2007

This is to certify that the
dissertation entitled

LIQUID CHROMATOGRAPHY/MASS SPECTROMETRY BASED METABOLITE PROFILING IN REVERSE GENETIC INVESTIGATIONS OF WOUNDING AND PATHOGEN STRESS RESPONSES IN *ARABIDOPSIS THALIANA*

presented by

Xiaoli Gao

has been accepted towards fulfillment
of the requirements for the

Ph.D. degree in Genetics

A. Daniel Jones
Major Professor's Signature

27 August 2009
Date

LIQUID CHROMATOGRAPHY/MASS SPECTROMETRY BASED METABOLITE PROFILING IN REVERSE GENETIC INVESTIGATIONS OF WOUNDING AND PATHOGEN STRESS RESPONSES IN *ARABIDOPSIS THALIANA*

By

Xiaoli Gao

A DISSERTATION

Submitted to
Michigan State University
in partial fulfillment of the requirements
for the degree of

DOCTOR OF PHILOSOPHY

Genetics

2009

ABSTRACT

LIQUID CHROMATOGRAPHY/MASS SPECTROMETRY BASED METABOLITE PROFILING IN REVERSE GENETIC INVESTIGATIONS OF WOUNDING AND PATHOGEN STRESS RESPONSES IN *ARABIDOPSIS THALIANA*

By

Xiaoli Gao

Investigations of gene functions have relied on two strategies known as forward genetics and reserve genetics. Both strategies are most powerful when phenotypes are described explicitly, and global phenotype profiling has emerged as a set of vital methodologies for functional genomics. This dissertation presents development and application of liquid chromatography/mass spectrometry (LC/MS) methods for metabolomic profiling for investigations of plant responses to wounding and pathogen stress. In the first study, liquid chromatography/time-of-flight mass spectrometry was used for nontargeted profiling of metabolites in leaves of wild type and *O*-methyltransferase (OMT) knockout mutants. *O*-methyltransferase (OMT) methylates the hydroxyl groups on phenols and produces methylated products. One of these mutants, *omt1*, exhibited metabolic phenotypes distinct from wild type plants, with notable accumulation of 5-hydroxyferuloyl malate in the mutant. After inoculation with pathogen *Pseudomonas syringae* DC3000, wild type plants exhibited five-fold greater bacterial counts relative to the *omt1* mutant. Profiling of metabolites in control and pathogen-infected *omt1* mutant and wild type plants pointed to several aspects of stress biochemistry associated with this specific mutation. Most notable was evidence of conversion of 5-hydroxyferuloyl malate to a reactive quinone metabolite in the pathogen-

infected *omt1* mutant. The quinone metabolite was converted to glutathione (GSH) conjugates *in vivo* in mutant plants. Further support for antimicrobial properties of the quinone metabolites came from *in vitro* screening of synthetic substances against *P. syringae*. Inhibition of bacterial growth was observed at low concentrations for 5-hydroxyferulic acid, its quinone, and the glutathione conjugate of the quinone, but not for the methylated analog sinapic acid. Though glutathione conjugation of quinones has been considered a detoxification step, the persistence of antagonism to *P. syringae* growth with the quinone-glutathione conjugate suggests this class of metabolites may undergo redox cycling, catalyzing formation of superoxide and hydrogen peroxide, as has been observed in studies of quinone toxicity in animals. Though some polyphenols have been documented in earlier studies to exhibit antimicrobial properties, roles for specific metabolites or metabolic genes have remained elusive. Furthermore, the *omt1* mutant displayed a more pronounced initial burst in levels of jasmonic acid, suggestive of crosstalk between polyphenol metabolism and jasmonate signaling.

The second part of this dissertation research has focused on development of ultraperformance LC (UPLC)-MS/MS methodology for rapid screening of multiple phytohormones in a single analysis. A fast, sensitive, and selective UPLC MS/MS method was developed for quantifying an assortment of jasmonic acid metabolites including bioactive amino acid conjugates, and an assortment of related phytohormones including salicylates, auxin, abscisic acid, and other oxylipins. These experimental approaches have been applied to study interactions among different metabolic pathways involved in gene regulation and signal transduction in wounding and pathogen stress.

Dedicated to my beloved: my husband and my parents

ACKNOWLEDGMENTS

I would like to express my earnest gratitude to my advisor and mentor, Dr. A. Daniel Jones for the guidance during these years. Dr. Jones has always been an admirable and brilliant mentor to me, has shown substantial support for my study and work with his inspiration and encouragement, and has strengthened my determination in pursuit of my dream. I still remember clearly the day when I went to his laboratory for the first time; he was very supportive to a genetics student who really wanted to study metabolomics. Luckily, I was accepted as one of his graduate students later. His persistent efforts and patience have assisted me through the most challenging but rewarding experiences to become a professional researcher. I will be grateful for his mentoring forever.

I also wish to show sincere appreciation to members of my guidance committee, Dr. Christoph Benning, Dr. Gregg Howe, and Dr. Lee Kroos for their constructive comments and insightful suggestions on my work. I have been extensively benefited from their marvelous instruction and treasured their friendship during my entire doctoral study.

I am grateful for the Plant Science Fellowship and Dissertation Completion Fellowship offered by the Michigan State University. I would like to thank Dr. Abraham J. K. Koo, Dr. Weiqing Zeng, and other colleagues for the collaboration. I would also like to thank the colleagues from Dr. Christoph Benning and Dr. Dean Della Penna's groups in Biochemistry second floor for their help.

I would like to express my special gratitude to Dr. Barbara Sears, the director of Genetics Program, who is like a big mum for every student in our program. I also would thank Genetics Program for enrolling me into Michigan State University, which gave me such a remarkable experience in my life.

I would like to acknowledge my friends and my colleagues in our laboratory who always bring joy and happiness to me. I would also like to thank their friendships and scientific interactions.

I owe countless thanks to my husband, Yanfeng Zhang, my parents, my parents-in-law, and my friends for years of unconditional love and support. Their encouragement and belief have pushed me to finish this work.

Finally, I would like to thank all of the people above. This work would not be possible without criticism, suggestion, support, and help from them.

TABLE OF CONTENTS

LIST OF TABLES

LIST OF FIGURES

(Images in this dissertation are presented in color)

ABBREVIATIONS

ABA	abscisic acid
ANOVA	analysis of variance
CCoAOMT	caffeoyl-CoA *O*-methyltransferase
[$^{13}C_6$]-JA Ile	[$^{13}C_6$]-jasmonyl-isoleucine
COMT	caffeic acid *O*-methyltransferase
Cor	coronatine
dJA	dihydrojasmonic acid
ESI	electrospray ionization
FT-ICR MS:	Fourier transform-ion cyclotron mass spectrometry
GC/MS	gas chromatography/mass spectrometry
GSA	β-O-D glucosylsalicylic acid
5HF	5-hydroxyferulic acid
5HFG	5-hydroxyferuloyl glucose
5HFM	5-hydroxyferuloyl malate
5HFMQ	5-hydroxyferuloyl malate quinone
5HFMQ-GS	5-hydroxyferuloyl malate quinone glutathione conjugate
5HFQ	5-hydroxyferulic acid quinone
5HFQ-GS	5-hydroxyferulic acid quinone glutathione conjugate
[$^2H_5$]-OPDA	[$^2H_5$]-12-oxo-phytodienoic acid
IAA	indole-3-acetic acid
IS	internal standard
JA	jasmonic acid

LA	linolenic acid
LC/MS	liquid chromatography/mass spectrometry
M	mutant without any treatment
MC	mutant control, with the infiltration of $MgCl_2$ buffer
MeJA	methyl jasmonate
MRM	multiple reaction monitoring
MP	mutant with the infiltration of *P. syringae*
NMR	nuclear magnetic resonance
OMT	*O*-methyltransferase
OPDA	12-oxo-phytodienoic acid
OPLS	orthogonal partial least squares
PCA	principal component analysis
PLS-DA	partial least squares - discriminant analysis
SA	salicylic acid
SAG	salicylic acid glucosides
SAM	S-adenosyl methionine
SIM	selected ion monitoring
SG	sinapoyl glucose
SGE	salicylic acid glucose ester (acylglucoside)
SM	sinapoyl malate
UPLC-MS/MS	ultraperformance liquid chromatography-tandem mass spectrometry
W	wild type without any treatment
WC	wild type control, with the infiltration of $MgCl_2$ buffer

WP	**wild type with the infiltration of *P. syringae***

CHAPTER 1

Introduction

1.1 The significance of plant disease control

As the world population grows, the world places increasing demands on natural resources to sustain supplies of food, energy, and materials. Photosynthetic organisms, in particular land plants, serve as the foundation for nearly all of the food supply for humans and animals. Plants can convert energy from sunlight into chemical energy, and these biochemical intermediates flow ultimately into macronutrients including carbohydrates, proteins, and fats. In this manner, the survival of all animals including humans depends on plants, but the ability of these resources to meet the demands of a growing human population is threatened by diseases and challenged by the desire to use plants as a source of bioenergy. Plant diseases are classified as infectious (or biotic) disease and noninfectious (abiotic disease). Biotic diseases in plants are caused by biotic pathogenic microorganisms, such as viruses, bacteria, fungi, protozoa, nematodes, and threats from insect damage. Abiotic diseases are caused by environmental conditions, such as lack or excess of nutrients, water or light, and the presence of toxic chemicals in air or soil (Agrios 2005).

Productivity of diseased plants can show dramatic decreases relative to healthy plants, and uncontrolled plant diseases result in economic losses or foods of poor quality that can threaten human health (Agrios 2005). In the United States, annual crop losses have been estimated at $9.1 billion lost to diseases, $7.7 billion to insects, and $6.2 billion to competition by weeds. Therefore, crop protection becomes even more important than increasing fertilization, irrigation, and other methods to avoid the losses (Agrios 2005). Diseased plants may also contain poisons that make them unfit for consumption and affect the environment. Many plant products, like grains, hay, and fruits are often

infected with fungi that produce toxic secondary metabolites known as mycotoxins (Blumenthal 2004; Serra et al. 2005). Animals and humans consuming such foods may develop severe diseases of organs, the nervous system, and the circulatory system that are sometimes lethal.

Improved control of plant disease can result in more food, better quality, lower production costs, and less environment contamination. Therefore, finding environmentally friendly ways to control plant disease serves as an important avenue of research. Over the last 100 years, the control of plant diseases has depended increasingly on the extensive use of pesticides, with associated risks of toxicity and environmental contamination (Blain 1990; Mattsson 2000). Modern research in plant control aims at finding other environmentally friendly approaches to reduce toxicity and negative environmental impacts. The most promising approaches employ biological approaches that enhance plant resistance to disease including conventional breeding, genetic engineering of disease-resistant plants, RNAi gene-silencing to silence some genes, and enhanced production of agents antagonistic to microorganisms that cause plant disease. New biotechnological products are currently being developed based on stimulation of the plant defense response, and on the use of plant-beneficial bacteria for biological control of plant diseases (biopesticides) and for plant growth promotion (biofertilizers) (Montesinos et al. 2002).

In this study, the long-term goal is to increase our knowledge about how plants might better resist disease and use the knowledge to manipulate the combinations of plant genetics with environment to better avoid or control those diseases. Specifically, I am studying how plants generate biochemical responses to biotic stress (pathogen stress) and

abiotic stress (wounding stress) using *Arabidopsis thaliana-Pseudomonas syringae* as a model plant and pathogen system. To establish the context for my efforts, this section explores and explains recent applications of LC/MS based metabolomics and systems biology to the area of plant stress response.

1.2 Plant-pathogen interaction studies

1.2.1 *Arabidopsis-Pseudomonas syringae* model system.

In this study, we investigated plant-pathogen interactions using a model system based on the model plant *Arabidopsis thaliana* and model pathogen *Pseudomonas syringae*. In this model interaction, the genomes of both the host and the pathogen have been sequenced, and plant-pathogen interactions are well-studied in this model system. *Arabidopsis thaliana* is a small flowering weed of mustard family (Brassica) and has a short life cycle of six weeks (Meinke et al. 1998; Dennis and Surridge 2000). Its genome is one of the smallest plant genomes and was the first plant genome to be sequenced in 2000 (Arabidopsis Genome Initiative, 2000). The genome of *P. syringae* pv. *tomato* DC3000 has also been sequenced (Buell et al. 2003) (http://www.pseudomonas-syringae.org/). *P. syringae* strains had been observed to be a natural pathogen of soybean, tomato, and bean (Keen 1990). Examples of disease symptoms caused by *P. syringae* DC3000 infection in Arabidopsis leaves are shown in Figure 1.1.

Figure 1.1 Disease symptoms in Arabidopsis leaves caused by *P. syringae* DC3000 infection at third day after inoculation with 1 x 10^6 cfu/ml DC3000. The infected leaves were in yellow.

However, some researchers have not been convinced that *Arabidopsis-P. syringae* provides a good model system for two reasons. First, *P. syringae* is not known as a natural pathogen for *Arabidopsis* in the wild. Second, artificial inoculation methods, either infiltration or use of surfactant, were required to develop infection in the laboratory (Katagiri et al. 2002). Despite these disadvantages, there are substantial advantages that make this a good model system, since no other systems have been studied for such a long time with well-developed information on genomes and mechanisms of the pathogenesis from the pathogen side and resistance from the plant side.

Current wisdom suggests that plant resistance to pathogens is correlated with the activation of a network of broad-spectrum defense mechanisms. The response involves initial bacterial invasion, recognition of the pathogen effectors, opening of ion channels, signal transduction, activation of protein kinases, transcriptional activation of defense-related genes, and activation of preformed enzymes to modify primary and secondary

metabolism (Buchanan et al. 2001). The most frequently encountered defense and signaling mechanisms are described below to give an overall picture how plants respond to pathogens. These include stomata-based defense against bacterial invasion, two-branched innate immune system: nonhost resistance (basal defense) and pathogen-specific resistance (gene-for-gene model) (Jones and Dangl 2006), and systemic acquired resistance (SAR).

1.2.2 Stomata-based defense against bacterial invasion

Stomata, which are microscopic surface openings on the leaf, provide the first entrance for microbial invasion of plants. They serve as the critical first step for bacteria to cause infection. Stomata have long been assumed to be passive ports of bacterial entry, but recent studies in the laboratory of Sheng Yang He at Michigan State University found that stomatal closure is part of the plant immune response and acts as an innate immunity barrier to restrict bacterial invasion. However, some *P. syringae* strains produce a polyketide toxin, coronatine, that triggers reopening of stomata, and circumvent this host defense (Melotto et al. 2006; Thilmony et al. 2006)

1.2.3 Innate immune system: nonhost resistance (basal defense)

When bacteria invade plant tissues into the apoplast through the stomata, the innate immune system presents the first line of defense. A key function of innate immunity is recognition of pathogen-associated molecular patterns (PAMP) produced by infectious agents such as bacterial flagellin. Such recognition events activate a cascade of mitogen-activated protein kinases (MAPKs) and production of WRKY transcription factors that

confer resistance by altering gene expression (Mizoguchi et al. 1997; Asai et al. 2002; Chisholm et al. 2006). A diagram representing these processes is shown in Figure 1.2A (Chisholm et al. 2006). Alterations of plant cell walls at infection sites and deposition of electron dense callose-rich papillae have also been reported as a major component of non-host resistance (Truman et al. 2006).

Figure 1.2 Model for the evolution of bacterial resistance in plants. (A) Recognition of pathogen-associated molecular patterns (PAMP) caused by bacterial flagellin promptly triggers basal immunity, which activates signaling through MAP kinase cascades and transcriptional reprogramming through WRKY transcription factors. (B) Pathogenic bacteria use the type III secretion system (TTSS) to deliver effector proteins (Avr gene product) that target multiple host proteins to suppress basal immune responses, allowing bacteria growth and cause disease. (C) Plant resistance proteins (R gene products) recognize effector activity and restore resistance through effector-triggered immune responses. Limited accumulation of bacteria occurs prior to effective initiation of effector-triggered immune responses (Chisholm et al. 2006). Reprinted from Host-microbe interactions: shaping the evolution of the plant immune response, 124/4, Chisholm, S. T., G. Coaker, B. Day and B. J. Staskawicz, Cell, 803-814, Copyright (2006), with permission from Elsevier.

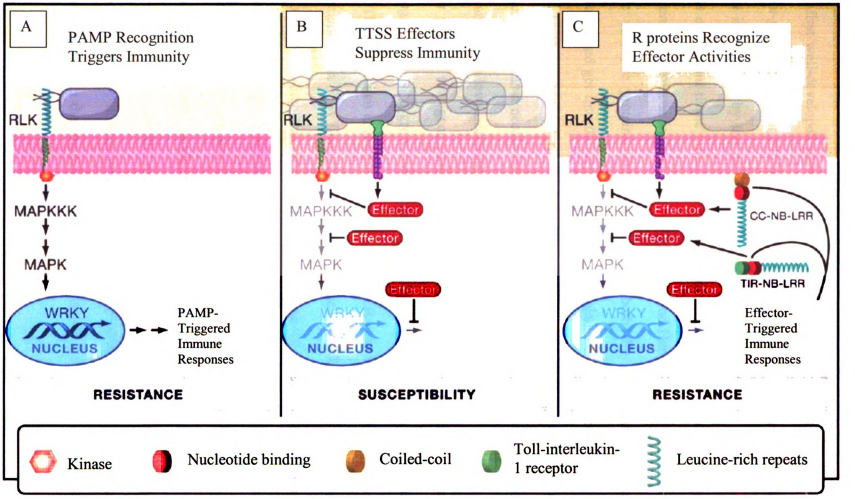
A
PAMP Recognition
Triggers Immunity
RLK
MAPKKK
MAPK
WRKY
NUCLEUS
PAMP-
Triggered
Immune
Responses
RESISTANCE
B
TTSS Effectors
Suppress Immunity
RLK
MAPKKK
Effector
Effector
MAPK
Effector
WRKY
NUCLEUS
SUSCEPTIBILITY
C
R proteins Recognize
Effector Activities
RLK
MAPKKK
Effector
CC-NB-LRR
Effector
MAPK
TIR-NB-LRR
Effector
WRKY
NUCLEUS
Effector-
Triggered
Immune
Responses
RESISTANCE
Kinase
Nucleotide binding
Coiled-coil
Toll-interleukin-
1 receptor
Leucine-rich repeats

1.2.4 Innate immune system: pathogen-specific resistance (Gene-for-gene model)

The first well-developed pathogen-specific resistance mechanism is described as the gene-for-gene model (Flor 1955), the specific recognition of the resistance gene (R gene) product in the plant by the pathogen avirulence *(avr)* gene product. After pathogenic bacteria enter plant tissue through stomata or wounding, they proliferate in the apoplast (the intercellular spaces between plant cells) (Jones and Dangl 2006). The Avr products, specific virulence proteins, are secreted across both the inner and outer bacterial membranes and get into the cytoplasm of the host plant cell. The secretion mechanism utilized by the pathogen, termed a type III secretion system (TTSS), involves a protein complex that forms a needle-like structure that spans both the inner and outer bacterial membranes and allows bacterial proteins to enter plant cells. The major function of these effector proteins (avr gene products) is to suppress the host innate immune response, allowing pathogens to grow and cause disease (Chisholm et al. 2005; Chisholm et al. 2006). The mechanism is shown in Figure 1.2B. The R proteins, operate as receptors and signal transducers. They first recognize any Avr gene-dependent ligand and then activate downstream signaling that leads to rapid induction of various defense responses (Buchanan et al. 2001). The mechanism is shown in Figure 1.2C. This recognition sets off a hypersensitive response (HR), a rapid and localized cell death with hydrogen peroxide concomitantly produced which effectively prevents further spread of the pathogen. The HR is generally recognized by the presence of brown and dead cells at the infection site and by "defense gene" expression (Heath 2000). Two mechanisms underlie HR formation. Either the attacked cell initiates a regulated cell death program (apoptosis)

or the responding cells are rapidly poisoned by the toxic compounds and free radicals they have synthesized, and thus die as a result of necrosis.

1.2.5 Systemic Acquired Resistance (SAR)

Within minutes of pathogen attack, plant defense responses are activated locally (as described above). Within hours, defense responses are sometimes activated in tissues far from the invasion site and even in neighboring plants to protect non-infected tissues from secondary infection. This mechanism of induced defense that confers long-lasting protection against a broad spectrum of microorganisms is called systemic acquired resistance (SAR) (Durrant and Dong 2004). SAR in plants is analogous to the innate immune system found in animals, in that both produce antimicrobial substances such as peptides and metabolites in response to infection (Traw et al. 2007). The combination of accumulation of the phytohormone salicylic acid (SA) and systemic activation of a specific subset of pathogenesis related (PR)-type genes is essential for the expression of SAR. (Hunt et al. 1996; Fobert and Despres 2005). This SA-mediated signal transduction cascade is modulated by interactions between a redox-sensitive protein known as the non expressor of pathogenesis-related genes 1 (NPR1) and the TGA family of transcription factors. These interactions regulate expression of an assortment of PR defense genes. The mechanisms underlying the influence of cellular redox state are not fully established, but it has been proposed that hydrogen peroxide may serve as a second messenger of SA. (Lebel et al. 1998; Zhang et al. 1999; Fobert and Despres 2005; Weigel et al. 2005; van Verk et al. 2008). Some PR proteins are chitinases and glycanases, enzymes that degrade

structural polysaccharides of pathogen cell walls and may reduce bacterial growth (Metzler et al. 1991; Rogers and Ausubel 1997).

The mechanisms of plant activation of defenses against pathogens using *Arabidopsis thaliana-Pseudomonas syringae* as a model system were reviewed above. However, the extent to which genetic diversity in plants contributes to resistance to pathogens remains a body of knowledge with several gaps. To understand exactly how these defense mechanisms work, we need to broaden our knowledge about functions of plant genes including aspects of protein localization, protein-protein interactions, endogenous substrates for enzymes and transporters, and the biological roles of these genes in plant interactions with microbes and other organisms.

1.3 Responses of plants to wound stress

Introduction of pathogens to plant tissues is often accompanied by mechanical wounding. Such wounding is an important aspect of plant responses to herbivory by insects. To dissect the contributions of plant responses to various stressors, plant responses to mechanical wounding have been investigated in detail.

Leaf wounding is well characterized for its stimulation of rapid activation of jasmonic acid (JA) synthesis (Weber et al. 1997; Schilmiller and Howe 2005; Chung et al. 2008; Glauser et al. 2008; Koo et al. 2009), and JA is widely considered as the main phytohormone produced as a wound response and an important regulator of gene expression following wounding. The precursors of JA, linolenic acid (C18:3) and its metabolite 12-oxo-phytodienoic acid (OPDA), are released from plastid membrane galactolipids by the catalytic action of lipases (Ishiguro et al. 2001; Buseman et al. 2006;

Kourtchenko et al. 2007; Hyun et al. 2008), and some basal levels of OPDA may be present prior to wounding. Conversion of OPDA and related intermediates to JA is believed to occur in the peroxisome, first through reduction to the intermediate OPC:8, followed by chain shortening by β-oxidation. JA can be further metabolized to assorted derivatives such as JA Ile and MeJA (Figure 1.3) that differ in biological activity.

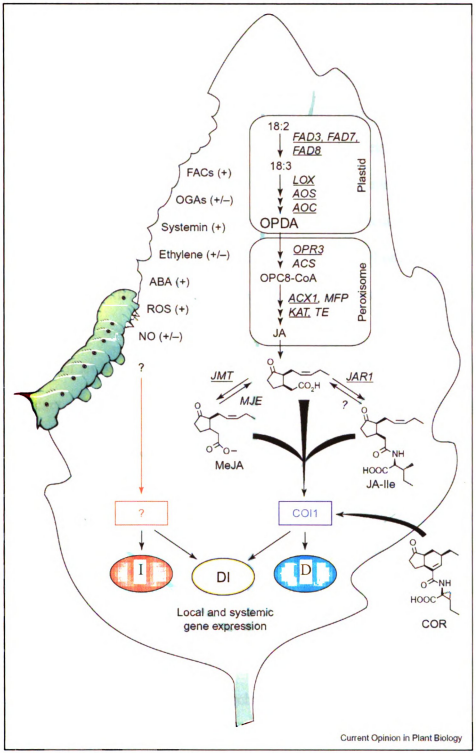

Figure 1.3 Systemic signaling in the wound response (Schilmiller and Howe 2005). Reprinted from Systemic signaling in the wound response, 8/4, Schilmiller, A. L. and G. A. Howe, Current opinion in plant biology, 369-377, Copyright (2005), with permission from Elsevier.

While JA and related oxylipins have attracted much attention for their role in plant responses to wounding, the early events that plants use to recognize and generate biochemical responses to wounding have remained a subject of intensive study and debate. Release of linolenic acid from membranes following wounding has been proposed as one of the early steps leading to increased JA levels following wounding.

Hydrolysis of membrane lipids to generate signaling molecules other than JA has been reported as a consequence of wounding in plants. Accumulation of phosphatidic acid (PA) has been observed in leaves following wounding (Lee et al. 1997), and PA is now recognized to activate an assortment of signaling pathways in plants. Though it has been proposed that wound-activated phospholipase D (PLD) could catalyze formation of PA upstream of JA biosynthesis (Wang et al. 2000), a recent study of *pld* mutants showed no significant differences in JA or related oxylipin levels following wounding (Bargmann et al. 2009).

Early events in responses to wounding have been associated with release of calcium from damaged cells, membrane depolarization, formation of systemin peptides, and activation of mitogen activated protein kinase (MAP kinase) activity (Ryan 2000). Within minutes, measurable increases in levels of JA and its amino acid conjugate, jasmonoyl-isoleucine (JA Ile), can be observed, and these jasmonates play important regulatory roles. Most members of the JASMONATE ZIM-domain (JAZ) transcriptional repressors were highly expressed in mechanical wounding within 5 min of mechanical tissue damage, coincident with a large rise in JA and JA Ile levels (Chung et al. 2008). JA and JA Ile activate wound-induced defense responses by promoting SCF^{COI1}-dependent

degradation of JAZ proteins that repress the expression of early response genes (Chung et al. 2008; Katsir et al. 2008; Koo et al. 2009).

The jasmonic acid (JA) pathway in plant responses to wounding is regulated by other signaling molecules which have been proposed to play important roles in wound signaling as well (Figure 1.3). Wounded plants also accumulate abscisic acid (ABA) (Birkenmeier and Ryan 1998), ethylene (O'Donnell et al. 1996), oligosaccharides (Doares et al. 1995), and the oligopeptide systemin (Constabel et al. 1995; Howe and Ryan 1999; Ryan 2000). Wound signal transduction cascades also involve secondary messager calcium which is released from damaged cells (Knight et al. 1993), fatty acid conjugates (FACs) (Ryu and Wang 1998), and hydrogen peroxide (Orozco-Cardenas and Ryan 1999; Guan and Scandalios 2000; Orozco-Cardenas et al. 2001). Nitric oxide (NO) may down regulate the expression of wound-inducible defense genes during pathogenesis (Orozco-Cardenas and Ryan 2002). Besides jasmonate-dependent signal transduction cascades, jasmonate-independent cascades also exist including gene expression activated by oligogalacturonides (Titarenko et al. 1997; Leon et al. 1998). Coronatine, a microbial metabolite and structural mimic of JA, exerts its effects by activating the JA singaling pathway through COI1. A summary of wound-induced signaling is shown in Figure 1.3 (Schilmiller and Howe 2005).

Tissue damage is associated with decompartmentalization, release of cellular contents, and a loss of water, similar to those occurring in water-stressed intact plants (Reymond et al. 2000). Therefore, wounding shares many biochemical consequences with osmotic stress (Denekamp and Smeekens 2003). The overlap was also observed

between wounding and pathogen response (Cheong et al. 2002), since mechanical wounding not only damages plant tissues, but also facilitates pathogen invasion.

1.4 Current knowledge and knowledge gaps pertaining to mechanisms of plant responses to stress and disease

1.4.1 Genetics in plant response to stress and disease: plant gene function studies

Association of individual plant genes with specific functions serves as a key step toward development of plants with improved productivity and resistance to pathogens and other environmental stresses. In order to determine biological function of a gene, a well-used genetics approach investigates the phenotypic effects of the perturbation of the gene by introducing genetic alterations. It is helpful to compare two genotypes: the wild type that can express a functional gene, and a mutant that lacks this gene. Identification of mutants and their corresponding phenotypes is achieved either by 'forward' or 'reverse' genetics (Alonso and Ecker 2006). Forward genetics involves working from a phenotype to identify a corresponding gene and its functions, following the approach developed by Mendel, the father of genetics, in his legendary experiments on garden pea plants in the mid-19th century. It is the traditional approach where groups of randomly generated mutants are screened based on their phenotype, and the gene responsible for the phenotype is identified by gene mapping (Jander et al. 2002). The advantage of forward genetics is that no prior assumptions need be made about the mutant genes and phenotypes, making this unbiased approach powerful for identifying roles for genes of unknown functions. Forward genetic approaches encounter challenges in gene mapping and discovery, particularly for those plants for which genomic sequence information is

limited. Reverse genetics approaches explore gene functions by working from specific mutant genes to identification of phenotype. Mutants with the depletion of specific genes are analyzed with a number of phenotypic assays (McCallum et al. 2000). The great advantage of reverse genetics is that more facile association of mutant phenotype with the affected gene can be achieved, and a broader array of phenotypes can be measured against mutants than in a forward genetics screen (Lahner et al. 2003; Messerli et al. 2007). A major disadvantage of the reverse genetics approach arises because most common phenotypic assays of mutants lacking specific genes have failed to associate functions with those genes. As a result, large-scale phenotypic profiling of numerous mutants may be necessary for gene function discovery.

In the model plant *Arabidopsis thaliana*, it has been estimated that the genome codes for about 25,000 genes (Poethig 2001). The Arabidopsis 2010 program, funded by the US National Science Foundation, has a stated aim of identifying all Arabidopsis gene functions by the year 2010. However, at this date, many genes remain with unidentified functions. Approximately one thousand predicted genes encode proteins assumed to function in secondary metabolism in Arabidopsis (von Roepenack-Lahaye et al. 2004). Sequence similarities have suggested >250 cytochrome P450, >100 acyl transferase, >300 glycosyl transferase, >300 glycoside hydrolase genes, and a large number of other putative genes encoding enzymes such as dioxygenases, *O*-methyltransferases, terpene synthases, or polyketide synthases. Compared with the huge number of these genes, the number of known reactions catalyzed by these types of enzymes is relatively low in Arabidopsis.

A large number of metabolites have yet to be identified as well (von Roepenack-Lahaye et al. 2004). Despite well-developed approaches of forward and reverse genetics, why is it so difficult to determine the functions of these genes? The answers come first from realization that gene annotation is most often based on similarity of DNA sequence to a gene of known function. However, sequence similarities do not always lead to identical functions, and single mutations can have dramatic effects on protein functions. Second, redundant genes often display no overt phenotypes. When a given biochemical function is redundantly encoded by two or more genes (so called genetic redundancy), mutations in one of these genes may have a small or negligible effect on the loss of phenotypes. Therefore, it is challenging to establish the function of a single gene with overlapping functions with other genes. Third, regardless of whether a study pursues forward or reserve genetic approaches, it is essential that the phenotypes be described as explicitly as possible, so that the functions of genes responsible for the phenotypes can be assigned accurately. The molecular phenotypes include all the levels of mRNAs, proteins, and metabolites. More commonly, however, the approaches that have been used to study cellular responses have focused on the transcript or the protein levels (transcriptomics and proteomics, respectively) because technologies and databases have been more advanced in these areas than for metabolites.

The traditional forward genetic and reverse genetic strategies have suffered from the interrogation of each mutant with a limited number of phenotypic assays, typically targeting only one or a limited number of pathways. This approach limits the likelihood that the full effects of a mutation will be discovered, and hinders researchers from discovering unexpected relationships between genes. Examples of comprehensive

screening of biochemical phenotypes have been few until recent years. In one prominent and recent study, previously characterized Arabidopsis mutants that have primary physiological defects were shown to have unexpected secondary phenotypes and syndromes based upon parallel assays of metabolites, physiology, and morphology (Lu et al. 2008). An important aspect of the novelty of this study lies in the depth of phenotypic screening of large numbers (~ 100) of mutants, and comparisons of numerous phenotypes including levels of numerous fatty acids and 25 amino acids and related metabolites. The findings of this study suggest that greater efficiencies in gene function discoveries result from parallel measurements of multiple phenotypes in a single study.

In view of these findings, this dissertation emphasizes development and application of approaches capable of profiling metabolites on a global level to accelerate the precise linkage of genes to their functions in plants. Most investigations of this kind have been centered on measurements of biochemical phenotypes under control environmental conditions, but the research described below aims to extend metabolite profiling to investigate gene functions in plant responses to stress.

1.4.2 Biochemistry of plant responses to stress and disease

1.4.2.1 Stress and metabolic homeostasis

Stress in a plant can be defined as any change that requires adjustments to metabolic fluxes to sustain homeostatic control (Shulaev et al. 2008), and these adjustments are usually referred to as acclimation (Mittler 2006). To thrive despite an assortment of environmental stresses, plants must be able to sense changes in environmental conditions and respond to these changes through regulation of gene expression and protein activity.

Because plants are immobile, they cannot avoid stress by moving to less stressful locations. Their successful resistance to pathogens depends on their ability to detect pathogens and generate biochemical responses that provide a defense against pathogens. These biochemical defenses will be described in greater detail below. Pathogen detection by plants is followed by a complex system of signal transduction events that ultimately result in dramatic changes in profiles of gene expression (Thilmony et al. 2006) and metabolites. Since metabolite levels change in response to levels and activities of protein gene products including enzymes and transporters, metabolic responses often lag behind changes in gene expression. Plant responses to pathogens often involve changes in expression of hundreds of genes and levels of metabolites, most of which remain unidentified and unmeasured. As a consequence, attribution of resistance functions to individual metabolic genes or metabolites remains challenging, and it has been difficult to prove roles for individual metabolites in resistance. One group of specialized metabolites, the phytoalexins, is defined as a group of antimicrobial metabolites synthesized by plants in response to pathogen infection, and these will be discussed in more detail below.

The plant kingdom produces a diverse suite of specialized secondary metabolites and other natural products that can confer disease resistance (Dixon 2001) including numerous metabolites with antimicrobial properties (Cowan 1999). Most specialized metabolites have functions that often remain unclear, although their modulations are likely to be the major result of the numerous induced changes in transcriptional activity occurring in infected plant cells (Scholthof 2001). Plant responses to pathogen infection and other environmental stress often involve increased production of secondary

metabolites (Bednarek and Osbourn 2009), but the extent of these changes has not been addressed in a comprehensive manner.

1.4.2.2 Classes of secondary metabolites associated with plant stress responses

Based on current knowledge of secondary metabolites involved in plant responses to pathogen stress, the metabolites can be classified based on their dynamics and functions in plant response and their chemical structures.

Metabolites with different dynamics in plant responses to stress

Several stages are thought to be involved in acclimation of plants to stress. In the initial stages, the change or attack is sensed by the plant, and a network of signaling pathways is activated. These signaling cascades involve changes in gene expression, protein function, and metabolite levels. Details of the early mechanisms in conversion of molecular stress to a biochemical signal are often unclear. In later stages, the activated signal transduction pathways trigger the production of different genes, proteins and metabolites that restore or achieve a new state of homeostasis (Mittler et al. 2004).

Metabolites with different functions in the plant response to stress

At least three different types of metabolites with different functions have been touted as important for acclimation: (1) compounds involved in the acclimation process such as antioxidants including ascorbic acid, glutathione, tocopherols, anthocyanins, and carotenoids, or osmoprotectants including the polyols mannitol and sorbitol, betaines and dimethylsulfonium compounds, and the amino acids proline and ectoine (Shulaev et al.

2008); these compounds offer protection against damage to cellular functions in the form of inactivation of reactive intermediates including free radicals, maintenance of cellular redox state, and stabilization of three-dimensional protein structures; (2) metabolic by-products of stress that result from the disturbance of normal homeostasis and resulting changes in gene expression and protein functions; these include compounds with suspected antimicrobial properties, classified as phytoalexins (Hammerschmidt 1999); and (3) signal transduction molecules involved in mediating the stress response (Shulaev et al. 2008).

The production of phytoalexins such as the indole alkaloid camalexin in Arabidopsis, tomatine (steroidal glycoalkaloid) in tomato, and avenacin (triterpene glycoside) in oat are phytochemicals with antimicrobial properties (Bednarek and Osbourn 2009). In 1994, the first report of a mutant Arabidopsis plants deficient in camalexin exhibited enhanced sensitivity to *P. syringae*, but one camalexin-deficient mutant (*pad3*) exhibited behavior in pathogen growth similar to wild type plants (Glazebrook and Ausubel 1994). The study was unable to reach definitive conclusions about the role of camalexin in these plant-pathogen interactions, having shown that levels of camalexin alone did not explain differences in pathogen susceptibility, but suggested that another metabolite in the camalexin biosynthetic pathway might show similar antimicrobial effects. Such findings point to the drawbacks of attributing antimicrobial functions to a single targeted metabolite.

One unanticipated finding, reported in 1988, identified the tripeptide glutathione (GSH) as a metabolite that stimulated induction of plant defense genes in cultured bean cells (Wingate et al. 1988). While GSH has long been recognized as a redox buffering

metabolite, mechanistic understanding has yet to explain these observations. One of the camalexin-deficient mutants (*pad2*) described above was recently used to demonstrate that the *PAD2* gene codes for γ-glutamylcysteine synthetase, a key enzyme in GSH biosynthesis. The *pad2-1* mutants showed enhanced susceptibility to additional pathogens, and these findings suggested an important, but mechanistically undefined role for GSH in pathogen resistance (Parisy et al. 2007).

A variety of studies have suggested that signaling metabolites involved in plant responses to pathogens could be newly synthesized or released from their conjugated forms. These substances could be by-products of stress-induced metabolism (similar to the second type of metabolites described above), degradation of membrane lipids and release of precursors of bioactive metabolites, an assortment of reactive oxygen species (ROS), oxidized metabolites such as oxidized phenolic compounds, or even some antioxidants (Mittler 2002). Salicylic acid (SA), methyl salicylate (Me SA), and abscisic acid (ABA) are induced and involved in the signal transduction for activating systemic defense and acclimation response under pathogen stress (Nawrath et al. 2002; Guo and Stotz 2007; Kachroo and Kachroo 2007). Jasmonic acid (JA), JA amino acid conjugates, methyl jasmonate (Me JA), 12-oxophytodienoic acid (OPDA) and other oxylipins and their conjugates that are produced as a result of wounding stress can also serve as signaling molecules. Crosstalk among those signals makes the study of signaling mechanisms more challenging (Gupta et al. 2000; Gutjahr and Paszkowski 2009), and it is in these studies where reverse genetics approaches offer prospects for identifying roles of specific individual genes.

Classes of metabolites important in plant stress response

Numerous classes of specialized plant metabolites have important roles in plant responses to stress including pathogen infection. Polyphenols are some of the most abundant secondary metabolites in plants and their induced production indicates change in relevant metabolic steps in plants under pathogen stress (Dixon and Paiva 1995). In addition, glucosinolates, oxylipins, indole conjugates, terpenes, and alkaloids are also thought to play important roles in plant responses to pathogens (Kliebenstein 2004), and these are discussed in greater detail below.

Polyphenols are specialized metabolites defined by the presence of at least one phenolic hydroxyl group per molecule. They are generally subdivided into tannins and phenylpropanoids such as lignins and flavonoids that are derived from simple polyphenolic units produced by the shikimate pathway (Dewick 1995). Polyphenols are important to the plant cell and have been assigned functions as phytoalexins, UV sunscreens, pigments, signaling molecules, and are precursors of major structural components including lignin and hemicelluloses (Winkel 2004). Polyphenols are also potent inhibitors of free radical oxidations owing to their ease of forming phenoxy radicals. Oxidative burst is a phrase that describes the rapid generation of superoxide and hydrogen peroxide that follows initial recognition of pathogen infection. Many polyphenols are potent scavengers of oxidants that are generated during this process, and may be oxidized to various forms by nonenzymatic and enzyme-catalyzed reactions with such oxidants.

Polyphenols are derived from the amino acid phenylalanine, which is transformed into a variety of important secondary products, including lignin, sinapate esters, stilbenes,

and flavonoids. Flavonoids are derived from a C15 skeleton, which is synthesized via the condensation of *p*-coumaroyl-CoA and three molecules of malonyl-CoA (Harborne 1988). Flavonoids occur widely in plants and have diverse subgroups that can be divided into anthocyanins, flavonols, flavones, flavanones, chalcones, dihydrochalcones and dihydroflavonols. (Treutter 2005; Treutter 2006). The distribution of specialized metabolites among these forms depends on the presence and expression of metabolic enzymes that catalyze key steps in their biosynthesis. The induced formation of flavonoids after injury by pathogens or pests is a well-known phenomenon (Barry 2002; Gallet 2004). The phenolic unit can often be modified through esterification, glycosylation, methylation, and in some plants, prenylation, and these modifications can influence reactivity and sequestration. Dimerization or further polymerization can create additional classes of polyphenols.

Some polyphenols are reported to be antifeeding compounds that inhibit herbivory by insects and other animals. However, roles of most polyphenols in microbial pathogen infection have often been postulated, but have remained uncertain (Harborne 1994; Treutter 2005).

Glucosinolates are also well-characterized antimicrobial and anti-insect metabolites (Grubb and Abel 2006; Mewis et al. 2006) that may exert their antimicrobial activity after metabolic conversion to reactive isothiocyanate metabolites. Glucosinolates share a common core structure of a β-D-thioglucose group linked to a sulfonated aldoxime moiety and variable aglycone side chains (Fahey et al. 2001). In *A. thaliana*, the source of the side chain defines three major classes of glucosinolates: aliphatic glucosinolates are derived principally from methionine via elongation of the alkyl chain, indolyl

glucosinolates are from tryptophan, and aromatic glucosinolates are derived from phenylalanine (Mewis et al. 2006). It was reported that aphid attacks increased indole-glucosinolate levels and suppressed methylsulfinylpropyl and propenyl-glucosinolate synthesis (Kusnierczyk et al. 2008). The metabolite 4-methylsulphinylbutyl isothiocyanate has been shown to have antimicrobial activity against DC3000 in vitro (Tierens et al. 2001). This activity may result from enzymatic transformation of glucosinolates to isothiocyanates, which are electrophilic intermediates reactive toward nucleophiles such as certain proteins and low molecular weight thiols.

Biosynthesis of secondary metabolites following pathogen infection and stress is often regulated by oxylipin metabolites that are central regulators of plant gene expression, including genes involved in responses to stress and pathogen infection. Among oxylipins, jasmonic acid (JA), its methyl ester (MeJA) and 12-oxophytodienoic acid (OPDA) are important mediators of signal transduction (Browse 2005; Koo et al. 2009). A growing research effort focuses on the roles of oxylipin conjugates including glycolipid conjugates and bioactive amino acid conjugates of jasmonates in signal transduction. Much work is underway and is needed to improve understanding of the roles of oxylipin metabolites in control of plant responses to stress (Staswick and Tiryaki 2004).

Accumulation of soluble and wall-bound indolic metabolites in *Arabidopsis* leaves has also been found to follow infection by *Pseudomonas syringae* (Hagemeier et al. 2001). Most prominent among the accumulating soluble substances were tryptophan, β-D-glucopyranosyl indole-3-carboxylic acid, 6-hydroxyindole-3-carboxylic acid 6-*O*-β-D-glucopyranoside, and the indolic phytoalexin camalexin.

Terpenes comprise another class of abundant specialized metabolites; many are volatile compounds that give plants their odors, and some are chemical insect attractants and repellents. They are based upon isoprene (C_5H_8) building blocks, with an enormous number of isomers possible within the class. Diterpenes (C_{20}), triterpenes (C_{30}) and tetraterpenes (C_{40}), hemiterpenes (C_5), and sesquiterpenes (C_{15}) are commonly found in plants. Terpenoids are terpenes with the addition of oxygen-containing functional groups (Cowan 1999). Within the Arabidopsis genome, over 30 genes have been identified that potentially encode terpene synthases (TPSs) (Chen et al. 2004). Volatile terpenoids have been implicated in plant defenses, particularly toward herbivory by insects, but demonstration of their direct role in pathogen resistance has remained elusive. Attribution of roles to specific terpenoids is complicated by concomitant changes in numerous other metabolites during the course of pathogen infection. In the case of volatile terpenoids, levels in Arabidopsis are considered low compared to other plants. A possible role of terpenoid metabolism was found in the induced defense of *A. thaliana* plants against *P. syringae*. Elevated emission of the volatile terpenoid (E,E)-4,8,12-trimethyl-1,3,7,11-tridecatetraene (TMTT) was suggested to be a by-product of activated JA signaling, rather than an effective defense response that contributes to resistance against *P. syringae* (Attaran et al. 2008).

Alkaloids are specialized metabolites having a nitrogen atom within a heterocyclic ring, as is the case for pharmacologically important compounds such as morphine (Cowan 1999). As was the case for other classes of metabolites, roles for alkaloids in pathogen resistance have been proposed but difficult to prove. In one recent paper (Kim and Sano 2008), transgenic tobacco plants developed to produce the alkaloid caffeine,

showed enhanced resistance to *P. syringae* and tobacco mosaic virus. Direct application of caffeine to wild-type plant leaves generated similar resistance. Since the transgenic plants constitutively expressed defense-related genes, the study concluded that a bifunctional mechanism was at work, involving a combination of direct antagonism toward the pathogen and indirect activation of host defense systems. Alkaloids are not known to be significant metabolites in *A. thaliana*.

Though many gene functions have been suggested by recent research, the roles of individual genes in plant defense responses and resistance to effects of stress and pathogens remain mysterious. Defining those genes whose functions are important from those whose expression is more an effect than a cause of stress resistance remains an important area for research. To answer such questions, combinations of genetic and biochemical efforts ought to take advantage of new technologies capable of providing rich information about gene functions. The study of plant biochemistry using comprehensive metabolite profiling, known as metabolomics, is a promising approach for discovery of new bioactive metabolites important for disease resistance.

1.5 Metabolomics as a new tool to close the gap between gene annotation and gene functions

1.5.1 The feasibility and utility of metabolomics in gene annotation

As biology moves increasingly away from reductionism and toward the more holistic systems biology approach, researchers have tools to explore comprehensive 'omics' studies, including genomics, transcriptomics, proteomics, and metabolomics. Like the other 'omics' studies in systems biology, metabolomics is, in theory, the study of all the

metabolites and metabolic pathways in an organism (Guy et al. 2008). Of course, no single analytical approach can measure all metabolites, but the spirit of this approach dictates that investigators should design analyses to measure as many metabolites as is feasible. Metabolomic approaches seek to profile metabolites in a nontargeted way, i.e. to reliably separate and detect as many metabolites as possible in a single analysis. Combined with information on transcript and protein abundance, metabolite profiles ideally lead to a complete molecular picture of the state of a particular biological system at a given time (von Roepenack-Lahaye et al. 2004).

In some of its earliest applications, metabolite profiling was used as a diagnostic tool to measure metabolite composition to ascertain metabolic responses to herbicide, and the classification of plant genotypes or treatments. Recently it has found growing application to decipher gene functions, investigate metabolic regulation, and as part of integrative analyses of systemic responses to environmental or genetic perturbations (Schauer and Fernie 2006). The real advantage of metabolomics lies not only in the characterization of the metabolic response to stress, but also provides utility in using metabolite profiles for gene annotation (Schauer and Fernie 2006). Since metabolites are the end products of cellular processes, their levels can be regarded as the ultimate responses of biological systems to genetic and/or environmental changes (Gu et al., 2009). Understanding the metabolome of each plant species is critical to understanding gene function and coupling each of these functions to plant traits (Shulaev et al. 2008). The effects of a single genetic mutation are often not limited to a single biochemical pathway. Indeed, levels of metabolites derived from seemingly unrelated biochemical pathways may be altered owing to pleiotropic effects. To understand the effects of loss of a metabolic enzyme,

comprehensive identification and quantification of all metabolites would be helpful (Fiehn 2001).

1.5.2 Methodology of metabolomics

Global metabolite analyses have taken one of two dominant approaches termed metabolic fingerprinting and metabolic profiling. Metabolic fingerprinting involves the analysis of the total composition of metabolites for comparison of patterns or fingerprints among samples (as opposed to identification and quantification of specific compounds) generated by analytical instruments. In this approach, the magnitudes of several hundreds to thousands of discrete analytical signals are used to compare different samples. These signals are usually generated using Nuclear Magnetic Resonance (NMR) spectroscopy (Ward et al. 2007) or Fourier Transform-Ion Cyclotron Resonance Mass Spectrometry (FT-ICR MS), the latter of which is a high resolution mass spectrometry method. Each metabolite may give several signals (e.g. peaks in NMR spectra or mass spectra), and the magnitude of each signal serves as a measure of the quantity of a metabolite. Profiles of these signals are quantitatively compared to identify signals that can define phenotypic differences, but it is uncommon to identify all of the metabolites responsible for the phenotype. Metabolite fingerprinting is considered a nontargeted analysis; the instrument detects signals from as many metabolites as possible. In contrast, metabolite profiling, a term first used in the 1970s, is defined as the qualitative and quantitative analysis of complex mixtures of physiological origin (Sumner et al. 2003). It consists of analyzing a known subset of metabolites, and is a technology increasingly used in functional genomics. Most work has focused on optimization of Gas

Chromatography/Mass Spectrometry (GC/MS) and Liquid Chromatography/Mass Spectrometry (LC/MS) analysis and demonstrations of their potential applications. The former is a more developed technology because extensive libraries of mass spectra are available to aid metabolite identification. Once optimized, these methods can be sensitive and quantitative, and are capable of detecting picomole quantities of numerous metabolites.

In addition to its role as a quantitative tool, mass spectrometry provides the first step toward metabolite identification owing to its ability to generate molecular and fragment mass information for nearly all compounds. The nontargeted LC/MS analyses of metabolites reported in this work were conducted on a time-of-flight mass spectrometer that is capable of measuring ion masses with great accuracy, usually to within 10 parts-per-million (ppm) of their true masses. For a metabolite ion mass of 400 Da, measurements accurate to ± 0.004 Da or better are common with this approach. Nearly all observed ions are derived from molecules that are mixtures of different combinations of naturally occurring stable isotopes. Common practice calls for reporting masses of monoisotopic ions, more specifically, the ions corresponding to only the most abundant isotopes (e.g. ^{12}C, ^{1}H, ^{16}O). It is possible for molecules of different elemental formulas to have the same nominal mass, which is the mass rounded to the nearest integer. This phenomenon arises because each element has a unique mass defect, which is the difference between the atomic mass and the nominal mass. For example, the nominal mass of ^{1}H is 1 Da, whereas the exact mass of this isotope is 1.0078. In this case, the mass defect is 0.0078 Da, or 7.8 milliDaltons (mDa). Substances that differ in their elemental formulas will have slight differences in their mass defects. As a result,

elemental formulas of compounds can often be determined from molecular mass measurements alone, providing that the mass measurement accuracy is sufficient. Additional information that supports elemental formula assignments comes from ratios of ion abundances for ions that contain naturally occurring stable isotopes such as ^{13}C and ^{34}S.

To date, both GC and LC in combination with various MS detection technologies and NMR have been employed to analyze complex mixtures of extracted metabolites. The use of GC allows separation of metabolites with high separation efficiency and sensitivity. In combination with MS, it provides very accurate, high resolution, sensitive and selective identification and quantification of chemical compounds (Fiehn 2008). In the past, GC-MS has been applied and optimized for simultaneous analyses of metabolites in many different plant species such as *Arabidopsis thaliana* (Fiehn et al. 2000; Fiehn 2006), *Solanum tuberosum* (Roessner et al. 2000), and *Cucurbita maxima* (Fiehn 2003). Despite the many advantages of GC/MS, GC can only be used for low molecular weight (<1000 Da) compounds, that are either volatile at relatively low temperatures or can be chemically transformed into volatile derivatives. Thus, for a comprehensive analysis of a greater range of plant metabolites, LC/MS offers more advantages. First, compounds do not have to be chemically altered by derivatization prior to analysis and second, highly polar, thermo-unstable and high-molecular weight compounds, such as oligosaccharides, glycoconjugates, and complex lipids, can be separated and quantified (Roessner 2007).

1.5.3 Challenges of metabolomics

The biggest challenge facing researchers wishing to perform metabolomic analyses lies in the identification of all the metabolites. Nowadays the significant challenge for plant metabolomics is the lack of a fully described and annotated metabolome for any plant species. The magnitude of such tasks is immense; it has been estimated that the plant kingdom produces 90,000-200,000 metabolites (Fiehn 2002), but these estimates are based on speculation. *Arabidopsis,* with a relatively simple secondary metabolism, has been estimated to produce more than 5,000 metabolites (Roessner et al. 2001). Because of the diverse chemical nature of metabolites and the lack of schemes that can predict metabolites structures from genetic information, the analysis of the metabolome is particularly challenging. Typical efforts have rarely identified more than 100 metabolites in a single analysis. The study of CBF cold response genes and metabolome in cold adaptation in *Arabidopsis* (Cook et al. 2004) is a strong example of the successes and limitations of GC/MS metabolite profiling. In this study, 434 metabolites were detected and 325 (75%) were found to increase in Arabidopsis plants in response to low temperature. However, the large majority (84 of 114) of metabolites increasing by > 5 fold remained unidentified despite the availability of libraries of metabolite mass spectra.

It is frequently the case that metabolites that are novel in stressed plants or specific mutants are present in tiny quantities that often preclude structure elucidation by NMR spectroscopy or x-ray crystallography. For this reason, information from mass spectra often provides the only information upon which metabolites can be identified. Perhaps the most important information obtained from a metabolite mass spectrum is the molecular mass of the compound. For LC/MS analyses, metabolite ionization is a gentle process. Most mass spectra contain only molecular mass information, with minimal

formation of fragment ions that are common in GC/MS analyses. Additional information about structure can be generated by inducing the molecular ions to fragment. This is accomplished using collision induced dissociation (CID), in which the molecular ion collides with gas molecules, and the collision leads to formation of fragment ions whose masses are also measured. This information can be used to construct a proposed chemical structure for the metabolite. Since CID spectrum libraries are limited and are not standardized, metabolite identification is a time- and labor-intensive process.

Although there are growing discussions and numbers of publications on the processing of metabolomics in biology, there are few examples of open-ended metabolomic approaches leading to novel biological insights. Most plant biologists are still using targeted metabolite profiling to discover functions for genes and their regulation (Gu et al., 2009). Furthermore, most metabolomic studies on plants have used plants grown under control environmental conditions using wild type plants, and have measured only a limited number of metabolite classes. There are great opportunities for research that employs metabolomic approaches for investigation of responses of wild type and mutant plants to various stresses including pathogen infection.

The second great challenge posed in metabolome analysis involves finding improved methods for interpretation of complex metabolite data sets that will allow for robust comparisons of metabolite profiles. One may anticipate that important changes in metabolite profiles may involve appearance of novel metabolites at low levels, and these are easily obscured by more abundant metabolites. Statistical evaluation and visualization software tools have been developed recently and enable researchers to identify those metabolites that exhibit significant differences between treatments or genotypes. These

tools enable investigators to recognize those metabolites that are highest priority for identifying, but confirmation of structure requires convincing evidence of structure. In addition, knowledge of metabolite structure often fails to reveal the substance's biological function. Linking changes in metabolite levels to meaningful biological interpretation often requires challenging follow-up experiments.

Most early metabolite profiling studies of plants demonstrated the capabilities of metabolomic methodologies in the form of distinguishing different plant species or tissues. Before 2006, most published reports largely demonstrated the capabilities of the technology for distinguishing plants or tissues without using metabolite profiles for hypothesis generation or testing. More exciting applications have appeared during the past five years. Profiling of metabolites in transgenic plants using GC/MS (Cook, Fowler et al. 2004) revealed functions of the CBF cold response pathway genes in regulating levels of amino acids, carbohydrates, and organic acids in cold stress. A somewhat different approach, used by Georg Jander and colleagues (Jander et al. 2004), employed high-throughput LC/MS/MS profiling of amino acids in thousands of mutant Arabidopsis lines to discover a role for threonine aldolase in controlling seed amino acid levels. Both targeted and nontargeted metabolite analyses were used by Saito and coworkers (Tohge et al. 2005) to generate results that documented participation of two genes as glycosyltransferases in anthocyanin biosynthesis.

Another challenge faced during the application of metabolite profiling results because the inherent variation in biological behavior usually exceeds analytical variance in metabolite measurement. It has been estimated that the biological variability exceeds analytical variability of gas chromatography-mass spectrometry by a factor of ten

(Roessner et al. 2000; Sumner et al. 2003). Quality control is important for any analysis, as it allows analysts to judge the reliability of analytical measurements. Some groups have reported spending comparable efforts on analysis of quality control samples as on biological extracts (Fiehn et al. 2008).

Absolute quantification of all metabolites presents enormous challenges. A shortage of reference standards makes comprehensive and absolute quantification of phytochemicals in plant extracts improbable (Bednarek and Osbourn 2009). As a result, most metabolite profiling efforts are usually limited to relative quantitative analyses, reporting analytical signals relative to an internal standard or relative to the sum of all metabolite signals. Phenotypes are thus defined in terms of differences in relative levels of individual metabolites between treatments, time points, or genotypes.

1.5.4 Introduction to my project

Metabolite profiling provides a powerful link between genotypes and phenotypes. LC/MS is just emerging as a tool for plant metabolite profiling, and is being used in this study as a primary screening method to determine changes in plant metabolite profiles associated with different genotypes or treatments in *Arabidopsis*. Such changes would provide powerful evidence for functions of specific genes or mutations. Specifically, I have used liquid chromatography coupled to electrospray ionization time-of-flight mass spectrometry (ESI-TOF-MS) for rapid identification and measurement of metabolites with high mass accuracy (to ~ 5 ppm). This analytical tool can measure hundreds of metabolites in a single analysis, and can discriminate between metabolites that have the same integer mass (and slightly different molecular masses) but different elemental

formulas. Under biotic and abiotic stress, plants may produce a wide variety of secondary metabolites that may differ both qualitatively (presence or absence) or quantitatively relative to control plants.

The impetus for this research came from preliminary studies performed by graduate student John Hanley in the Jones laboratory, then at Penn State University (Hanley JC, PhD Dissertation, 2005). His tentative metabolite identifications, performed without the benefit of high resolution mass spectrometry, suggested that O-methyltransferases (OMTs) involved in polyphenol metabolism might be induced in Arabidopsis leaves upon *P. syringae* infection, and to a lesser extent, following herbivory by two insects. To explore the functions of OMTs during pathogen infection, the studies described in Chapter 2 report assessment of leaf metabolic phenotypes in infected and control mutant and wild type Arabidopsis using LC/TOF MS.

The first step for analyzing metabolite profile data involves extraction and organization of LC/MS data and determination of whether there are meaningful statistical changes in metabolite levels. In this study, automated processing of LC/MS data using Masslynx software was used for chromatographic peak detection, alignment, and integration. Statistical analyses using Principal Component Analysis (PCA), Partial Least Squares for Discriminant Analysis (PLS-DA), Orthogonal Partial Least Squares (OPLS), and two-way ANOVA were used to aid recognition of those metabolites most affected by genetic or environmental changes (Eriksson et al. 2004; Trygg et al. 2007). PCA is an unsupervised data reduction technique that is used to reduce the dimensionality of a multi-dimensional dataset while retaining the characteristics of the dataset that contribute most to data variance. PLS-DA is a supervised regression extension of PCA that takes

advantage of class information to attempt to maximize the separation between groups of observations. OPLS is a modification of the usual PLS method that filters out variation that is not directly related to the response.

Identification of novel metabolites relevant to pathogen stress represents a central aspect of this work, but metabolite identification remains a challenging activity. Ten years ago, a summary of *A. thaliana* metabolism reported 36 secondary metabolites from four major classes (Chapple et al. 1994). This list now includes more than 170 secondary metabolites from seven major classes (D'Auria and Gershenzon 2005), and this still represents only a small fraction (about 3%) of expected *Arabidopsis* metabolites. Many important metabolites and novel pathways still need to be identified and studied. The research described in this dissertation will help expand understanding of *Arabidopsis* secondary metabolism and develop the research tools for analyzing metabolic networks, cross-talk between different pathways (Bostock 1999), and identifying novel pathways. Furthermore, pathogens and other stresses can induce extensive changes in gene expression and thereby reprogramming of cellular metabolism. The roles of and connections between these responses remain mysterious to a great extent. It is often not clear which defense reactions are fundamental to plant survival and which are simply an effect of the perturbation of an interconnected network. One promising approach to address these questions involves large-scale profiling of metabolites in mutant plants to identify genes and their functions (Last et al. 2007). In this study, I have been investigating the functions of OMT genes using metabolite profiling. It is expected this work will be helpful to determine whether OMT and plant resistance pathways are coordinately regulated or are activated by independent mechanisms.

In this study, I applied metabolite profiling to expanding functional annotation of genes to help develop a more comprehensive understanding of cellular responses to biological conditions. In Chapter 2, I used a reverse genetic approach to investigate OMT gene function using metabolite profiling to recognize genes important in leaf secondary metabolism and explore their broader biological functions under conditions of pathogen infection. In Chapter 3, a comprehensive and fast analytical method was developed to support studies of the dynamics of multiple phytohormones in wounding stress.

1.6 Research objectives

The primary purpose was to develop high-throughput LC/MS methods to measure metabolite profiles, and apply them to help us to understand gene functions and gene regulation in plant responses to wounding and pathogen stress.

CHAPTER 2

Reverse genetic investigation of functions of *O*-methyltransferases in *Arabidopsis thaliana* responses to *Pseudomonas syringae* infection using liquid chromatography/mass spectrometry for nontargeted metabolite profiling

2.1 Introduction

Discoveries of functions of plant genes hold central importance in efforts to improve global food supplies and develop biological energy resources. Investigations of gene functions have relied on two strategies known as forward genetics and reserve genetics. Both tactics are most powerful when phenotypes are described explicitly, and global phenotype profiling has emerged as a set of vital methodologies for functional genomics. Plants synthesize a huge repository of metabolites, but most conventional approaches have employed a small number of phenotypic assays that cover a limited number of biochemical pathways. Recent years have seen emergence of a research area known as metabolomics, which aims to describe the biological state of an organism by measuring the entire set of metabolites.

This dissertation presents development and application of LC/MS methods for metabolomic profiling for investigations of plant responses to wounding and pathogen stress. In the first study, LC/time-of-flight MS was used for nontargeted profiling of metabolites in leaves of wild type and *O*-methyltransferase (OMT) knockout mutants.

2.1.1 Preliminary studies in our laboratory

The impetus for this research came from preliminary studies performed by graduate student John Hanley in the Jones laboratory at Penn State University (Hanley 2005). When *Arabidopsis* plants were infected by *Pseudomonas syringae*, one of the most striking changes in metabolite profiles was a sharp decrease in the abundant metabolite sinapoyl malate (SM) and the less abundant 5-hydroxyferuloyl malate (5HFM), with concomitant increases in a metabolite with molecular mass 14 Da greater than SM. Since

this mass was consistent with methylation, and the fragmentation pattern was indicative of a malate ester, the report identified the new metabolite as 3,4,5-trimethoxycinnamoyl malate (TMCM) (Hanley 2005). The chemical structure of TMCM has the unusual trait among Arabidopsis metabolites as being methylated in the 4-position (Figure 2.1), and methylation in this position posed a potential effect on lignin formation. These enzymatic *O*-methylations are proposed to occur via catalysis by OMTs. There are 31 loci with 45 distinct gene models encoding members of the OMT family in *Arabidopsis*. Therefore, the original aim of this project was to identify which genes code for the enzyme that methylates sinapoyl malate to 3,4,5-trimethoxycinnamoyl malate.

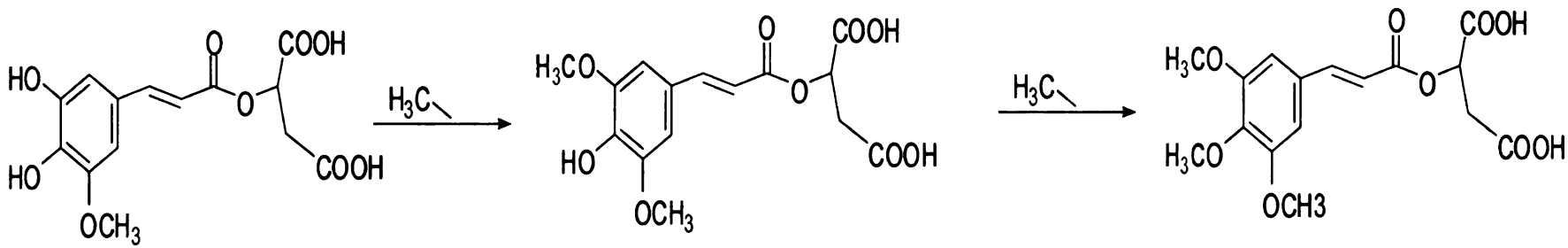

5-Hydroxyferuloyl malate(5HFM) Sinapoyl malate(SM) 3,4,5-Trimethoxycinnamoyl malate(TMCM)

Figure 2.1 Proposed *O*-methylation from 5-hydroxyferuloyl malate and sinapoyl malate to 3,4,5-trimethoxycinnamoyl malate, based on work by Hanley (Hanley 2005).

However, while my early experiments replicated detection of a metabolite with this mass that appeared following *P. syringae* infection, its assignment as TMCM was called into question as described in more detail in the Results section below. High resolution mass measurements determined the mass of the ionized metabolite to be m/z 353.1600. This experimental result disproved the identification of 3,4,5-trimethoxycinnamoyl malate ($C_{16}H_{18}O_9$) with its calculated monoisotopic ion mass of m/z 353.0873, and suggested instead a formula consistent with an oxylipin conjugate OPC:4 malate of formula $C_{18}H_{26}O_7$ with the structure shown in Figure 2.2.

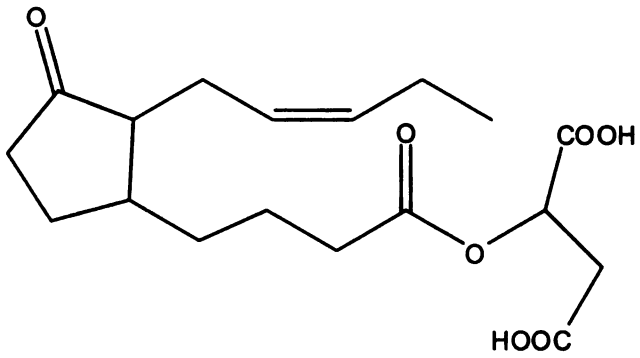

Figure 2.2 Chemical structure of OPC:4 malate ($C_{18}H_{26}O_7$) with accurate molecular mass of 354.1679.

An unexpected turn in this research came about a short time later, as *omt1* showed distinct differences in metabolite profile compared to wild type plants and showed evidence of slower development of pathogen colonization than wild-type plants. More extensive investigation of these processes is presented in the research described below.

2.1.2 Introduction to *O*-methyltransferase (OMT)

Metabolic methylation plays important roles in secondary metabolism in animals, microbes, and plants, and methylation of hydroxyl groups is catalyzed by members of a family of O-methyltransferases. *O*-methylation catalyzed by OMTs [EC 2.1.1.6.x] involves the transfer of the methyl group from *S*-adenosyl-L-methionine (SAM) to the hydroxyl group (-OH) of an acceptor molecule, with the formation of its methylated product ($-OCH_3$) and *S*-adenosyl-L-homocysteine (SAH) (Ibrahim et al. 1998). Methylation of polyphenols by OMTs is considered a critical step for several biological functions, since methylation of a phenolic hydroxyl can block glycosylation and other chemical transformations, particularly those that convert phenolic groups to phenoxy radical intermediates. For example, lignin, one of the polymeric products of the general phenylpropanoid pathway, is an abundant biopolymer that adds mechanical strength to plant tissues and is thought to be an important component of some disease resistance mechanisms. Monomeric precursors of lignin include two methylated polyphenols, sinapyl alcohol and coniferyl alcohol, which contribute syringyl and guaiacyl groups respectively. Two classes of "lignin-specific" OMTs have been found (Joshi and Chiang 1998; Burga et al. 2005). Class I consists of low molecular weight (23–27 kDa subunits), Mg^{2+}-dependent OMTs. Class I enzymes were initially identified as caffeoyl-CoA OMTs (CCoAOMTs), and these enzymes catalyze methylation involved in formation of the guaiacyl moiety of phenolic CoA esters in lignin biosynthesis. Class II enzymes are larger OMTs (38–43 kDa subunits) that methylate the phenolic hydroxyl groups of caffeic acid, caffeoyl aldehyde, and caffeoyl alcohol (COMTs) independent of Mg^{2+}, and were considered to methylate primarily 5-hydroxyconiferaldehyde residues during lignin biosynthesis (Joshi and Chiang 1998; Burga et al. 2005). COMT-deficient plants exhibit

altered lignin structures and properties. In this mutant, lignins are deficient in syringyl (S) units and contain more 5-hydroxyguaiacyl units (5-OH-G), which are S-units lacking a single methyl group. Therefore, the enzymatic activity of COMT appears to be involved in lignin S-unit biosynthesis. However, COMT1 is not a limiting enzyme for the lignin synthesis since the over-expression of poplar COMT1 in wild-type Arabidopsis did not increase the S-lignin content (Goujon et al. 2003; Do et al. 2007).

The *Arabidopsis thaliana* genome contains 31 loci that encode members of the OMT family (TAIR 2007), but only a few of these *OMT* genes have been studied so far (Zhang et al. 1997; Muzac et al. 2000; Goujon et al. 2003; Deem et al. 2006; Pontier et al. 2007). Caffeic acid *O*-methyltransferase 1 (OMT1) (At5g54160) is one of the most studied OMTs in *Arabidopsis*. OMT1 was originally thought to be a bifunctional enzyme that methylates caffeic acid and 5-hydroxyferulic acid (Zhang et al. 1997), based on high sequence similarity to COMT from other species. Transgenic studies revealed that another predominant role of COMT is the methylation of 5-hydroxyconiferaldehyde and 5-hydroxyconiferyl alcohol to sinapaldehyde and sinapyl alcohol, respectively, which are also metabolites in the lignin synthesis pathway (Goujon et al. 2003; Raes et al. 2003). In contrast in a report from the year 2000, OMT1 was cloned and reported to use the flavanol quercetin as the preferred substrate, but no significant activity was observed toward the hydroxycinnamic acids, caffeic or 5-hydroxyferulic acid (Muzac et al. 2000). More recently, it was reported that stem extracts of the OMT1 T-DNA knockout mutant exhibited only about 7% of activity toward caffeic acid and 5-hydroxyferulic acid relative to that of wild type, and stem extracts from an overexpressing line gave a 5-fold increase in activity toward these two substrates relative to wild type (Goujon et al. 2003). Since

the finding from the T-DNA mutant is inconsistent with the biochemical observations regarding OMT1 activities, a more complete assessment of the kinetic properties of OMT1 is needed to resolve these differences.

In a related study, the group of Kazuki Saito (Tohge et al. 2007) recently used targeted profiling of flavonoids using LC/MS and photodiode array detection, and transcript analysis to propose that OMT1 in *Arabidopsis* root extracts is also involved in the methylation of the flavonol quercetin to form isorhamnetin. Quercetin and its derivatives are not abundant in leaves of the Col-0 ecotype of Arabidopsis, where kaempferol derivatives, which lack a hydroxyl group in the position methylated for quercetin, are the dominant flavonols.

Minor sequence modifications are known to result in significant changes in substrate affinity for the enzymes (Gauthier et al. 1998; Wang and Pichersky 1999). As a result, enzymes may be somewhat promiscuous in their use of substrates. OMTs are involved in many different biosynthetic pathways. Thus, comparisons of sequence similarity/identity are not sufficient to determine the functions of *OMT* gene family members. To fill in the gaps between gene annotations and proven gene functions, metabolite profiles of leaves from wild-type plants and T-DNA insertion mutants were used in the research described below to provide evidence for the metabolic role of different *OMT* genes.

In Arabidopsis leaves, sinapoyl malate is one of the most abundant metabolites. This polyphenolic compound has two methyl ether groups, and presence of these groups is attributed to *OMT* genes. The reduction of sinapoyl malate levels was observed in several mutants in *Arabidopsis* phenylpropanoid pathway for lignin synthesis. An Arabidopsis mutant defective in the conversion of ferulate to 5-hydroxyferulate exhibited lower levels

of sinapoyl esters in leaves, a trait recognized by a characteristic red fluorescence under UV light, compared with blue-green color in the wild type plants (Chapple et al. 1992); (Ruegger et al. 1999; Ruegger and Chapple 2001). One mutant, *fah1-2*, was unable to produce sinapoyl malate but exhibited growth indistinguishable from wildtype under laboratory conditions. This finding demonstrated that these compounds are not essential for normal development, but a separate study (Landry et al. 1995) demonstrated that sinapoyl esters confer protection against damage by ultraviolet radiation. An Arabidopsis mutant deficient in the expression of a specific *O*-methyltransferase (*AtOMT1*) increased 5-hydroxyguaiacyl groups in lignin and decreased, but did not eliminate, levels of sinapoyl esters in leaves and stems (Goujon et al. 2003). This finding implicated more than one *O*-methyltransferase in sinapoyl malate biosynthesis. These studies preceded comprehensive metabolite profiling, and none explored the responses of mutants deficient in polyphenolics to wounding or pathogen infection.

During the course of the research described in this dissertation, it was reported that *OMT1* functions important in biosynthesis of sinapoyl esters and lignin are somewhat redundant with methylation catalyzed by caffeoyl CoA *O*-methyltransferase (CCoAOMT1). The development of homozygous double mutants was arrested at the plantlet stage, with the absence of sinapoyl malate and isorhamnetin (Do et al. 2007). This report concluded that the methylation functions of these enzymes play crucial roles in plant development.

2.1.3 Specific aims

The goal of this research project has been to develop and apply metabolite profiling approaches to learn about biochemical and biological functions of OMT genes and related metabolites in plant-pathogen interactions.

2.2 Materials and methods

2.2.1 Chemicals

All commercially available compounds and mobile phase additives were purchased from Sigma (St. Louis, MO, USA), and HPLC-grade solvents were purchased from VWR Scientific.

2.2.2 Confirmation of homozygous T-DNA insertion lines using PCR (DNA level)

The seeds of the *A. thaliana* T-DNA insertion mutant lines of At5g54160 (SALK_135290 and SALK_002373), and all other mutants, were purchased from the *Arabidopsis* Biological Resource Center (Ohio State University, Columbus, OH). All of the mutants used in this study were derived from the Col-0 ecotype.

Genomic DNA isolation

Genomic DNA was extracted as a template for PCR for amplification and isolation of the OMT gene. Around 0.5 cm^2 of leaf tissue was cut and ground in 20 µl 0.5 N aqueous NaOH and 180 µl 0.1 M Tris buffer (pH 8.0). The tissue was centrifuged (8000×g, 5 mins) and 5 µl supernatant containing genomic DNA was used for PCR.

Primer Design

SALK T-DNA primer is designed using the protocol from Salk Institute Genomic Analysis Laboratory as shown in Figure 2.3 (http://signal.salk.edu/tdnaprimers.2.html).

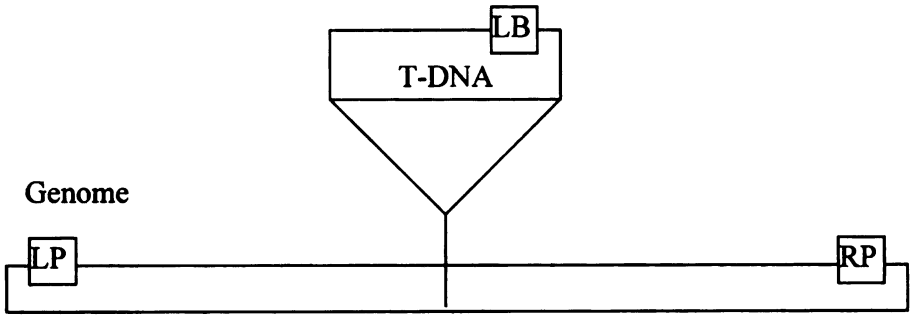

Figure 2.3 Diagram of primer design for SALK T-DNA insertion lines. LP and RP are left and right genomic primers. LB is the left T-DNA border primer.

Two sets of primers (LP + RP and LB + RP) were used in PCR. The primers were LP 5'-GAACGTGATTGATTGTAATCGG-3', RP 5'-AATTCTTGATGGTGGGATTCC-3', and LB 5'- GCGTGGACCGCTTGCTGCAACT-3'). For heterozygous T-DNA insertion, two bands in PCR were observed: one for LP+RP and the other one from RP+LB. For homozygous T-DNA insertion, only one band was observed from RP+LB.

PCR reaction

Amplification using LP and RP was performed using 1× PCR buffer without $MgCl_2$, 2 mM $MgCl_2$, 0.2 mM for each dNTP, <0.5 μg genomic DNA, 1.25 unit Taq polymerase, 0.5 μM of primers LP and RP. H_2O was added to adjust to final volume of 50 μl.

Amplification using LB and RP was performed in the same PCR reaction as described above, except 0.5 μM of LB and RP were used as primers.

PCR program was run at 94 °C for 5 min to denature, followed by 30 cycles as follows: 94 °C for 45 seconds, 53 °C for 45 seconds, and 72 °C for 80 seconds, and 72 °C for 10 min. At the end of 30 cycles, the solutions were kept at 4 °C until analysis by gel electrophoresis.

2.2.3 RT-PCR for gene expression analysis

Total RNA was extracted using RNeasy plant mini kits (QIAGEN, Valencia, CA, USA) from both wild type and mutant plants (five weeks seedlings). Primers corresponding to OMT1 cDNA sequence were designed according to the T-DNA insertion position on genomic sequence. Since the T-DNA is inserted at the second exon, one primer is set at the 5'UTR sequence (5'- CCCATCACA CAATCCTCAA AACAG-3') and the other one is set in the second exon (5'- GCATAGTT TTGGAACCGT GGAAGG-3'). Reverse transcription (RT)-PCR was performed using SuperScript™ III One-Step RT-PCR System with Platinum® Taq High Fidelity kits (Invitrogen, Carlsbad, California). The wild type will have a piece of 490 bp PCR product while *omt1* mutant is not expected to express this product.

2.2.4 Plant culture and pathogen stress

For pathogen stress treatment, 5-week-old non-bolting wild type and mutant plants (12 h light/12 h dark, 22 °C) were inoculated with *Pseudomonas syringae* DC3000 (~10^6 cfu/ml in 10 mM $MgCl_2$). About 20 µl of the bacterial suspension was inoculated with a syringe via the stomata into the lower surface of half of the leaf. Control leaves were treated similarly with a sterile solution of 10 mM $MgCl_2$. Local leaf tissues were

harvested from control and stressed plants for both the wild type and the mutant at 0 hour, 1 hour, 24 hours, 48 hours, and 72 hours after inoculation. Five biological replicates were performed.

2.2.5 Quantification of bacterial growth procedure

The classic phytopathological technique for quantifying bacterial virulence is to measure bacterial growth within the host tissue (plant leaves in this study) (Katagiri et al. 2002). A standard enumeration procedure involves pathogen inoculation (syringe injection at ~10^6 cfu/ml) followed by assaying bacterial populations present within host tissues daily. Briefly, leaves were harvested and surface sterilized with 70% ethanol for 1 min. Leaf disks were excised from leaves with a cork borer and ground with plastic pestle in a microfuge tube with 100 µl sterile distilled water. The pestle was rinsed with 900 µl of water, with the rinse being collected in the original tube such that the sample was now in a volume of 1.0 ml. An aliquot of 100 µl sample was removed and diluted in 900 µl sterile distilled water. A serial 1:10 dilution series was created for each sample by repeating this process. The samples were plated on King's medium B with antibiotics to select for the inoculated bacterial strain. The plates were placed at 28 °C for 2 days and then the colony forming units (cfu) for each dilution of each sample were counted.

2.2.6 LC/MS and LC MS/MS methods

In this study, fast LC/MS and LC MS/MS methods were developed for the identification and quantification of metabolites. The former employed high resolution time-of-flight mass spectrometry analysis with multiplexed CID, whereas the latter used a

triple quadrupole mass spectrometer to ensure that observed fragment ions were derived from specific molecular ion species.

Leaves were collected, weighed, frozen in liquid nitrogen, and extracted with methanol/0.15% aqueous formic acid (50:50 v/v) at 4 °C for 24 h. An aliquot (10 µl of 20 µM) of internal standard solution of 2 µM (final concentration) propyl 4-hydroxybenzoate was added as internal standard into 90 µl leaf extracts. 10 µl of leaf extract was injected and separated using a Thermo BetaBasic C18 column with a gradient of 0.15% aqueous formic acid (solvent A), methanol (solvent B), and acetone (solvent C) over 25 mins with a mobile phase flow rate of 0.1 ml/min. The gradient consisted of a linear increase from 5% A/95% B to 100% B in 17 min, and maintenance of 100% C for 4 min. The gradient was then adjusted to 5% A/95% B in 1 min. The column was re-equilibrated for 3 min prior to running the next sample. The column, which was maintained at 30°C, was interfaced to a Waters LCT Premier time-of-flight mass spectrometer (Waters Corporation, Milford, MA) operated using electrospray ionization. Negative mode electrospray ionization was applied for all analyses. Accurate mass data were collected using multiplexed Collision Induced Dissociation (CID) acquisition through modulation of the Aperture 1 potential. Spectra were acquired in quasi-simultaneous acquisition with five different CID conditions (10, 30, 50, 70, and 90 volts) in a single analysis to generate fragmentation patterns useful for metabolite identification. Peak integration and alignment were performed using Markerlynx and Quanlynx from Masslynx 4.1 software.

Additional support for metabolite identifications was generated using LC-MS/MS using a Quattro Premier XE mass spectrometer, employing LC gradients similar to those described above.

2.2.6.1 Identification of secondary metabolites

Leaf metabolites were identified based on accurate molecular masses, fragment ion masses, isotopic patterns of naturally occurring stable isotopes, and mass defects. An example is shown in Figure 2.4 about how accurate mass measurement was used to help identify a secondary metabolite.

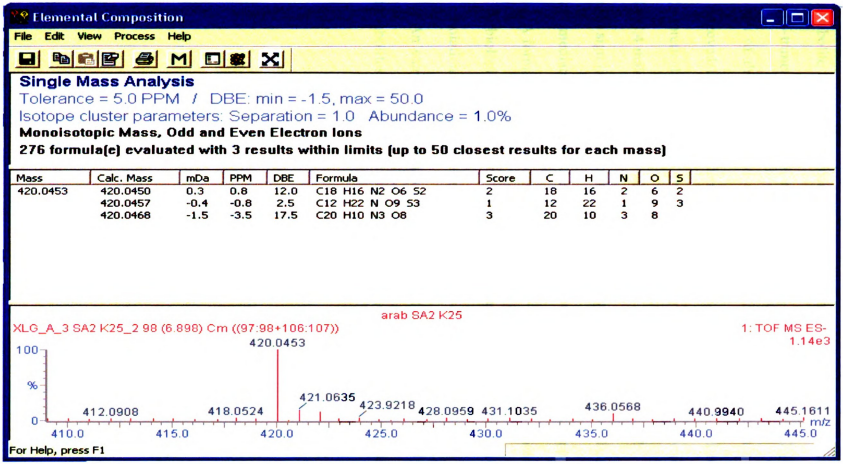

Figure 2.4 Identification of 4-methylthiobutyl glucosinolate ($C_{12}H_{23}NO_9S_3$) by accurate mass measurement. High mass accuracy was achieved using a LockSpray accessory which allows comparisons of metabolite masses with a reference compound that is continuously infused into the mass spectrometer. The high mass accuracy limits the range of possible elemental compositions corresponding to an ion's measured mass. In this case, the measured mass for the $[M-H]^-$ ion (m/z 420.0453) differs from the calculated value (m/z 420.0457) by only 0.8 ppm.

An example to demonstrate the importance of accurate mass measurement for metabolite identification comes from my correction of the previous identification of 3,4,5-trimethoxycinnamoyl malate ($C_{16}H_{18}O_9$) to OPC:4 malate ($C_{18}H_{26}O_7$). Measured mass of this deprotonated compound in negative ion mode is m/z 353.1610, which disproved the previous identification of 3,4,5-trimethoxycinnamoyl malate ($C_{16}H_{18}O_9$) (theoretical m/z 353.0873 for $[M-H]^-$), but suggested instead a new oxylipin conjugate OPC:4 malate ($C_{18}H_{26}O_7$) with theoretical m/z 353.1600. (Figure 2.2). This finding may hold significance to jasmonate signaling during pathogen infection because OPC:4 is an intermediate in JA biosynthesis. Its conjugation to malate presents a competing pathway to JA formation and a potential mechanism for sequestration of a potential JA precursor. The biological properties of OPC:4 malate have yet to be established, and await synthesis or isolation of sufficient quantities of this compound.

An example is shown in Figure 2.5 about how our laboratory identifies secondary metabolites using multiplexed in-source collision induced dissociation (CID) in LC/MS.

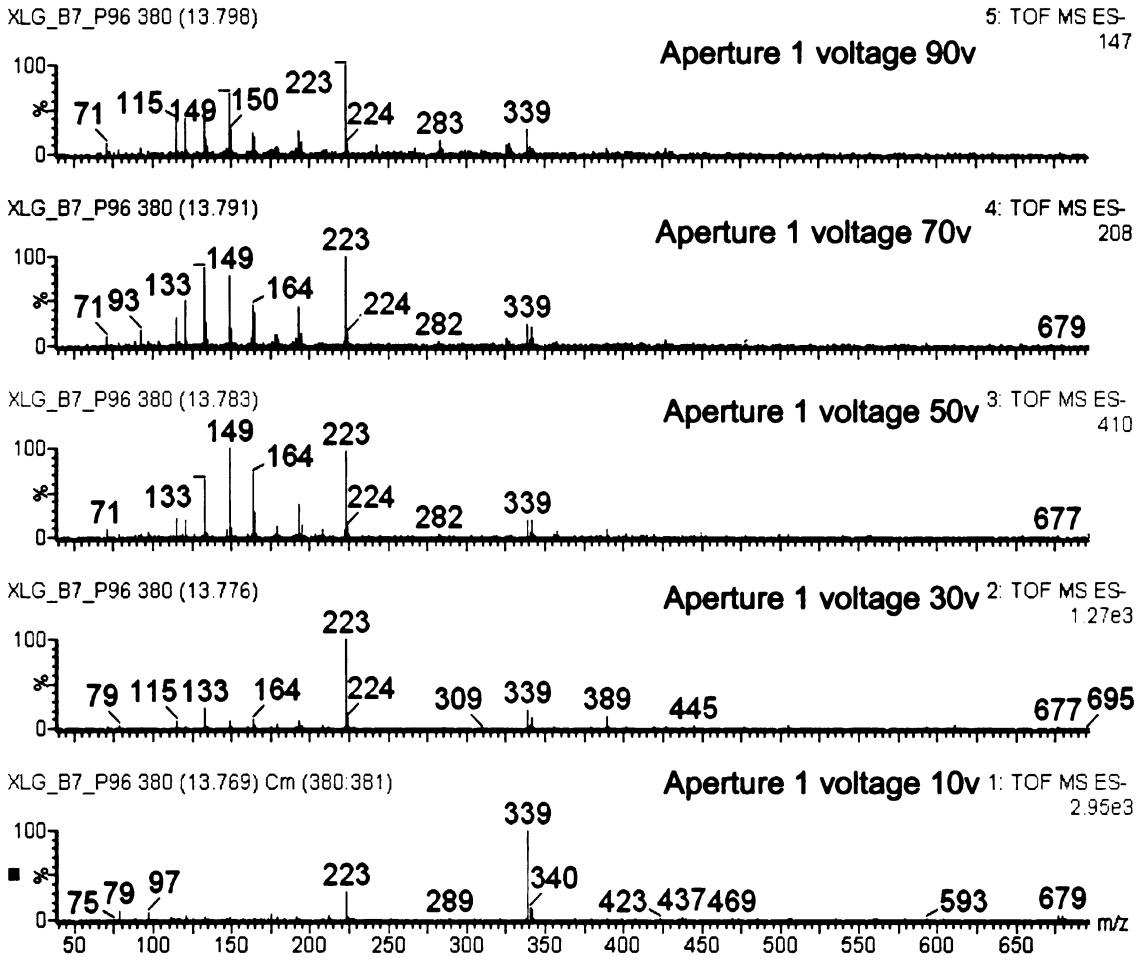

Figure 2.5 Identification of sinapoyl malate ($C_{15}H_{16}O_9$) based upon fragment ions from multiplexed CID. Five different functions were used to generate these spectra:
Function 1: Cone voltage 40v; Aperture 1 voltage 10v
Function 2: Cone voltage 40v; Aperture 1 voltage 30v
Function 3: Cone voltage 40v; Aperture 1 voltage 50v
Function 4: Cone voltage 40v; Aperture 1 voltage 70v
Function 5: Cone voltage 40v; Aperture 1 voltage 90v

The major fragments are observed at m/z 223 and 133. The assignments of these fragments are shown in the following fragmentation reactions (Figure 2.6).

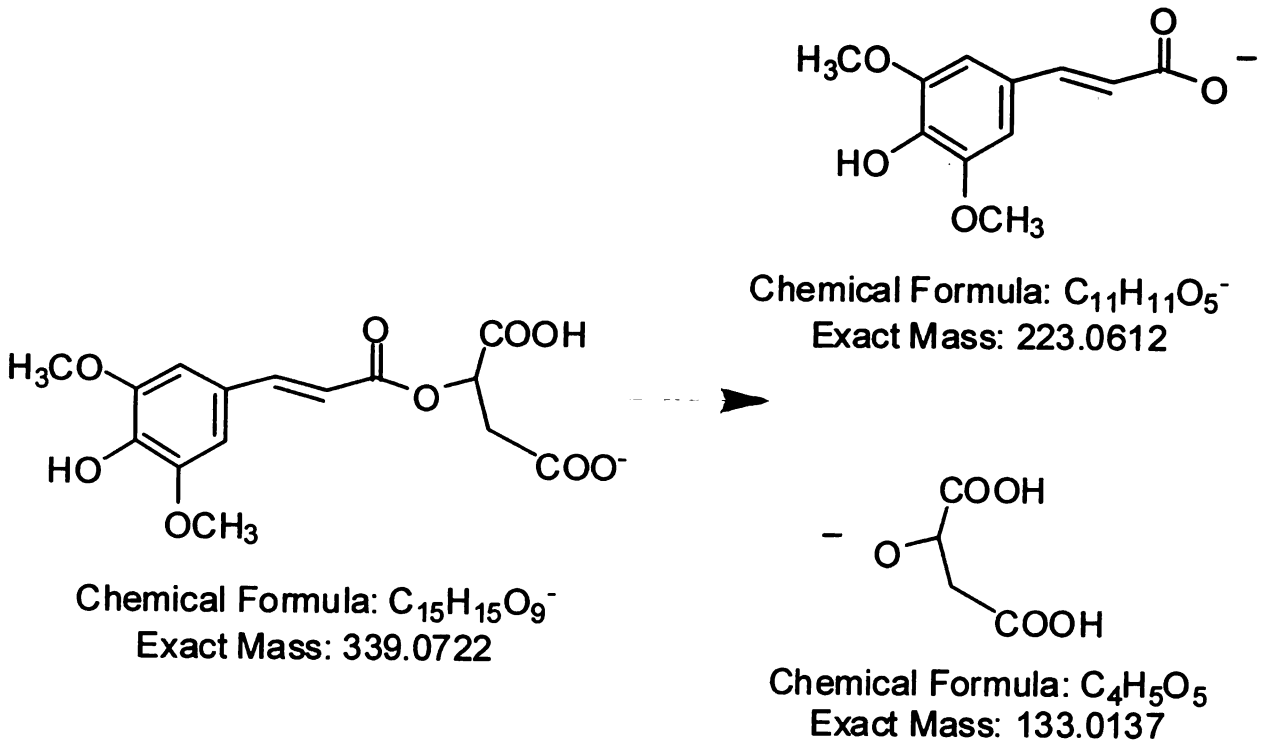

Figure 2.6 Fragmentation reactions for sinapoyl malate ($C_{15}H_{16}O_9$) in negative ion mass spectra.

Some characteristic fragment ions can be used for identifying compounds with common functional groups. For example, the following fragment ions can help the analyst recognize the presence of specific classes of metabolites: m/z 97 for glucosinolates (fragment ion of the sulfate group HSO_4^-) or phosphorylated metabolites (as $H_2PO_4^-$), m/z 291 (deprotonated OPDA anion) for conjugates of the oxylipin OPDA, and m/z 306 (deprotonated glutathione) for various glutathione conjugates. Metabolite structures can also be assigned through the assistance of fragmentation through loss of group-specific neutral fragments.

2.2.6.2 Quantification of secondary metabolites

Metabolite levels were normalized to the integrated peak area for a constant amount (2 μM) of added internal standard propyl 4-hydroxybenzoate, then normalized to fresh leaf weight. Such normalization is essential for relative quantification, because measurements of absolute amounts were not possible owing to the unavailability of authentic metabolite standards. Here is an example (Figure 2.7) to show how to quantify a secondary metabolite 5-hydroxyferuloyl malate (5HFM).

Figure 2.7 Relative quantification of 5-hydroxyferuloyl malate (5HFM) in two leaf extracts.
Fgure A: ES- total ion chromatogram (TIC) of metabolites in leaf tissue extract from *omt1* mutant (Ma1, upper TIC) and wild type plants (Wa1, lower TIC). 5-Hydroxyferuloyl malate (5HFM) appeared at a retention time of 5.86 min at m/z 325. Sinapoyl malate (SM) appeared at a retention time of 6.12 min at m/z 339.
Figure B: ES- extracted ion chromatogram (XIC) of 5HFM with m/z 325 and internal standard propyl 4-hydroxybenzoate with m/z 179 from OMT mutant (Ma1, upper XIC) and wild type plants (Wa1, lower XIC). In the upper XIC, 5.86 is the retention time. 325 is the mass to charge ratio (m/z), and 3384 is the integrated peak area for m/z 325. Integrated peak area under an XIC peak is a measure of the amount of metabolite. Relative quantification of 5HFM is determined by peak area ratio of 5HFM (m/z 325) to standard propyl 4-hydroxybenzoate (m/z 179), and this value is then divided by the fresh leaf weight. 5HFM is accumulated in OMT(At5g54160) mutant plants (Ma1 sample, the upper XIC).

A

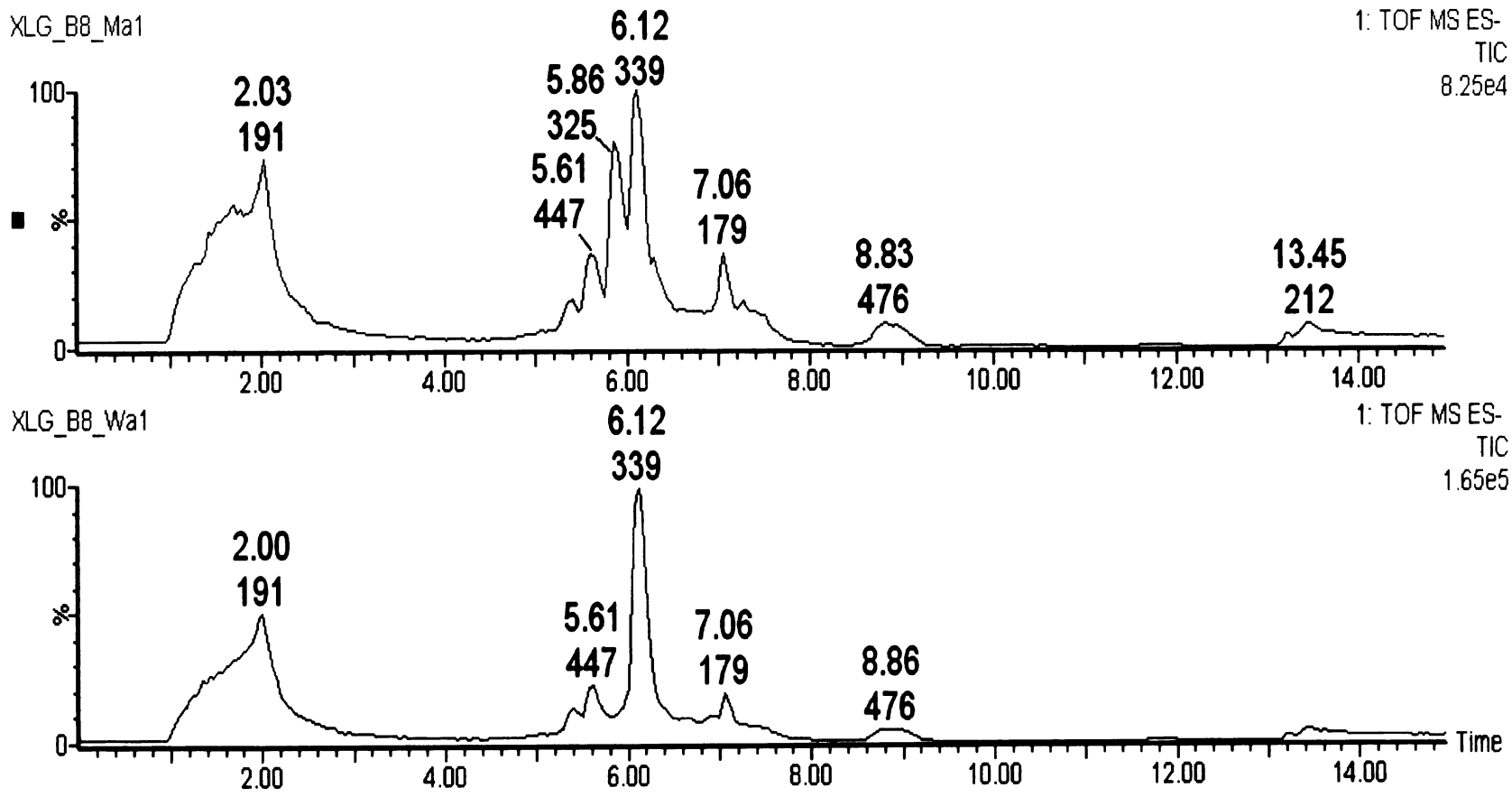
XLG_B8_Ma1
1: TOF MS ES-
TIC
8.25e4
100
%
0
2.03
191
5.86
325
6.12
339
5.61
447
7.06
179
8.83
476
13.45
212
2.00
4.00
6.00
8.00
10.00
12.00
14.00
XLG_B8_Wa1
1: TOF MS ES-
TIC
1.65e5
100
%
0
2.00
191
6.12
339
5.61
447
7.06
179
8.86
476
Time
2.00
4.00
6.00
8.00
10.00
12.00
14.00

Figure 2.7 continued

B

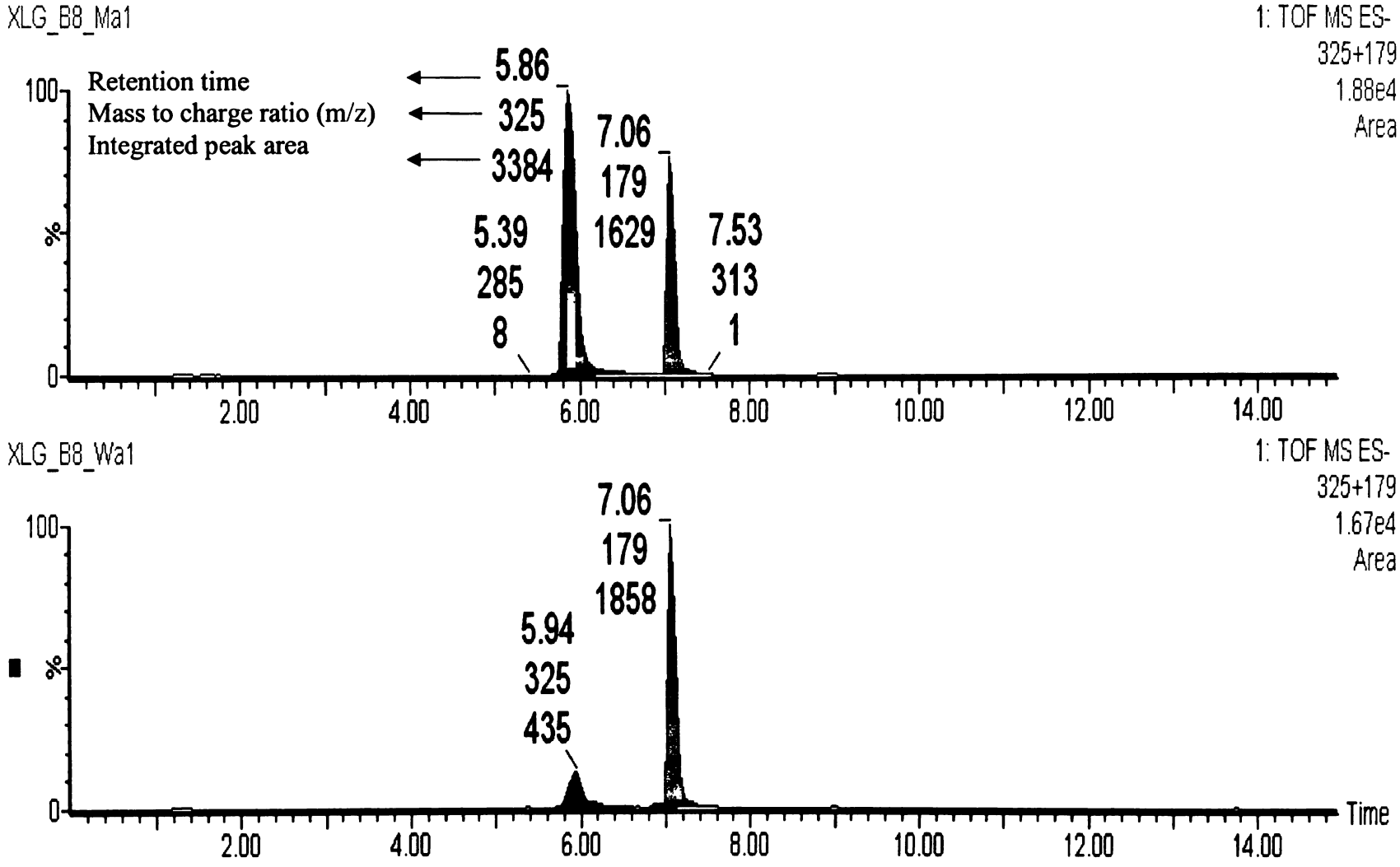

Automatic peak measurement and alignment were performed using Markerlynx from Masslynx 4.1 software. The integrated peak area values (without scaling) were exported, then normalized to peak area of internal standard propyl 4-hydroxybenzoate and fresh leaf weight.

By using LC/MS analyses performed on the Waters LCT Premier instrument, multiplexed collision induced dissociation (CID) with accurate mass (<5 ppm) was used to collect the molecular ions and fragment ions together in a single analysis using experimental parameters common to all analyses. This approach, developed in the Jones laboratory at Michigan State University, provides a powerful tool to discover, identify, and quantify metabolites in nontargeted analyses. By using LC MS/MS with the Waters Quattro Premier triple quadrupole mass spectrometer, daughter ion MS/MS scans were used to ensure that observed fragment ions were generated by fragmentation of specific molecular ions, which helps further identify and confirm the structures of metabolites after LC separations. Daughter ion MS/MS scans were performed by selecting one specific precursor ion (the molecular ion of a selected metabolite) in the first mass analyzer and inducing it to fragment through ion-molecule collisions in the collision cell. A spectrum of the fragment ions derived from the selected molecular ion was generated by scanning the second mass analyzer, and these product ion spectra were used for annotating the structure of the metabolite. The advantage of using LC MS/MS daughter scan is that the precursor ion can be selected specifically without interference from fragment ions generated from other coeluting metabolites. For more precise quantification of target metabolites, multiple reaction monitoring (MRM) was used. This approach uses the first mass analyzer to filter all but the selected molecular ion, and the

second mass analyzer allows only a selected and characteristic fragment ion to reach the detector. This approach yields chromatograms selective for the target metabolite(s). Details regarding MRM methodology and its performance in analysis of phytohormone metabolites generated during wounding stress are discussed in Chapter 3.

2.2.7 Statistical analysis

Statistical analyses were performed on multivariate data using SIMCA-P (Umetrics, San Jose, CA, USA) for Principal Component Analysis (PCA), Orthogonal Partial Least Squares (OPLS) and Partial Least Squares for Discriminant Analysis (PLS-DA), and SAS software for two-way Analysis of Variance (ANOVA) was applied as appropriate.

2.2.8 Chemical synthesis

Chemical synthesis of 5-hydroxyferulic acid (5HF)

5-Hydroxyferulic acid was prepared by dissolving 1 g of 4,5-dihydroxy-3-methoxy-benzaldehyde with 2.9 g of diethyl malonate in 6 ml of dry pyridine and 600 µl piperidine (as a base) and allowed to sit overnight. 30 ml of ice water was added and then evaporated off using a rotary evaporator. This step was repeated once more using room temperature water to ensure the removal of pyridine. A 10:1 ratio of 10% NaOH was added to hydrolyze the ester groups, and the solution incubated for 2 days. After 2 days, the solution was acidified using 88% formic acid to a pH of 2.0-3.0 and incubated again for 3 days. The 5-HFA was then extracted using methylene chloride. Methylene chloride was evaporated under a stream of nitrogen, and product was redissolved in a 1:1 methanol/water mixture. Evidence for the structure of the 5-hydroxyferulic acid product

was confirmed using negative mode electrospray ionization mass spectrometry ($[M-H]^-$ at m/z 209).

Chemical synthesis of 5-hydroxyferuloyl malate (5HFM)

5HFM was prepared by heating 1 g of malic acid with 5 g of acetic anhydride, and then adding 25 ml of water to quench the acetylation. The mixture was then evaporated using a rotary evaporator to remove any leftover acetic acid and acetic anhydride. This was repeated using 10 ml of water. The acid was then dissolved in 150-200 ml of diethyl ether in a 500 ml three neck round bottom flask. 1 ml of H_2SO_4 was added and mixed thoroughly into the solution. The flask was placed in a dry ice bath with acetone and cooled. Isobutylene gas was charged into the flask for approximately 5 minutes or until the liquid volume increased sufficiently to guarantee that an excess amount was dissolved into the ether, while maintaining the flask at cold temperature using the dry ice bath. The flask was incubated for 2 days while maintaining the dry ice bath. The mixture was recharged with isobutylene gas if the volume visibly decreased. After 2 days, the flask was allowed to warm to room temperature, and the reaction was quenched with 25 ml of ice water and solid Na_2CO_3 was added until bubbling ceased. The water layer was removed, and 25 ml of water was again added and drawn off. The ether was evaporated to dryness using the rotary evaporator, and the di-tert butyl ester of malic acid was then re-dissolved in 50 ml of THF. Evidence to support the structure of the product was confirmed using GC/MS at the MSU Mass Spectrometry Facility.

In the next step of the synthesis, solid 5-hydroxyferulic acid was incubated with 0.25 ml of $SOCl_2$ and 2 ml of THF. Once all residues were completely dissolved, the reaction

was left at room temperature for 5-10 minutes. The di-tert-butyl malate was then added as a THF solution, and mixed thoroughly. Reaction was incubated for 3 days and then pH tested. TFA was added to hydrolyze the tert-butyl groups. Evidence for the structure of the 5-hydroxyferuloyl malate product was confirmed using negative mode electrospray ionization mass spectrometry ($[M-H]^-$ at m/z 325).

Chemical synthesis of 5HF quinone and 5HF quinone-GS

Synthesis of 5HF quinone was modified from previous methods on the synthesis of caffeic acid quinone (Fulcrand et al. 1994). One milliliter of a 10 mM 5HF solution (50% acetonitrile in water) and 1.0 ml of a 20 mM $NaIO_4$ solution (50% acetonitrile in water) with 1% acetic acid were mixed and then incubated for 10 min at room temperature. Low pH (pH < 4) was essential for this reaction and to minimize side reactions. The formation and disappearance of quinones from phenols are dependent on solvent and pH. Quinones disappear more rapidly in aqueous solution, because water could act as a nucleophile towards the quinones and produce hydroxylated adducts. The quinone is stable in the pH range 3-5 (Fulcrand et al. 1994). The product was passed through a C18 solid phase extraction cartridge which retained the product while eluting inorganic salts. Following loading on to the column, the cartridge was washed with 10%, 35%, 65%, and 100% acetonitrile respectively and eluted within 65% acetonitrile, with each fraction analyzed by mass spectrometry to determine product identity. The solution containing purified 5HF quinone was characterized using LC/MS to determine product purity, and the reaction product extracted twice into dichloromethane (v:v = 1:2). The combined lower dichloromethane layers were collected, solvent was removed by rotary evaporation, and

the residue was kept dry for storage. Confirmation of chemical structure was by electrospray ionization mass spectrometry. 5HF quinone was dissolved in dimethyl sulfoxide (DMSO) for introduction into bacterial cultures.

5HF quinone-GS was synthesized by incubating GSH with 5HF quinone. A 1 mM solution of 5HF quinone in 50% acetonitrile in water was mixed with 10 mM GSH in potassium phosphate (K_2HPO_4) buffer at pH 8 for 10 min at room temperature. The mixture was passed through a C18 solid phase extraction cartridge for purification, washed with 10%, 35%, 65%, and 100% methanol respectively. Flow injection analysis mass spectrometry showed the desired product eluted with 35% methanol. The structure and purity of the 5HF quinone-GS product was confirmed by LC/MS. The purified product was evaporated to dryness under a stream of nitrogen and finally dissolved in dimethyl sulfoxide (DMSO) for bacterial culture.

2.2.9 Cloning, Expression and Characterization of OMT1

2.2.9.1 Cloning of *OMT1* gene

The DNA encoding OMT1 was amplified from an *Arabidopsis* Columbia-0 ecotype (Col-0) cDNA library by PCR using forward primer: CATG **CCATG G**GT TCA ACG GCA GAG ACA CA (*NcoI* site in bold), and reverse primer: CCG **CTC GAG** CTT CTT GAG TAA CTC AAT AAG (*XhoI* site in bold). An extra glycine near the N-terminus and one extra leucine and glutamate near the C-terminus were created together with the C-terminal 6 X His-tag during cloning. The PCR amplification consisted of 35 cycles of denaturing at 94 °C for 45 sec, annealing at 53 °C for 1 min, and elongation at 72 °C for 1 min and 30 sec, followed by 72 °C for 10 min. The PCR products were purified by

QIAquick PCR purification kit (QIAGEN, CA, USA) and digested with NcoI and XhoI. The pLW01 expression vector (Bridges, Gruenke et al. 1998) digested with NcoI and XhoI, and ligated with the digested PCR product, was transformed into competent *E.coli* DH5α cells. Positive clones growing on LB plates containing 100 μg/ml ampicillin were picked, and plasmid DNA was isolated and sequenced.

2.2.9.2 Expression and purification of OMT1

The sequenced plasmid was transformed into expression host *E. coli* BL21 (DE3) competent cells. A single colony from a freshly-streaked selection plate was used to inoculate 100 ml of LB medium containing 100 μg /ml ampicillin and was incubated overnight at 37 °C with shaking at 200 rpm. Twenty ml of this culture was transferred into 1L of fresh LB medium containing antibiotics and the cells were grown at 37 °C to an A_{600} of 0.6-0.8. The cells were then induced by adding 0.1 mM IPTG and incubated with shaking at room temperature for 17 hours. Cells were harvested by centrifugation and stored at –80 °C.

To purify OMT1, the cell pellets were resuspended in Buffer A (50 mM sodium phosphate, 300 mM sodium chloride, 250 mM sucrose, 10% glycerol, 10 mM β-mercaptoethanol, and 0.1 mM EDTA, pH 8.0). After sonication, the crude cell extract was centrifuged at 4 °C for 20 min at 12,000 g. The supernatant was loaded onto a pre-equilibrated column containing 20 ml Ni-NTA agarose slurry. The column was washed with buffer B (50 mM sodium phosphate, 300 mM sodium chloride, 10% glycerol, 10 mM β-mercaptoethanol, and 20 mM imidazole, pH 8.0). Protein was eluted from the column using Buffer C (50 mM sodium phosphate, 300 mM sodium chloride, 10%

glycerol, 10 mM β-mercaptoethanol, and 200 mM imidazole, pH 8.0). The protein-containing fractions were pooled and concentrated to 1 ml using an Amicon 30000 MWCO ultrafilter. To further purify the OMT1, the protein was loaded onto a 1 ml Hightrap Q ion exchanger, eluted with a gradient based upon buffer D (20 mM Tris-HCl, pH 8.5) and buffer E (20 mM Tris-HCl, 1 M sodium chloride, pH 8.5) at a rate of 1 ml/min. To determine the oligomeric state of OMT1, size exclusion chromatography was performed. A Superdex 75 10/30 GL column was equilibrated with buffer F (20 mM Tris-HCl, 150 mM sodium chloride, and 10% glycerol, pH 7.5). The protein was loaded and eluted at a flow rate of 0.5 ml/min. Fractions containing homogenous OMT1 were combined and concentrated as above. Protein concentration was determined by the method of Bradford (Bradford, 1976) with bovine serum albumin as the standard. Precast NuPAGE 4-12% Bis-Tris polyacrylamide gels (Invitrogen, CA, USA) were used for SDS-PAGE. Proteins were visualized with Coomassie blue staining.

2.2.9.3 Mass spectrometry analysis of OMT1 molecular weight (MW)

The molecular weight of purified OMT1 was analyzed using positive mode electrospray ionization on a Waters LCT Premier time-of-flight mass spectrometer coupled with Shimadzu LC-20AD HPLC pumps and a SIL-5000 autosampler. Separation was performed using a Thermo BetaBasic cyano column (1 x 10 mm) with a gradient of 0.15% aqueous formic acid and 75% acetonitrile over 10 min for online desalting and elution. MassLynx data system (version 4.1) (Waters Ltd, Manchester, UK) provides instrument control, data acquisition and data processing. The protein molecular mass is

calculated based on spectrum deconvolution to a zero charge state spectrum using the MaxEnt1 algorithm.

2.2.9.4 Enzymatic assay

The activity of recombinant OMT1 was determined by measuring the decrease of substrate concentrations using LC/MS. Assays were carried out in Buffer G (100 mM Tris-HCl, 150 mM sodium chloride, pH 7.5) at 30 °C. The 500 µl reaction volume contained 1 mM SAM, various concentrations of substrate and purified enzyme (10-25 µg/ml). The reaction was stopped by adding 50 µl quench solution containing 1% formic acid in methanol: water (1:1, v/v). The control sample containing all assay components was stopped at time 0. Fifty µl was withdrawn from the reaction after 60 seconds and tranfered to autosampler vial for LC/MS analysis. The decrease of substrate concentrations and the formation of enzymatic reaction products were identified and quantified using the LCT Premier time-of-flight mass spectrometer (Waters, Milford, MA, USA). Negative mode electrospray ionization was used for all samples. Fast separation of analytes as performed by a Thermo BetaBasic C18 (1 x 150 mm, 5 µm particles) column using a gradient of 0.15% aqueous formic acid and methanol over 10 min for every substrate. Accurate mass (<5 ppm) LC/MS data were collected using multiplexed collision induced dissociation (CID) acquisition through modulation of the Aperture 1 potentials. Spectra were acquired under two different CID conditions (10 and 50 V) in a single analysis to get fragmentation information for structure confirmation. Accurate mass, fragmentation pattern, and retention time were used for identifying the substrates and products. Substrates were also quantified on the basis of integrated areas of

the peaks in extracted ion chromatograms of $[M-H]^-$ ions, using linear calibration curves generated using each standard compound for known concentrations. Peak integration and quantitative analyses were performed using Quanlynx from Masslynx 4.1 software.

2.2.9.5 Determination of kinetic properties

Substrates at different concentrations, ranging from 1 μM to 100 μM, were prepared for the determination of *Km* values of purified OMT1. LC/MS based assays were carried out with the same amount of enzyme against initial velocity of the purified enzyme. V_{max} and K_m were obtained through nonlinear curve fitting model with the Michaelis–Menten kinetics equation of $V=V_{max}*[S]/(K_m+[S])$ using Origin 7 software (OriginLab, Northampton, MA, USA).

2.2.10 Determination of antibacterial activity

The procedure is modified from previous report (Franklin et al. 2009). Both the plate and liquid media were augmented with 100 μg/ml rifampicin. For the disc diffusion assay, sterile paper discs loaded with 10 μl of two different concentrations (2 μM and 20 μM) of 5-hydroxyferulic acid quinone conjugate (5HFQ), 5-hydroxyferulic acid quinone glutathione conjugate (5HFQ-GS), 5-hydroxyferulic acid (5HFA), and sinapic acid (S) were placed onto Luria-Bertani (LB) media spread with 100 μl *P. syringae* DC3000 suspension (5×10^7 cfu/ml). DMSO was used as the negative control and H_2O_2 was used as the positive control for antibacterial activity. For each plate, 10 μl of DMSO, 10 mM H_2O_2, 2 μM and 20 μM chemicals were added to each corner on one single plate and cultured at 28 °C for 24 h. A series of different concentrations of H_2O_2 (100 mM, 10 mM,

1 mM, 0.1 mM, 0.01 mM) was loaded on one plate to see which concentration of H_2O_2 can inhibit bacterial growth successfully.

For suspension bacterial culture, 100 µl of chemicals or controls were added into 2ml media and maintained in a shaking incubator at 200 rpm at 28 °C for 12 h. After 8 h, 100 µl aliquot from each sample was serially diluted to 10^{-6} and spread on plates. The colony forming units (cfu) on each plate were counted after incubation for 24 h and percentage of viability was calculated.

2.2.11 Extraction of apoplast sap by centrifugation

The plant above ground level was cut and soaked in buffer (50 mM $NaPO_4$, 150 mM NaCl, pH 7.0). The apoplast was infiltrated with the buffer using vacuum infiltration (Katagiri et al. 2002). The plant tissue was centrifuged at 1,000 g for 15 min. Repeated centrifugation was occasionally required to remove all visible liquid from the leaves. The residual liquid removed during centrifugation contained a solution of Arabidopsis apoplast sap.

2.2.12 H_2O_2 measurement

The standard curve of H_2O_2 (0-25 µM) was made using FOX assays (Delong et al. 2002). The FOX reagent contained 90 ml MeOH (90% (v/v), 10 ml of 250 mM H_2SO_4 (10%), 88 mg BHT (4 mM final), 9.8 mg ferrous ammonium sulfate hexahydrate (250 µM final), and 7.6 mg Xylenol Orange (100 µM final). The reagent was mixed well with different concentration of H_2O_2 (0-25 µM) and measured under OD_{560nm}. A standard curve was drawn based on OD values measured. The water extracted leaf samples were

also mixed with FOX reagent and measured under OD_{560nm}. OD values were used to quantify H_2O_2 based on the standard curve.

2.3 Results and discussion

2.3.1 Identify the principal *OMT* genes responsible for phenolic metabolism in *Arabidopsis thaliana* leaves

Before exploring *OMT* gene functions in pathogen stress, *omt* mutant plants were studied to understand basic functions of OMTs without stress in this study. To identify *OMT* genes that significantly affect phenolic metabolism in *Arabidopsis*, *omt* T-DNA insertion mutants were screened using nontargeted metabolite profiling to identify differenes in metabolite profiles associated with each mutation. Sixteen different *omt* T-DNA insertion mutant plants (13 *OMT* genes), as shown in phylogenetic tree of Arabidopsis OMT family in Figure 2.8, were cultured in a growth chamber (12 h light/12 h dark, 105 $\mu E\ m^{-2}\ s^{-1}$ light, 22 °C) for five weeks. The metabolites were extracted from leaf tissues of individual plants and analyzed using LC/MS. The metabolite profiles in leaves of all mutants were compared to the metabolite profiles of wild type plants after chromatographic peak integration and retention time alignment using MarkerLynx software. Principal Component Analysis (PCA) showed that a cluster of the *omt1* (At5g54160) mutants, including both alleles tested, separated from wild type and other mutants (Figure 2.9). Therefore, OMT1, which appears to have the most profound difference of metabolite profiles compared to wild type plants, was chosen for further study.

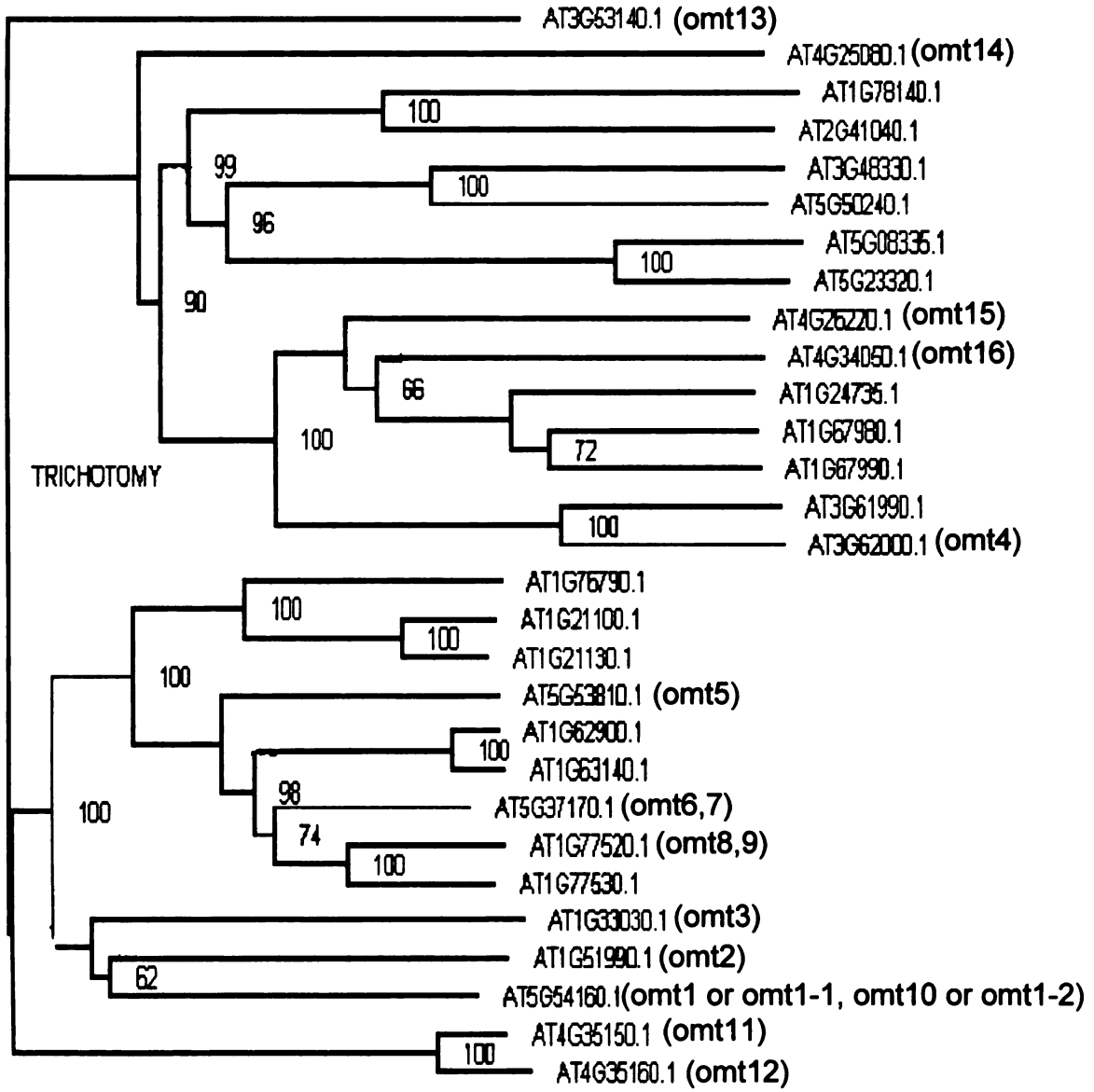

Figure 2.8 Phylogenetic tree with annotation of the 16 *OMT* T-DNA insertion mutant lines with 13 *omt* mutant genes in the phylogenetic tree of Arabidopsis OMT family.

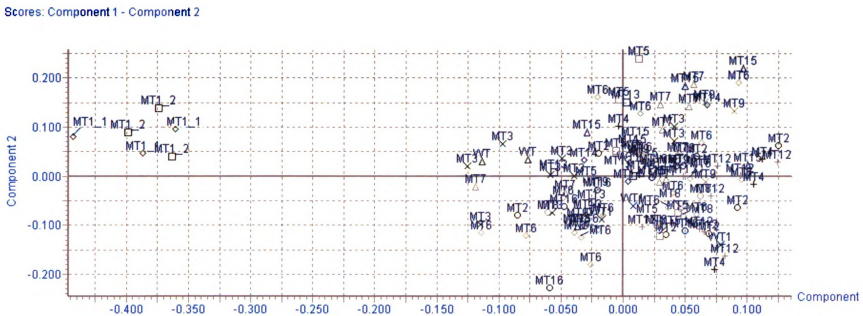

Figure 2.9 PCA scores plot of metabolite data from wild type (WT) and 16 *omt* T-DNA insertion mutants (MT) leaves measured using LC/MS, and showing the first two principal components. The *omt1* mutant plants cluster toward the left side of the graph, separated from wild type and all other mutants. Two insertion mutant alleles of *omt1* mutant were used. The *omt1* insertion mutant allele of At5g54160 (SALK_135290) is marked by MT1_1 and At5g54160 (SALK_002373) is marked by MT1_2.

2.3.2 Confirmation of homozygous T-DNA insertion lines using PCR, RT-PCR, and sequencing

Genomic DNA (as the template) extracted from the leaves of *A. thaliana* T-DNA insertion mutant line of At5g54160 (SALK_135290) was subjected to PCR using specific primers (primer design is shown in Method 2.2.2). PCR products were separated on 1.2% agarose gel (Figure 2.10). Only one band for PCR products (~ 500 bp) amplified using primers of RP and LB was observed, which confirmed the homozygous T-DNA insertion of the SALK line (Figure 2.10A). By using the primers of LP and RP for the wild type, a PCR product with the size of 1091 bps (the size of *OMT1* gene) was observed (Figure 2.10B). However, for the homozygous T-DNA insertion mutant, there is no product since the normal Taq enzyme cannot amplify the template with size of more than 2 kb for *OMT1* gene with T-DNA insertion.

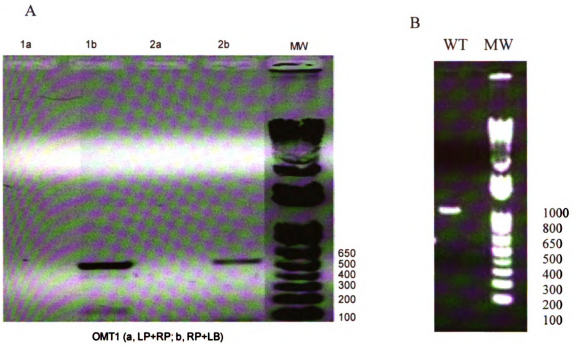

Figure 2.10 PCR products separated on 1.2% agarose gel. (A) Lane a, PCR products amplified using primers of LP and RP for the homozygous T-DNA insertion of the SALK line. Lane b, PCR products amplified using primers of RP and LB the homozygous T-DNA insertion of the SALK line. MW, 1 kb DNA ladder. (B) Lane WT, PCR products amplified using primers of LP and RP for the wild type. MW, 1 kb DNA ladder.

Total RNA extracted from the leaves was submitted to reverse-transcription (RT) PCR, so that the absence of functional transcripts was confirmed. RT-PCR products are separated on 1.2% agarose gel (Figure 2.11). The positions of primers for RT-PCR are shown in Figure 2.12. The absence of functional transcripts was confirmed since no PCR product was produced for the mutant. The product is only amplied from cDNA, but not genomic DNA since the size of the product from DNA is much larger than 448 bp (more than 1kb) with the intron.

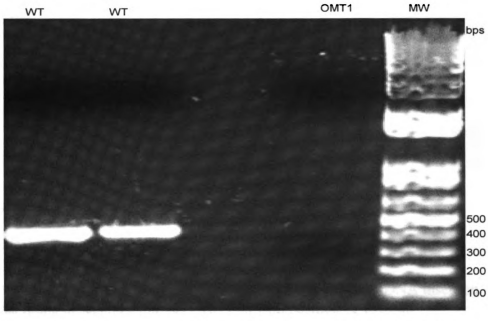

Figure 2.11 RT-PCR products separated on 1.2% agarose gel. Lane WT, PCR products (448 bp) for the wild type. Lane OMT1, no PCR product was produced for the mutant. MW, 1 kb DNA ladder.

The PCR amplification product generated using primers of LB and RP was purified with QIAquick Gel Extraction Kit (Qiagen, CA, USA) and sequenced in the Research Technology Support Facility (RTSF) at Michigan State University. The sequence was BLASTed with genomic DNA and the T-DNA insertion position was found at second exon 1299-1609 bp with position of 1319 bp, as shown in Figure 2.12.

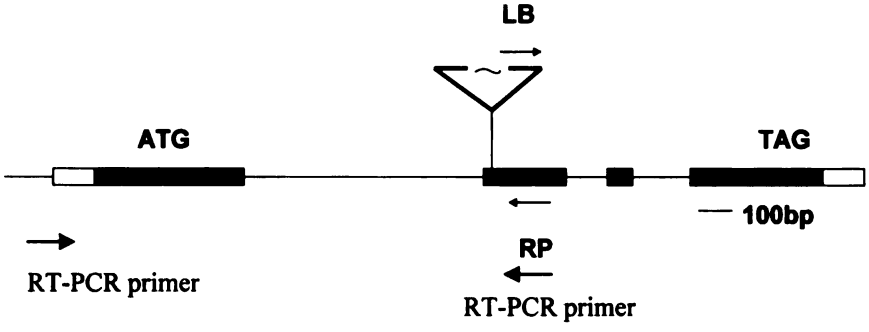

Figure 2.12 T-DNA insertion position for *omt1* gene (At5g54160). T-DNA insertion position was found at second exon 1299-1609 bp with position of 1319 bp.

2.3.3 Phenotypes of *omt* mutant compared with the wild type

When homozygous *omt1*(At5g 54160) mutant plants were cultivated under control conditions, there was no discernable morphological phenotypic difference between the wild type and mutant plants; their growth and fertility were comparable to those of wild type *Arabidopsis*. To quantify bacterial virulence, bacterial growth within the host tissue was assayed based on a bacterial pathogen enumeration procedure (Katagiri et al. 2002). Under pathogen stress, a 5-fold decrease in colony forming units was observed for the *omt1* mutant plant leaves relative to the wild type after three days infection (Figure 2.13A), and *omt1* mutant plants showed slower infection rate than the wild type (Figure 2.13B).

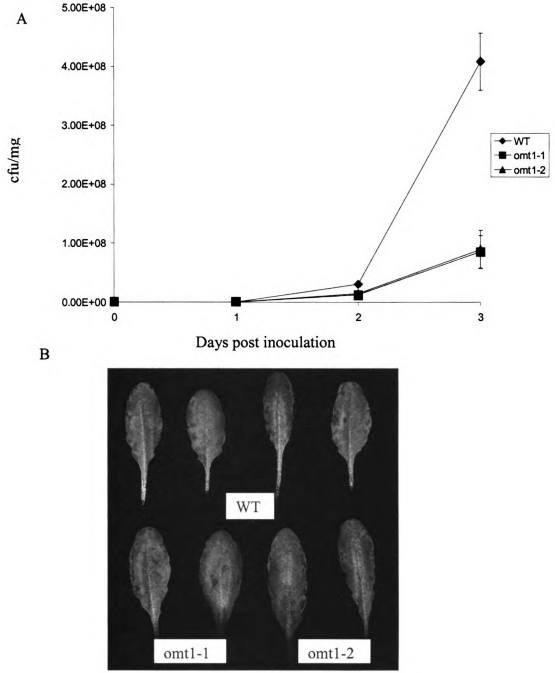

Figure 2.13 Bacterial growth on the wild type and the *omt1* mutant plant leaves. omt1-1 stands for insert line of SALK_135290 and omt1-2 stands for insert line of SALK_002373. (A) Leaves were inoculated with 1 x 10^6 cfu/mL of *P. syringae* DC3000 and *in planta* bacterial populations were determined daily. The error bars indicate the standard deviation within the 3 replicate samples for each treatment. (B) Leaf appearances at 3 day infection with *P. syringae* DC3000.

To study *OMT1* gene function in pathogen stress, employing a virulent strain of *P. syringae* offers advantages relative to use of an avirulent strain. Many resistance genes are induced in the interaction between plant and avirulent pathogen strain, but the virulent pathogen avoids activation of the plant's hypersensitive response. Therefore, this report studied the responses of *omt1* mutant with virulent pathogen stress to avoid the complexity of activation of resistance factors.

2.3.4 Comparison of *omt* mutant lines with two different mutant alleles in At5g54160

Mutant lines of two *omt1* alleles of At5g54160 (SALK_135290 and SALK_002373) showed indistinguishable phenotypes of growth, bacterial virulence, and metabolite profiles from one another. Both displayed no recognizable morphological phenotypic difference relative to wild type without stress. Both mutant alleles have similar bacterial virulence after pathogen inoculation, as shown in Figure 2.13. PCA display of metabolite profiles is shown in Figure 2.9, with the *omt1* insertion mutant line of At5g54160 (SALK_135290) marked as MT1_1 and At5g54160 (SALK_002373) marked as MT1_2 grouping together but separated from wild type and other mutants.

2.3.5 LC/MS based metabolic profiling to discover new metabolic phenotypes for gene function prediction

2.3.5.1 Data processing and statistical analysis for discovery and visualization of interesting metabolites

Automatic peak measurement and alignment were performed using Markerlynx from Masslynx 4.1 software. The integrated peak areas (after Pareto scaling) were then

exported to statistical software SIMCA-P or SAS. Statistical analyses based on Principal Component Analysis (PCA), Partial Least Squares for Discriminant Analysis (PLS-DA), Orthogonal Partial Least Squares (OPLS), and two-way ANOVA were used to aid recognition of those metabolites are most affected by genetic or environmental changes. PCA is an unsupervised data reduction technique that is used to reduce the dimensionality of a multi-dimensional dataset while retaining the characteristics of the dataset that contribute most to data variance. PLS-DA is a supervised regression extension of PCA that takes advantage of sample class information to maximize the separation between groups of observations from different sample classes. OPLS is a modification of the usual PLS method that filters out variation that is not directly related to the response (Umetrics SIMCA-P 11.0 software website).

As shown in the Figure 2.14A, PCA scores plot showed segregation of metabolite profiles of different genotypes of the wild type and the mutant. The PCA analysis is an unsupervised statistical method, and the separation between groups in the scores plot is weighted heavily on abundant metabolites. An alternative supervised method such as OPLS-DA can draw attention to less abundant metabolites whose levels provide effective discrimination between sample classes. For example, a comparison between the wild type and the mutant using OPLS-DA (Figure 2.14B) generates a 3D plot using the first three components that shows clearer separation of wild type and mutant, since OPLS uses sample class information to sharpen the separation and minimize variation that is not directly related to the response. An OPLS S-plot (Figure 2.14C) was used to highlight those metabolites whose levels most distinguish wild type and mutant plants. The S-plot is a loading plot to show the weighting coefficients of X-variable, here referring to the

influence of one single metabolite with a specific retention time and mass to charge ratio (m/z) value (such as 5.88_325.0 on the S-plot means signal with retention time of 5.88 min and m/z 325.0).

Figure 2.14 Statistical analysis of LC/MS metabolite data (using Umetrics SIMCA-P 11.0 software) from the wild type (w) and *comt1* mutant (m) leaves without stress. (A) PCA shows segregation of metabolite profiles of w and m. (B) Orthogonal partial least squares (OPLS) 3D plot is displayed using the first three components and showed better separation of classes of the wild type and mutant, since OPLS takes the advantage of class information to sharpen the separation and filters out variation that is not directly related to the response. (C) OPLS S plot was used to rank those metabolites whose levels changed most between wild type and mutant plants. The S plot is a loadings plot that shows the weighting coefficients of X-variable, here referring to the influence of one single metabolite with a specific retention time and mass/charge (m/z) value (such as 5.88_325.0 on the S plot means signal with the retention at 5.88 mins and m/z 325.0). X-axis shows the p score for covariances and y-axis shows the p(corr) score for correlations. Signals with the greatest y-axis values have high p(corr) scores which are measures of confidence in differing between the m and w samples. On the top-right side, it shows the signals which are more abundant in mutant (m) than the wild type (w). On the bottom-left side, it shows the signals that are more abundant in w than m. (D) Loading list of top 35 spectra sorted by descending p(corr) scores. The list at the right shows the spectra from the top-right side in (C). The list at the left shows the spectra from the bottom-left side in (C). Signals with m/z 325 and m/z 339, m/z 371 and m/z 385 are different in molecular mass by 14 Da (the mass change upon adding a methyl group) and are significantly different in mutant and wild type.

A

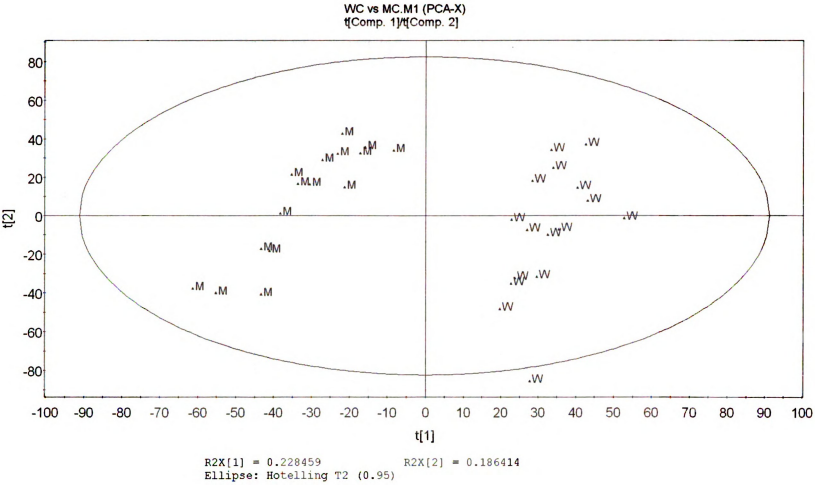
WC vs MC.M1 (PCA-X)
t[Comp. 1]/t[Comp. 2]
t[2]
t[1]
R2X[1] = 0.228459
R2X[2] = 0.186414
Ellipse: Hotelling T2 (0.95)

Figure 2.14 continued
B

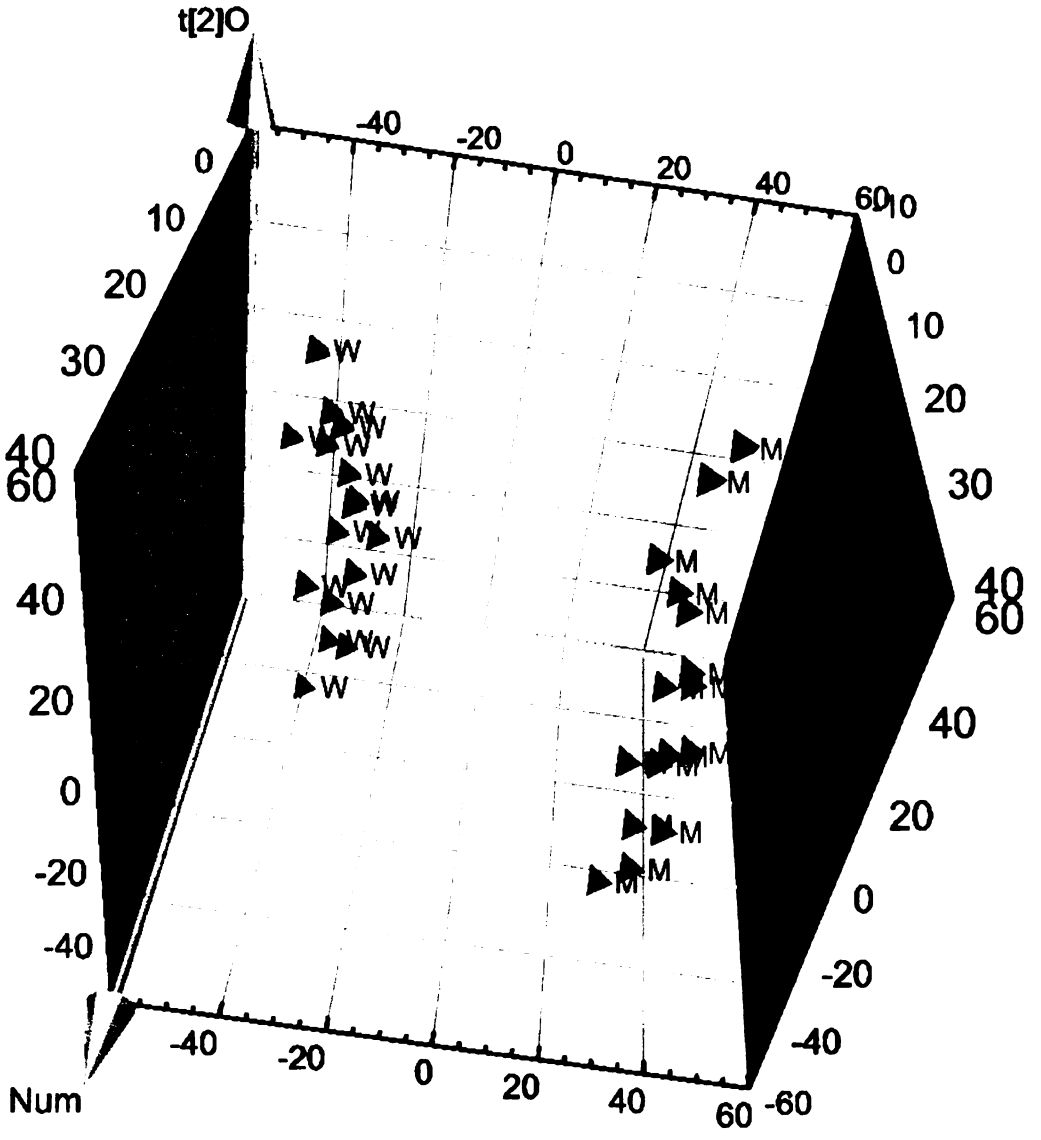

Figure 2.14 continued

C

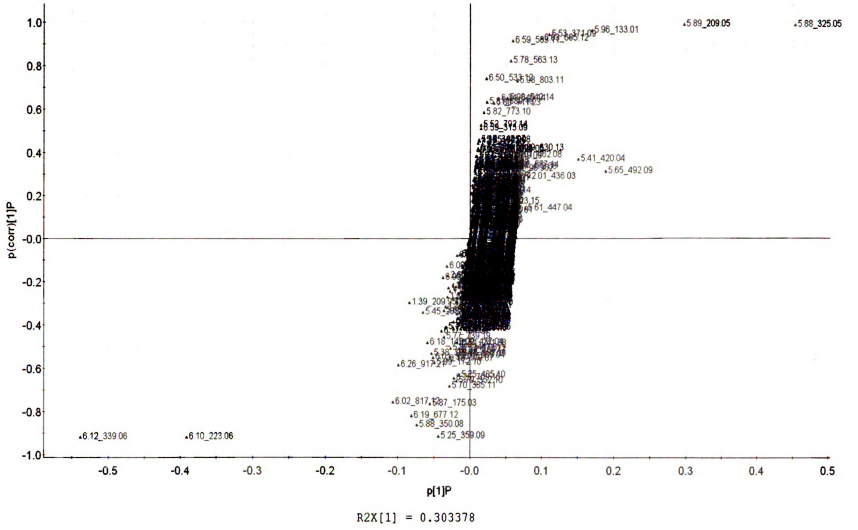

Figure 2.14 continued
D

More abundant in the wild type (w)		More abundant in mutant (m)	
Var ID (Primary)	M3.p(corr)[1]P	Var ID (Primary)	M3.p(corr)[1]P
6.12_339.0696	-0.91875	5.89_209.0506	0.987803
6.10_223.0650	-0.91824	5.88_325.0564	0.98465
5.25_359.0989	-0.91385	5.96_133.0182	0.959144
5.88_350.0869	-0.86152	5.53_371.0958	0.941066
6.19_677.1227	-0.82063	6.03_665.1243	0.923777
5.87_175.0338	-0.7639	6.59_503.1150	0.912133
6.02_817.1290	-0.75747	5.78_563.1331	0.818733
5.70_385.1152	-0.68327	6.50_533.1233	0.737952
5.79_352.1071	-0.65813	5.98_803.1141	0.72801
6.25_709.1529	-0.64474	5.98_542.1432	0.648108
5.25_405.1070	-0.63319	6.34_640.1421	0.64545
6.26_917.2190	-0.58419	5.81_889.1912	0.631097
5.99_172.1000	-0.57378	5.80_711.2322	0.626145
6.18_179.0755	-0.55862	5.82_773.1082	0.583353
6.01_556.1589	-0.55171	5.52_792.1418	0.524987
2.61_565.0407	-0.54219	6.59_313.0980	0.508955
6.47_353.0961	-0.53471	5.15_343.0710	0.457385
5.38_323.1334	-0.53214	5.25_345.0823	0.45498
5.82_389.1770	-0.5229	1.16_102.9928	0.451123
6.53_677.1285	-0.51223	7.42_801.4026	0.440745
5.87_244.0652	-0.5096	6.31_903.2083	0.418297
5.51_241.0873	-0.48678	5.89_630.1342	0.416202
6.20_437.0452	-0.48299	5.56_819.1454	0.414853
6.18_149.0265	-0.48124	5.86_323.0583	0.411867
5.77_739.1946	-0.45576	6.58_675.2071	0.40975
6.17_164.0520	-0.42867	7.43_873.4580	0.40743
7.68_836.4308	-0.42053	7.01_462.0874	0.384537
7.67_819.4406	-0.42016	5.90_649.0941	0.381557
8.71_226.0635	-0.41494	7.67_61.9897	0.38131
5.77_785.1991	-0.41151	5.77_165.0279	0.380935
7.65_854.4417	-0.41015	7.65_531.2759	0.371233
8.87_99.9298	-0.40828	5.41_420.0425	0.366732
2.67_224.0602	-0.39984	6.27_289.0948	0.362378
6.23_338.0662	-0.39349	6.47_402.0892	0.358752
5.77_775.1730	-0.39118	7.40_785.3805	0.354099

To calculate the probability (p) values that metabolite levels differ between sample classes, two-way ANOVA with mixed model and student t-test was performed using SAS software.

2.3.5.2 Interpretation of metabolite data

More than 3000 metabolite signals were detected in LC/TOF analyses of most leaf extracts. These signals were thought to come from more than 500 distinct compounds. A total of about one hundred compounds with five hundreds peaks were identified by annotation with chemical structures. Major groups are polyphenols (flavonoid and phenolic acid derivatives), lipids (oxylipins), glucosinolates, phytoalexins, and the bacterial metabolite coronatine. Metabolites showing significant differences in their levels in the various genotypes or treatments ($p<0.05$) are discussed below.

Result 1: Comparison of leaf metabolite profiles in WT and *omt* mutants without treatments (W vs M) to characterize the OMT function in absence of stress

One early question to be answered was whether the *omt* mutants showed evidence of OMT substrate accumulation or analogs of metabolites downstream from methylation events that might accumulate in the mutants. Nontargeted metabolite analysis using LC/TOF MS was performed for 16 OMT T-DNA insertion mutant lines with 13 mutant genes (Figure 2.8) to help recognize metabolites influenced by OMT activities (Figure 2.9), to establish differences between two alleles of *omt1* mutants (Figure 2.9), and to assess whether other pleiotropic effects of T-DNA mutations on metabolite profiles could be observed (Figure 2.14).

To identify putative substrates and products of OMT1, data analysis of metabolites aimed to identify metabolites whose spectra are different in molecular mass by 14 Da (the mass increase upon replacing a hydrogen with a methyl group) across sample classes. For example, a pair of signals at m/z 325 and m/z 339 was selected from the complete metabolite lists with p(corr) and p scores for each signal list after calculation using OPLS-DA, and also a prominent pair with m/z 371 and 385 (Figure 2.14D). For each pair of metabolites, the lower mass metabolite (m/z 325 and m/z 371) were more abundant in *omt1* mutants, whereas the higher mass metabolites (m/z 339 and m/z 385) as prevalent in wild type. Signals with m/z 325 and m/z 339 have the highest OPLS-DA p(corr) scores on the loading lists that exhibit the most significant differences between the wild type and mutant. Compounds with molecular ions $[M-H]^-$ of m/z 325 and m/z 339 were identified as 5-hydroxyferuloyl malate (5HFM) and its methylation product sinapoyl malate (SM), respectively, based on accurate mass measurements and fragmentation patterns. The measured mass for 5HFM is m/z 325.0564 (calculated mass is m/z 325.0560). The major fragment is m/z 209 for deprotonated 5-hydroxyferulic acid fragment ion and m/z 133 for deprotonated malate fragment ion. These fragments lend support to structure assignment as 5HFM. The measured mass for SM is m/z 339.0696 (calculated mass is m/z 339.0716), with major fragments at m/z 209 for deprotonated sinapic acid and m/z 133 for deprotonated malate. Relative quantification of 5HFM and SM in the wild type and the OMT1 mutant is shown in Figure 2.15A. In the *omt1* mutant, 5HFM showed a ten-fold increase and SM showed a three-fold reduction compared with the wild type. The continued presence of SM in the *omt1* mutant is indicative of an alternative methylation pathway. This result suggests that the loss of OMT1 activity

decreases, but does not eliminate, methylation in the 5-position that yields SM, and points to the possibility that OMT1 may play an important role in methylation of 5-hydroxyferuloyl metabolites. OMT activity toward malate esters has not previously been determined, in part due to the unavailability of malate ester standards. Proposed *O*-methylation by OMT1 from 5HFM to SM is shown in Figure 2.16A. In addition to the malate esters, compounds with molecular ions $[M-H]^-$ of m/z 371 and m/z 385 were identified as 5-hydroxyferuloyl glucose (5HFG), present in *omt1* mutants, and sinapoyl glucose (SG), abundant in wild type, respectively. Relative amount of 5HFG and SG in the wild type and the OMT1 mutant is shown in Figure 2.15B. In the *omt1* mutant, 5HFG showed a ten-fold increase and SG showed a five-fold reduction compared with the wild type. These results are consistent with a relationship between 5HFG and SG being substrate and product catalyzed by OMT1. A scheme depicting *O*-methylation by OMT1 from 5HFG to SG is also shown in Figure 2.16B.

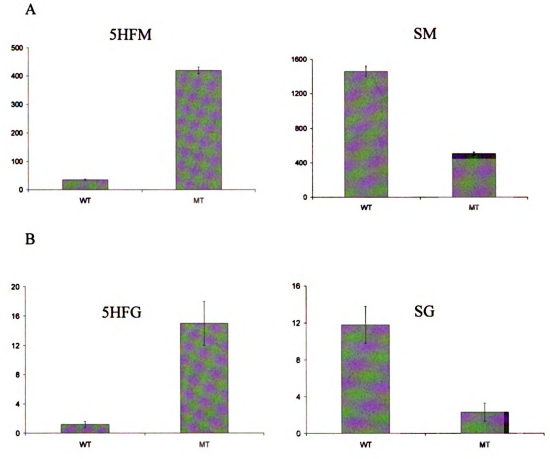

Figure 2.15 Relative quantification of (A) 5-hydroxyferuloyl malate (5FHM) and sinapoyl malate (SM) (B) 5-hydroxyferuloyl glucose (5HFG) and sinapoyl glucose (SG) in leaves of wild type (WT) and *oml1* (AT5G54160) mutant (MT) *Arabidopsis thaliana.* Y-axis is integrated XIC peak areas / mg fresh leaf weight, which is obtained by dividing the peak areas of metabolites to the internal standard propyl 4-hydroxybenzoate and normalizing to wet leaf weight. Data are means $\pm$ SE (N=8).

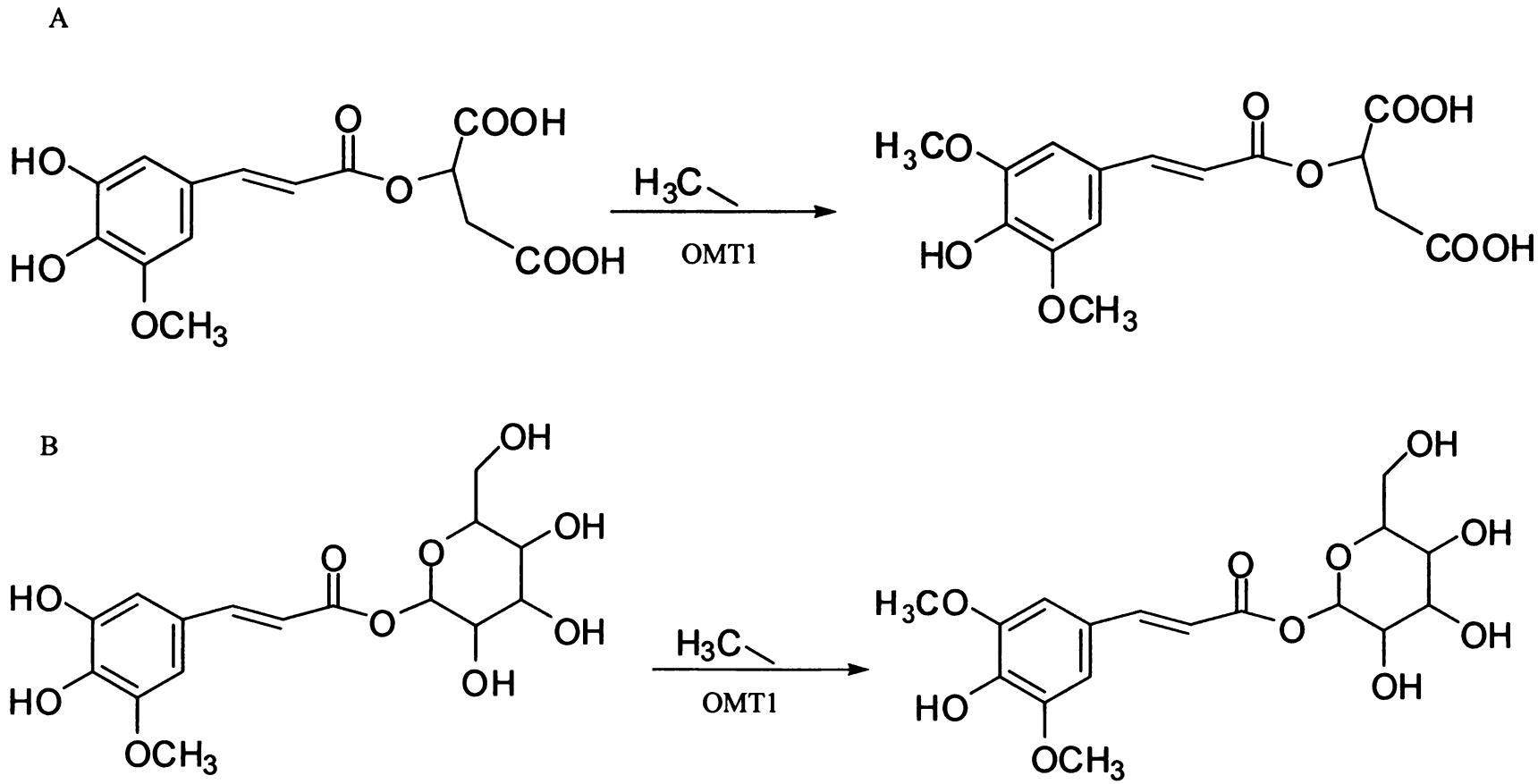

Figure 2.16 Proposed *O*-methylations catalyzed by OMT1 (A) from 5-hydroxyferuloyl malate (5HFM) to sinapoyl malate (SM) and (B) from 5-hydroxyferuloyl glucose (5HFG) to sinapoyl glucose (SG).

Biochemical characterization of OMT1: Cloning of the omt1 gene and assessment of its biochemical activities using an assortment of polyphenolic substrates

To confirm the catalytic activity of OMT1 toward various polyphenol substrates, the omt1 gene was cloned from cDNA and over-expressed in *E. coli* as a C-terminal His-tagged protein. OMT1 was purified and characterized using 12 polyphenolic substrates including the putative substrate, 5HFM, which was synthesized in our laboratory.

OMT1 was annotated as caffeic acid/5-hydroxyferulic acid OMT based on its high sequence similarity to *Populus tremuloides* CAOMT (Zhang et al. 1997), but current annotation (http://www.uniprot.org/) for accession #Q9FK25 describes it as quercetin 3-O-methyltransferase. Muzac, et al. (2000) reported that OMT1 catalyzed methylation of quercetin and myricetin when it was expressed as a recombinant protein in *E. coli*, but activities toward the hydroxycinnamic acids caffeic acid and 5-hydroxyferulic acid were reported as minimal (< 5% of activity toward quercetin). Values were not provided for V_{max} or K_m. In contrast, support for the earlier annotation came from analyses of crude enzyme activity in the stem extracts from an *omt1* mutant, which found that the activity for methylating caffeic acid and 5-hydroxyferulic acid was decreased to about 7% of the wild type for both compounds (Goujon *et al.*, 2003). This suggested that OMT1 may be involved in the catalysis of caffeic acid/5-hydroxyferulic acid. However, neither of these metabolites are known to be abundant in leaves of *Arabidopsis* ecotype Col-0. To resolve these differences regarding substrate specificity and better understand the functions of OMT1, this gene was cloned and expressed in *E. coli* and purified. The recombinant protein was used to measure catalytic activities and affinities for caffeic acid, 5-hydroxyferulic acid, and luteolin in the current study.

Cloning and over-expression of the omt1 gene

The *OMT1* gene was amplified from cDNA of *Arabidopsis* Col-0 using PCR, and was directly cloned into the 6× His-tagged pLW01 vector. *OMT1* was expressed in *E. coli* BL21 (DE3) and purified using Ni-NTA column chromatography to obtain >600 mg/L of pure protein (Fig. 2.17A). The protein was further purified using a 1 ml Hightrap Q ion exchange column. OMT1 was eluted at 15% - 20% sodium chloride and was purified to homogeneity based on SDS-PAGE (Fig. 2.17B). Using ESI-TOF MS, the mass of OMT1 was identified to be 40,436 Da (Fig. 2.18), which is consistent with that predicted for His-tagged protein (40,441 Da). Size exclusion chromatography showed elution of OMT1 as 80 ± 5 kDa, consistent with a dimeric native state (Fig. 2.19). This finding stands in contrast with the report by Muzac *et al.* (2000) that native recombinant OMT1 existed in solution as a monomer. The solved crystal structure of OMT from alfalfa suggested that it forms a dimer in solution and the dimeric arrangement is critical for its activity (Zubieta et al. 2001; Zubieta et al. 2002). The dimeric form of the protein is thought to exclude solvent from its active site, which is critical for substrate binding.

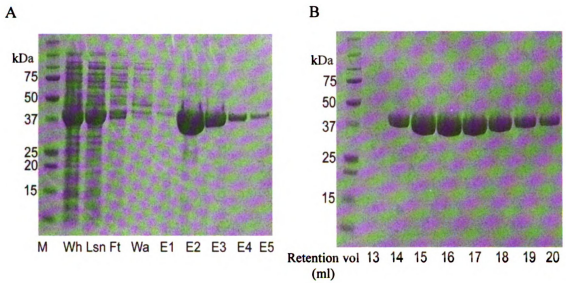

Figure 2.17 Purification of OMT1. (A) SDS-PAGE of OMT1 purified from Ni-NTA column. M, marker BioRad precision plus protein standards; Wh, whole cell lysate; Lsn, supernatant of low speed centrifugation; Ft, flow through from Ni-NTA column; Wa, wash fraction from Ni-NTA column; E1-E5, elution 1-5 from Ni-NTA column. (B) SDS-PAGE of fractions containing OMT1.

Figure 2.18 Molecular mass of OMT1 determined by ESI-TOF MS and MaxEnt1 spectrum deconvolution. (A) Electrospray ionization mass spectrum of His-tagged OMT1 showing multiple charge states. (B) Zero charge state spectrum deconvoluted using MaxEnt1 software. The experimentally determined mass of OMT1 is 40,436 Da. Separation was performed using a Thermo BetaBasic cyano column (1 x 10 mm) with a gradient of 0.15% aqueous formic acid and 75% acetonitrile over 10 min for online desalting and elution.

A

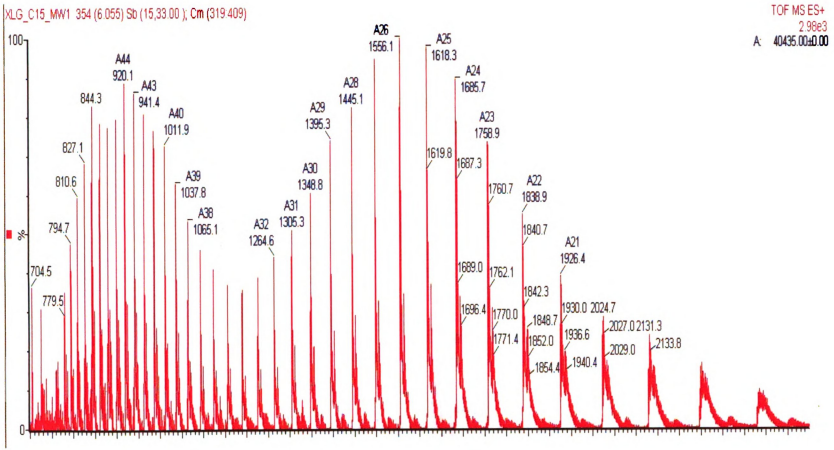
XLG_C15_MW1 354 (6.055) Sb (15,33.00); Cm (319.409)
TOF MS ES+
2.98e3
A 40435.00±0.00
100
%
0
704.5
779.5
794.7
810.6
827.1
844.3
A44
920.1
A43
941.4
A40
1011.9
A39
1037.8
A38
1065.1
A32
1264.6
A31
1305.3
A30
1348.8
A29
1395.3
A28
1445.1
A26
1556.1
A25
1618.3
1619.8
A24
1685.7
1687.3
A23
1758.9
1760.7
A22
1836.9
1840.7
1689.0
1762.1
1696.4
1770.0
1771.4
1842.3
1848.7
1852.0
1854.4
A21
1926.4
1930.0
2024.7
1936.6
2027.0
2029.0
2131.3
1940.4
2133.8

Figure 2.18 continued
B

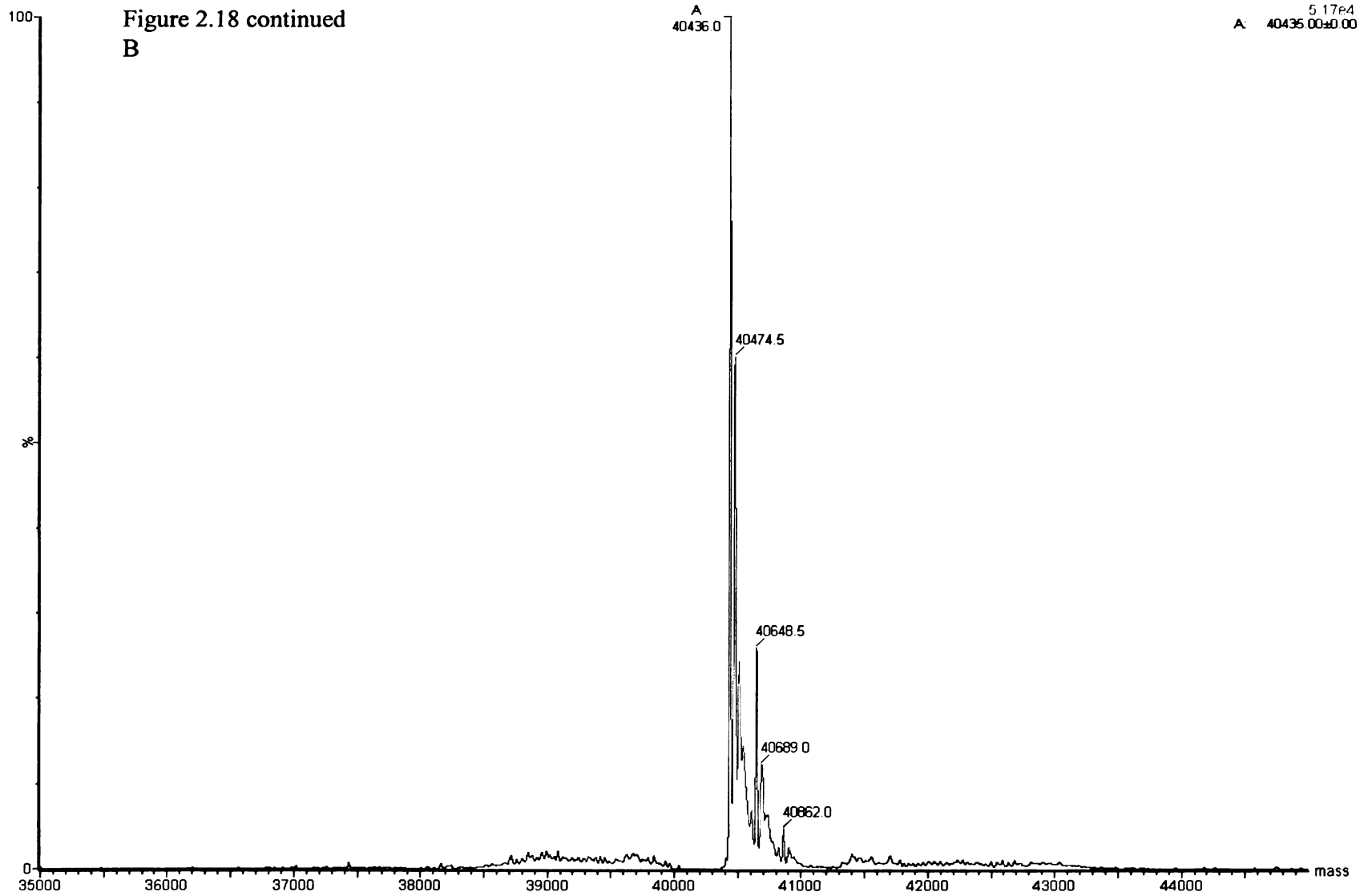

Absorbance at 280 nm (mAU)

Fig
of
Th
13

ra

D

2

p

a

o

s

a

d

g

d

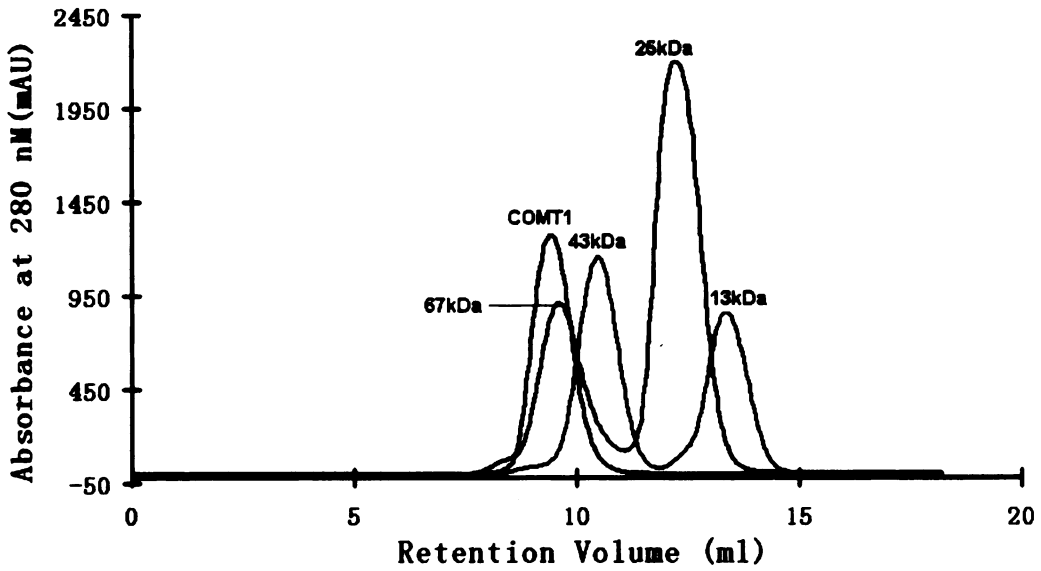

Figure 2.19 Size exclusion chromatography (with Superdex 75 column) showed elution of OMT1 as 80±5 kDa, consistent with a dimeric native state. The blue peak is OMT1. The green and red peaks are protein standards with sizes of 67 kDa, 43 kDa, 25 kDa and 13 kDa.

The optimum pH value for the activity of the enzyme was determined to be in the range of 7-8 and the enzyme is stable when stored at -80 °C with 10% glycerol and 1 mM DTT. Thirteen different putative substrates for OMT1 were screened for activity (Figure 2.20 and Table 2.1). OMT1 catalyzes the transfer of the methyl group of SAM to the 3'-position OH group of the phenolic ring of caffeic acid, 5-hydroxyferulic acid, quercetin and luteolin. The enzyme also methylates two hydroxyl groups in myricetin, the positions of the hydroxyl groups are most likely to be the 3'- and 5'-positions based on structural similarities of the phenolic acids. No methylation was detected at the 4'-position in apigenin, the 4-position in sinapic acid, or the 2-position in salicylic acid. No activity was detected toward compounds such as protocatechuic acid, gallic acid or the flavonol glycosides substituted in the 3-position as in quercetin 3-L-rhamnoside and rutin. From the structures of active substrates (Figure 2.20), it is concluded that the position of the

OH group and the size of the substrate are both critical for OMT1 activty. The enzyme also specifically methylates 3- and 5-position phenols of p-hydroxycinnamic acid derivatives (e.g. caffeic acid and 5-hydroxyferulic acid) or the 3'- and 5'-positions with C15 flavonoid skeleton (quercetin, myricetin, and luteolin), but not smaller hydroxybenzoic acids (gallic acid and protocatechuic acid) lacking the three-carbon side chain, or flavonol glycosides (quercetin 3-L-rhamnoside and rutin) which are conjugated to carbohydrate at the 3-position.

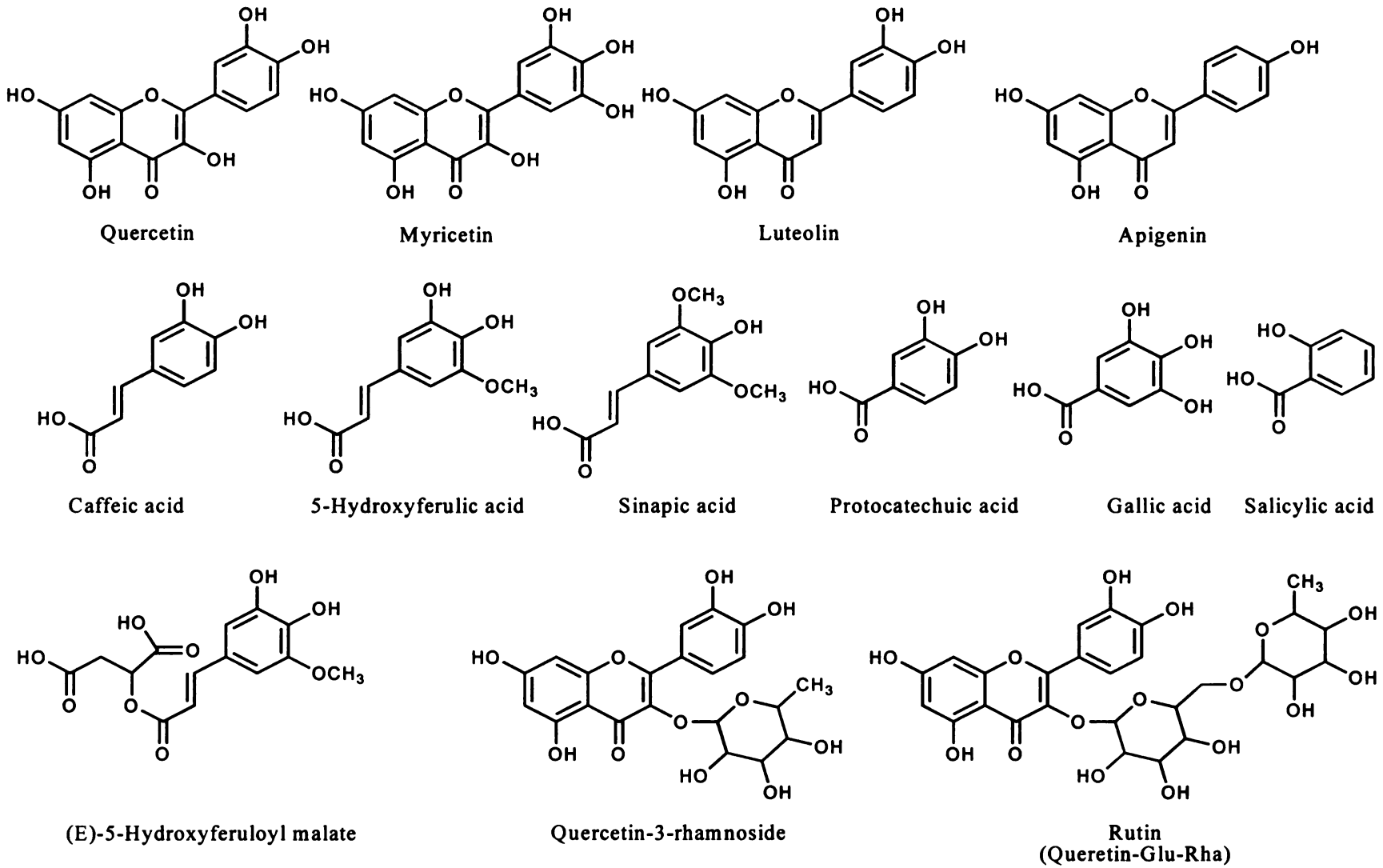

Figure 2.20 Structures of substrates tested for OMT1 activity in this study.

Label-free OMT activity assays using LC/MS

Before this study, several methods have been used to measure methyltransferase activity, but since spectroscopic differences between substrate and product are minimal, spectrophotometric assays are not normally used. One of the commonly used methods was described by Dumas *et al.* (1998) and is based on radiolabeled S-adenosylmethionine as substrate. There are two approaches that can be used – one is to measure the amount of residual SAM (by titration), but this is not sensitive when conversion of SAM is low. The second approach would physically separate radiolabeled product from SAM, and measure the radiolabel in the product. Both cases are time- and labor-consuming. A recent report described a new LC/MS based assay for detection and quantitation of methyltransferase activity, based on monitoring the conversion of S-adenosylmethionine (SAM) to S-adenosylhomocysteine (SAH) (Salyan et al. 2006). In the current study, a new assay method was developed to measure the OMT activity using LC/MS. This approach allows direct measurements of the decrease of phenolic substrates and increase of products by LC/MS. The enzymatic assay method is described in the Materials and Methods section. Briefly, the LCT Premier time-of-flight mass spectrometer was used to measure the decrease of substrate in the reaction. A Thermo Betabasic C18 column allows fast separation (10 min) of analytes with limits of detection less than 1 μM for all substrates tested. The linear range of LC/MS detection is substance-dependent, and typically ranges from about 0.1 μM to 50 μM. For enzymatic reactions involving higher concentrations, the reaction was diluted by buffer G to be in the linear range when the concentration of substrate is above 50 μM.

Taking caffeic acid as an example, after the enzyme reaction, caffeic acid substrate was identified (with m/z 179.04) and the decrease of caffeic acid was quantified by comparing integrated peak areas for the extracted ion chromatogram for m/z 179 with a calibration curve generated using standard solutions of varied concentrations. Values for V_{max} (0.795 μmol/min/mg) and K_m (27 μM) were obtained through nonlinear curve fitting model with the Michaelis–Menten kinetics equation of $V=V_{max}*[S]/(K_m+[S])$ using Origin 7 software (OriginLab, Northampton, MA, USA) (Figure 2.21).

Fig
fit
plo

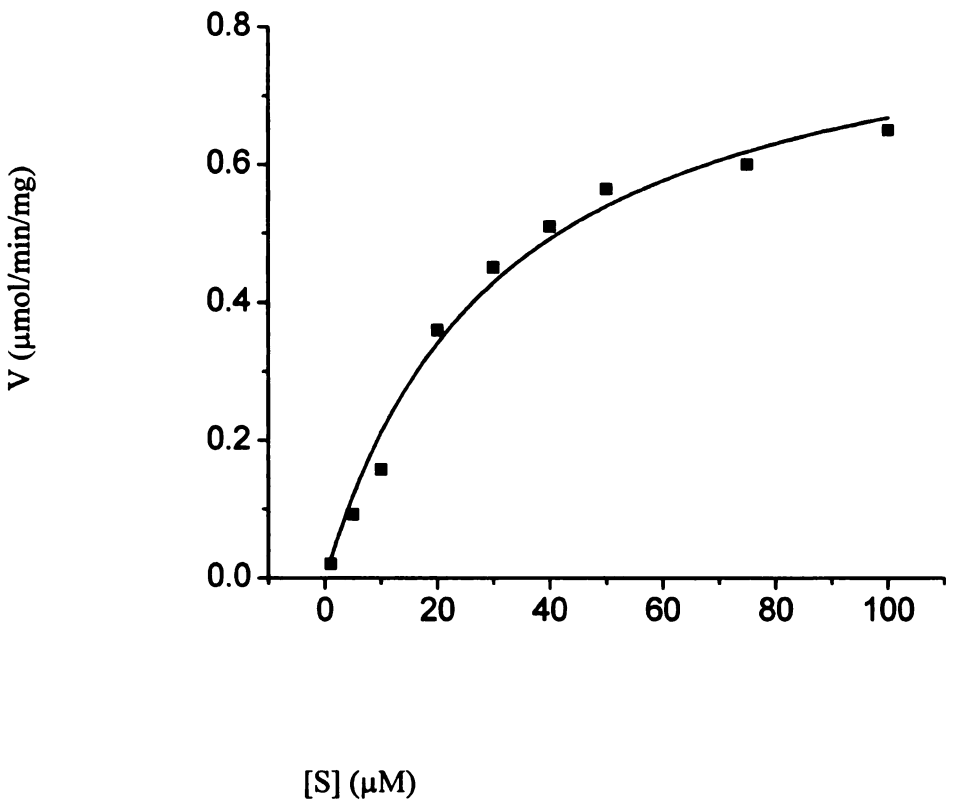

Figure 2.21 Recombinant OMT1 enzyme kinetics towards caffeic acid. Nonlinear curve fitting model with the Michaelis–Menten kinetics equation of $V=V_{max}*[S]/(K_m+[S])$ to plot V again [S].

The same procedure was used for other substrates with the mass for generating the extracted ion chromatogram differing for each substrate. 5-Hydroxyferulic acid was measured using m/z 209.04, quercetin with m/z 301.04, myricetin with m/z 317.03, and luteolin with m/z 285.03.

Results from kinetics studies of OMT1 with different phenolic substrates are shown in Table 2.1. The best substrates of recombinant OMT1 are quercetin, myricetin and luteolin, better than caffeic acid and 5-hydroxyferulic acid, based on their low K_m, high V_{max}, and K_{cat}/K_m. The flavonol aglycones with hydroxyl groups in 3' positions gave K_m values ranging from 7-8 μM, slightly lower than the hydroxycinnamic acids which were 27 and 35 μM for caffeic and 5-hydroxyferulic acids, respectively. Values for K_{cat}/K_m were about 10- to 20-fold greater for the flavonols. Muzac *et al.* (2000) reported minimal methyltransferase activity of OMT1 toward caffeic acid and 5-hydroxyferulic acid and luteolin, and activity was so low that no values were reported for V_{max} or K_m. Since they found that the protein was a monomer, a dimer may be critical for certain functions of the enzyme. Therefore, we cannot discount the possibility that the OMT1 they purified either failed to fold into a dimer during expression, or the activity was partially lost during the purification. Since Muzac *et al.* (2000) did obtain activity with quercetin and myricetin, which indicates the enzyme they purified was at least partially active, it could be that their enzyme assay was not sensitive enough to measure activities toward caffeic acid and 5- hydroxyferulic acid.

Substra
Caffeic
5-Hydr
Querce
Myrice
Luteol

Table
phenol
protoc

Alth

myrice

accum

LCM

consu

with t

(e.g.,

(e.g.,

OMT

gluco

sinap

Loren

meth

N

Krist

recor

defin

Substrate	$K_m(\mu M)$	V_{max} (μmol/min/mg)	$K_{cat}(s^{-1})$	$K_{cat}/K_m(\mu M^{-1}s^{-1})$
Caffeic acid	27	0.795	0.53	0.020
5-Hydroxyferulic acid	35	1.525	1.24	0.035
Quercetin	7.7	6.818	4.55	0.491
Myricetin	7.5	3.044	2.03	0.270
Luteolin	7.0	3.884	2.59	0.369

Table 2.1 Affinities and activities of purified *Arabidopsis* recombinant OMT1 toward phenolic substrates. No activities toward sinapic acid, salicylic acid, gallic acid, protocatechuic acid, quercetin 3-L-rhamnoside, rutin, and apigenin were detected.

Although high OMT1 activities toward caffeic acid, 5-hydroxyferulic acid, quercetin, myricetin and luteolin were detected *in vitro*, none of these, or their methylated products accumulate to significant levels in wild type or mutant *Arabidopsis* leaves based on LC/MS metabolite profiles. It may be because some substrates are intermediates and are consumed in the cell, or some substrates are not present in the same organelle or tissue with the enzyme. It also may be because the free acids are usually conjugated to sugars (e.g., glucose conjugates), cell wall carbohydrates (e.g., ferulate esters), or organic acids (e.g., sinapate esters, chlorogenic acid). The main evidence for *in vivo* functions of OMT1 in Arabidopsis leaves comes from levels of malate esters 5HFM and SM, and glucose esters 5HFG and SG. It has been reported that SG can be converted to SM by sinapoyl-glucose:L-malate O-sinapoyltransferase in *Arabidopsis* (Mock et al. 1992; Lorenzen et al. 1996; Lim et al. 2001). Therefore, SM may be synthesized either from the methylation of 5HFM, or from SG, the product of the methylation of 5HFG.

Neither 5HFM nor 5HFG is commercially available, therefore undergraduate student Kristina Knight and I worked together to synthesize 5HFM. Specific activities of purified recombinant OMT1 against 5HFM is 0.21 U/mg $\pm$ 0.02. One unit of enzyme activity is defined as the conversion of 1 μmol of 5HFM to SM per min at 30°C. Relative activity of

5HFM to 5HFA is about 10%. One finding of note is that incubation of the recombinant OMT1 with a crude metabolite extract from *omt1* mutant leaves gave 100% conversion of 5HFM to SM and 5HFG to SG in less than one hour, suggesting that the enzyme is capable of methylating malate and glucose esters of hydroxycinnamic acids. The malate esters are some of the dominant polyphenols in *Arabidopsis* leaves. To our knowledge this is the first direct demonstration of OMT activity toward malate esters.

OMT1 can use the flavonoids quercetin, myricetin, and luteolin as substrates. Quercetin and its glycosidic and rhamnosidic derivatives are major flavonoids found in *Arabidopsis thaliana* (Kerhoas et al. 2006; Stobiecki et al. 2006) in certain tissues such as roots, but are uncommon in leaves. The induced production of flavonoids under stress of pathogens and pests is a well-known phenomenon in plants (Barry 2002; Gallet 2004). Based on these earlier findings, we anticipated that quercetin glycosides or rhamnosides may be impacted in roots and other tissues of *omt1* mutant plants under pathogen stress.

Result 2: Comparison of metabolite profiles between control and pathogen stress both in the wild type plants (WC vs WP) and in the mutant (MC vs MP) to characterize the biomarkers in plant-pathogen interaction

One of the goals of this study is to identify the biomarkers, the indicators of pathogen infection or plant defense-involved secondary metabolites. In this experiment, the control leaves were inoculated using a syringe with a sterile solution of 10 mM $MgCl_2$ via the stomata into the lower surface of half of the leaf. Therefore, the control samples were also under wounding stress. Some metabolites were induced both in control and pathogen samples due to the wounding stress. However, the biomarkers in pathogen stress are the

metabolites induced only after pathogen stress but not in control samples, both in the wild type and the mutant. The amounts of the metabolites discussed below were calculated as integrated extracted ion current (XIC) peak areas divided by fresh leaf weight (mg). The amount the metabolites and their corresponding mass to charge ratios (m/z) are shown either in the content or in the Appendix A.

Some biomarkers are pathogen produced metabolites such as coronatine (m/z 318.17), or induced plant metabolites such as the phytoalexin camalexin (m/z 199.04). Both of them were induced gradually after pathogen stress and reach their highest levels at three days (Figure 2.29 and 2.30).

Some biomarkers of interest in pathogen stress are signaling metabolites such as salicylic acid (SA) (m/z 137.04), two isomeric forms of salicylic acid glucoside (SAG) (m/z 299.07), ABA (m/z 263.13), jasmonic acid (JA) (m/z 209.12), 12-OH JA (m/z 225.15), JA Ile (m/z 322.20), 12-oxo-phytodienoic acid (OPDA) (m/z 291.20), OPC:8 (m/z 293.2), linolenic acid (LA) (m/z 277.22), and oxylipin glycolipid conjugates Arabidopsides A-E (either in the content or in the Appendix A).

Metabolite profiling also detects an assortment of candidate biomarkers including glucosinolates. Quantification of glucosinolates is shown in Appendix A. Methylsulfinyl glucosinolates have sulfoxide groups, e.g. 4-methylsulfinylbutyl glucosinolate (m/z 436) and 8-methylsulfinyloctyl glucosinolate (m/z 492), their reduced methylthio glucosinolate analogs, e.g. 4-methylthiobutyl glucosinolates (m/z 420) and 8-methylthiooctyl glucosinolate (m/z 476), and phenethyl glucosinolate 3-methylsulfinylpropyl glucosinolate (m/z 422) decreased after pathogen stress, which corresponds to previous transcription results showing down-regulation of glucosinolate

biosynthesis genes (Tierens et al. 2001). Indole glucosinolates, e.g. 4-methoxyindolyl or 1-methoxyindolyl glucosinolates (m/z 477.07) did not exhibit obvious increases as shown in the previous transcription results (Tierens et al. 2001).

Polyphenols and quinone metabolites were changed after pathogen stress such as the decrease of 5HFM (m/z 325.06) and SM (m/z 339.07) and increase of 5HFM-GS (m/z 630.13) and 5HFM quinone-GS (m/z 628.11). The measured masses for 5HFM-GS (630.13) and 5HFM quinone-GS (628.11) are within 5 ppm of theoretical values. The major fragment ion for 5HFM-GS (630.13) is m/z 325.06 for deprotonated 5HFM and m/z 306.08 for deprotonated GSH. The major fragment ion for 5HFM quinone-GS (628.11) is m/z 323.04 for deprotonated 5HFM quinone and m/z 306.08 for deprotonated GSH.

Some biomarkers were present in different amounts in the wild type and the mutant, such as coronatine, camalexin, SA (m/z 137.04), ABA (m/z 263.13), JA (m/z 209.12), 12OH-JA (m/z 225.15), JA Ile (m/z 322.20), 5HFM (m/z 325.06), SM (m/z 339.07), 5HFM-GS and 5HFM quinone-GS. Some of them showed no differences between the wild type and the mutant, like OPDA, OPC:8, and LA. The metabolites that were different between the wild type and the mutant are discussed in the next section.

Result 3: Comparison of leaf metabolite profiles between WT and the *omt1* mutant after pathogen attack (WP vs MP) to characterize the OMT function under stress

Comparing metabolite profiles of the *omt1* mutant under pathogen stress with wild type plants was used to investigate the functions of this gene in pathogen response. Plant defense response is a time-dependent event; therefore metabolome changes were studied

at 1 hour, 24 hours, 48 hours, and 72 hours after inoculation to monitor the progress of early to late induced responses. Metabolites with significantly different between WT and the *omt1* mutant after pathogen attack (WP vs MP) were identified and quantified to interpret the role of OMT in modulating metabolic responses in Arabidopsis during *P. syringae* infection, as discussed below.

5HFM, SM, 5HFM-GS, 5HFM Quinone-GS, and GSH

The levels of 5HFM, the proposed substrate of OMT1, were decreased gradually after pathogen stress in the mutant (Figure 2.22), and so did the level of SM, the product of OMT1 (Figure 2.23). The structurally related compounds 5HFM glutathione conjugate (5HFM-GS) (Figure 2.24) and 5HFM quinone glutathione conjugate (5HFM Quinone-GS) (Figure 2.25) were found to increase gradually after pathogen stress in the mutant, with the depletion of GSH (Figure 2.26). 5HFM quinone-GS was only induced in the mutant, but not in the wild type. In the mutant, it increased two-fold more during pathogen stress than in the control. 5HFM-GS was also induced mostly in the mutant. In the mutant, it increased two-fold more during pathogen stress than in the control. 5HFM-GS was present at one time point in wild type plants. We have no explanation for the appearance in the wild type. Depletion of GSH was observed following pathogen inoculation. In the mutant, GSH was completely consumed after pathogen stress (relative amount dropped from 30 to 0), while the decrease of GSH in control was less (relative amount dropped from 30 to 10). The control sample had wounding stress during the infiltration of Mg_2Cl_2 at 0 h. That is may account for why 5HFM-GS and 5HFM quinone-

GS were also induced in control samples, though two-fold less than during pathogen stress.

The correlated relationship of the decrease of 5HFM and the increase of 5HFM quinone-GS and 5HFM-GS, as well as the depletion of GSH is consistent with the suggestion that 5HFM was oxidized to quinone following pathogen infection, and the quinone was then conjugated to GSH to produce 5HFM-GS. 5HFM-GS could be oxidized to 5HFM quinone-GS by various oxidants including H_2O_2, which could be reduced to 5HFM-GS by cellular reducing agents such as GSH as well. These quinones and hydroquinones may undergo redox cycling, giving catalytic generation of superoxide and H_2O_2 from O_2 as shown Figure 2.27 and discussed below. GSH is consumed both in the conjugation and redox cycling, and such biochemical events can lead to depletion of other cellular reducing agents. This assumption is made based on previous redox cycling studies in animals (Wilson et al. 1986; Galati et al. 1999; Stephensen et al. 2002). One notable finding was that the oxidized form of GSH, GSSG, was not observed in substantial amounts in any of the metabolite extracts.

The abbreviation of samples with different genotypes or treatments are: WC for the wild type control with the infiltration of $MgCl_2$ buffer, MC for the mutant control with the infiltration of $MgCl_2$ buffer, WP for the wild type with the infiltration of *P. syringae*, and MP for the mutant with the infiltration of *P. syringae*.

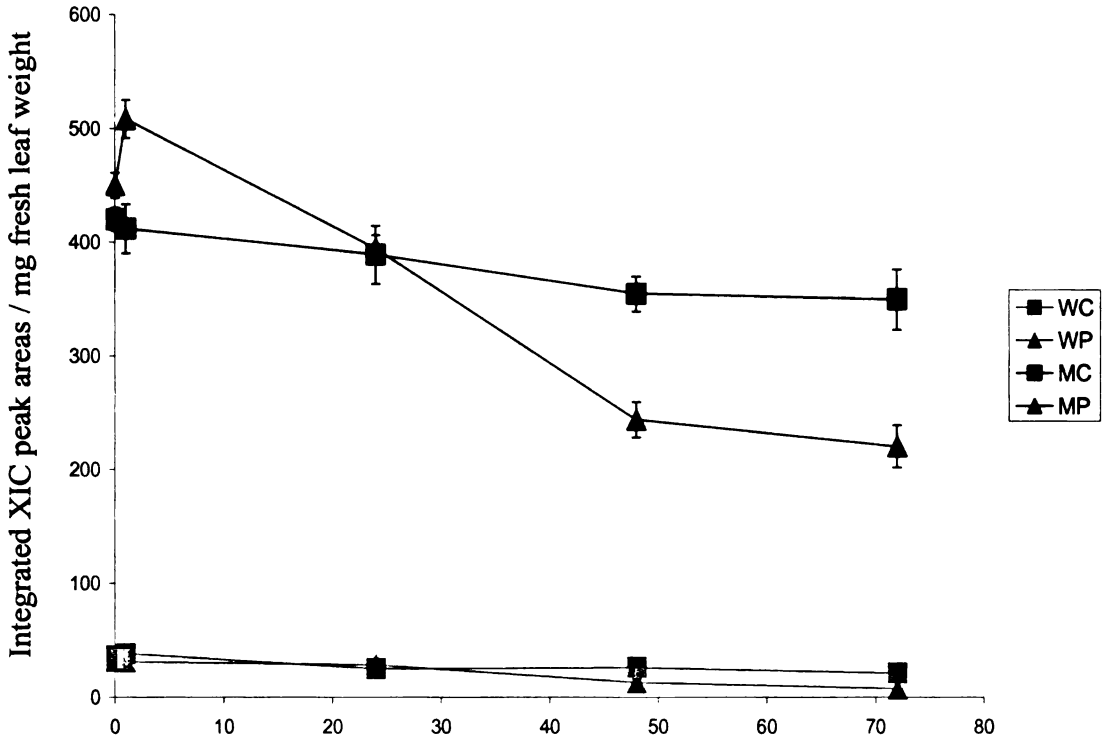

T-test analysis on metabolite levels

	1h	1d	2d	3d
WC vs MC	*	*	*	*
WP vs MP	*	*	*	*
WC vs WP	N.S.	N.S.	N.S.	N.S.
MC vs MP	*	N.S.	*	*

"*" significant, $p < 0.05$
"N.S." not significant

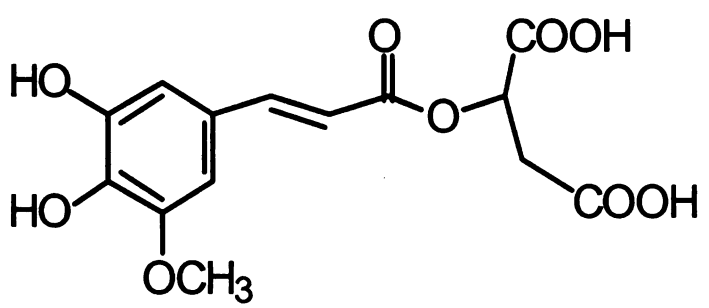

Figure 2.22 Levels and chemical structure of 5HFM (m/z 325.06)

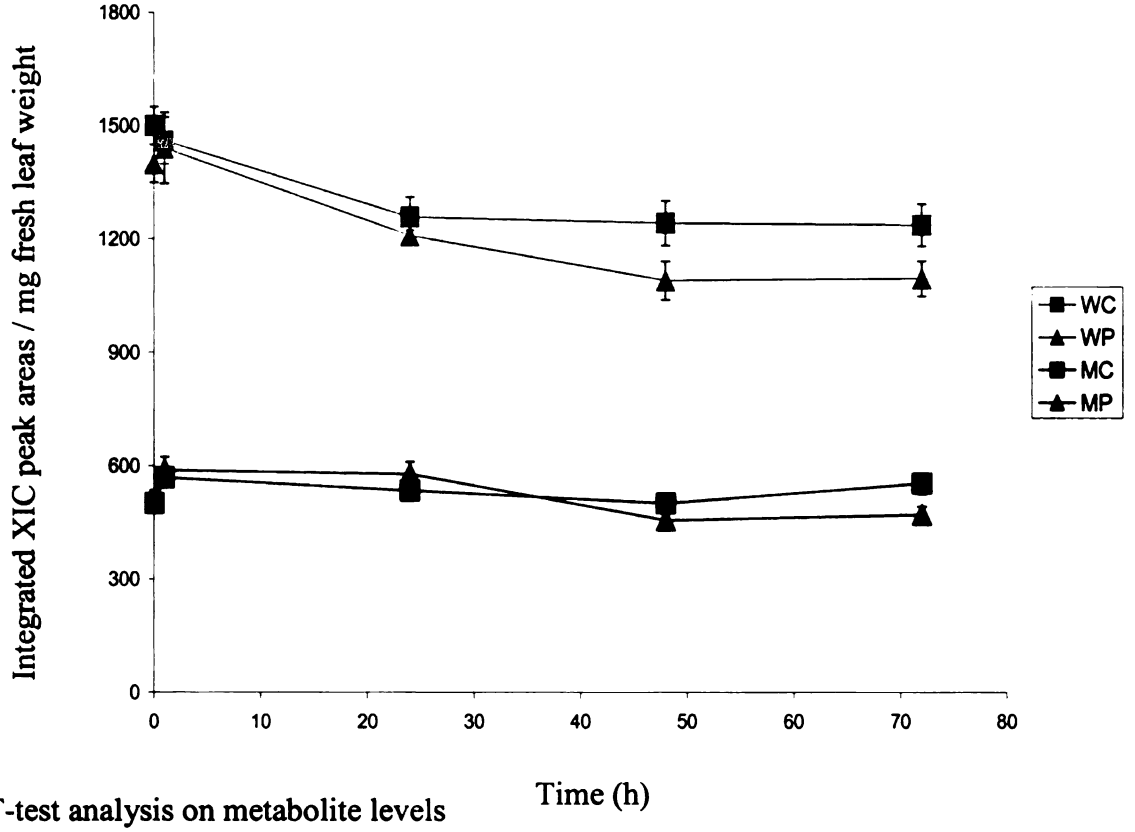

T-test analysis on metabolite levels

	1h	1d	2d	3d
WC vs MC	*	*	*	*
WP vs MP	*	*	*	*
WC vs WP	N.S.	N.S.	*	*
MC vs MP	N.S.	N.S.	N.S.	N.S.

"*" significant, $p < 0.05$
"N.S." not significant

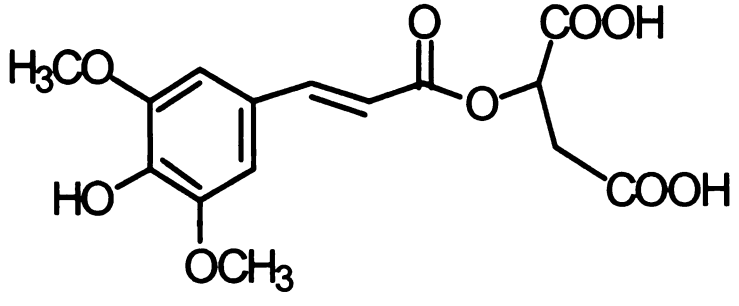

Figure 2.23 Levels and chemical structure of SM (m/z 339.07)

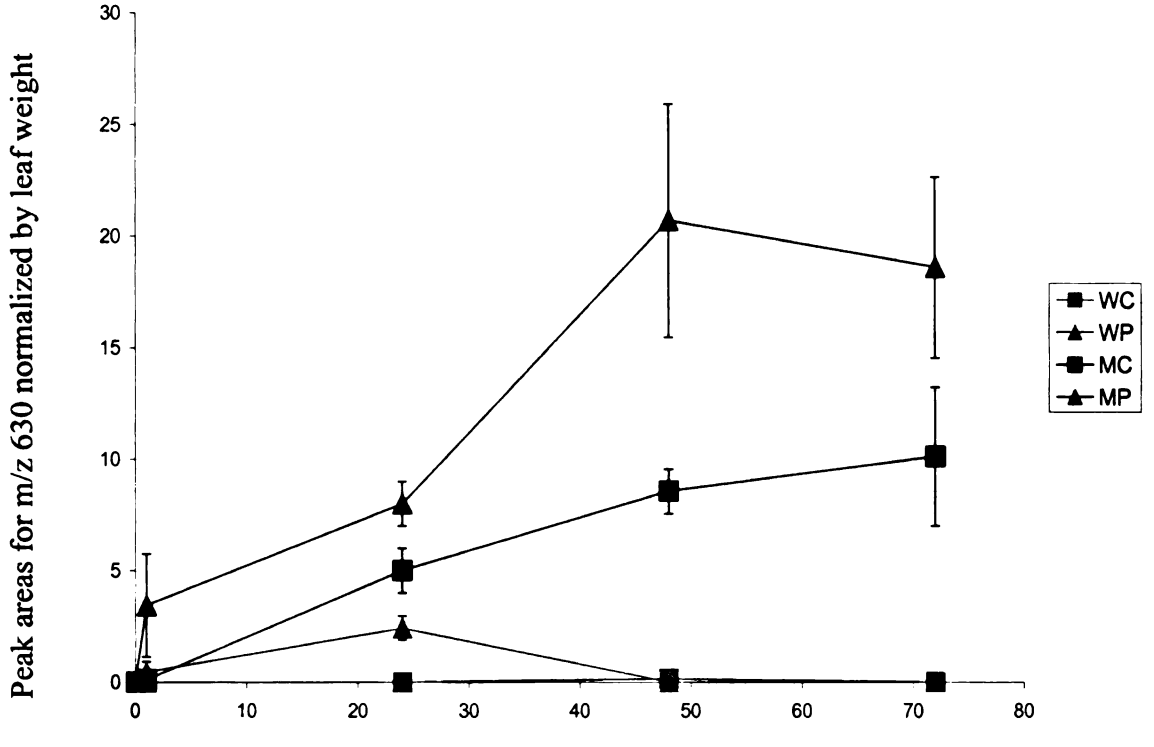

T-test analysis on metabolite levels

	1h	1d	2d	3d
WC vs MC	N.S.	*	*	*
WP vs MP	*	*	*	*
WC vs WP	N.S.	*	N.S.	N.S.
MC vs MP	*	*	*	*

"*" significant, $p < 0.05$

"N.S." not significant

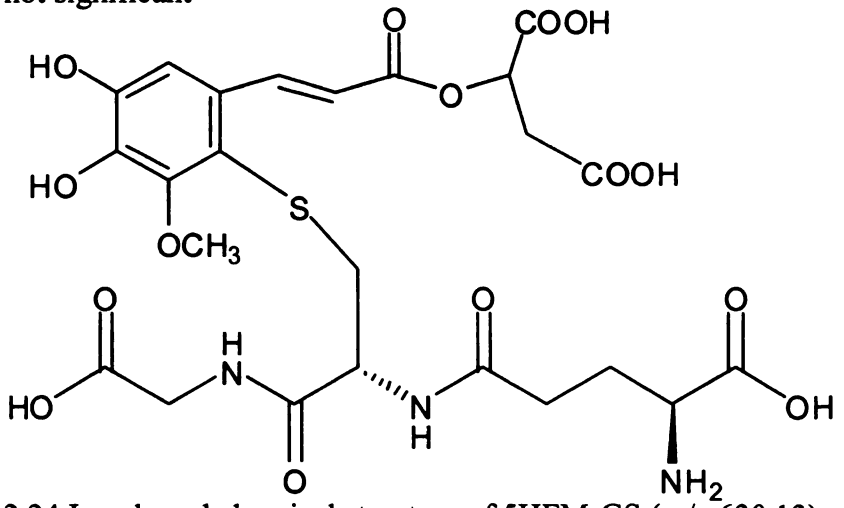

Figure 2.24 Levels and chemical structure of 5HFM-GS (m/z 630.13)

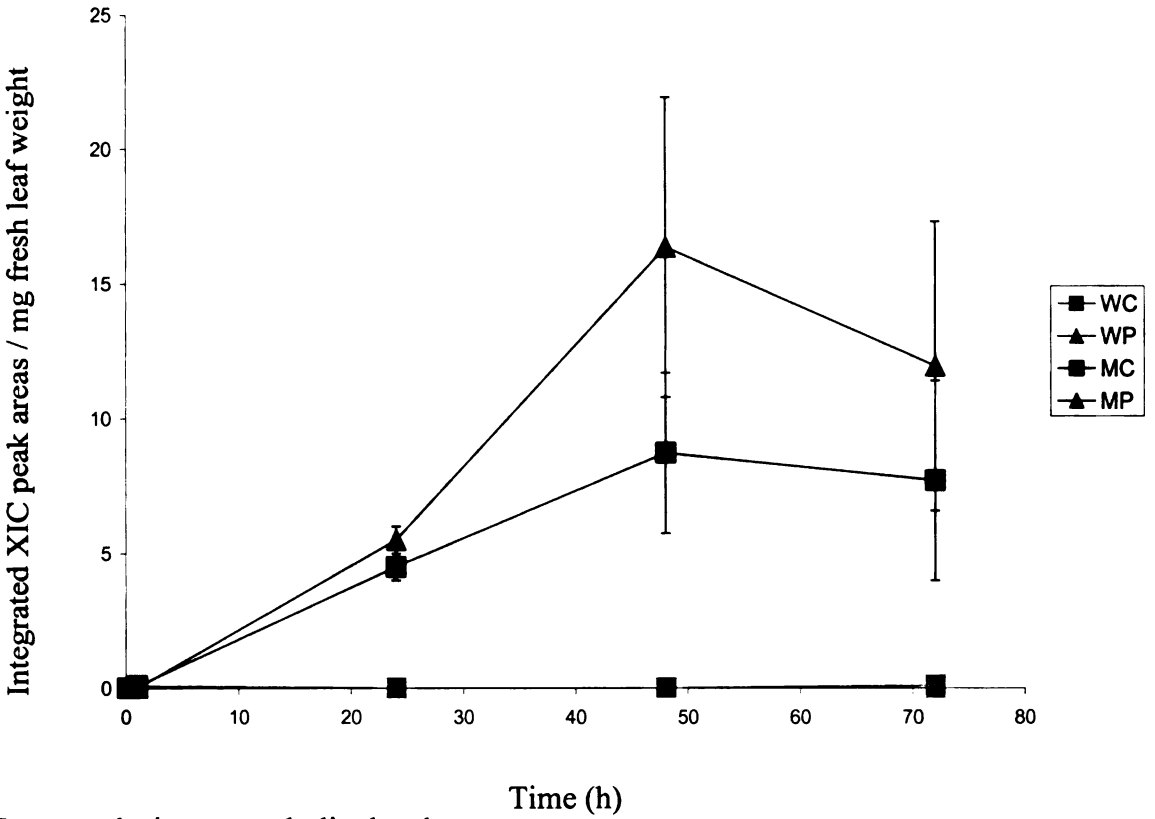

T-test analysis on metabolite levels

	1h	1d	2d	3d
WC vs MC	N.S.	*	*	*
WP vs MP	N.S.	N.S.	N.S.	N.S.
WC vs WP	N.S.	N.S.	N.S.	N.S.
MC vs MP	N.S.	N.S.	*	*

"*" significant, $p < 0.05$

"N.S." not significant

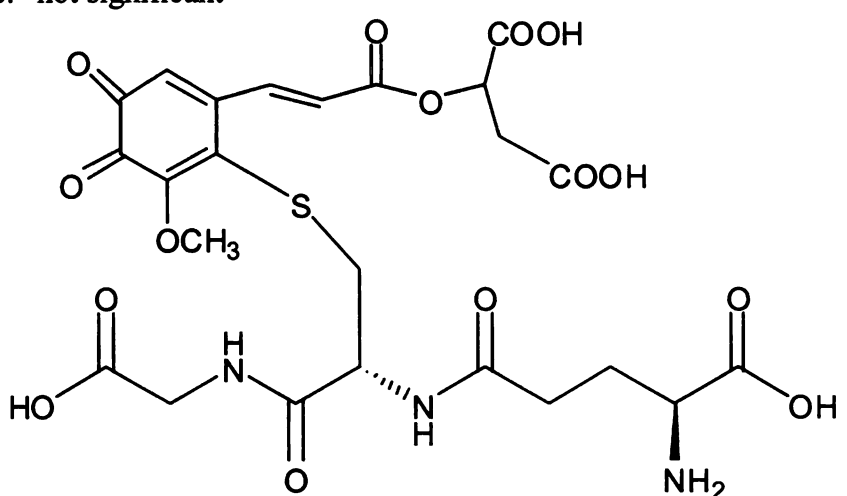

Figure 2.25 Levels and chemical structure of 5HFM quinone-GS (m/z 628.11)

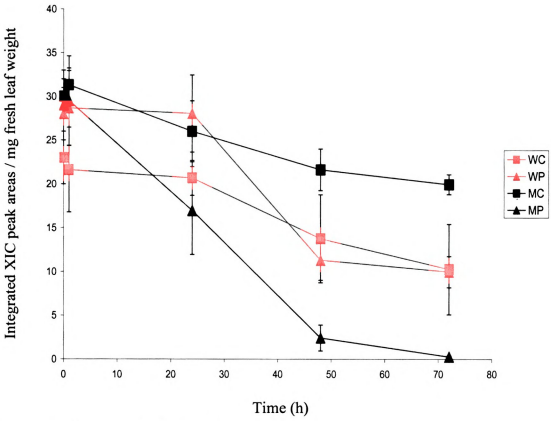

T-test analysis on metabolite levels

	1h	1d	2d	3d
WC vs MC	N.S.	N.S.	*	*
WP vs MP	N.S.	N.S.	*	*
WC vs WP	N.S.	N.S.	N.S.	N.S.
MC vs MP	N.S.	N.S.	*	*

"*" significant, $p < 0.05$
"N.S." not significant

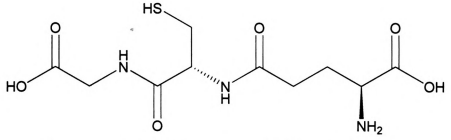

Figure 2.26 Levels and chemical structure of GSH (m/z 306.08)

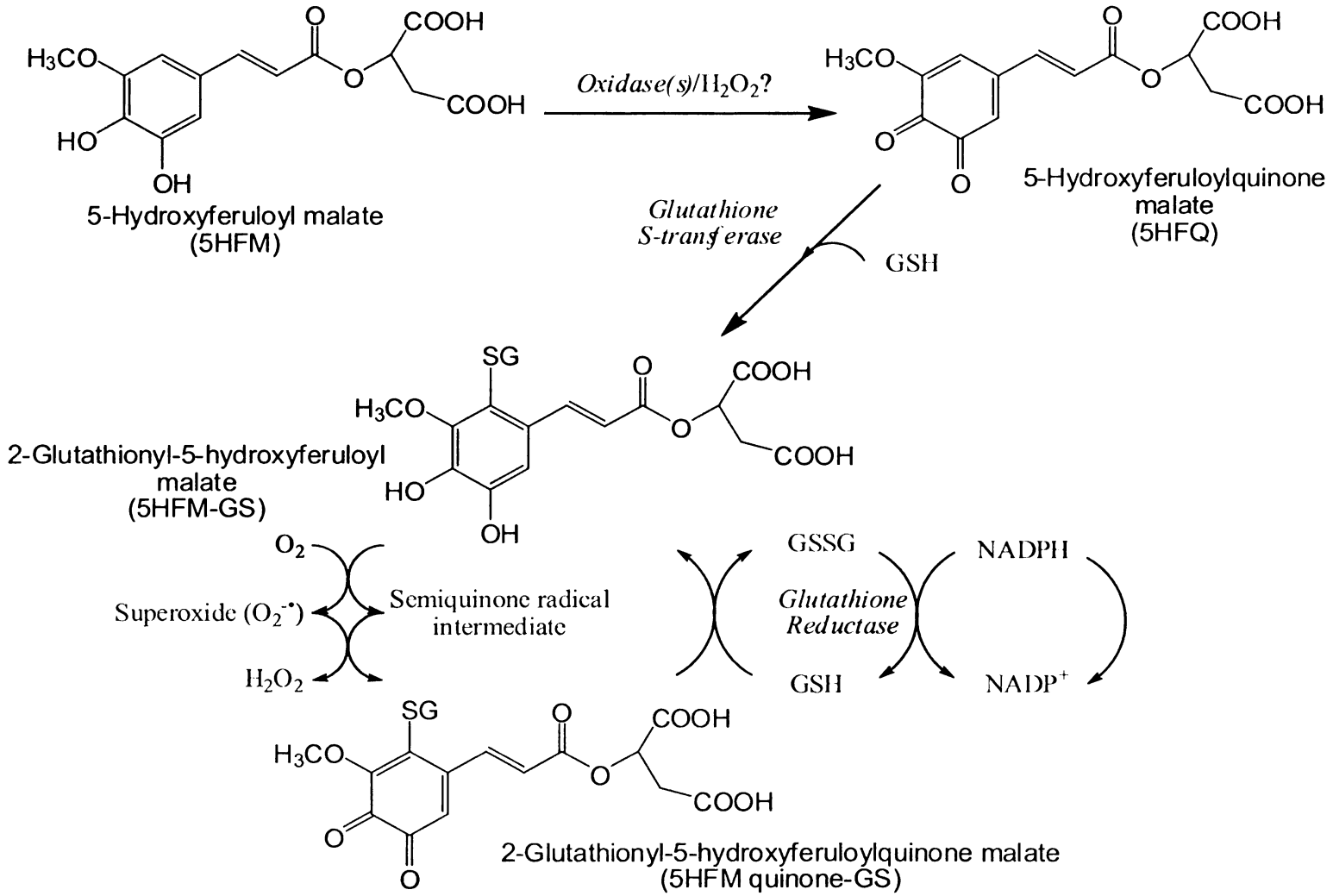

Figure 2.27 Proposed pathway for production of 5HFM-GS and 5HFM quinone-GS and catalytic formation of superoxide and H_2O_2 via redox cycling.

5HFM-OH and 5HFM-OH-GS

Evidence to support that quinones and hydroquinones undergo redox cycling and give catalytic generation of H_2O_2 is that more oxidized metabolites were induced in the mutant after pathogen stress such as 5HFM-OH (Figure 2.28) and 5HFM-OH-GS (Figure 2.29). The precise nature of the additional oxidation step is not yet clear, but the results are consistent with formation of reactive oxygen species that could introduce an additional oxygen atom into these acids and GSH conjugates. It suggests the mutant was under more oxidative stress than the wild type.

Figure 2.28 Levels and chemical structure of 5HFM-OH (m/z 341.06). Two possible structures are proposed.

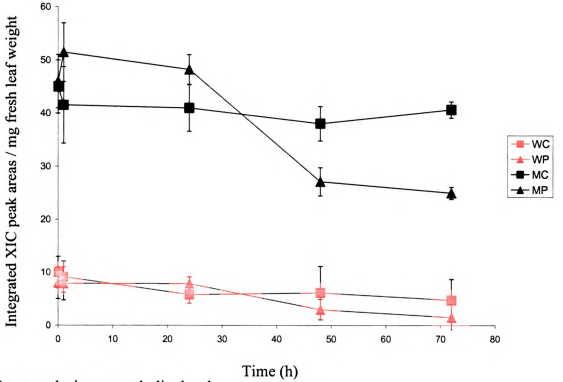

T-test analysis on metabolite levels

	1h	1d	2d	3d
WC vs MC	N.S.	N.S.	*	*
WP vs MP	N.S.	N.S.	*	*
WC vs WP	N.S.	N.S.	N.S.	N.S.
MC vs MP	N.S.	N.S.	*	*

"*" significant, $p < 0.05$
"N.S." not significant

Figure 2.28 continued

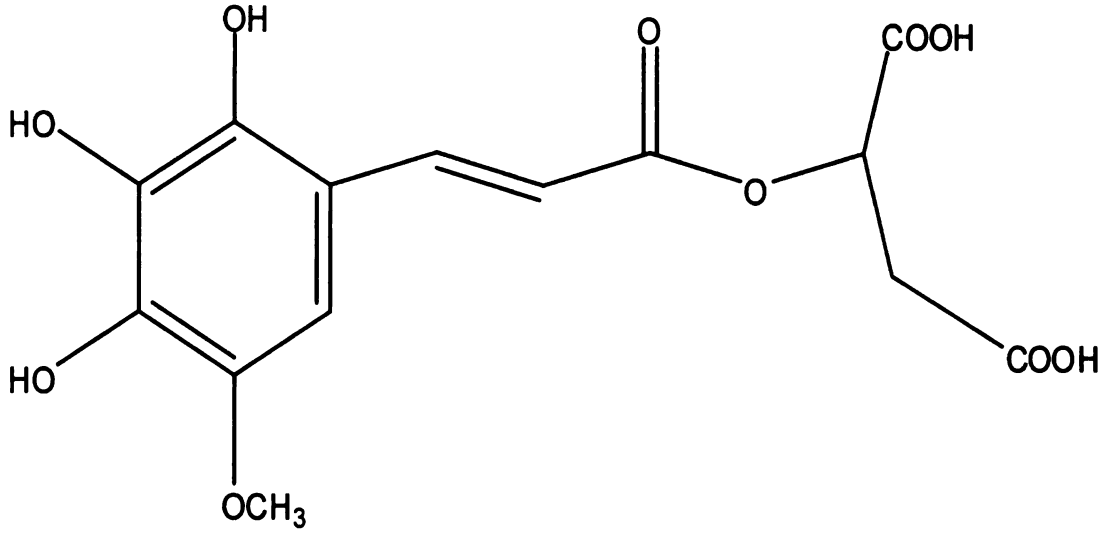

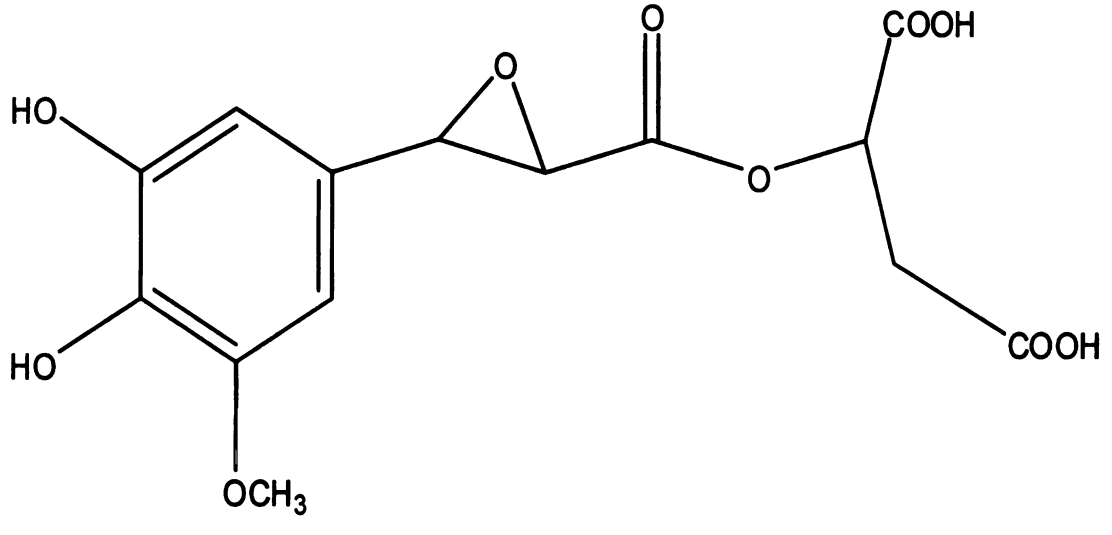

Figure 2.29 Levels and chemical structure of 5HFM-OH-GS (m/z 646.12). Two possible structures are proposed.

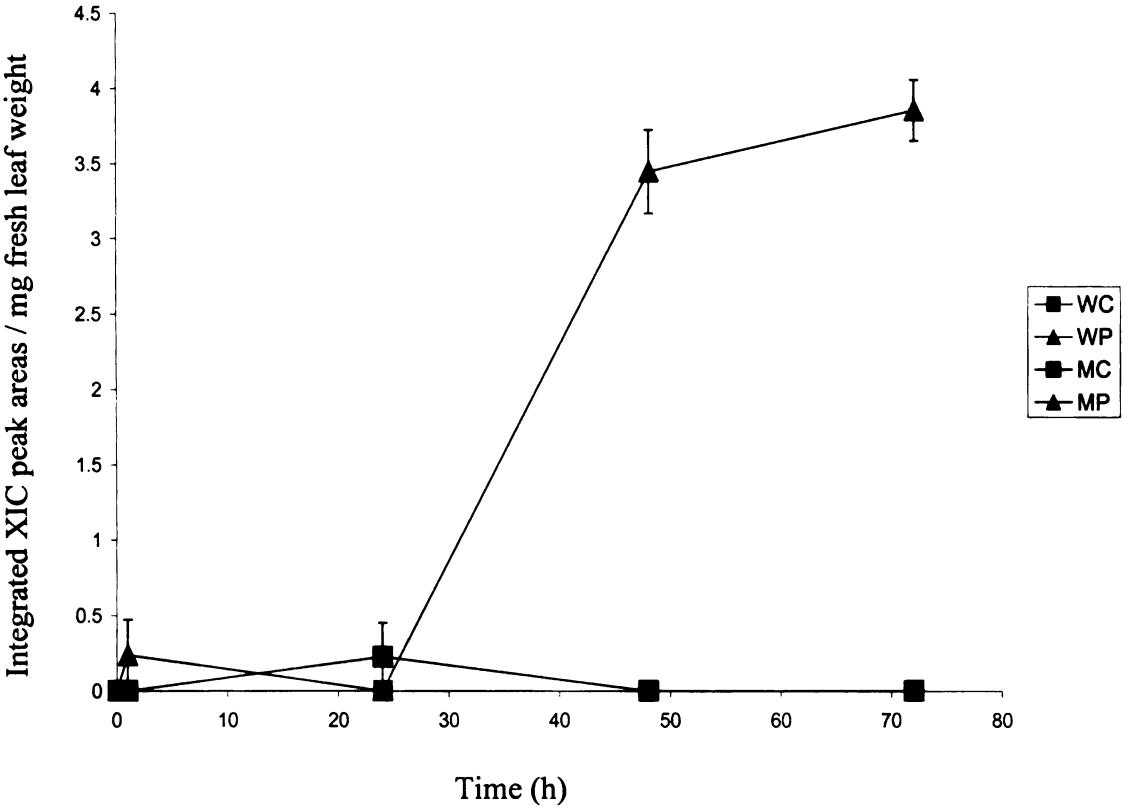

T-test analysis on metabolite levels

	1h	1d	2d	3d
WC vs MC	N.S.	N.S.	N.S.	N.S.
WP vs MP	N.S.	N.S.	*	*
WC vs WP	N.S.	N.S.	N.S.	N.S.
MC vs MP	N.S.	N.S.	*	*

"*" significant, $p < 0.05$
"N.S." not significant

Figure 2.29 continued

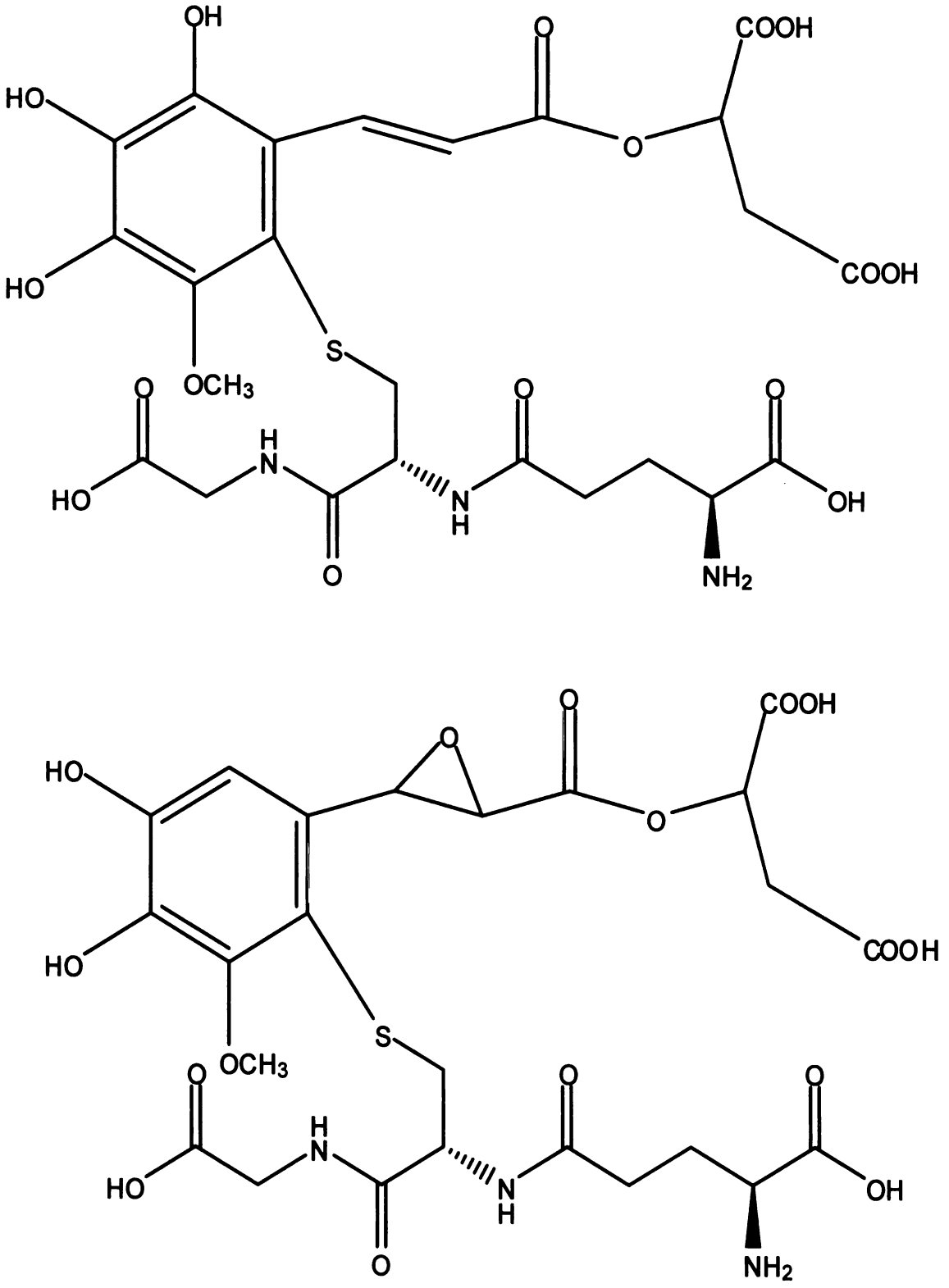

Coronatine

Coronatine levels (Figure 2.30) increased in both mutant and wild type after inoculation, but this increase was about two-fold less in the mutant than in the wild type after three days of pathogen treatment. Increases in the mutant were also less for SA, ABA, JA, 12OH JA, and JA Ile. Coronatine is an important virulence factor for *P. syringae* DC3000 infection in Arabidopsis plants and a pathogen-derived functional and structural mimic of the phytohormone jasmonic acid (JA) and it is thought to be involved in the reopening of stomata (Cui et al. 2005; Melotto et al. 2006). It is a metabolite which the pathogen secretes and is a biomarker for pathogen stress. In the mutant, the slower increase in coronatine levels may be explained by the inhibition of bacterial growth relative to wild type plants.

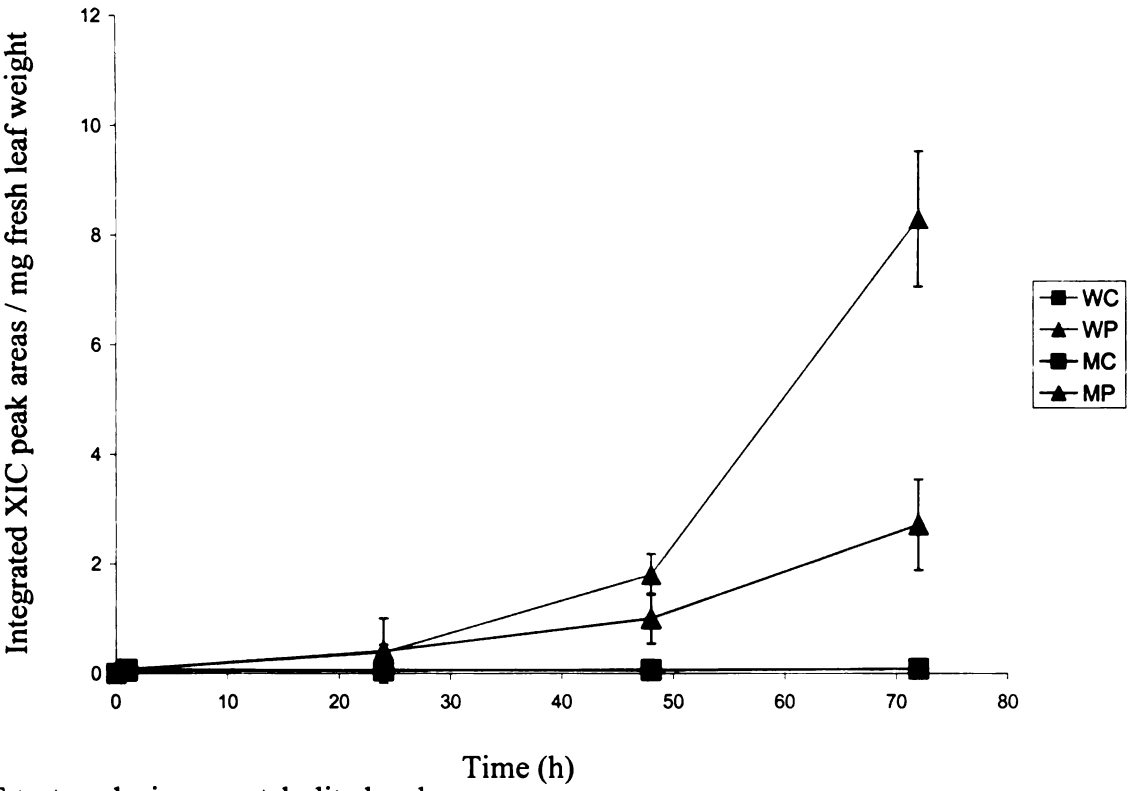

T-test analysis on metabolite levels

	1h	1d	2d	3d
WC vs MC	N.S.	N.S.	N.S.	N.S.
WP vs MP	N.S.	N.S.	N.S.	*
WC vs WP	N.S.	N.S.	*	*
MC vs MP	N.S.	N.S.	*	*

"*" significant, $p < 0.05$

"N.S." not significant

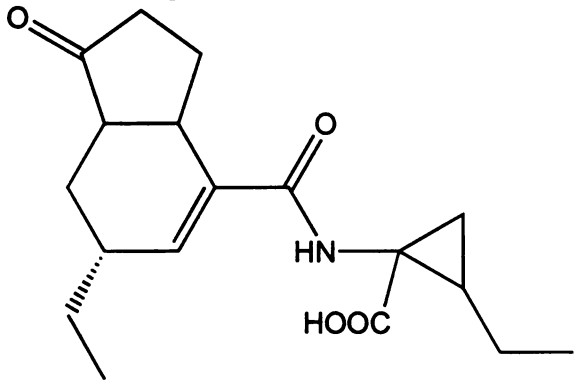

Figure 2.30 Levels and chemical structure of Coronatine (m/z 318.17).

Camalexin

Camalexin was induced two-fold more in the mutant than in the wild type after two days of pathogen stress (Figure 2.31). Camalexin is a phytoalexin which plants produce and has anti-microbial properties (Zook 1998). It is also a candidate biomarker for pathogen stress. Therefore, the higher levels of camalexin in the mutant are consistent with stronger activation of plant defense in the mutant despite slower progression of infection in the mutant than the wild type.

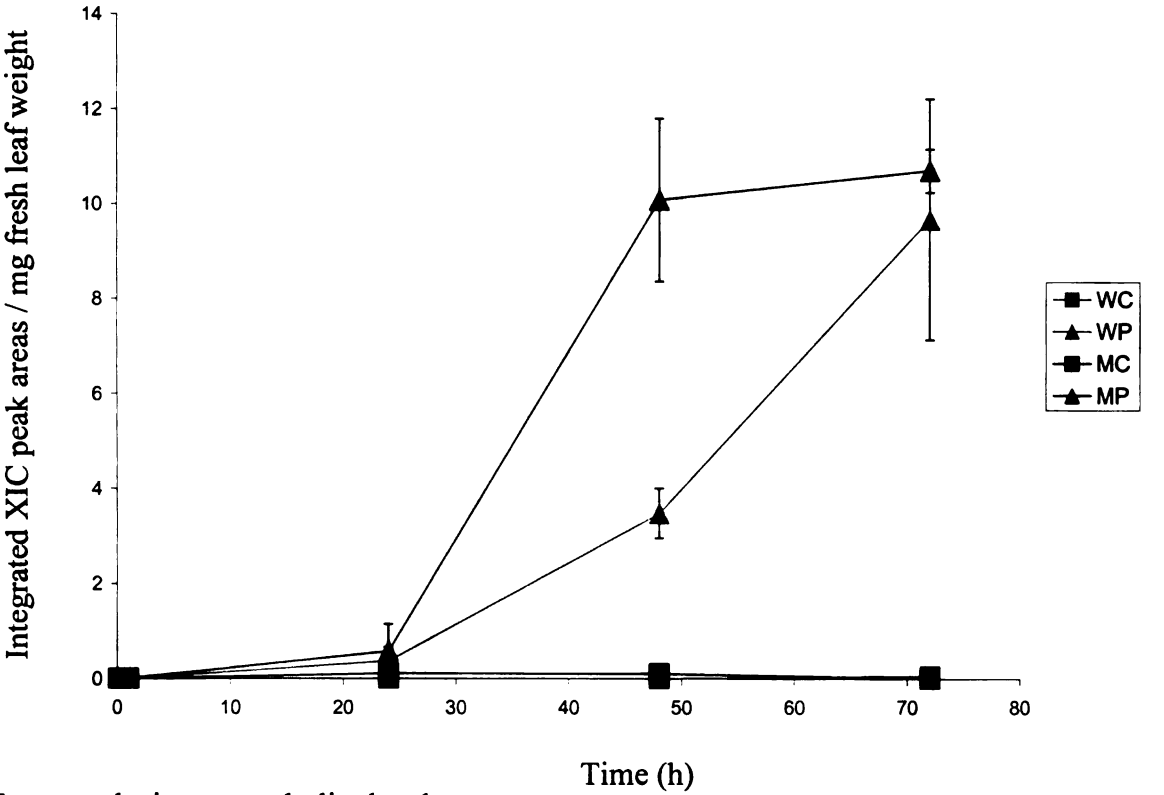

T-test analysis on metabolite levels

	1h	1d	2d	3d
WC vs MC	N.S.	N.S.	N.S.	N.S.
WP vs MP	N.S.	N.S.	*	N.S.
WC vs WP	N.S.	N.S.	*	*
MC vs MP	N.S.	N.S.	*	*

"*" significant, $p < 0.05$
"N.S." not significant

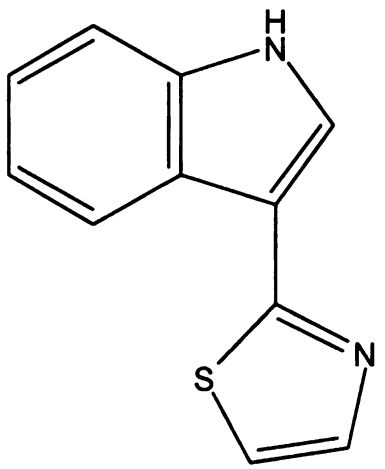

Figure 2.31 Levels and chemical structure of camalexin (m/z 199.04).

SA, ABA, JA, 12OH JA and JA Ile

At 1 h post inoculation, SA, ABA, JA, 12-OH JA and JA Ile were induced suddenly. Levels of JA are presented in Figure 2.32. Levels of SA, ABA, 12-OH JA and JA Ile are shown in Appendix A. They were increased at least two-fold more (with the exception of ABA) in the mutant relative to the wild type both in pathogen inoculated and control samples at 72 hours. Taking JA as an example, the mutant (both control and pathogen-infected) produces a quick surge in JA that is about 2-fold greater than the wild-type (both control and pathogen-infected) at 1 h. It is noted that 5HFM-GS was observed as early as at 1 h treatment, but not before treatment. The enhanced JA burst in the mutant suggests participation of OMT functions, manifested in the form of higher levels of quinone or other non-methylated metabolites in enhancement of the oxidative burst following pathogen inoculation.

Though levels of JA increased at 1 h post-inoculation, these levels dropped after 24 hours and increased again from 48-72 hours. The early increase is thought to result largely from wounding stress during inoculation, since JA is known to be the major signal compound induced after wounding. The late increase is attributed to the consequences of pathogen infection, which is greater for wild-type infected plants than for mutant infected plants. JA and JA Ile exhibited same behavior. SA, ABA, JA, 12-OH JA, and JA Ile exhibited similar behavior at 1h and 72 hour. Interestingly, JA and its precursors in the oxylipin pathway were observed in different patterns. Oxylipins OPDA, OPC:8, and LA showed no difference between the wild type and the mutant (Appendix A).

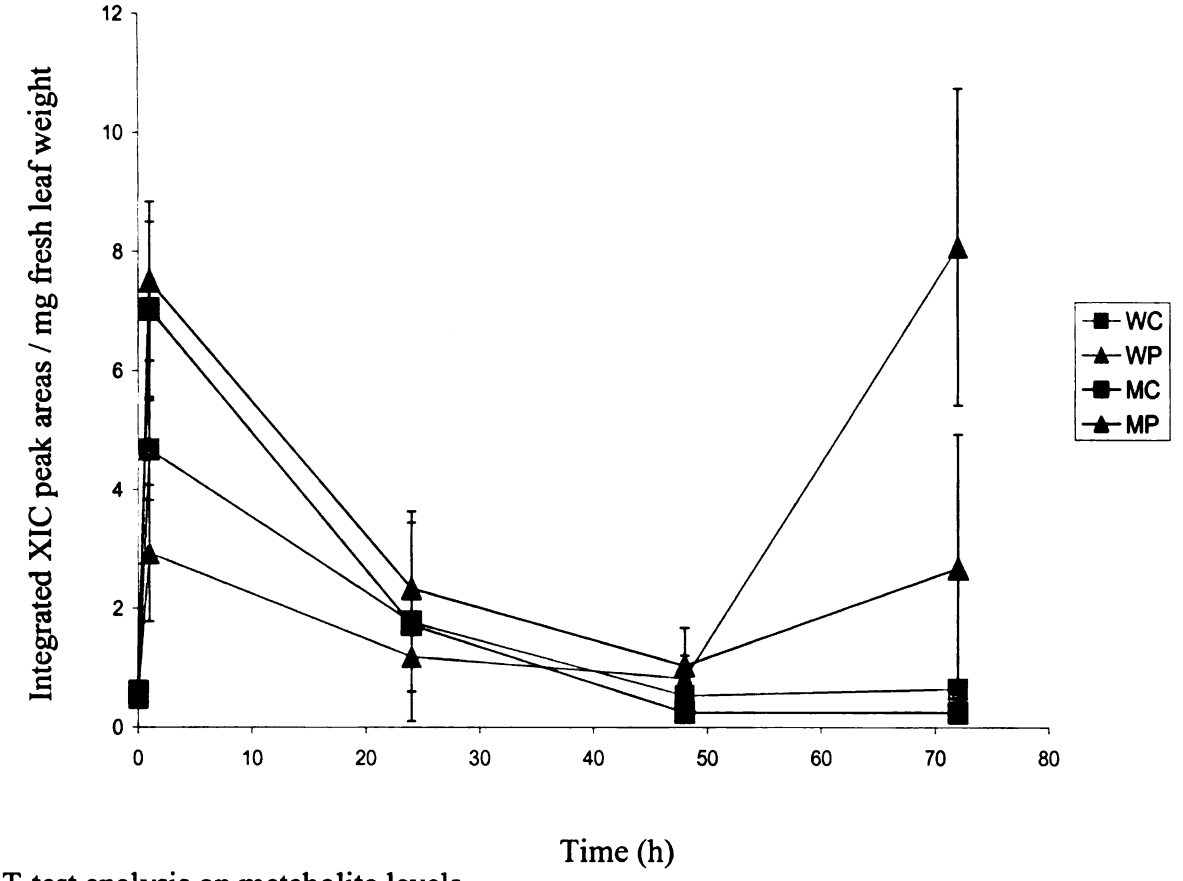

T-test analysis on metabolite levels

	1h	1d	2d	3d
WC vs MC	N.S.	N.S.	N.S.	N.S.
WP vs MP	N.S.	N.S.	N.S.	N.S.
WC vs WP	N.S.	N.S.	N.S.	*
MC vs MP	N.S.	N.S.	N.S.	*

"*" significant, $p < 0.05$
"N.S." not significant

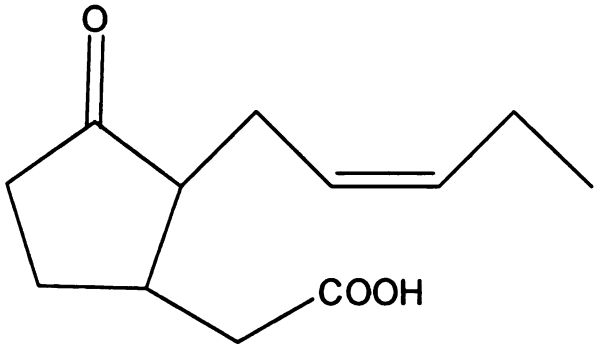

Figure 2.32 Levels and chemical structure of JA (m/z 209.12).

Flavonoids

The major flavonoids in leaf extracts, 3-O-,7-O-dirhamnosyl kaempferol and 3-O-glucosyl, 7-O-rhamnosyl kaempferol, accumulated slightly more (less than 10% of total amount) in mutant relative to wild type (Appendix A). Those flavonoids are not substrates of OMT1, as they lack hydroxyl groups in the 3'- and 5'- positions. Levels showed slight decrease both in pathogen stress and control conditions, while flavonoid 3-O-glucosylkaempferol (Appendix A) was increased gradually after pathogen stress, perhaps due to increased hydrolysis of the 7-position glycosides. Flavonoid synthesis is part of the phenylpropanoid pathway and is a competing biosynthetic branch of phenylpropanoid biosynthesis with the synthesis of phenolic acids, the latter of which serve as precursors of lignins (Nair et al. 2004; Rogers et al. 2005). Therefore, defects in *omt1*, which may affect phenols in the phenylpropanoid pathway and lignin synthesis, may also impact the levels of flavonoids. However, the results of this study do not provide definitive information in this regard.

Minor amounts of oxidized 3-O-glucosyl, 7-O-rhamnosyl kaempferol, appearing as a product with an additional hydroxyl group at position undetermined, were elevated slightly in the mutant relative to the wild type. This finding supports the suggestion that mutant plants are capable of generating more ROS than wild type plants in both control and pathogen stressed plants.

OPDA-GS and dinor OPDA-GS

GSH depletion was observed after pathogen stress, dropping to undetectable levels in the mutant by the third day after inoculation. To assess whether GSH depletion arises

largely via conjugations to quinone metabolites, other GSH conjugates such as oxylipin GSH conjugates were also quantified. Levels of OPDA-GS (m/z 598) and dinor OPDA-GS (m/z 570) decreased after one day pathogen stress, but did not change further after two days (Appendix A). There was no difference between mutant and the wild type, so it is concluded that GSH depletion was not accelerated in the mutant owing to more conjugation to oxylipins.

Taken in total, metabolite profiling has revealed a substantial decrease in GSH levels in infected mutant plants, relatively modest increases in the sum of all glutathione conjugates, and the absence of evidence for an increase in GSSG. These findings provide indirect evidence to suggest that some GSH is not accounted for. One explanation that deserves further study is that oxidant stress in infected mutants leads to increased formation of mixed protein-GSH disulfides, as these would not be detected using the current methodology.

2.3.5.3 Anti-microbial properties of quinones, quinone-GS conjugates, and H_2O_2

The metabolite data suggest that 5HFM quinone metabolites and their GSH conjugates may provide direct toxicity to pathogenic *P. syringae*. To probe whether polyphenolic quinone and quinone-GS conjugates pose chemical mechanisms leading to direct toxicity to *P. syringae*, *in vitro* cultures of *P. syringae* were dosed with polyphenols, quinone, quinone-GSH conjugate, and H_2O_2 (Figure 2.33). 5HF was used instead of 5HFM because adequate supplies of 5HFM were not available and 5HF has the same functional group and similar physical properties.

5HF quinone and 5HF quinone-GS were synthesized and used in bacterial culture, both in liquid and solid plates with the concentrations chosen to mimic the estimated *in vivo* concentrations of the malate ester analogs based on the LC/MS peak areas of the quinonoid compounds in extracts of the pathogen stressed leaves (Figure 2.33). Inhibition of bacterial growth was observed at low μM concentrations (~ 2 μM) for 5-hydroxyferulic acid, its quinone, and the GSH conjugate of the quinone, but not for the methylated analog sinapic acid. Though GSH conjugation of quinones has been considered a detoxification step, the persistence of antagonism to *P. syringae* growth in the quinone-GSH conjugate suggests this class of metabolites may undergo redox cycling, catalyzing formation of superoxide and hydrogen peroxide, as has been observed in studies of quinone toxicity in animals (Monks and Lau, 1998).

To probe whether H_2O_2 leads to direct toxicity to *P. syringae*, a series of different concentrations of H_2O_2 (100, 10, 1, 0.1, and 0.01 mM) were incubated in bacteria culture. Growth of *P. syringae* was inhibited by the highest H_2O_2 concentrations (100 mM and 10 mM) but inhibition was not observed at 1 mM or lower concentrations (Figure 2.33A).

Figure 2.33 Concentration dependence of antimicrobial potential of H_2O_2, 5-hydroxyferulic acid quinone conjugate (5HFQ), 5-hydroxyferulic acid quinone with glutathione conjugate (5HFQ-GS), 5-hydroxyferulic acid (5HFA), and sinapic acid (S) against *P. syringae* DC3000. Higher concentration (100 mM and 10 mM) of H_2O_2, 2 μM and 20 μM 5HFQ, 5HFQ-GS, and 5HFA showed clear zones of *P. syringae* DC3000 inhibition in disc diffusion method (A). When 5HFQ, 5HFQ-GS, or 5HFA was incorporated into *P. syringae* DC3000 suspension, it showed a concentration dependent colony forming unit reduction (B). In figure (B), all data points represent the average of three independent experiments.

A

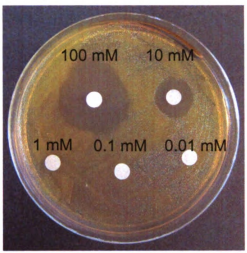

5 µl of a series of different concentration of H_2O_2 (100 mM, 10 mM, 1 mM, 0.1 mM, 0.01 mM)

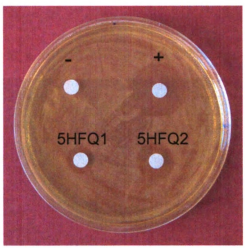

-: negative control: 10 µl of DMSO
+: positive control: 10 µl of 10 mM H_2O_2
5HFQ1: 10 µl of ~2 µM 5-hydroxyferulic acid quinone conjugate
5HFQ2: 10 µl of ~20 µM 5-hydroxyferulic acid quinone conjugate

Figure 2.33 continued

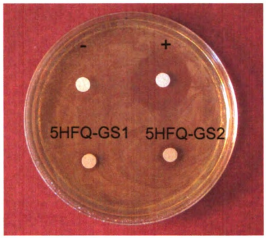

-: negative control: 10 µl of DMSO
+: positive control: 10 µl of 10 mM H_2O_2
5HFQ-GS1: 10 µl of ~2 µM 5-hydroxyferulic acid quinone and glutathione conjugate
5HFQ2-GS2: 10 µl of ~20 µM 5-hydroxyferulic acid quinone and glutathione conjugate

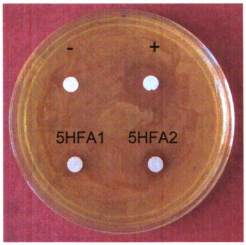

-: negative control: 10 µl of DMSO
+: positive control: 10 µl of 10 mM H_2O_2
5HFA1: 10 µl of ~2 µM 5-hydroxyferulic acid
5HFA2: 10 µl of ~20 µM 5-hydroxyferulic acid

Figure 2.33 continued

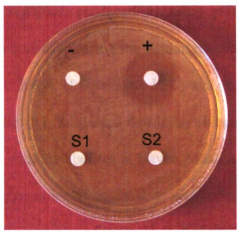

-: negative control: 10 µl of DMSO
+: positive control: 10 µl of 10 mM H_2O_2
S1: 10 µl of 10 µM sinapic acid
S2: 10 µl of 20 µM sinapic acid

B

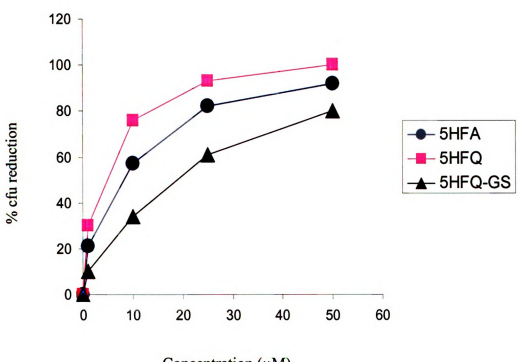

2.3.5.4 Quantification of H_2O_2 in leaf tissue

To see if H_2O_2 was produced in Arabidopsis leaves after pathogen stress. Hydrogen peroxide was quantified using the Fenton reaction with FOX assays (Delong et al. 2002; Franklin et al. 2009). However, no H_2O_2 was detected in extracts of the leaf tissues after pathogen stress. It is suspected that H_2O_2 was degraded by enzymes such as catalases or H_2O_2 reacted with metabolites in leaves. Many microbes are capable of producing H_2O_2-degrading enzymes including catalase and peroxidases as well. In the experiment to test anti-microbial properties of H_2O_2, H_2O_2 had no effect to inhibit the growth of *P. syringae* DC3000 when the concentration was lower than 1 mM in this study. (Figure 2.33A). Therefore, the results do not allow us to conclude whether enough H_2O_2 was produced in leaves of mutant plants to inhibit the growth of *P. syringae* DC3000.

2.3.5.5 Localization of 5HFM-GS and 5HFM Quinone-GS in apoplast

Plant apoplast, the intercellular space, is the first site of contact with a pathogen. (Bolwell et al. 2001). Sometimes metabolites will be secreted from the plant cell to the apoplast. One consequence of pathogen infection is that the cell may die when the resistant response fails or becomes overwhelmed. When cell death occurs, membrane integrity is lost, and the metabolites in the cell may flow into the apoplast. To determine whether 5HFM-GS and 5HFM quinone-GS could diffuse into the apoplast to suppress pathogen growth, apoplast extracts were prepared by centrifugation, and these extracts were analyzed for metabolites. After 1 day post-inoculation, the extract from the apoplast was collected before evidence of cell death was visible. Apoplast extracts were analyzed using LC/MS. 5HFM-GS and 5HFM Quinone-GS were not found in the apoplast. At two

days post-inoculation, cell death was evident from leaf discoloration. The extraction from the apoplast was therefore expected to sample from not only live cells but also damaged dead cells. LC/MS analyses for this time point also showed low levels of 5HFM quinone glutathione conjugate were released into the sampled volume, which may explain why the bacteria were inhibited *in planta* after two days.

Discussion

Polyphenols, quinones and glutathione conjugates

The polyphenols are important specialized metabolites of plants, known for their role in browning in plants (Antolovich et al. 2004). Many are oxidized to their corresponding quinones by polyphenol oxidase when plant tissue is damaged. Quinones are reactive substances that have structural similarities to aromatic compounds, being based upon a six-membered ring with two double bonds and two ketone substitutions, arranged either ortho (in the 1,2- positions) or para (in 1,4 positions). Some quinones are further polymerized by reactions with quinones or amines to form a brown pigment in fruit and vegetables (Murata et al. 2002). Enzymatic browning involves several steps, including the hydroxylation of monophenols into *o*-diphenols and further oxidation of *o*-diphenols into quinones. The mechanism of nonenzymatic browning is not well understood (Antolovich et al. 2004), in large part because the structures of the browning products are not well characterized.

Quinones are electrophiles and oxidants, with both properties arising from their electron deficient nature. Quinones are electrophilic (seeking electrons) because the addition of two electrons can convert them into more stable aromatic molecules

containing benzene ring structures. They undergo rapid reactions with the nucleotide groups in DNA and with amino or thiol groups in proteins and peptides to form covalent adducts. They are also oxidants, capable of oxidizing other substances that have lower redox potentials, including some other phenols. The electrophilic and oxidant properties of quinones can result in the destruction of molecules essential for cell survival including the tripeptide glutathione, which is an important cellular redox buffer (Fulcrand et al. 1994; Monks and Lau 1998). Quinones are also mutagenic and carcinogenic (Ames 1983; Chesis et al. 1984; Patrineli et al. 1996; Cornwell et al. 2002) and may provide direct toxicity in the cell through redox cycling (Lilienblum et al. 1985).

Metabolic conjugation of GSH to reactive electrophilic metabolites is well documented as a detoxification mechanism in animals (Chroust et al. 2001; Coles and Kadlubar 2003; Pastore et al. 2003), but our understanding of GSH conjugation in plants is still an emerging field of study. The potential importance of GSH conjugation is suggested by 54 glutathione S-transferase genes in the genome of *Arabidopsis thaliana* (Marrs 1996; Neuefeind et al. 1997; Dixon et al. 2009), but their importance has remained unclear aside from having roles in herbicide resistance and accumulation of anthocyanins in vacuoles (Alfenito et al. 1998; Mueller et al. 2000; Weisel et al. 2006). Several electrophilic oxylipin metabolites have been observed to form GSH conjugates (Davoine et al. 2005), but their significance remains unclear. Glutathione (GSH) is the major non-protein sulfhydryl in cells, and conjugation of potentially toxic electrophiles with GSH is usually associated with detoxication and excretion in animals. When GSH conjugates to quinones, the reaction is generally considered cytoprotective because the thiol function in GSH serves as a "sacrificial" nucleophile. However, polyphenolic-GSH

conjugates still possess a variety of biological activities. For example, quinone-thioether conjugates may participate in redox cycling, as substrates or inhibitors of enzymes, or as DNA-reactive mutagens, and may contribute to quinone-mediated carcinogenicity and neurotoxicity in animals (Monks and Lau 1992; Monks and Lau 1998).

In this study, glutathione conjugates of polyphenolic quinones were discovered in plants, with levels in pathogen-infected leaves of *omt1* mutant plants estimated to reach low- to mid- μM levels. Based on *in vitro* assays, 5HFA, 5HFA quinone, and its GSH conjugate showed marked inhibition of *P. syringae* growth at comparable concentrations. To our knowledge, these metabolites represent a novel finding, not just for Arabidopsis, but for the plant kingdom in general. Glutathione conjugation of quinones generates thioether-quinol adducts that are more reactive toward oxidation than the precursor polyphenol, and are more efficient at generating superoxide (Bratton et al. 1997; Bratton et al. 2000). The studies in animals showed that cytotoxicity of quinones is enhanced after GSH conjugation, owing in part to increased formation of reactive oxygen species (ROS). Studies of benzoquinone and its GSH conjugate demonstrated that the quinol-thioether conjugates readily form semiquinone radicals and undergo redox cycling, converting O_2 to superoxide by one-electron reduction, and providing a path to other ROS including H_2O_2. ROS are known to induce phytoalexin in Arabidopsis and other plants (Rusterucci et al. 1996; Thoma et al. 2003; Zhao et al. 2007).

After *P. syringae* inoculation, camalexin was induced two-fold more in the mutant as shown in the results above, which may be toxic the bacteria. H_2O_2 may be directly toxic to bacteria, but many microbes are capable of producing H_2O_2-degrading enzymes including catalase and peroxidases. After two days of pathogen treatment, some of the

plant cells started to die and lyse; the quinone and other anti-microbial compounds entered the apoplast and presumably killed the bacteria, or H_2O_2 produced through redox cycling may have killed the bacteria. Fewer bacteria in the mutant plant may explain why less coronatine was found than in the wild type.

GSH depletion – an alternative explanation for inhibition of pathogen growth

In humans, GSH depletion is linked to a number of disease states including cancer, neurodegenerative, and cardiovascular diseases (Pastore et al. 2003) as well as liver toxicity of drugs (Hentze et al. 2000; Jimenez-Lopez et al. 2008). In this study, GSH depletion was shown in the mutant after pathogen infection. During oxidant stress, GSH may be transformed to its oxidized dimer GSSG, and the latter may form mixed glutathione-protein disulfides (not measured in this study), or it can be conjugated to metabolites such as quinones and electrophilic oxylipins such as OPDA. GSSG could not be detected in leaf extract. OPDA-GS and dinor OPDA-GS were observed in a small amount at all the time points under both control and pathogen stress, but differences in oxylipin glutathione conjugates between mutant and the wild type were minimal. However, substantial differences in conjugation of GSH to 5HFM quinone distinguished pathogen-infected *omt1* mutant and wild type plants. Therefore, GSH depletion was due to the mutation of the *omt1* gene and may cause the inhibition of pathogen growth.

Function of OMT1 and its relevance to the metabolome and pathogen resistance

This study has demonstrated a role for OMT1 in the methylation of one of the most abundant secondary metabolites, 5HFM, converting it to SM. This function of OMT1

was proposed from the results of metabolite profiling without stress and the function was confirmed by biochemical characterization. OMT1 was found to methylate 3' or 5'OH group on the phenolic ring of polyphenols, including caffeic acid, 5-hydroxyferulic acid, quercetin and luteolin, and our findings are consistent with one other report (Goujon, 2003). SM is one of the most abundant secondary metabolites in leaves of the Col-0 ecotype. In this study, we found that one of the important functions of OMT1 is its methylation during its biosynthesis, and experiments with recombinant OMT1 demonstrate, in contrast with an earlier study (Muzac, 2000), that 5HFM is a substrate for this enzyme. In the absence of the *omt1* gene, 5HFM accumulates in leaf tissue, and this catechol derivative is oxidized to a reactive quinone upon pathogen stress, and to a lesser extent, following wounding in inoculated controls. Levels of 5HFM quinone and its GSH conjugate, in both oxidized and reduced forms, increased after pathogen stress. These are some of the few metabolic differences observed between *omt1* and wild type plants and their anti-microbial properties were observed.

2.4 Conclusion and perspective

Metabolite profiling of *omt1*(At5g54160) mutant and wild type plants cultivated in control conditions gave no significant morphological phenotype and the only pronounced metabolic phenotype in the mutant was a ~35% reduction in SM and a stoichiometrically similar increase in 5HFM, a metabolite containing a catechol (quinol) moiety. These findings are in agreement with methylation of 5HFM by recombinant OMT1, and confirm the *in vivo* function of OMT1 in SM biosynthesis. The functional consequences of the lack of near-complete methylation were only evident under conditions of

inoculation with *P. syringae*, where bacterial counts were higher ($p < 0.05$) in the wild type by about 5-fold. *In vitro* assessment of the antibacterial properties of 5HF, its quinone, and quinone glutathione conjugate, all showed inhibition of bacterial growth at low μM concentrations, which are in the range of levels observed in leaf extracts using LC/MS. In addition, the *omt1* mutants exhibited enhanced yields of JA at 1 hr past inoculation, suggestive of crosstalk between polyphenol metabolic pathways and jasmonate signaling.

The mutation of one single gene, *omt1*, led to changes in metabolite profiles both in control and pathogen stress conditions, but these are most evident after pathogen stress. This research has presented an original approach in conducting a wide-range of simultaneous analyses of specialized metabolites on genotypes with well-defined differences (a specific T-DNA mutation). When coupled with assessment of pathogen infection, the findings suggest that nontargeted metabolomic profiling, with emphasis on specialized metabolites, may draw more useful functional conclusions by studying stressed rather than control growth environments. The new methodology developed also provides a broad-based analysis of plant metabolic responses to pathogen infection.

The broader importance of this work will best be assessed by using this information in the study of other plant and pathogen systems. Leaves of the Col-0 ecotype of wild type *Arabidopsis thaliana* have low levels of catechol-containing metabolites owing to OMT enzymes which convert metabolic intermediates into methylated polyphenols such as SM. The work described in this chapter points to opportunities to manipulate expression of OMTs and genes in the phenylpropanoid and glutathione pathways to enhance resistance to pathogens, and perhaps herbivores, without substantial detriment to

the host plant. The results also highlight the biochemistry of quinones and GSH conjugation, which are well-studied topics in mammalian toxicology, and suggest that greater awareness of their importance in plant systems could provide fruitful areas for future research.

CHAPTER 3

UPLC MS/MS assay of jasmonates and related phytohormones for large-scale screening of plant metabolic phenotypes

Portions of this Chapter describe a collaborative work that has been published, to which I contributed by performing LC MS/MS method development and validation.

Chung, H. S., A. J. Koo, X. Gao, S. Jayanty, B. Thines, A. D. Jones and G. A. Howe (2008). "Regulation and function of Arabidopsis JASMONATE ZIM-domain genes in response to wounding and herbivory." Plant Physiol 146(3): 952-64.

Koo, A. J., X. Gao, A. Daniel Jones and G. A. Howe (2009). "A rapid wound signal activates the systemic synthesis of bioactive jasmonates in Arabidopsis." Plant J. In press.

3.1 Abstract

This report presents a selective and sensitive ultraperformance liquid chromatography tandem mass spectrometry (UPLC-MS/MS) method for simultaneous analysis of jasmonates and related phytohormones for large-scale screening of plant metabolic phenotypes. Twenty-four jasmonates and related phytohormones are measured within 5 min using multiple reaction monitoring and a fast reversed phase gradient. Multiple reaction monitoring (MRM) transitions were developed to distinguish leucine and isoleucine conjugates of jasmonic acid (JA) even when chromatographic resolution is incomplete. Isotope-labeled or dihydro analogs of these compounds were used as internal standards to yield accurate quantification. Sample preparation requires no derivatization, and the method gives detection at low fmol levels for all target metabolites. Endogenous levels of JA, 12-hydroxy JA, ten different JA amino acid conjugates, and methyl ester metabolites were measured. In the same analysis, the oxylipins OPDA, OPC:8 and OPC:6 were also quantified, along with their precursor linolenic acid (LA) and phytohormones salicylic acid, abscisic acid, indole-3-acetic acid and the bacterial phytotoxin coronatine. This method demonstrated presence of some JA metabolites in *Arabidopsis* leaves for the first time, and was applied to the analysis of plant hormones and metabolites from *Arabidopsis thaliana* leaves induced by wounding and the pathogen *Pseudomonas syringae* DC3000 infection.

3.2 Introduction

Plants regulate growth and developmental processes by producing a diverse array of specialized metabolite hormones (phytohormones). Since plant responses to biotic and

abiotic stress rely on changes in plant chemistry, phytohormones play an essential role in evoking physiological responses that are essential for survival. Phytohormones act at micromolar or lower concentrations that have presented challenges to the study of plant hormones, and only since the 1970s have researchers made great strides in clarifying their effects and importance (Srivastava 2002).

Among phytohormones, jasmonates are oxylipins that hold central importance in plant responses to wounding and stress (Chiwocha et al. 2003). Jasmonates regulate plant responses to biotic stresses including insect herbivory and pathogen infections as well as abiotic stresses including high UV light intensity, air pollutants including ozone, and osmotic stress. Shifts between growth- and defense-oriented metabolisms regulated by jasmonates enable plants to adapt to rapid environmental change (Chung et al. 2008). During pathogen infection, microbial metabolites also contribute to related signaling networks. Coronatine, a bacterial toxin with structural and functional similarity to JA and its amino acid conjugates, functions both as a signal mimic (Weiler et al. 1994) and inducer of JA biosynthesis (Laudert and Weiler 1998)

Plants convert jasmonic acid (JA) to a suite of modified metabolites, collectively known as jasmonates, including JA methyl ester (MeJA), glycosyl esters, and amide-linked conjugates with various amino acids (Staswick and Tiryaki 2004). Many jasmonates regulate gene expression upward or downward in a regulatory network with other plant hormones including salicylic acid (SA), auxin (indole-3-acetic acid, IAA), and abscisic acid (ABA) (Wasternack 2007). Recent findings show that amino acid conjugates of JA are more potent signaling compounds than JA itself (Staswick and

Tiryaki 2004; Thines et al. 2007), and these findings have stimulated a growing recognition of the importance of JA metabolism in plant signaling.

Few analytical approaches have assessed crosstalk among these signaling mechanisms through simultaneous and comprehensive measurements across a broad range of phytohormones at multiple time points. Low throughput in sample processing and metabolite analysis has limited such efforts, particularly with regard to the spatial and temporal responses of plants to biotic and abiotic stresses. Since plants need to produce hormones at specific times and locations, a comprehensive approach that yields simultaneous quantification of numerous plant metabolites is essential for elucidating their dynamics and functions. A GC/MS-based approach for measuring multiple phytohormones was described recently (Schmelz et al. 2004), but GC/MS analyses often require solvent evaporation and chemical derivatization steps (Wilbert et al. 1998; Glassbrook et al. 2000; Chiwocha et al. 2003; Engelberth et al. 2003) that present barriers to large-scale investigations.

An efficient analytical method is needed to provide selective and comprehensive quantification of phytohormones with low detection limits, high precision and accuracy, and experimental simplicity compatible with analyses for many treatments and time points. While GC/MS methods have provided outstanding resolution, dynamic range, and low susceptibility to matrix effects, LC methods offer advantages in simplicity and speed of sample preparation coupled with short analysis times. Recent development of sub-2 μm particles for ultraperformance LC (UPLC) provides separations that give superior throughput with chromatographic peak widths competitive with capillary GC.

LC/MS/MS methods add selectivity of analyte detection, yielding fmol detection limits for many analytes.

LC/MS/MS methods have been reported for a limited number of jasmonates such as JA, JA Leu and JA Ile (Tamogami and Kodama 1998), and UPLC/TOF MS has been employed to monitor an assortment of phytohormones and metabolites including several hydroxylated JA derivatives (Glauser et al. 2008). Both of these reports describe LC separations running more than 30 min/sample.

For more precise quantification of target metabolites, multiple reaction monitoring (MRM) has emerged as the standard approach for quantitative LC/MS analyses, and was used in the experiments described below. This approach uses the first mass analyzer (MS1) to filter all but the selected molecular ion, and the second mass analyzer (MS2) allows only a selected and characteristic fragment ion to reach the detector. This approach yields chromatograms selective for the target metabolite(s), filtering out signals from all other substances that cannot satisfy the requirements for both molecular and fragment ion masses and for chromatographic retention time. The specific experiment is known as a "transition" and can be written as parent ion > fragment ion. For example, m/z 209 > m/z 59 is MRM for jasmonic acid (Figure 3.1).

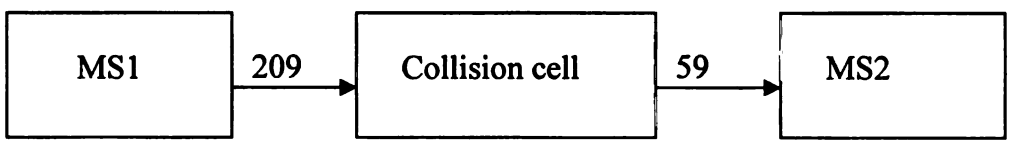

Figure 3.1 Diagram for triple quatrupole and multiple reaction monitoring (MRM). MS1 stands for first mass analyzer and MS2 stands for second mass analyzer. For example, m/z 209 > m/z 59 is MRM for jasmonic acid. m/z 209 is the parent ion, which was allowed to pass through MS1. m/z 59 is the fragment ion which was allowed to pass through MS2.

In this study, we report a fast, sensitive, and selective UPLC MS/MS method for quantifying JA metabolites, additional oxylipins, salicylates, abscisic acid, and auxin without need for derivatization. We demonstrate the most comprehensive profiles of jasmonates and related phytohormones using LC/MS/MS, including measurements of some metabolites in *Arabidopsis* for the first time. Selective MRM transitions were optimized to distinguish two coeluting isomers. Performance of the method is evaluated for measurements of phytohormone levels in leaves upon wounding and pathogen stress.

3.3 Materials and methods

3.3.1 Chemicals

All commercially available compounds and mobile phase additives were purchased from Sigma (St. Louis, MO), and HPLC-grade solvents were purchased from VWR Scientific. Structures of the phytohormones measured in this study are presented in Figure 3.2.

Figure 3.2 Chemical structures of the 24 compounds and the internal standards used in this study.

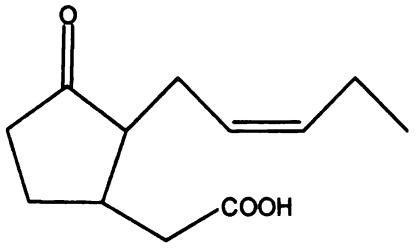

JA

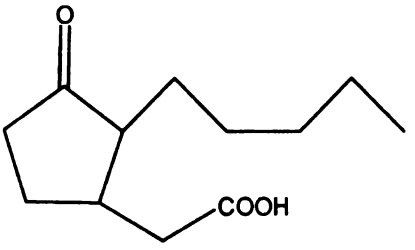

dJA

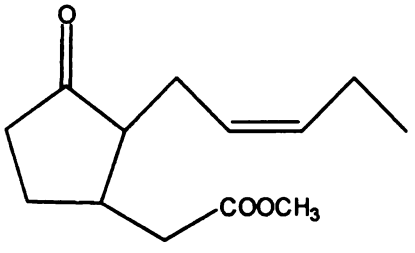

Me JA

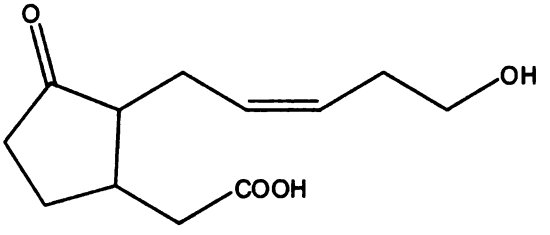

12OH JA

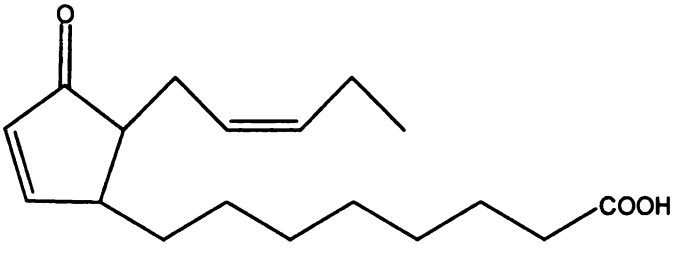

OPDA

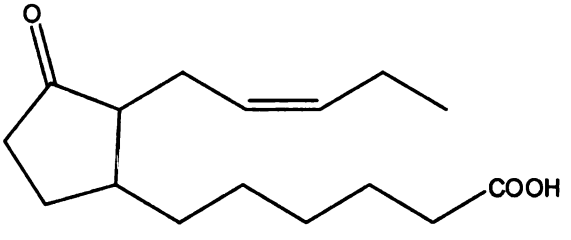

OPC:6

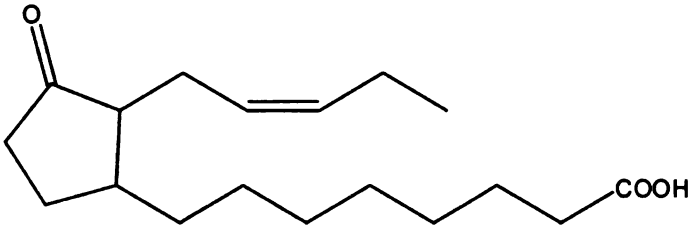

OPC:8

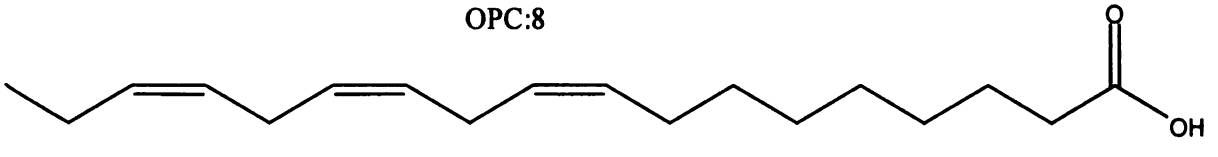

LA

Figure 3.2 continued

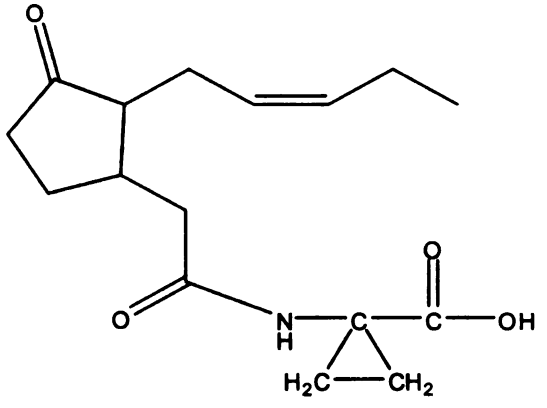

JA ACC

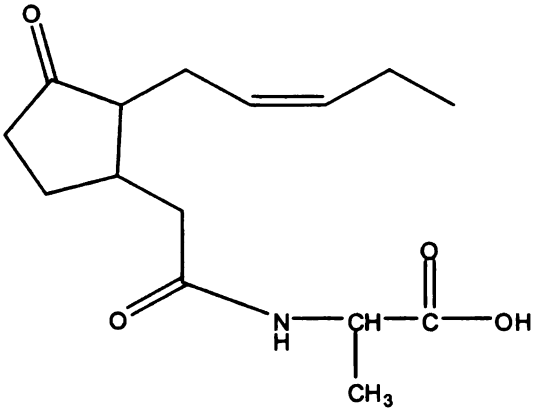

JA Ala

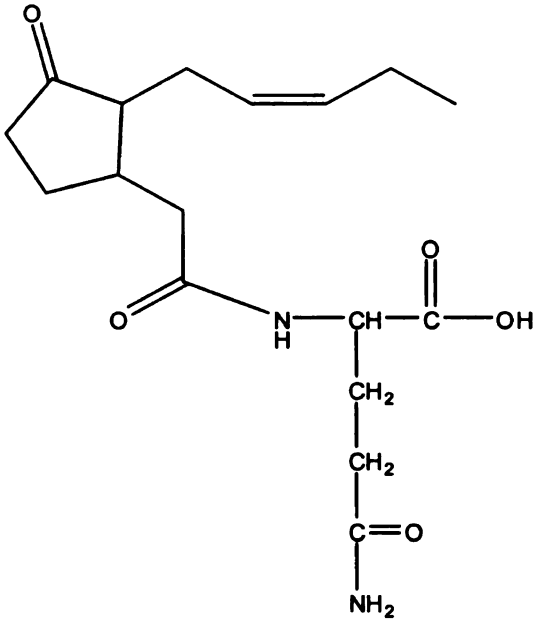

JA Gln

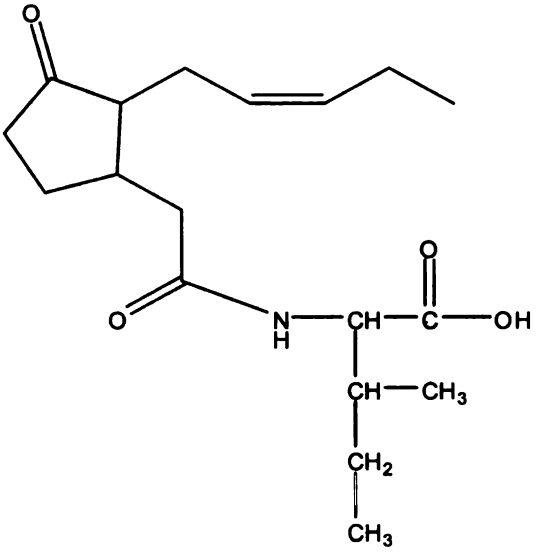

JA Ile

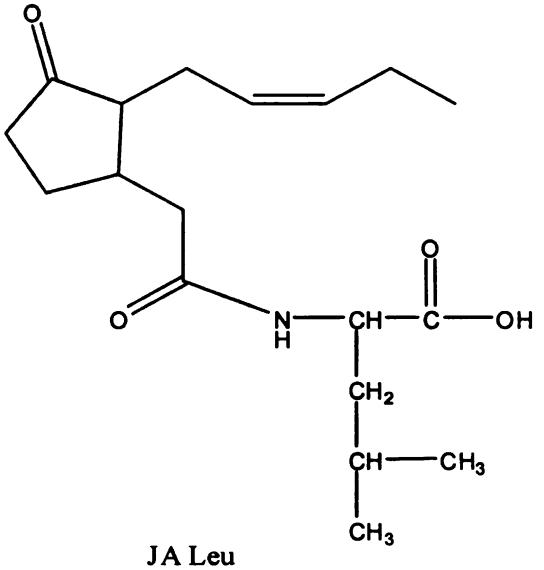

JA Leu

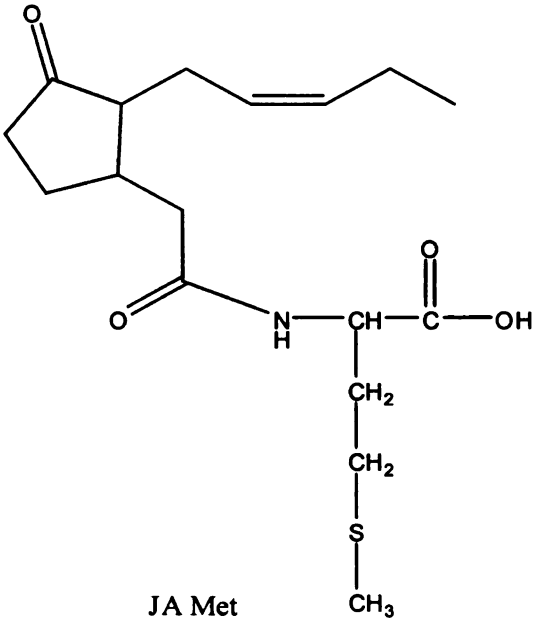

JA Met

Figure 3.2 continued

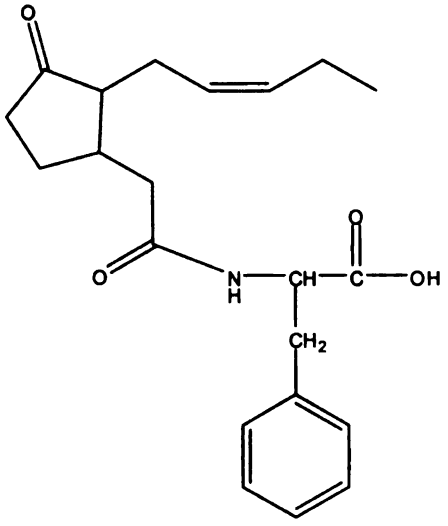

JA Phe

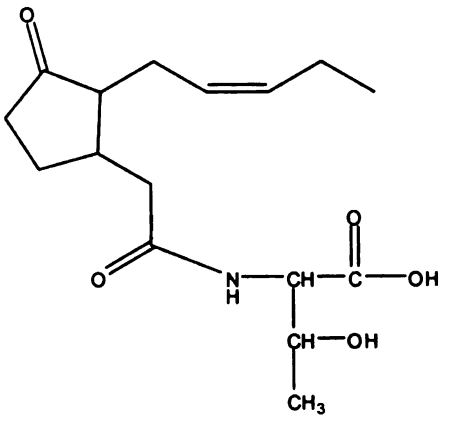

JA Thr

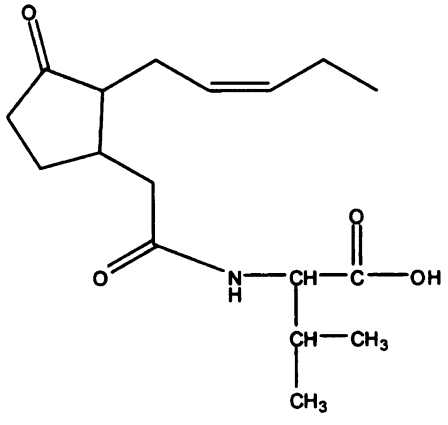

JA Val

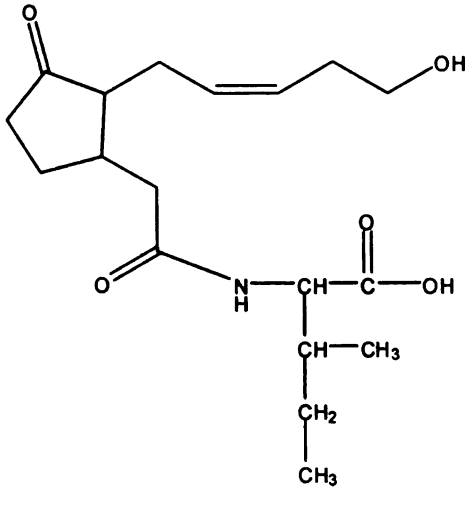

12-OH JA Ile

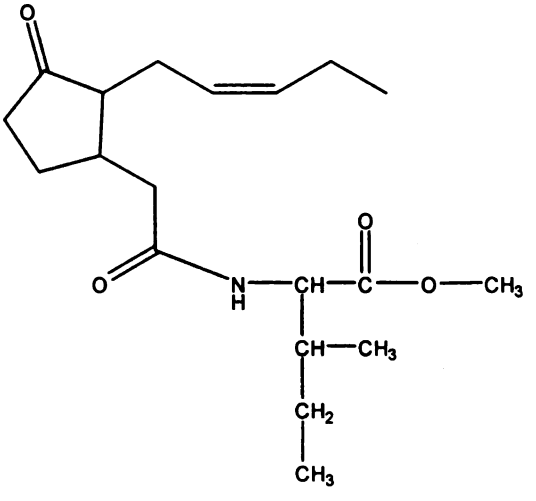

JA Ile Me

Figure 3.2 continued

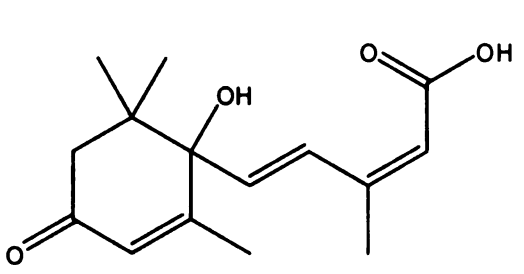

ABA

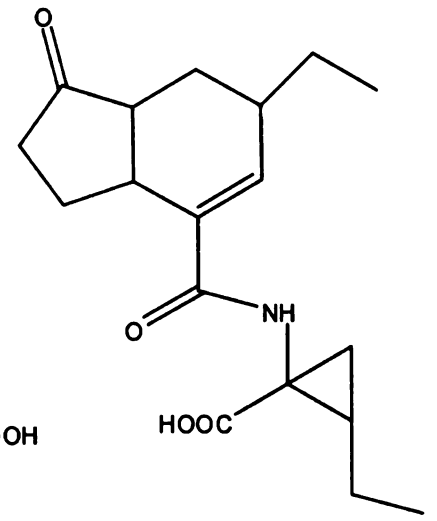

Cor

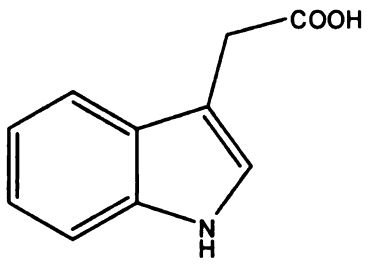

IAA

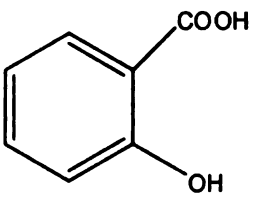

SA

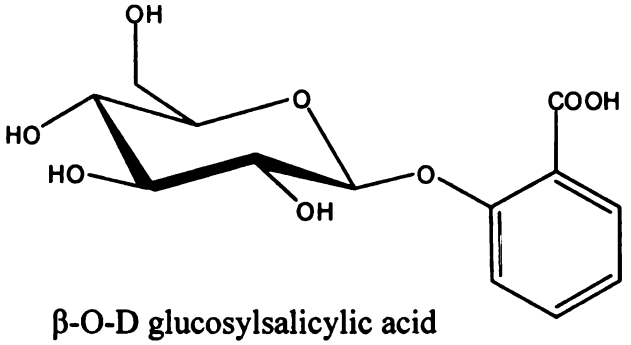

β-O-D glucosylsalicylic acid

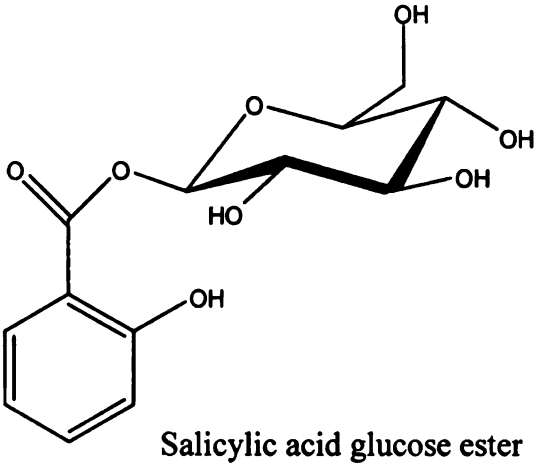

Salicylic acid glucose ester

SA glucosides

3.3.2 Plant Material, Growth Conditions and Plant Treatments

Arabidopsis thaliana ecotype Columbia-0 (Col-0) was used for all experiments. Soil-grown plants were maintained in a growth chamber at 22°C under 12 h light (100 μE m^{-2} s^{-1}) and 12 h dark.

For mechanical wounding treatments, fully expanded rosette leaves on 5-week-old plants were wounded three times by crushing the leaf across the midrib with a hemostat. This wounding protocol, which resulted in damage to approximately 40% of the leaf area, was administered to approximately six rosette leaves per plant (Chiwocha et al. 2003). For the pathogen stress treatment, 5-week-old plants were inoculated with *Pseudomonas syringae* DC3000 (~10^6 cfu/ml in 10 mM $MgCl_2$) via the stomata into the lower surface of half of the leaf. About 20 μL of the bacterial suspension was injected with a syringe via the stomata into the lower surface of half of the leaf. Control leaves were treated similarly with a sterile solution of 10 mM $MgCl_2$ (Katagiri et al. 2002). Local and systemic leaf tissues were harvested from control and stressed plants at 1 hour, 12 hours, one day and two days after inoculation. Tissues were immediately frozen in liquid nitrogen. Five biological replicates were performed.

3.3.3 Sample Preparation

Around 300 mg (10-14 leaves) of *Arabidopsis thaliana* leaves were harvested, immediately frozen in liquid nitrogen, ground and extracted with 2 ml methanol/water (80:20 v/v) containing 0.1% formic acid and 0.1 g/L butylated hydroxytoluene (BHT) at 4□ for 24 h. An aliquot of each internal standard solution was added to deliver 1.0 nmol each of internal standards dihydro-JA, [$^{13}C_6$]-JA-isoleucine and [$^{2}H_5$]-12-oxo-

phytodienoic acid ([$^2H_5$]-OPDA). Homogenates were mixed and centrifuged at 12,000*g* for 10 min at 4°C. Supernatants were filtered through a 0.2 μM PTFE membrane (Millipore, Bedford, MA) and transferred to autosampler vials without additional processing.

3.3.4 Liquid Chromatography and Mass Spectrometry

Plant extracts (5 μL extract per injection) were separated on a UPLC BEH C18 column (2.1 × 50 mm, 1.7 μm particles, Waters, Milford, MA) installed in the column oven of an Acquity Ultra Performance Liquid Chromatography (UPLC) binary pump and autosampler (Waters Corporation, Milford, MA). The performance of two additional LC columns was tested: a fused core Ascentis Express C18 column (2.1 × 50 mm, 2.7 μm; Supelco, Bellefonte, PA) and BetaBasic C18 column (1 × 150 mm, 5 μm; Thermo, Bellefonte, PA). A gradient of 0.15% aqueous formic acid (solvent A) and methanol (solvent B) was applied in a 5 min program with a mobile phase flow rate of 0.4 ml/min (0.15 ml/min for the 1 mm ID column) as shown in Table 3.1. The column, which was maintained at 50°C, was interfaced to a Quattro Premier XE tandem quadrupole mass spectrometer (Waters Corporation, Milford, MA) operated using electrospray ionization. The capillary, cone, and extractor potentials were set at 3 kV, 30 V, and 3V respectively. Flow rates of cone gas and desolvation gas were 100 and 800 L/h, respectively. Ion source and desolvation temperatures were 120 and 350 °C, respectively. Collision-induced dissociation employed argon as collision gas at a manifold pressure of 3×10^{-3} mbar, and collision energies and source cone potentials were optimized for each transition using Waters QuanOptimize software. This method was composed of two

negative ion functions (0-1.5 and 1.5-5.0 min) and one positive ion mode function covering full run time to allow for adequate dwell time for each analyte. Data were acquired under the control of MassLynx 4.0 software and processed for calibration and for quantification of the analytes using QuanLynx software.

Time (min)	Mobile phase A	Mobile phase B
0.0	60%	40%
1.0	40%	60%
3.0	25%	75%
3.5	0%	100%
4.51	60%	40%
5.0	60%	40%

Table 3.1 Mobile phase gradient in HPLC separation. Mobile phase A =0.15% aqueous formic acid, Mobile phase B= Methanol

3.3.5 Standard solutions

Jasmonoyl-amino acid conjugates were prepared and the structures were verified by GC-MS as described previously (Kramell et al. 1997; Staswick and Tiryaki 2004). OPC:6, OPC:8, OPDA, and dJA were prepared as previously described (Koo et al. 2006). [$^{13}C_6$]-JA Ile was synthesized by conjugation of cis-(±)-JA (Sigma, St Louis, MO, USA) to [$^{13}C_6$]-JA Ile (Cambridge Isotope Laboratories, Andover, MA, USA) as previously described (Kramell et al. 1997; Staswick and Tiryaki 2004). [$^{2}H_5$]-OPDA was prepared according to Delker et al. (Delker et al. 2007).

3.3.6 Quantification of JA Ile in mixtures of JA Ile and JA Leu.

Two positive mode MRM transitions established capability to distinguish isomeric Leu and Ile conjugates of JA based upon transitions of $[M+H]^+$ to m/z 30 and 69, respectively, even when chromatographic resolution is incomplete. To quantify of JA Ile

in mixtures of JA Ile and JA Leu, quantification curves were generated by plotting the percentage of JA Ile verses the peak area ratios of the transition 324 > 69 to 324 > 30.

3.3.7 Annotation of SA glucoside (SAG) isomers.

To confirm assignments of the two isomers of SAG, extracts of pathogen-infected leaves with high SAG levels were subjected to base hydrolysis by adding 10% aqueous NaOH to a final pH of 12.5). The reaction was stopped after 24 hours by adding formic acid to adjust the pH to 7. Levels of SAG and SA were assessed by LC MS/MS using the protocol described above.

3.3.8 Method Validation.

3.3.8.1 Limit of Detection (LOD)

The limit of detection (LOD) for each analyte was determined, using method calibration standard solutions, as three times the signal-to-noise ratio (S/N) as calculated using MassLynx software. Noise levels were determined for a 1-minute wide region of each MRM transition chromatogram.

3.3.8.2 Linearity and calibration curve

For the creation of calibration curves, 20 μM stock solutions of each of the 22 unlabeled compounds were used to prepare different concentration of standard solutions range from 2.5 nM to 5.0 μM. Dihydro-JA, [$^{13}C_6$]-JA Ile and [$^{2}H_5$]-OPDA were added as internal standards to give fixed concentration of 0.5 μM each, as was the case for all plant extracts. Data from analyses of these standards were used to create the calibration curves

for each compound by plotting the known concentration of each unlabeled compound as x-axis and peak area ratio of unlabeled compound/fixed concentration of labeled internal standard as y-axis using linear regression.

3.3.8.3 Calculations of matrix effect (ME %), recovery efficiency (RE %), and process efficiency (PE %)

Preextracts. To measure the efficiency of recovery of the target compounds from plant leaf extracts, dihydro-JA, [$^{13}C_6$]-JA Ile and [$^{2}H_5$]-OPDA internal standards were added to extraction buffer to make final preextracts with internal standards in each sample.

Postextracts. To measure matrix effects for dihydro-JA, [$^{13}C_6$]-JA Ile and [$^{2}H_5$]-OPDA internal standards and provide a comparison with the preextracts, we evaluated the effects of adding internal standards directly to filtered leaf extract to make final postextracts with internal standards in the sample.

3.3.8.4 Validate intra- and interday accuracy and reproducibility.

The accuracy of the method was examined by analyzing quality control samples in *Arabidopsis* leaf extracts using the method of standard additions. Four different concentrations of three unlabeled oxylipin conjugates standards JA, JA Ile and OPDA mix (0, 1, 3, or 5 μM) with fixed concentration of [$^{13}C_6$]-JA Ile internal standards (0.5 μM) were spiked in 1x, 0.5x, and 0.25x extracts for four replicates. Standard curves were generated by plotting the added concentration versus peak area ratio of phytohormone standards/internal standards, and the intra- and inter-day accuracies were calculated by

the following equation: accuracy (%) = 100 x calculated concentration/nominal concentration.

3.4 Results and discussion

The purpose of this study was to develop a method capable of large-scale measurements of target jasmonate and related phytohormones compatible with the needs of comprehensive studies of plant responses to wounding and disease. Development of the method was achieved by optimizing extraction, LC separation, and MS ionization and fragmentation to resolve and distinguish all target metabolites. At the end, the potential of this method as an aid to modeling plant metabolite profiles is evaluated.

3.4.1 Extraction procedure optimization

Six alternative suitable extraction systems were compared to optimize peak areas and recoveries of the phytohormones from *Arabidopsis* leaves after pathogen infection. Around 300 mg of leaves (10-14 leaves) from wounded *Arabidopsis thaliana* plants were frozen in liquid nitrogen, ground, and extracted with 2 ml of different extraction solvents at 4□ for 24 h. The six extraction solvents were (A) 50% methanol in water, (B) 80% methanol in water, (C) isopropanol, (D) ethyl acetate, (E) 3:2 hexane:isopropanol (v/v), and (F) 2:1 chloroform: methanol (v/v), with all solvents containing 0.1% formic acid and 0.1 g/L BHT. Target phytohormones were quantified in each extract using LC/MS/MS. Solvents B (80% methanol) and D (ethyl acetate) gave consistently higher phytohormone levels (10-20% more) compared with other solvents. Solvent B was

chosen for this study owing to its miscibility with water – a trait desirable for HPLC separations.

3.4.2 Development of LC separations for the simultaneous quantification of jasmonates and related phytohormones.

The method was developed and applied using a BEH C18 column (2.1 × 50 mm, 1.7 μm) (Waters, Milford, MA). Both the Waters and Supelco sub-3 μm particle columns gave exceptional separation efficiencies that allowed for steep solvent gradients and improved chromatographic resolution relative to the longer BetaBasic C18 column (5 μm particles) while yielding narrow chromatographic peaks ($w_{1/2}$ = 2.2 sec for JA Ile).

A mixture of 24 target analyte standards and 3 internal standards were separated using a 5-minute LC separation and detected by MS/MS as shown in Figure 3.3. Many synthetic JA amino acid conjugates and JA itself elute as two peaks because they are mixtures of isomers.

Figure 3.3 Extracted ion MRM chromatograms of 27 standard compounds. A mixture of 24 standards for the target analytes and 3 internal standards were separated and detected by HPLC-MS/MS using the transitions described in Table 3.2. The X-axis shows the retention time, and Y-axis indicates the relative intensity being set as 100% with the height of the highest peak of each measurement.

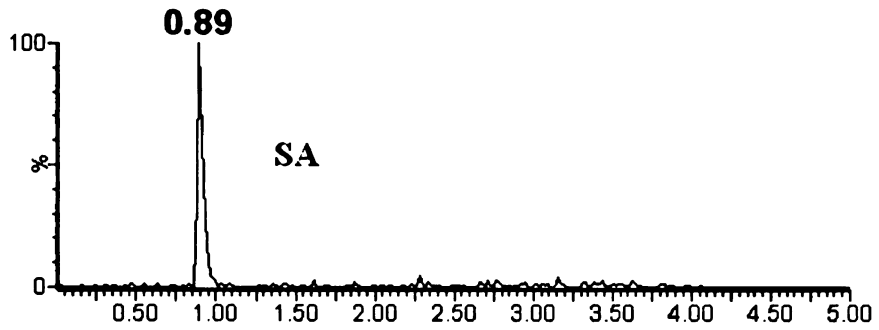
0.89
100
%
0
SA
0.50 1.00 1.50 2.00 2.50 3.00 3.50 4.00 4.50 5.00

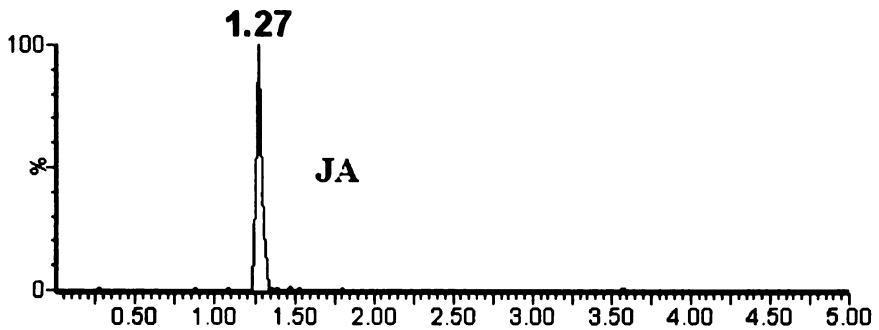
1.27
100
%
0
JA
0.50 1.00 1.50 2.00 2.50 3.00 3.50 4.00 4.50 5.00

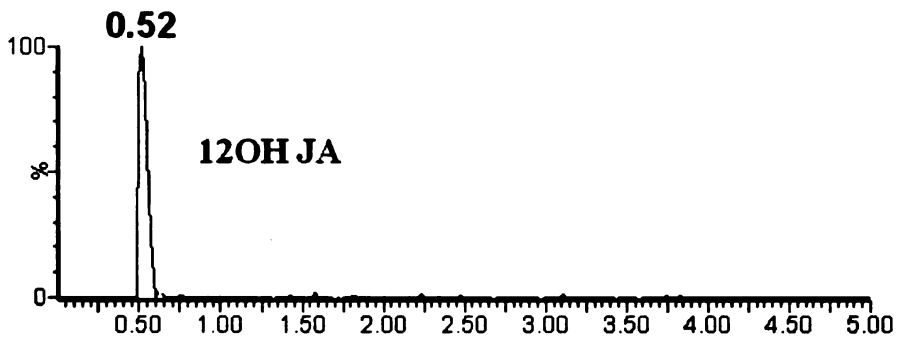
0.52
100
%
0
12OH JA
0.50 1.00 1.50 2.00 2.50 3.00 3.50 4.00 4.50 5.00

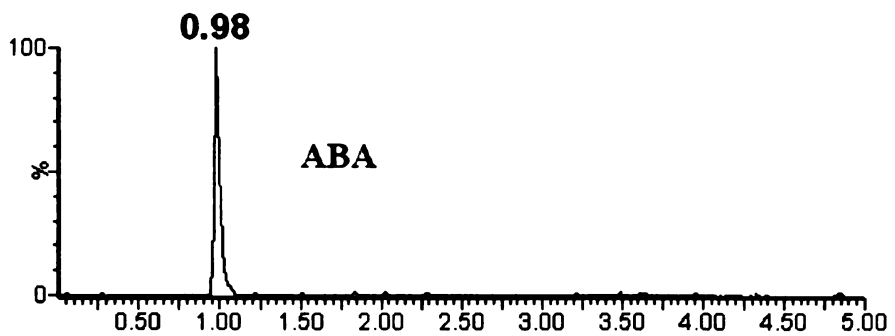
0.98
100
%
0
ABA
0.50 1.00 1.50 2.00 2.50 3.00 3.50 4.00 4.50 5.00


1.10
1.03
100
%
0
JA Ala
0.50 1.00 1.50 2.00 2.50 3.00 3.50 4.00 4.50 5.00

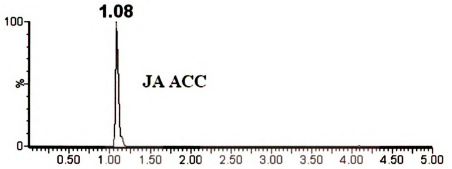
1.08
JA ACC
100
%
0
0.50 1.00 1.50 2.00 2.50 3.00 3.50 4.00 4.50 5.00

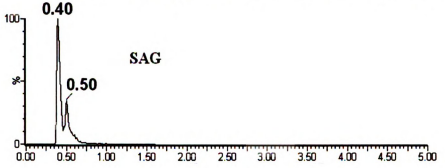
0.40
SAG
0.50
100
%
0
0.00 0.50 1.00 1.50 2.00 2.50 3.00 3.50 4.00 4.50 5.00

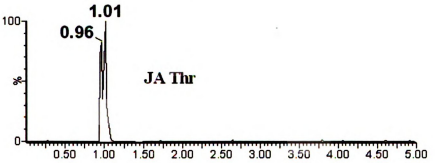
1.01
0.96
JA Thr
100
%
0
0.50 1.00 1.50 2.00 2.50 3.00 3.50 4.00 4.50 5.00

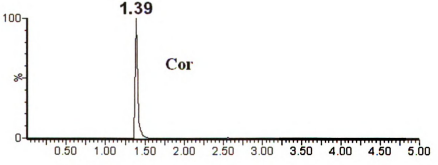
1.39
Cor
100
%
0
0.50 1.00 1.50 2.00 2.50 3.00 3.50 4.00 4.50 5.00

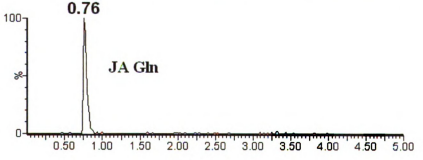
0.76
JA Gln
100
%
0
0.50 1.00 1.50 2.00 2.50 3.00 3.50 4.00 4.50 5.00

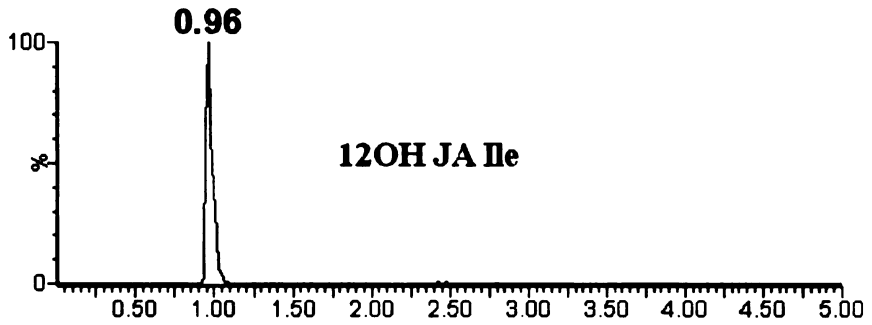
0.96
100
%
0
12OH JA Ile
0.50 1.00 1.50 2.00 2.50 3.00 3.50 4.00 4.50 5.00

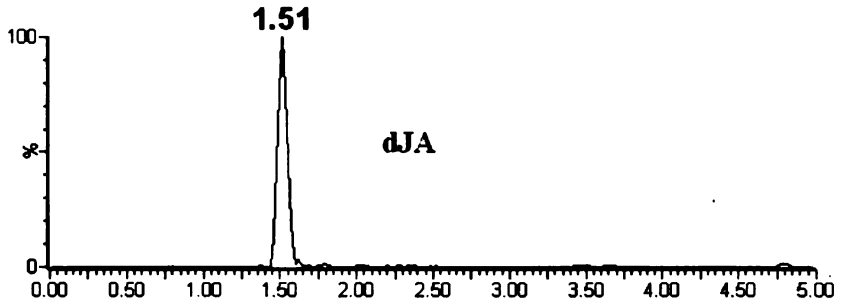
1.51
100
%
0
dJA
0.00 0.50 1.00 1.50 2.00 2.50 3.00 3.50 4.00 4.50 5.00

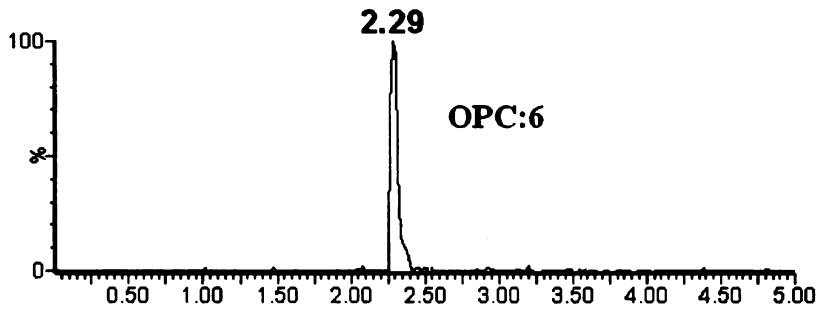
2.29
100
%
0
OPC:6
0.50 1.00 1.50 2.00 2.50 3.00 3.50 4.00 4.50 5.00

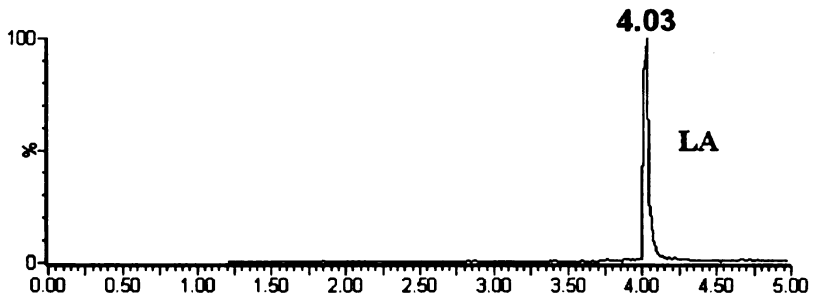
4.03
100
%
0
LA
0.00 0.50 1.00 1.50 2.00 2.50 3.00 3.50 4.00 4.50 5.00

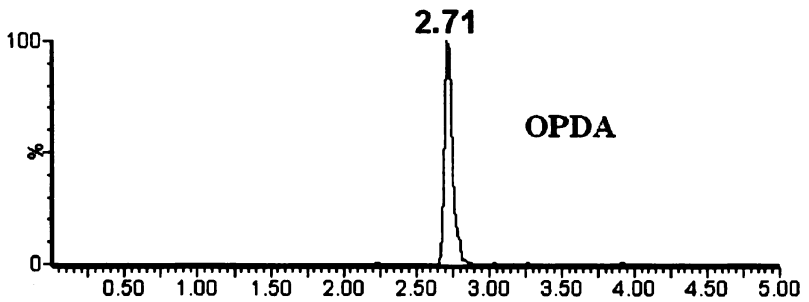
2.71
100
%
0
OPDA
0.50 1.00 1.50 2.00 2.50 3.00 3.50 4.00 4.50 5.00

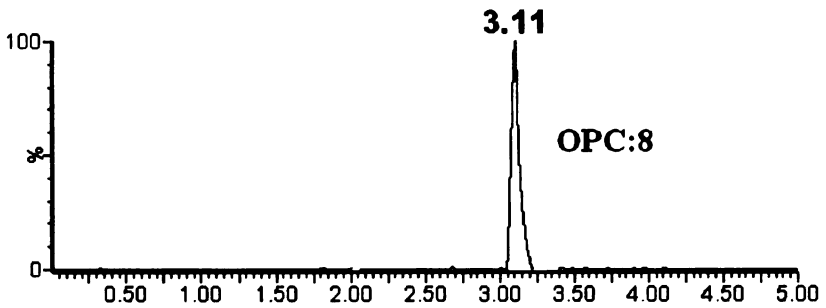
3.11
OPC:8
100
%
0
0.50 1.00 1.50 2.00 2.50 3.00 3.50 4.00 4.50 5.00

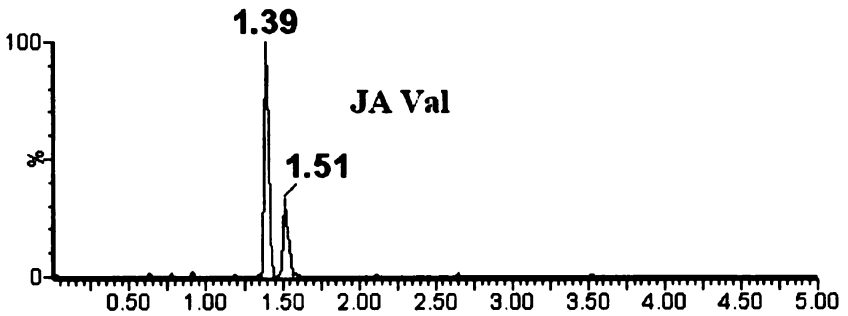
1.39
JA Val
1.51
100
%
0
0.50 1.00 1.50 2.00 2.50 3.00 3.50 4.00 4.50 5.00

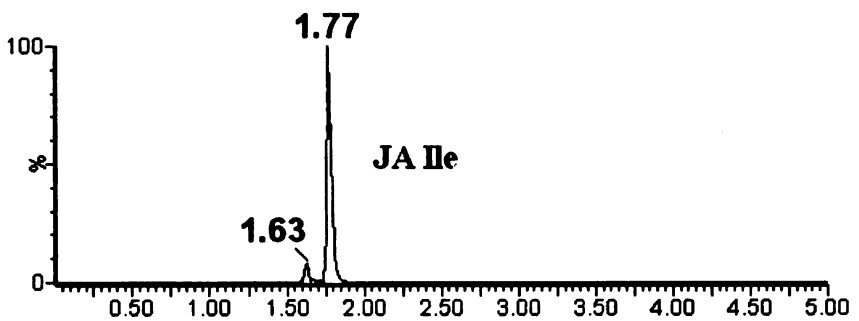
1.77
JA Ile
1.63
100
%
0
0.50 1.00 1.50 2.00 2.50 3.00 3.50 4.00 4.50 5.00

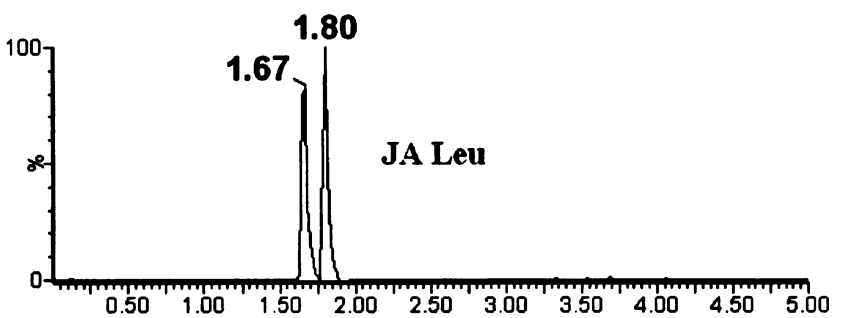
1.80
1.67
JA Leu
100
%
0
0.50 1.00 1.50 2.00 2.50 3.00 3.50 4.00 4.50 5.00

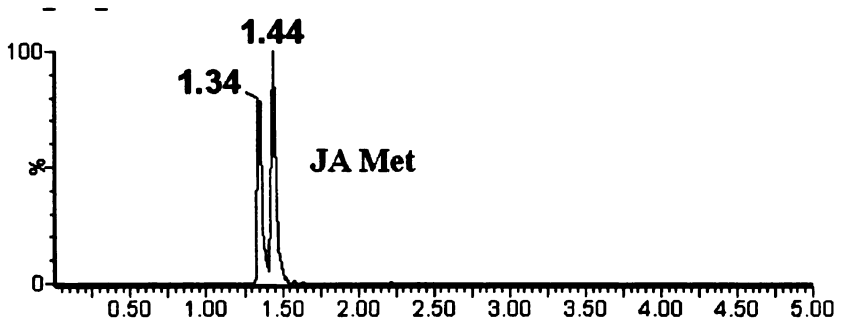
1.44
1.34
JA Met
100
%
0
0.50 1.00 1.50 2.00 2.50 3.00 3.50 4.00 4.50 5.00

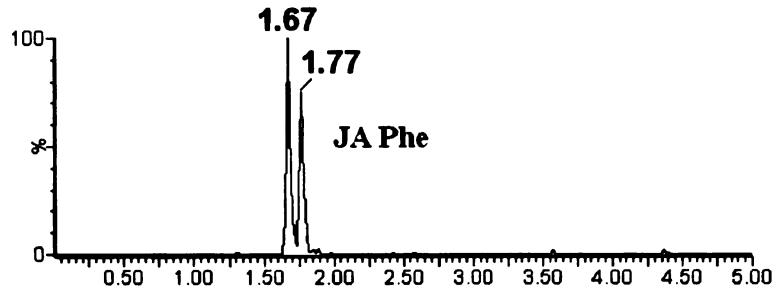
1.67
1.77
JA Phe
100
%
0
0.50 1.00 1.50 2.00 2.50 3.00 3.50 4.00 4.50 5.00

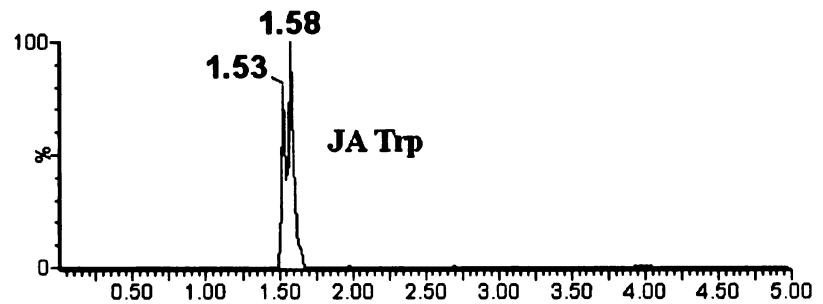
1.58
1.53
JA Trp
100
%
0
0.50 1.00 1.50 2.00 2.50 3.00 3.50 4.00 4.50 5.00

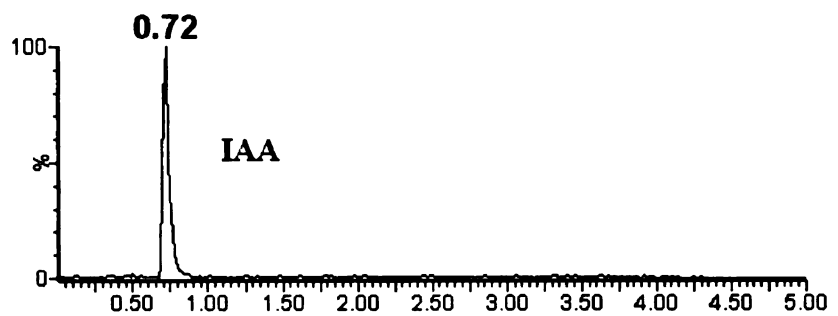
0.72
IAA
100
%
0
0.50 1.00 1.50 2.00 2.50 3.00 3.50 4.00 4.50 5.00

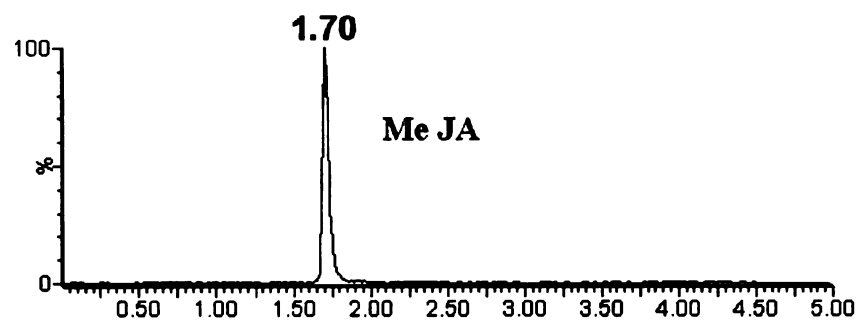
1.70
Me JA
100
%
0
0.50 1.00 1.50 2.00 2.50 3.00 3.50 4.00 4.50 5.00

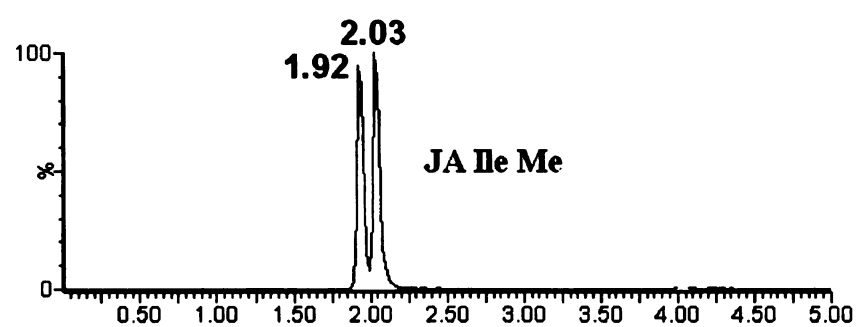
2.03
1.92
JA Ile Me
100
%
0
0.50 1.00 1.50 2.00 2.50 3.00 3.50 4.00 4.50 5.00

3.4.3 Development of multiple reaction monitoring (MRM) transitions for phytohormone analysis.

All target compounds were detectable using electrospray ionization. Positive mode ESI was employed to quantify IAA, the methyl esters Me JA, Me JA Ile, and for the purpose of distinguishing JA Leu and JA Ile based on isomer-selective fragmentation. All other phytohormones were measured using negative mode ESI. A pilot study demonstrated that IAA yielded about 10-fold greater MRM signal in positive mode than in negative mode. Despite the lack of a clearly basic functional group, the methyl esters Me JA and Me JA Ile yielded abundant $[M+H]^+$ ions in positive mode but $[M-H]^-$ ions were not detected in negative mode.

All of the JA amino acid conjugates were detected in both positive and negative modes. Negative mode has more than 10 times higher transition efficiency than the positive mode owing to fewer competitive fragmentation pathways. Product ion spectra of deprotonated JA amino acid conjugates were dominated by deprotonated amino acid ions (e.g. m/z 130 for JA Ile) as the dominant fragment ions. In positive mode, CID produced signal distributed over multiple fragment ions with none being dominant

JA Ile and JA Leu have similar structures, differing only the position of the side chain branch point. A recently reported LC/MS/MS method does not distinguish JA Ile from JA Leu, and values reported represent the sum of JA Ile plus JA Leu (Wang et al. 2007). In the current study, these isomers were chromatographically resolved during analysis of standard solutions (see Figure 3.3), but the minor isomer (JA Leu) could not be resolved from the more abundant JA Ile in the plant extracts using an MRM transition common to both metabolites. The fast UPLC separation did not resolve these isomers, and both gave

indistinguishable product ion spectra in negative mode. To solve this problem, collision induced dissociation (CID) spectra were generated in positive mode for $[M+H]^+$ ions. Selective transitions were discovered: m/z 324 > 69 and 324 > 30 for JA Ile and JA Leu, respectively. These transitions are analogous to those recently reported as selective product ions from protonated Ile and Leu respectively (Gu et al. 2007). To quantify JA Ile in mixtures of JA Ile and JA Leu, calibration curves were generated using standards with varying JA Ile/JA Leu ratios, and by plotting the percentage of JA Ile against the peak area ratios of the transitions m/z 324 > 69: 324 > 30 (Figure 3.4).

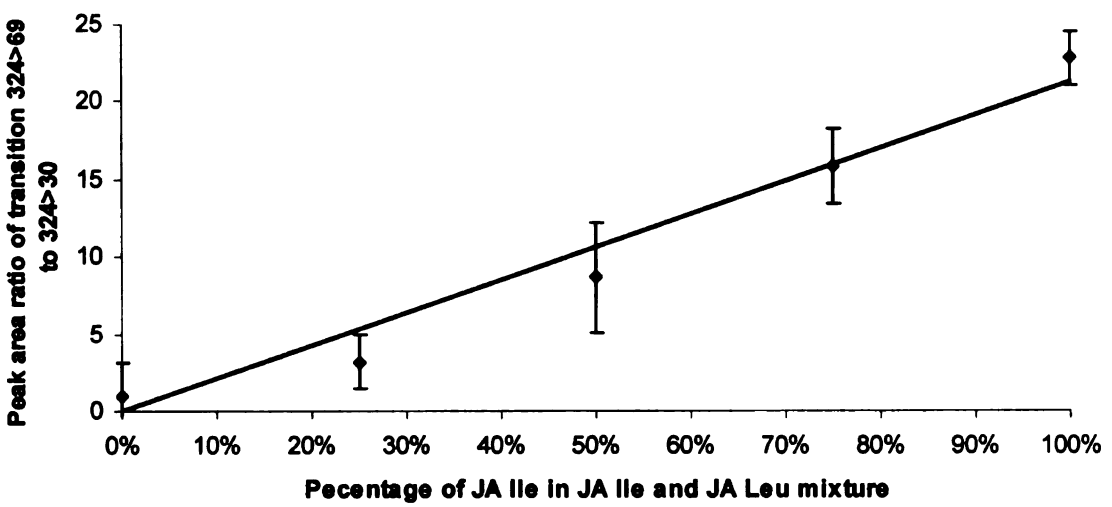

Figure 3.4 Quantification of JA Ile in mixtures of JA Ile and JA Leu. Two positive mode MRM transitions established capability to distinguish isomeric Leu and Ile conjugates of jasmonic acid based upon transitions of $[M+H]^+$ to m/z 30 and 69, respectively, even when chromatographic resolution is incomplete.

Oxylipins OPC:6, OPC:8, and precursor fatty acid LA yielded strong $[M-H]^-$ ions in negative ion mode, but none yielded abundant and analytically useful fragments. Although deprotonated ions fragmented by loss of CO_2, the high collision voltages (~60 V) needed to generate these fragments resulted in low ion transmission efficiencies (<

10%) in the mass spectrometer. Therefore, to provide low detection limits for these three analytes, MRM channels were set up with collision energy set to zero and both analyzers transmitted $[M-H]^-$, yielding selected ion monitoring (SIM) of these ions instead of MRM. It is noteworthy that while JA and OPDA fragment efficiently, the analogs OPC:6 and OPC:8 are resistant to fragmentation. These differences are attributed to the greater distances between the carboxylic acid group (where the charge is likely to be localized) and carbonyl or double bonds. For these oxylipins and LA, SIM analysis yielded nearly 100-fold lower detection limits for standards (~ 1 fmol injected) than could be achieved using MRM.

Analyses of *Arabidopsis* leaf extracts revealed several chromatographic peaks in the MRM channel for m/z 291 > 165 (Figure 3.5). This transition detects the oxylipin OPDA but only two isomers are commonly formed in plants, which result from two stereochemical configurations at the 13-position. The additional peaks are attributed to OPDA-containing glycerolipids that undergo partial fragmentation in the mass spectrometer ion source (Buseman et al. 2006).

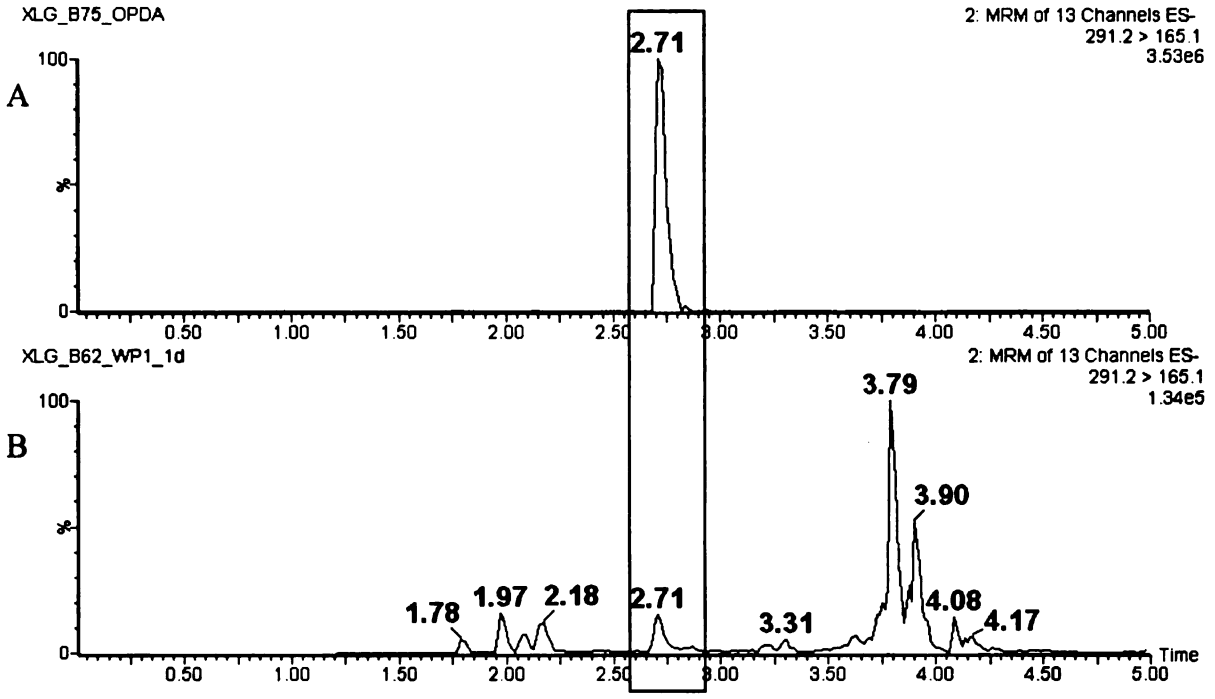

Figure 3.5 MRM transition of m/z 291.2 > m/z 165.1 from OPDA standard (A) and OPDA in pathogen stressed leave tissue (B). More than ten peaks showed up in Figure B. The peak with same retention time (2.71min) to OPDA standard is the free OPDA in the leave tissue. The other peaks are from the fragments of glycerolipids with OPDA conjugates.

This method provides for simultaneous measurements of the phytohormone salicylic acid (SA) and its two isomeric glucosides (SAGs): β-O-D glucosylsalicylic acid (GSA) and the acylglucoside salicylic acid glucose ester (SGE) (Figure 3.3). To distinguish SGE from GSA in an extract of *Arabidopsis* leaves, the extract was treated with base to effect selective hydrolysis of the acylglucoside, as the phenolic glucoside is resistant to base hydrolysis (Figure 3.6). The LC/MS/MS analyses of the untreated extract showed two SAG peaks with the minor peak (t_R = 0.50 min) giving a peak area 19% of the area of the major isomer (t_R = 0.40 min). After 24 h of base treatment, the peak for the minor isomer disappeared (from 3703 to 0), the major SAG peak remained largely unchanged (from 19637 to 20780), and the signal corresponding to the hydrolysis product SA increased

(from 7023 to 11643). Based on this result, we assign the early-eluting major isomer as GSA and the minor isomer is identified as SGE. LC/MS detection and quantification of SA glucoside isomers before and after base hydrolysis are shown in the Figure 3.7. Additional evidence for the SAG annotation came from product ion MS/MS spectra upon collision induced dissociation of $[M-H]^-$ for each isomer. The early eluting isomer gave products at m/z 137 and 93 corresponding to the salicylate anion and decarboxylated fragment respectively, whereas the later eluting isomer showed products at m/z 179 (deprotonated glucose), 161 (deprotonated anhydroglucose), 137, 93, and a radical ion at m/z 136 that is attributed to homolytic cleavage of the glucose ester bond. These results support the assignments made based on the hydrolysis result. Since the fragment at m/z 137 dominated the product ion spectra, the transition of m/z 299>137 was employed for both isomeric SAGs.

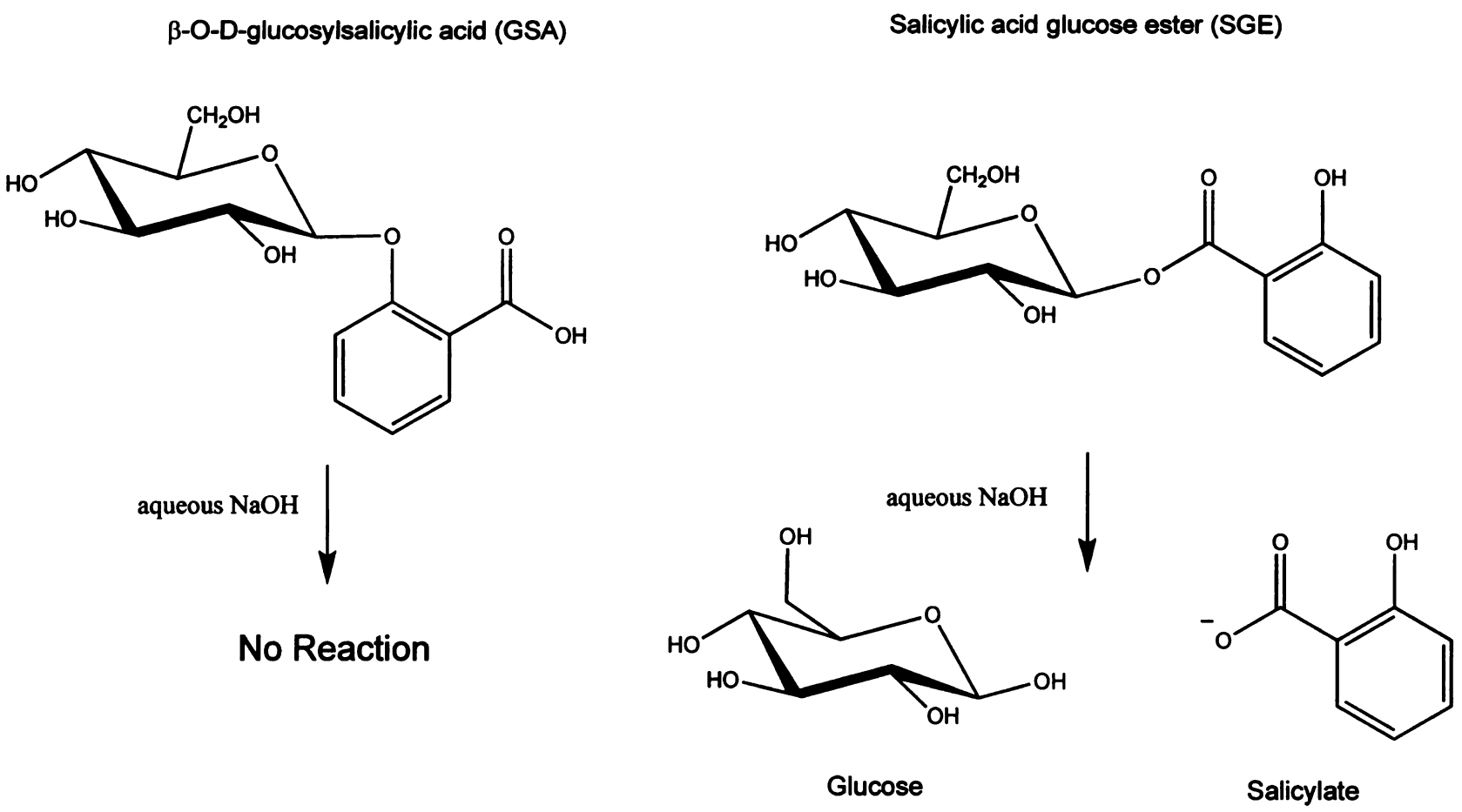

Figure 3.6 Distinguishing SA glucoside isomers through base hydrolysis.

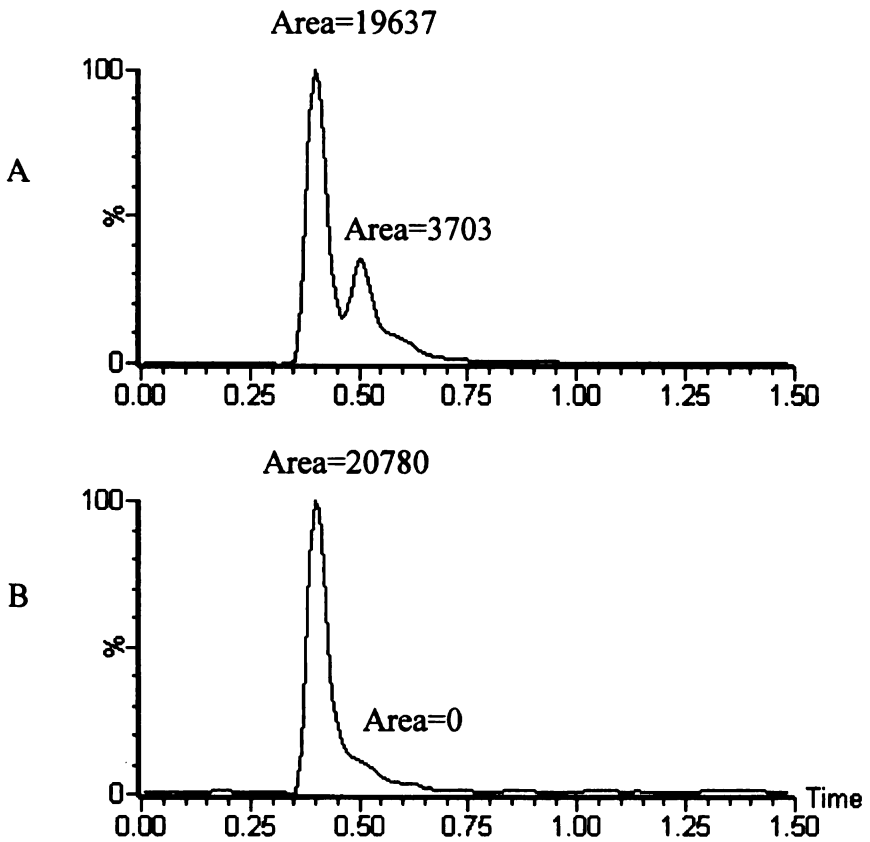

Figure 3.7 LC/MS detection and quantification of SA glucoside isomers before and after base hydrolysis. (A) Before base hydrolysis. (B) After base hydrolysis. MRM transition of m/z 299.1 > m/z 137.0 was used to select SA glucoside isomers.

After optimization of ion source cone and collision cell potentials, the data acquisition was split between two negative ion mode functions, with the first monitoring 11 MRM transitions from 0 to 1.5 min and the second monitoring 12 MRM transitions from 1.5 to 5.0 min. Eleven MRM transitions were included in function 1 and twelve in function 2. The HPLC retention times and optimized MRM parameters for these 24 compounds are summarized in Table 3.2.

Table 3.2 MRM transitions, optimized source cone voltages, collision cell voltages, and analyte retention times.
Notes: 1. When one single standard gives more than one peak, the different retention times of the peaks are separated by comas.
2. The internal standards(ISs) for quantification purpose are marked by asterisk (*).
3. Three internal standards(ISs) were used. A stands for dihydro-JA, B stands for [$^{13}C_6$] JA Ile and C stands for [$^{2}H_5$]12-oxo-phytodienoic acid (d_5-OPDA)

ES-	compound	Precursor ion> product ion (m/z)	Cone voltage(V)	Collision voltage (V)	Retention time (min)	function no.	Internal standard
	SA	137.0 > 93.0	34	22	0.89	1	B
	JA	209.1 > 59.0	28	16	1.27	1	A
	12-OH JA	225.2 > 59.0	28	16	0.52	1	A
	ABA	263.1 > 153.1	28	10	0.98	1	B
	JA Ala	280.2 > 88.1	28	22	1.03,1.10	1	B
	JA ACC	292.2 > 100.0	28	16	1.08	1	B
	SA Glucosides	299.1 > 137.0	34	22	0.40, 0.50	1	B
	JA Thr	310.2 > 266.2	34	16	0.96,1.01	1	B
	Cor	318.2 > 163.1	22	28	1.39	1	B
	JA Gln	337.2 > 145.0	34	22	0.76	1	B
	12-OH JA Ile	338.2 > 130.1	46	22	0.96	1	B
	*dJA	211.1 > 59.0	34	16	1.51	2	IS
	OPC:6	265.2 > 265.2	34	0	2.29	2	B
	LA	277.2 > 277.2	46	0	4.03	2	B
	OPDA	291.2 > 165.1	46	22	2.71	2	C
	*d5 OPDA	296.2 > 170.1	46	28	2.71	2	IS
	OPC:8	293.2 > 293.2	28	0	3.11	2	B
	JA Val	308.2 > 116.1	34	22	1.39,1.51	2	B
	JA Leu	322.2 > 130.1	34	22	1.67,1.80	2	B
	JA Ile	322.2 > 130.1	34	22	1.63,1.77	2	B
	*^{13}C JA Ile	328.2 > 136.1	34	22	1.63,1.77	2	IS
	JA Met	340.2 > 148.1	40	22	1.34,1.44	2	B
	JA Phe	356.2 > 164.1	34	22	1.67,1.77	2	B
	JA Trp	395.2 > 203.1	28	22	1.53,1.58	2	B

Table 3.2 continued.

ES+							
	IAA	176.1 > 130.0	22	10	0.72	1	B
	Me JA	225.1 > 151.1	22	16	1.7	1	B
	JA Leu	324.2 > 30.0	30	34	1.77,1.80	1	B
	JA Ile	324.2 > 69.0	30	34	1.66,1.77,1.85	1	B
	JA Leu/Ile	324.2 > 86.0	30	34	1.66,1.77,1.85	1	B
	*^{13}C JA Ile	330.2 > 91.1	28	28	1.66,1.78	1	IS
	JA Ile Me	338.2 > 86.0	34	28	1.94,2.05	1	B

3.4.4 Method validation

3.4.4.1 LOD

Detection limits ranged from 0.4 fmol for SA to 10 fmol for JA Val, which enable quantification of the relative lower level plant hormones (Table 3.3).

3.4.4.2 Linearity and calibration curve

For JA Ile quantification, [$^{13}C_6$]-JA Ile, obtained from chemical synthesis, is six Da heavier than JA Ile and can be used as an IS using isotope dilution methodology. The same method can be used to quantify OPDA with [$^{2}H_5$]-OPDA as IS. For JA and 12-OH JA analysis, dihydro-JA (dJA) has often been used. dJA is easily prepared compared with isotope labeled JA and is two mass units heavier than JA. For the other phytohormones, standards that are stable isotope-labeled versions or structurally-related analogs are scarce, therefore [$^{13}C_6$]-JA Ile was used as their IS instead.

Solutions containing varying amounts of each unlabeled analyte compound and a known, fixed amount of the corresponding internal standard (IS) were used to create calibration curves. Calibration curves were linear over the range of 2.5 nM to 5 μM. Average correlation coefficient limits (R^2 values) are from 0.980-0.999.

The precision of the method is also dependent on the ratio of IS and analyte compound and yields best precision when standard and analyte levels are within an order of magnitude of one another. Thus, the amount of IS added to samples should be in the range of the expected amount of the target compound. Though it is difficult to predict the change of levels of phytohormones, 0.5 μM dihydro-JA, [$^{13}C_6$]-JA Ile and [$^{2}H_5$]-OPDA internal standards were used in this study according to our previous experience.

3.4.4.3 Matrix effect (ME %), recovery efficiency (RE %), and process efficiency (PE %)

Matrix effect (ME %), recovery efficiency (RE %), and process efficiency (PE %) were calculated according to Matuszewski et al [Matuszewski, 2003 #92] with ME (%) = 100 ($area_{spiked\ after\ extraction}/area_{standard\ solution}$), RE (%) = 100($area_{spiked\ before\ extraction}/area_{spiked\ after\ extraction}$), and PE (%) = 100($area_{spiked\ before\ extraction}/area_{standard\ solution}$). The overall method efficiencies ranged from 60%-90% (Figure 3.4), which indicates that ion suppression by matrix constituents was not severe. The results suggest that the method is sufficiently robust for reliable quantification at levels found in wounded Arabidopsis leaves.

	ME (%)		RE (%)		PE (%)	
	mean	CV(%)	mean	CV(%)	mean	CV(%)
dJA (1 μM)	89.3	4.3	71.2	5.7	63.6	6.5
^{13}C JA Ile (0.5 μM)	61.2	5.9	83.9	3.7	51.4	7.3
d5 OPDA (1 μM)	63.3	13.2	80.8	10.1	52.0	15.4

Table 3.3 Matrix Effect (ME %), Recovery Efficiency (RE %), Process Efficiency (PE %) of the three internal standards. (n=6)

3.4.4.4 Intra- and interday accuracy and reproducibility

The retention times only shifted 0.01 min for all of the phytohormones, and the interday retention time precision (CV) ranged from 0.5 to 2%. These results indicate that the HPLC conditions are reproducible from run to run. Next, the intra- and interday precisions of peak area ratios of JA, JA Ile and OPDA versus their individual stable isotopically labeled internal standard were examined to evaluate the reproducibility of the system. The intra- and inter-day CVs were less than or equal to 5%.

3.4.5 Quantification of 24 plant hormones in wounding and pathogen stress samples.

To test the feasibility of using this method to analyze plant samples, *Arabidopsis* leaves were either mechanically wounded or infected with bacterial pathogen *P. syringae*, followed by UPLC MS/MS analysis of leaf extracts.

In the control samples without any treatment, most of the phytohormones were at levels less than 100 fmol/mg fresh weight except GSA, OPDA and LA. Eight (JA Ala, JA ACC, JA Met, JA Trp, Me JA, JA Ile Me, Cor, and IAA) were not present at detectable levels. After wounding stress, JA, 12OH JA, 12OH JA Ile, LA, OPDA, OPC:6, and OPC:8 were induced to more than 100-fold greater levels than basal levels in unwounded plants. JA-Ala, JA-Gln, JA-Phe, JA-Thr, and JA-Val were also induced but only 10- to several hundred-fold. The biological functions of these signaling compounds, especially JA and JA Ile, were described in a recent report resulting from our collaborative efforts that employed a variation on this method (Koo et al. 2009). In Arabidopsis leaves, we found JA Ile is more abundant than JA Leu after wounding stress, accounting for 85-100% of the total amount of JA Ile and JA Leu. Previous reports documenting the steep rise and fall of JA levels in response to wounding imply the existence of an efficient mechanism to metabolize them, which may involve hydroxylation, conjugation with amino acids, and glycosylation. In this study, we reported levels of hydroxylated and amino acid conjugates ran parallel with the induction of JA such as 12OH JA and JA Ile.

After pathogen stress, the major induced compounds in leaf extracts were SA, ABA, GSA, and SGE, increasing by as much as several thousand-fold. Cor was produced *de novo* by the pathogen, and its levels may provide a measure of the extent of pathogen infection. The SGE was barely above limits of detection in control samples, but levels

increased by 50-fold after pathogen stress. However, GSA was shown as an abundant compound both in control and pathogen stress samples. LA, OPC:6, OPC:8, and OPDA were also induced, but less than 10-fold.

From Table 3.4, we conclude all phytohormones in this study can be detected in stressed plants, with JA-Ala and JA-Phe only observed in wounding stress. Although the mechanisms of induction of jasmonates and related compounds remain to be elucidate, the changes in the levels of these compounds provides substantial evidence that they play an important role in regulating gene expression and metabolite profiles. An in-depth analysis of the dynamics of these compounds and their functional consequences is of utmost importance in order to give an accurate description of metabolic responses in plant-pathogen interactions.

Table 3.4 Levels of phytohormones in extracts of control, wounded, and *P. syringae* infected *Arabidopsis* leaves[a].

[a] Phytohormone levels are expressed as mean ± SD (fmol/mg fresh weight) for three biological replicates.

[b] LOD = Limit of detection. Reported limits of detection were determined as the amount injected on column that gave a signal-to-noise ratio (with noise determined as the root-mean-square level remote from the metabolite MRM peak) equal to 3.

[c] Wounding: Leaves were wounded three times across the midvein using a hemostat. Local wounded tissue was harvested 1 h after wounding.

[d] Pathogen infection: Leaves of Arabidopsis plants were infiltrated with the virulent strain of *P. syringae* and harvested after 1 day. Inoculation control plants were infiltrated with $MgCl_2$ solution as described in the text.

[e] Limits of detection were not established owing to the unavailability of authenticated reference standards of known concentration.

Compound	LOD[b] (fmol injected)	Wounding Control[c]	Wounded Leaves[c]	Inoculation Control[d]	Pathogen infected [d]
Salicylates					
SA	0.4	242 ± 41	740 ± 122	276 ± 50	4430 ± 200
GSA	not established[e]	2540 ± 110	2850 ± 95	2910 ± 89	11800 ± 1680
SGE	not established[e]	7 ± 1	6 ± 1	15 ± 1	800 ± 4
Jasmonates					
JA	6.9	41 ± 3	20300 ± 1000	50 ± 4	1590 ± 3
JA Ile	2.5	12 ± 4	1690 ± 81	10 ± 3	15 ± 1
12-OH JA	7.2	8 ± 2	3790 ± 150	18 ± 2	99 ± 4
12-OH JA Ile	3.2	43 ± 3	3380 ± 180	40 ± 3	47 ± 2
JA Val	10.0	7 ± 1	279 ± 13	7 ± 1	172 ± 8
JA Leu	2.5	3 ± 4	145 ± 7	3 ± 3	3 ± 3
JA Gln	8.4	7 ± 1	135 ± 12	6 ± 1	17 ± 2
JA Thr	9.5	8 ± 2	31 ± 2	10 ± 3	14 ± 2
JA Phe	4.5	7 ± 1	24 ± 2	<LOD	<LOD
JA Ala	5.4	<LOD	23 ± 2	<LOD	<LOD
JA ACC	8.0	<LOD	8 ± 2	<LOD	6 ± 1
JA Met	9.3	<LOD	8 ± 1	<LOD	5 ± 1
JA Trp	7.3	<LOD	5 ± 1	<LOD	4 ± 1
Me JA	1.6	<LOD	41 ± 3	<LOD	25 ± 2
JA Ile Me	1.4	<LOD	13 ± 2	<LOD	<LOD
Jasmonate analogs					
Cor	4.5	< LOD	< LOD	< LOD	300 ± 14
Linolenic acid and related oxylipins					
OPDA	1.0	335 ± 15	18200 ± 890	410 ± 15	989 ± 49
OPC:8	1.2	50 ± 3	620 ± 28	46 ± 5	817 ± 37
OPC:6	1.6	59 ± 3	397 ± 18	69 ± 3	110 ± 16
LA	1.0	677 ± 26	3160 ± 150	577 ± 26	773 ± 37
Other phytohormones					
ABA	3.3	10 ± 3	12 ± 3	15 ± 4	297 ± 13
IAA	1.1	<LOD	5 ± 1	15 ± 1	246 ± 12

3.5 Conclusions

A fast UPLC MS/MS method was used to generate quantitative profiles of 24 jasmonate-related metabolites. Six different extraction procedures were compared and the procedure with the most consistently high efficiency involved extraction with methanol/water (80:20). Twenty-three oxylipin and salicylate phytohormones are measured within 5 min using a UPLC BEH C18 column and rapid gradient multiple reaction monitoring (MRM) transitions selective for each compound. Most compounds were analyzed using negative mode electrospray ionization. Positive mode ESI was chosen for methylated conjugates methyl jasmonate, JA-isoleucine methyl ester, JA Leu and JA Ile. Two positive mode MRM transitions established capability to distinguish isomeric Leu and Ile conjugates of jasmonic acid based upon transitions of $[M+H]^+$ to product ions at m/z 30 and 69, respectively, even when chromatographic resolution is incomplete. For acidic lipids (OPC:6, OPC:8, linolenic acid) that are ionized well but are difficult to fragment, collision energy is set to zero and selected ion monitoring is performed within the same method. Compared to derivatization-based GC/MS methods, this UPLC-MS/MS approach involves minimal sample processing and avoids sample losses during evaporation and derivatization, requires only 5 min instrument time per sample, and yields precise quantification of a broad range of jasmonates and related metabolites down to less than five femtomoles. The method is well-suited for monitoring the dynamics of signaling metabolites in studies of wounding, pathogen stress, and other plant stress, and is recommended to laboratories as a practical alternative to measurements of single phytohormones.

CHAPTER 4

Conclusions and perspectives

4. Conclusions and perspectives

4.1 Conclusion of thesis project

At the outset of this project, nearly all published reports on metabolomics relied on mature GC/MS technologies. These experimental approaches provided extensive data sets, but were limited to detection of small primary metabolites such as amino acids, organic acids, and simple sugars. Prior to my dissertation research, published reports of nontargeted profiling of metabolites using LC/MS were rare and were limited by the lack of LC/MS spectrum databases and long HPLC separations that precluded analyses of large sample sets. For these reasons, LC/MS was viewed as a powerful method for measuring known secondary metabolites, but successes in identifying new and unanticipated metabolites were few. In addition, developments of LC/MS metabolomic approaches for identifying gene functions were in their infancy when these projects were initiated.

Despite the slow start, metabolite profiling has emerged a fast-growing technology for phenotyping and diagnostic analyses of plants (Schauer and Fernie 2006). In this study, my efforts have focused on developing and applying two complementary approaches for using metabolite profiling to expand functional annotation of genes and to build a more comprehensive understanding of the cellular responses to changing environments. In Chapter 2, nontargeted LC/MS metabolite profiling of wild type and *omt1* mutant Arabidopsis plants was performed under control and pathogen stress conditions to reveal mechanisms of direct and pleiotropic influences of the OMT1 gene. The findings identified roles for specific polyphenols, their quinone metabolites, and glutathione in pathogen resistance. The results of this study suggested potential

mechanisms by which changing the extent of polyphenol methylation could modulate levels of metabolites capable of redox cycling, generating ROS, and influencing phytohormone and phytoalexin signaling networks. In Chapter 3, a fast, accurate, and targeted analytical method was developed to measure a wide assortment of phytohormones in regulation of gene expression and signal transduction in wounding stress. These two approaches bear similarities to nontargeted and targeted measurements of gene expression, in the manner that microarrays and quantitative real-time PCR are used in modern research.

Most previous publications on the subject of nontargeted metabolite profiling in plants have employed plants grown under carefully controlled environments to minimize unintended phenotypic variations. Though a few concurrent studies have broken with this tradition to study stress responses (Boccard et al. 2007; Kim et al. 2007; Alvarez et al. 2008; Glauser et al. 2008), there remain great opportunities to pursue this kind of approach to learn about roles for specific genes and environmental conditions on plant phenotypes.

4.2 Opportunities for future research

4.2.1 Designer plants for control of OMT function

Since the *omt1* mutant showed the ability to inhibit bacterial growth, metabolic engineering of plants for optimal production of o-dihydroxylated polyphenols may be useful to increase plant resistance to pathogen infection.

4.2.2 More studies on quinones and glutathione conjugates

It is hoped that the finding of polyphenol quinone metabolites that exhibit anti-microbial properties will raise awareness of their potential in enhancing plant resistance to pathogens, and perhaps, other stress conditions. Since there are such big pools of polyphenols (flavonoids) which have the potential to be oxidized to quinones, it will be interesting to identify more quinones and study the functions of these compounds.

Metabolic conjugation of GSH to reactive electrophilic metabolites is well-documented as a detoxification mechanism in animals (Chroust et al. 2001; Coles and Kadlubar 2003; Pastore et al. 2003), but our understanding of GSH conjugation in plants is still an emerging field of study. The potential importance of GSH conjugation is suggested by 54 glutathione S-transferase genes in the genome of *Arabidopsis thaliana* (Marrs 1996; Neuefeind et al. 1997; Dixon et al. 2009).

Furthermore, several electrophilic oxylipin metabolites have been observed to form GSH conjugates (Davoine et al. 2005), and this may represent a competing sink for quinone metabolites. In this study, some polyphenolic-glutathione conjugates were discovered. My preliminary studies that have employed LC/multiplexed CID for metabolite profiling have suggested the presence of dozens of glutathione conjugates in extracts of plant leaves. Understanding the interaction of secondary metabolite biosynthetic pathways with glutathione S-transferase functions may lead to novel discoveries in the area of plant biochemistry.

4.2.3 New trends in plant metabolomics

Integration of 'omics' studies

Currently, most plant stress response studies use one or two "omics" approaches of those 'omics' studies (Weckwerth 2008). Integrated analysis of metabolite, transcript, and protein levels in plant systems identified several important features of plant metabolic regulation (Hirai et al. 2005; Le Lay et al. 2006). In the future, using a combination of all three "omics" approaches or more will unleash the potential of systems biology to uncover mechanisms regulating plant stress response on various levels (Shulaev et al. 2008).

Plant micrometabolomics: the analysis of single cells or tissues

Most metabolomic studies have been conducted at the whole tissue level. Metabolomics within specific cell types or single cells is of particular interest for natural product chemistry, chemical ecology, and biochemistry (Moco et al. 2009) because functions are organized at cellular and subcellular levels. Plants are considered to have about 40 different cell types, therefore, they are likely to have different metabolites profiles in different cell types (Martin et al. 2001). Localization of particular metabolites in certain organelles is important to interpret functions of those metabolites.

Several technical challenges confront investigators hoping to use metabolomics to discover new gene functions and enhance understanding of cellular physiology. As mentioned above, metabolomic studies would be most useful if they integrated nontargeted and targeted metabolite data for multiple genotypes, treatments, time points, and tissue or cell types. For this to become practical, further improvements in pipeline throughput and analytical limits of detection will be needed. Ongoing efforts in these areas promise to make important advances over the coming years, and we may expect

metabolome analyses to have more prominence in functional genomic studies of plants and other organisms.

Appendix A

Levels and chemical structures of metabolites

WC: wild type control, with the infiltration of $MgCl_2$ buffer

MC: mutant control, with the infiltration of $MgCl_2$ buffer

WP: wild type with the infiltration of *P. syringae*

MP: mutant with the infiltration of *P. syringae*.

4-Methylsulfinylbutyl glucosinolate (m/z 436.04)

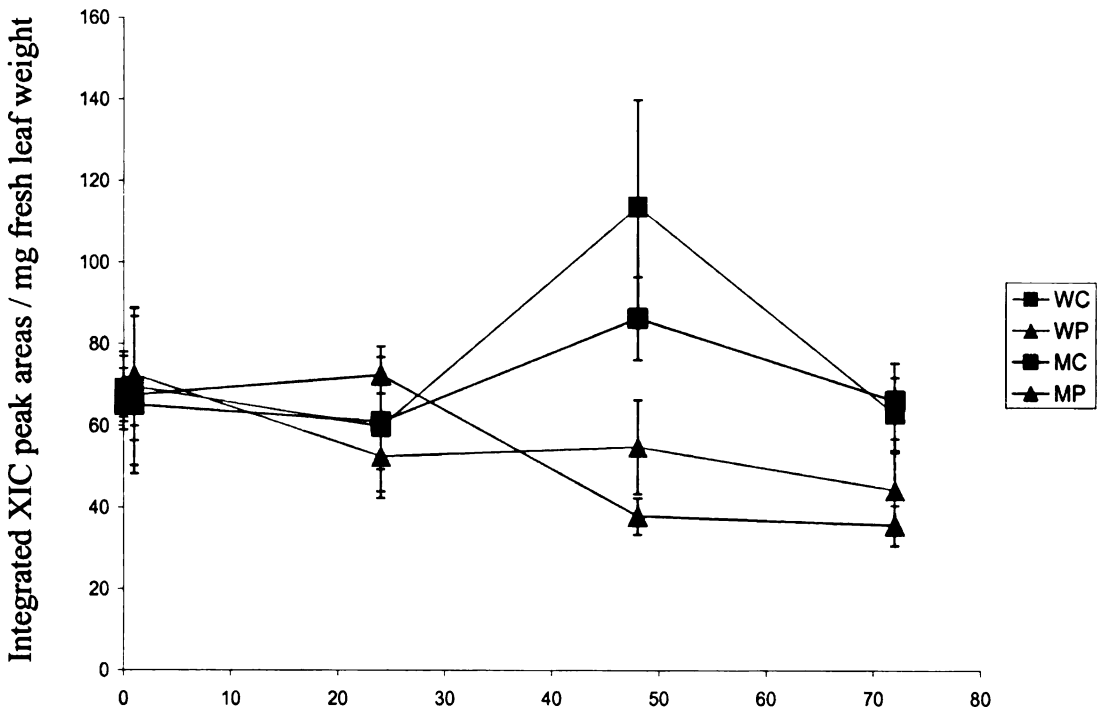

T-test analysis on metabolite levels

	1h	1d	2d	3d
WC vs MC	N.S.	N.S.	N.S.	N.S.
WP vs MP	N.S.	N.S.	N.S.	N.S.
WC vs WP	N.S.	N.S.	*	*
MC vs MP	N.S.	N.S.	*	*

"*" significant, $p < 0.05$

"N.S." not significant

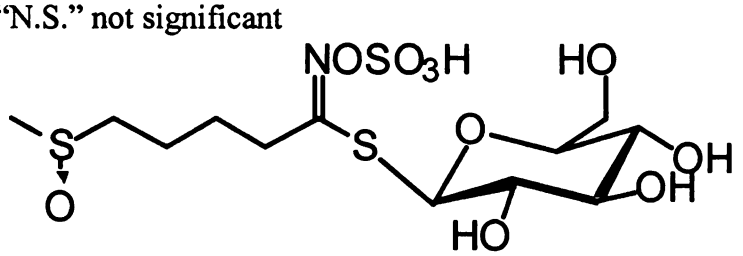

8-Methylsulfinyloctyl glucosinolate (m/z 492.11)

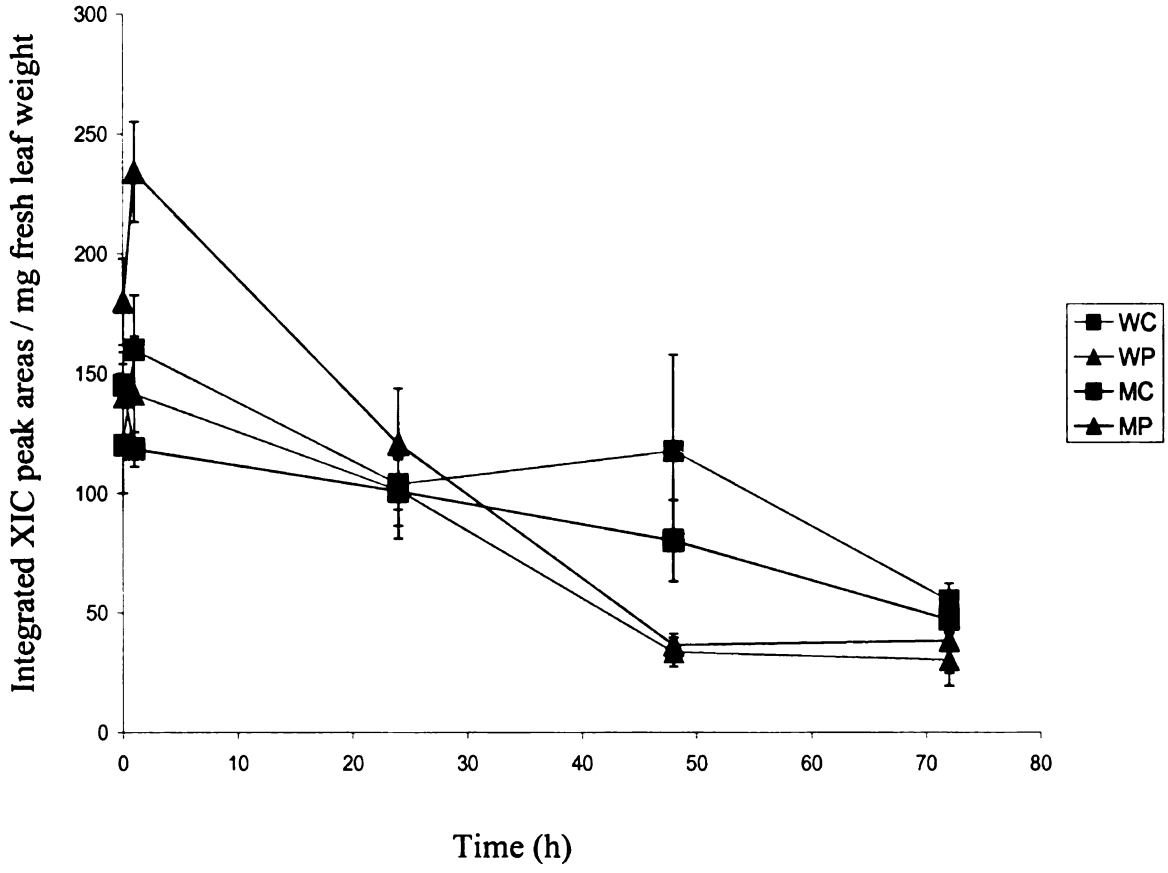

T-test analysis on metabolite levels

	1h	1d	2d	3d
WC vs MC	N.S.	N.S.	N.S.	N.S.
WP vs MP	*	N.S.	N.S.	N.S.
WC vs WP	N.S.	N.S.	*	N.S.
MC vs MP	*	N.S.	*	N.S.

"*" significant, $p < 0.05$
"N.S." not significant

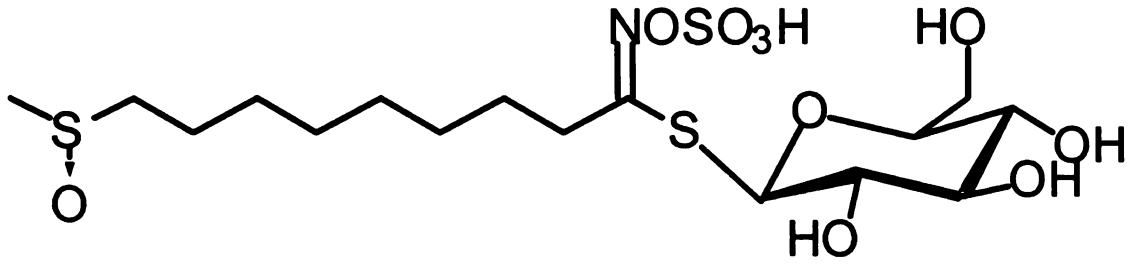

4-Methylthiobutyl glucosinolates (m/z 420.05)

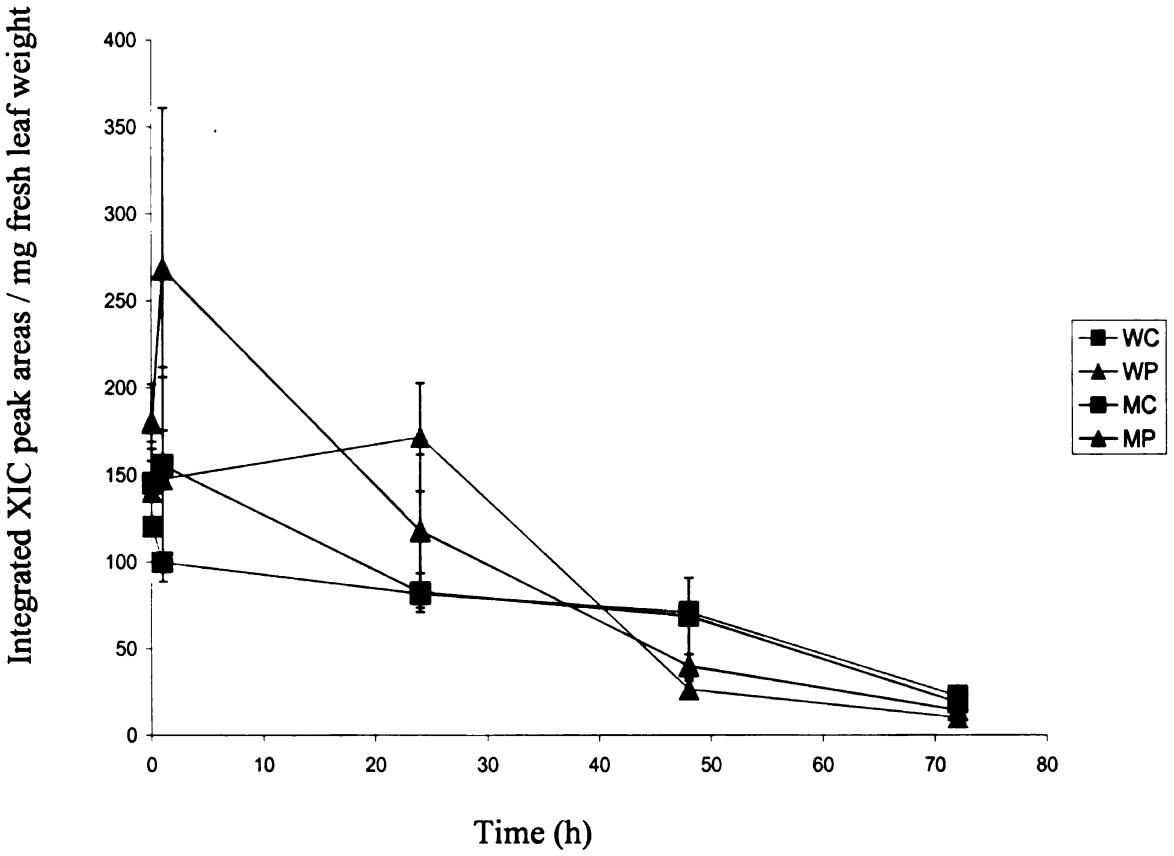

T-test analysis on metabolite levels

	1h	1d	2d	3d
WC vs MC	N.S.	N.S.	N.S.	N.S.
WP vs MP	N.S.	N.S.	N.S.	N.S.
WC vs WP	N.S.	N.S.	*	N.S.
MC vs MP	N.S.	N.S.	*	N.S.

"*" significant, $p < 0.05$
"N.S." not significant

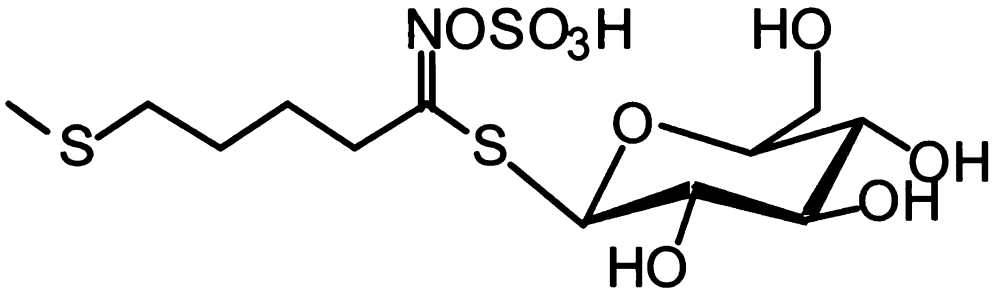

8-Methylthiooctyl glucosinolate (m/z 476.11)

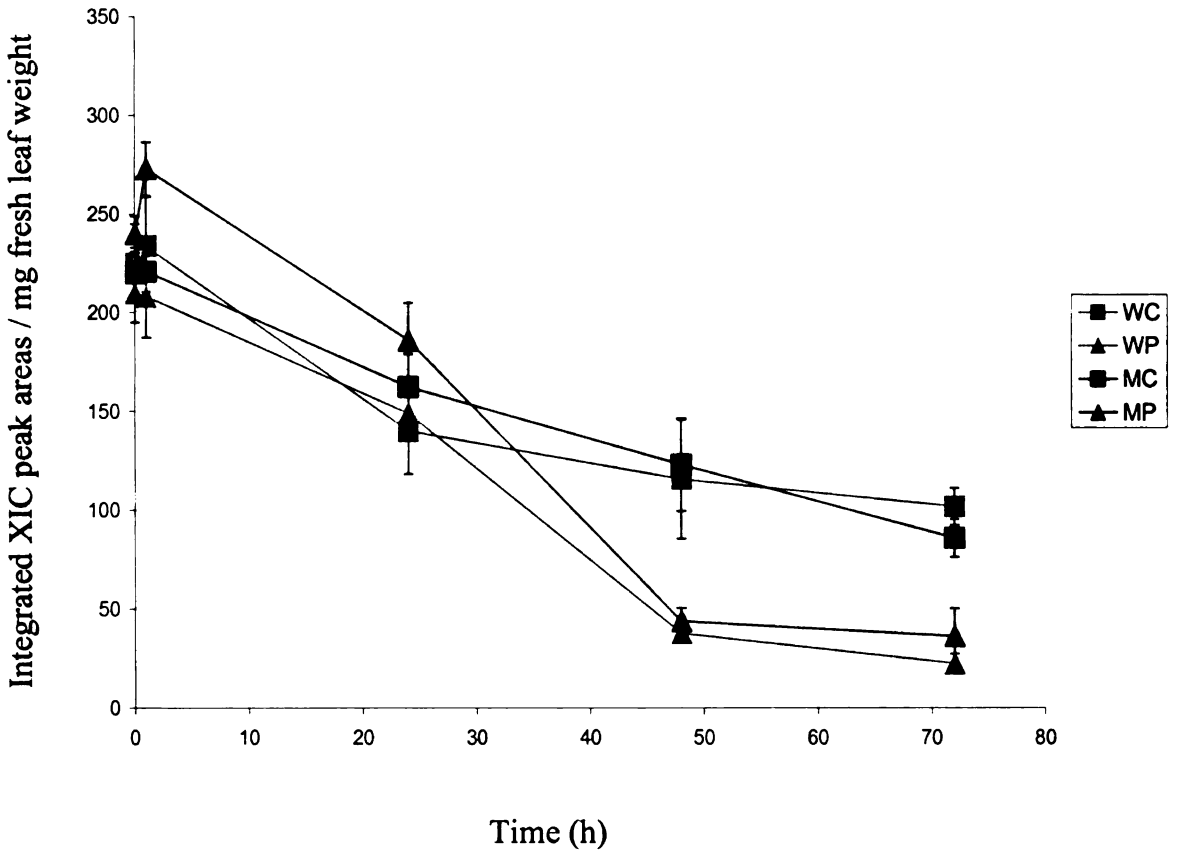

T-test analysis on metabolite levels

	1h	1d	2d	3d
WC vs MC	N.S.	N.S.	N.S.	N.S.
WP vs MP	N.S.	N.S.	N.S.	N.S.
WC vs WP	N.S.	N.S.	*	*
MC vs MP	N.S.	N.S.	*	*

"*" significant, $p < 0.05$
"N.S." not significant

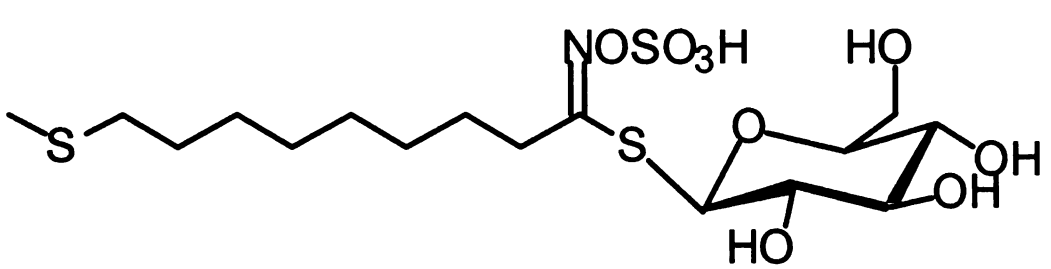

3-Methylsulfinylpropyl glucosinolate (m/z 422.06)

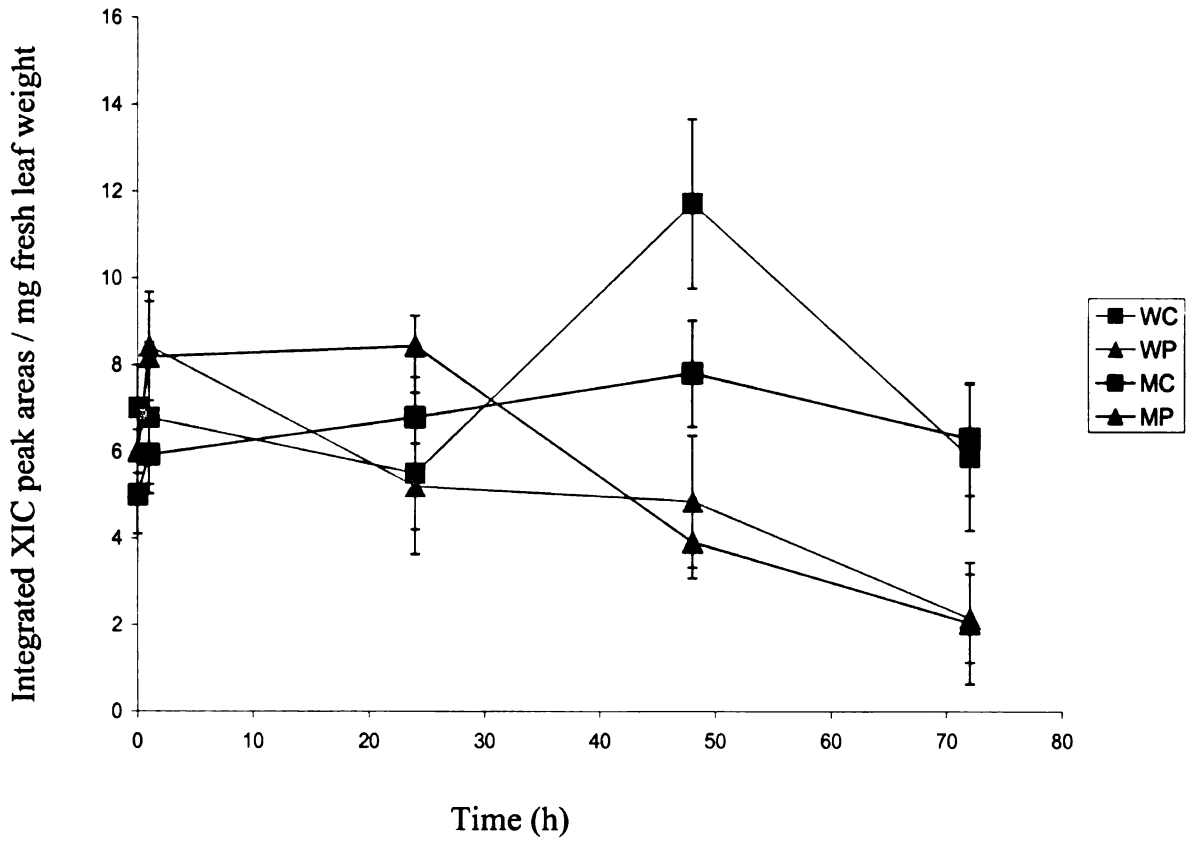

T-test analysis on metabolite levels

	1h	1d	2d	3d
WC vs MC	N.S.	N.S.	N.S.	N.S.
WP vs MP	N.S.	N.S.	N.S.	N.S.
WC vs WP	N.S.	N.S.	*	*
MC vs MP	N.S.	N.S.	*	*

"*" significant, $p < 0.05$
"N.S." not significant

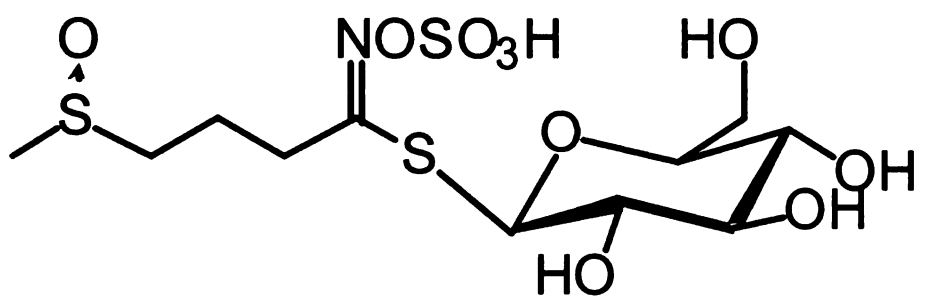

4-Methoxyindolyl or 1-Methoxyindolyl glucosinolates (m/z 477.07)

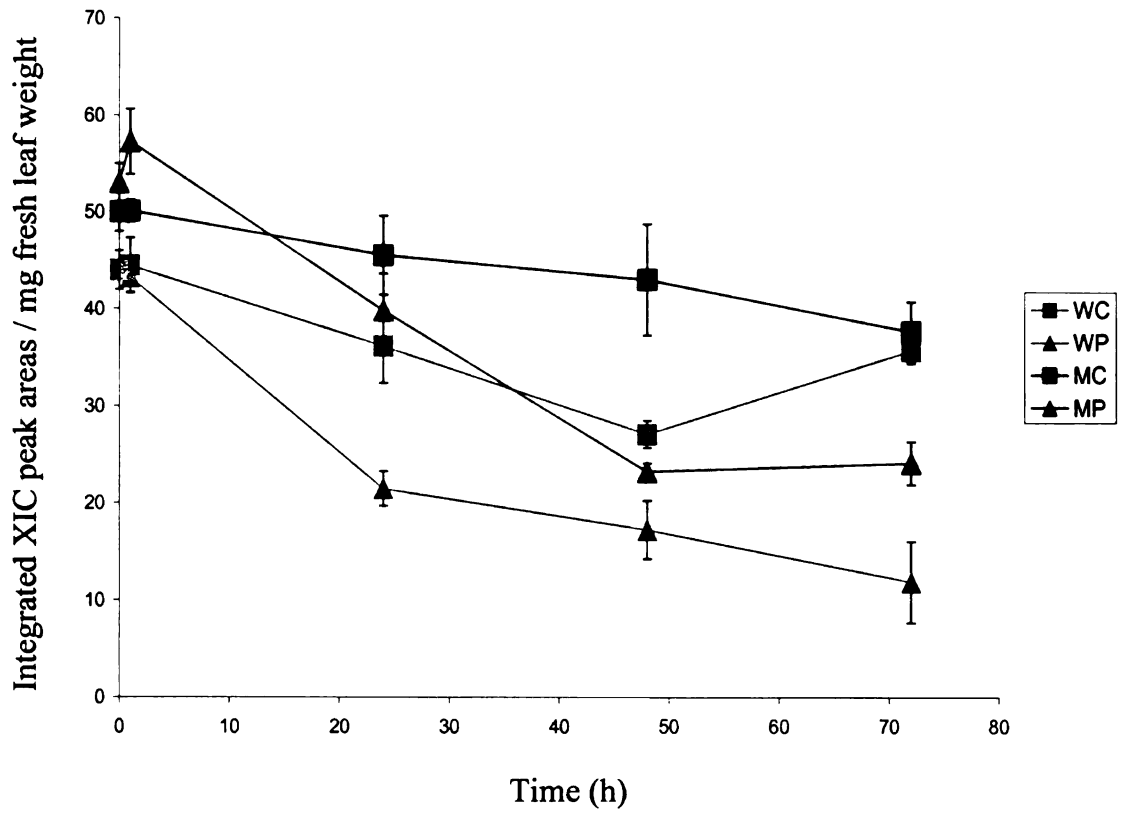

T-test analysis on metabolite levels

	1h	1d	2d	3d
WC vs MC	N.S.	N.S.	*	N.S.
WP vs MP	N.S.	*	N.S.	*
WC vs WP	N.S.	*	*	*
MC vs MP	N.S.	N.S.	*	*

"*" significant, $p < 0.05$

"N.S." not significant

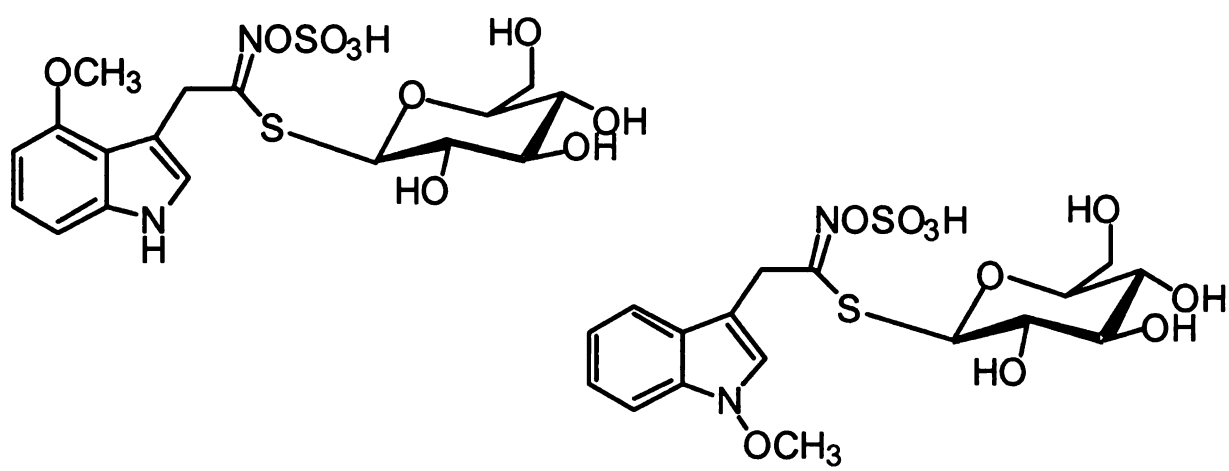

SA (m/z 137.04)

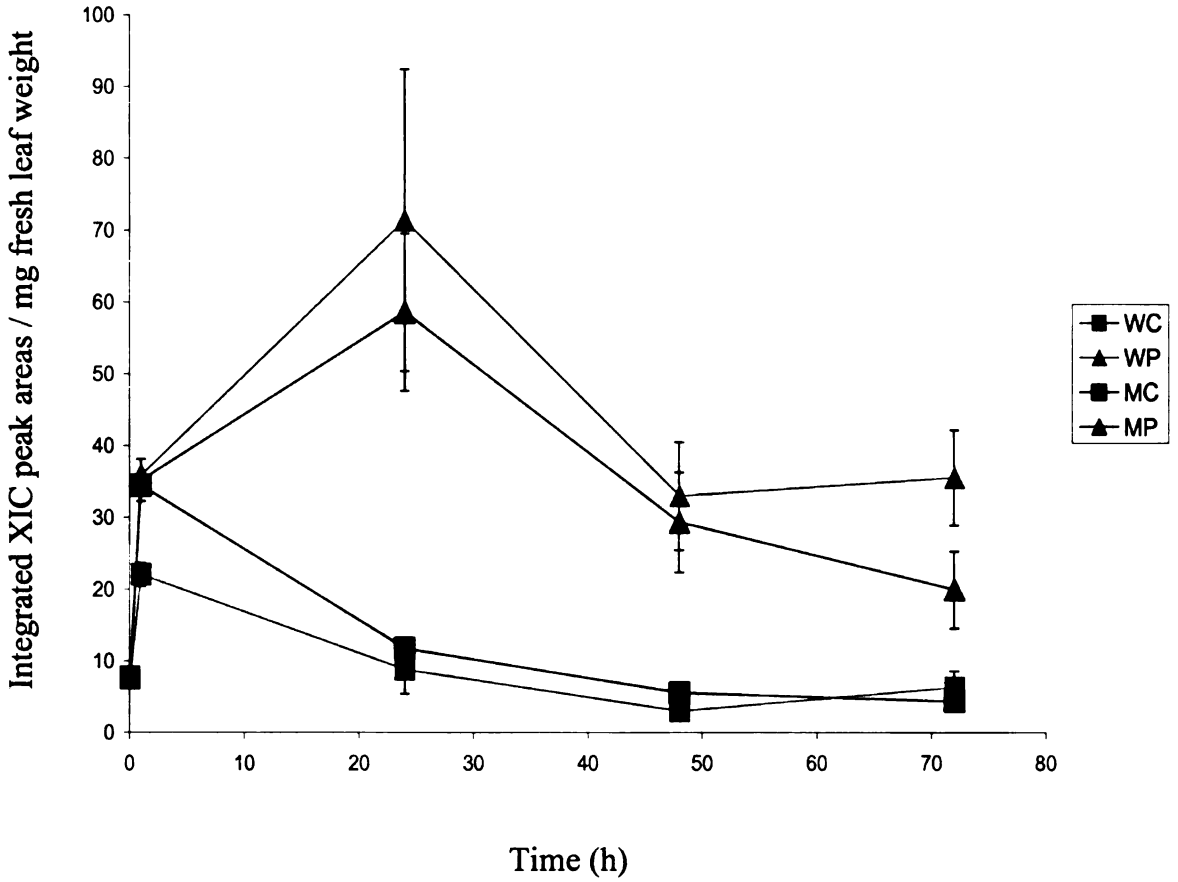

T-test analysis on metabolite levels

	1h	1d	2d	3d
WC vs MC	*	N.S.	N.S.	N.S.
WP vs MP	N.S.	N.S.	N.S.	*
WC vs WP	*	*	*	*
MC vs MP	N.S.	*	*	*

"*" significant, $p < 0.05$

"N.S." not significant

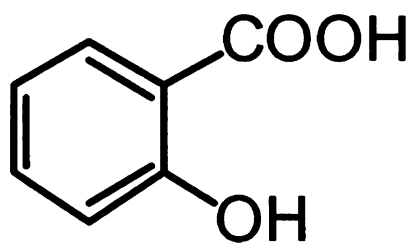

ABA (m/z 263.13)

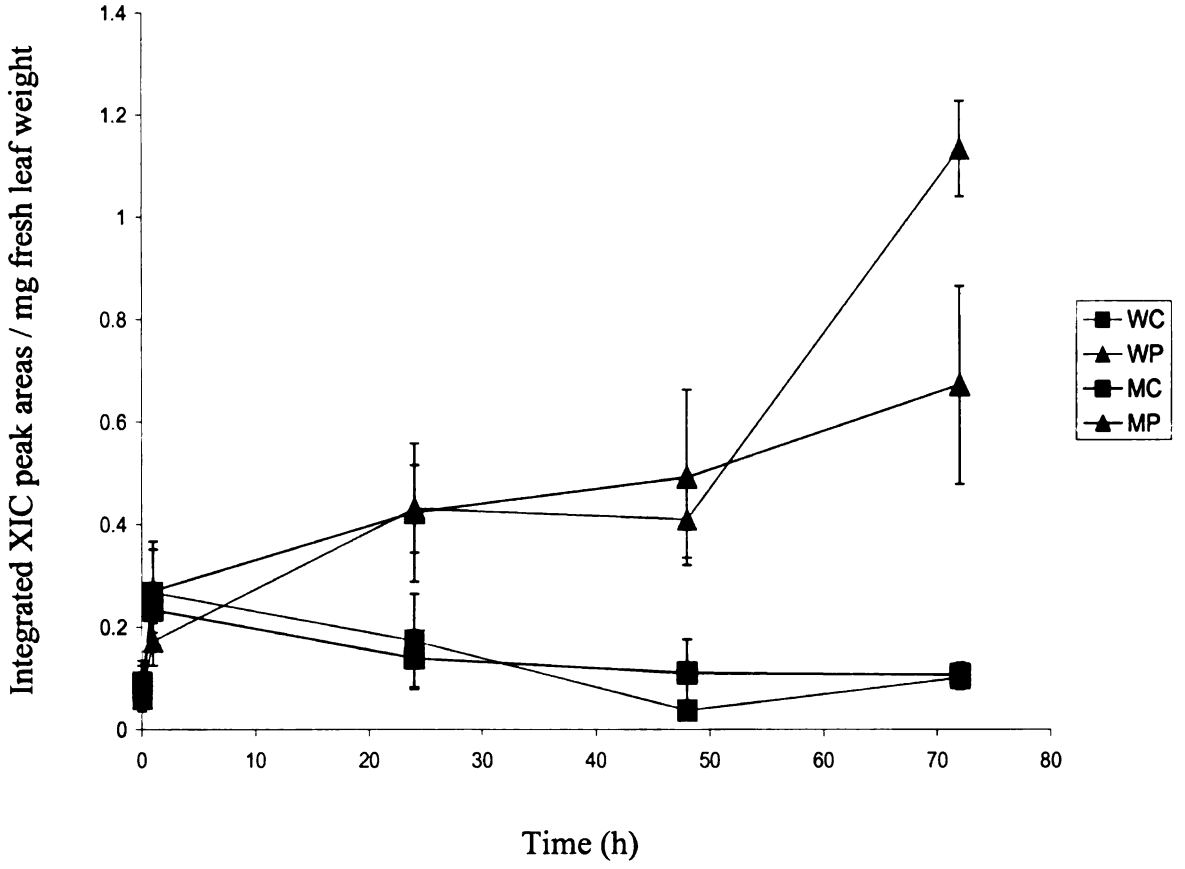

T-test analysis on metabolite levels

	1h	1d	2d	3d
WC vs MC	N.S.	N.S.	N.S.	N.S.
WP vs MP	N.S.	N.S.	N.S.	*
WC vs WP	N.S.	*	*	*
MC vs MP	N.S.	*	*	*

"*" significant, $p < 0.05$

"N.S." not significant

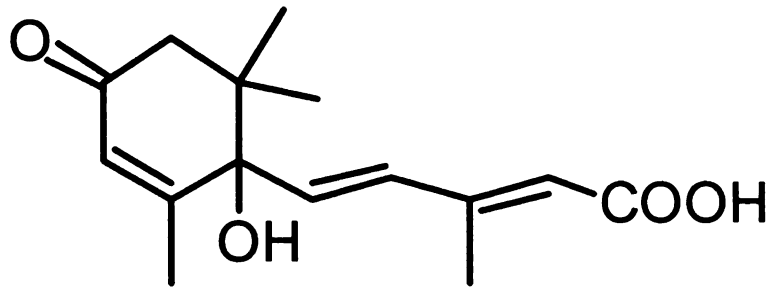

12OH JA (m/z 225.15)

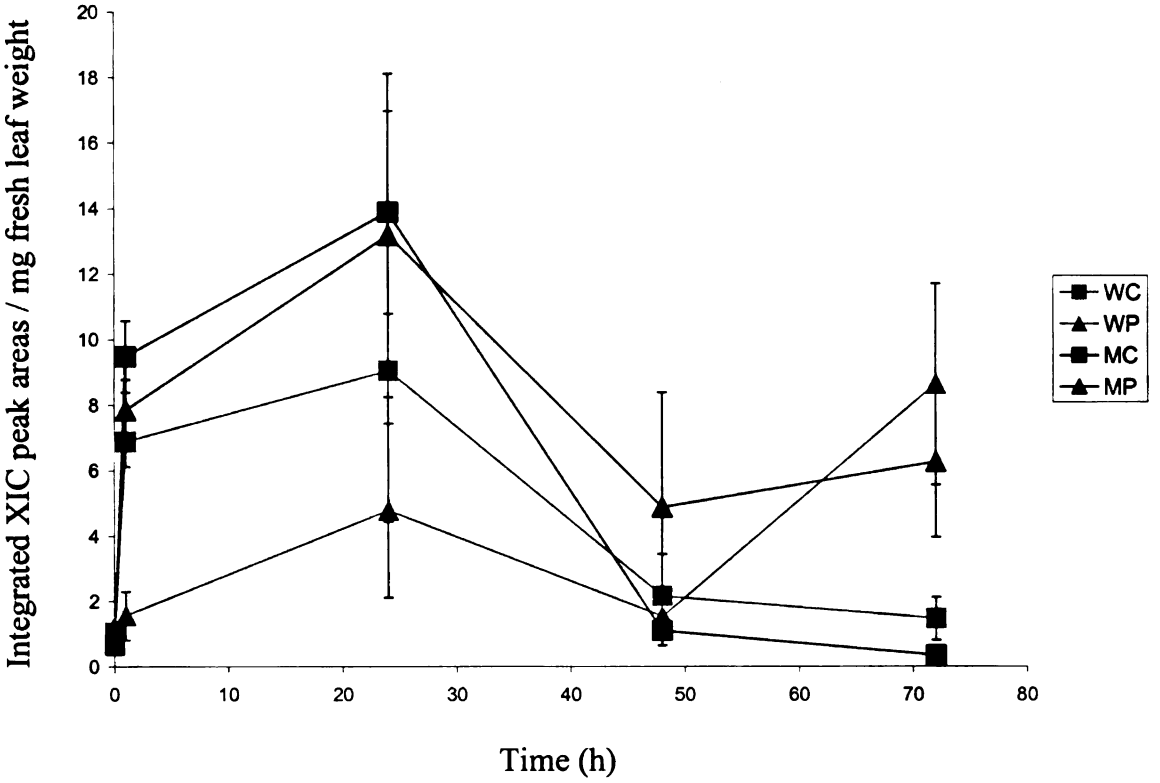

T-test analysis on metabolite levels

	1h	1d	2d	3d
WC vs MC	*	N.S.	N.S.	N.S.
WP vs MP	*.	N.S.	N.S.	N.S.
WC vs WP	N.S.	N.S.	N.S.	*
MC vs MP	*	N.S.	N.S.	*

"*" significant, $p < 0.05$
"N.S." not significant

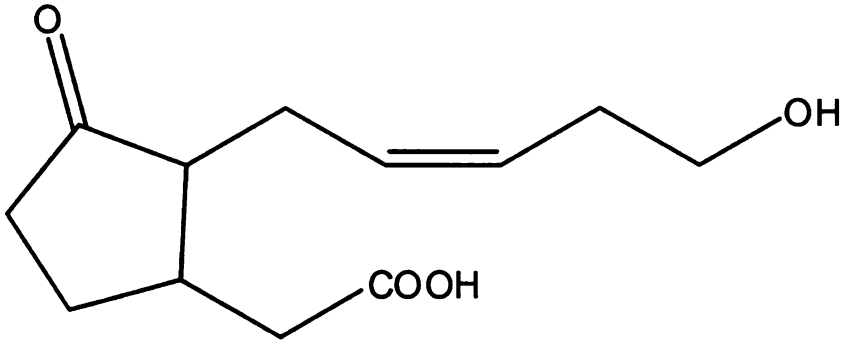

JA Ile (m/z 322.20)

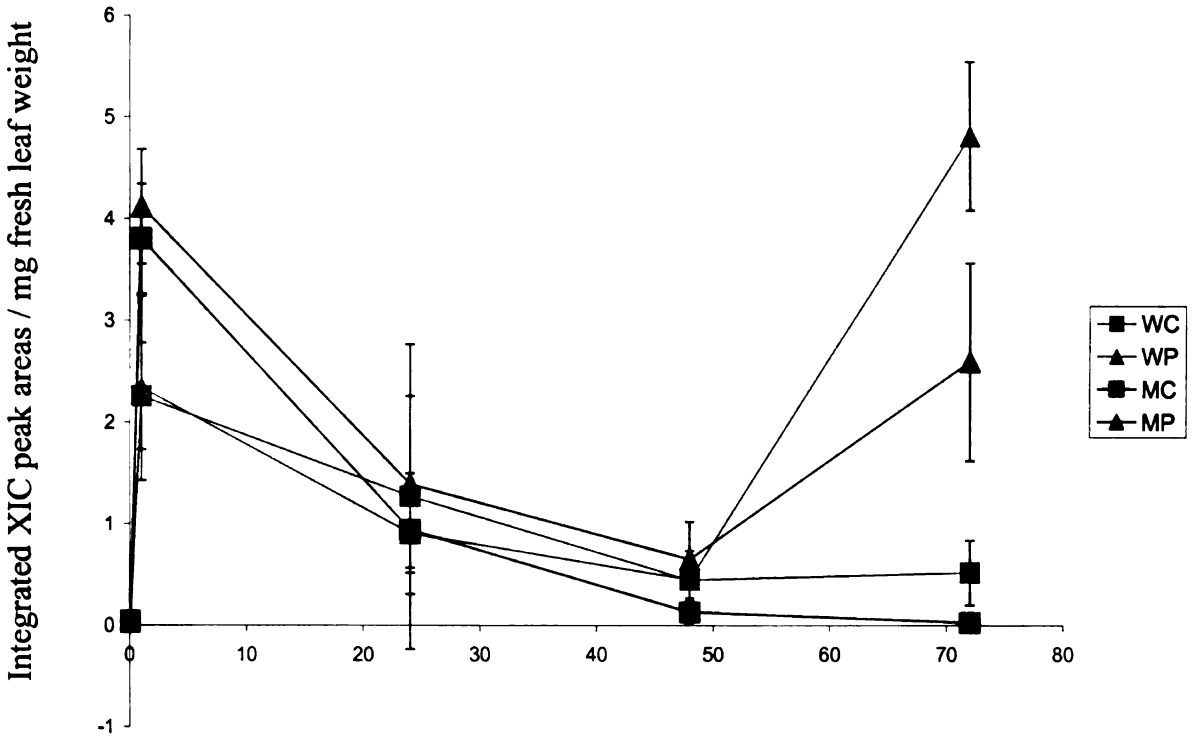

T-test analysis on metabolite leve

	1h	1d	2d	3d
WC vs MC	*	N.S.	N.S.	N.S.
WP vs MP	*.	N.S.	N.S.	*
WC vs WP	N.S.	N.S.	N.S.	*
MC vs MP	N.S.	N.S.	N.S.	*

"*" significant, $p < 0.05$

"N.S." not significant

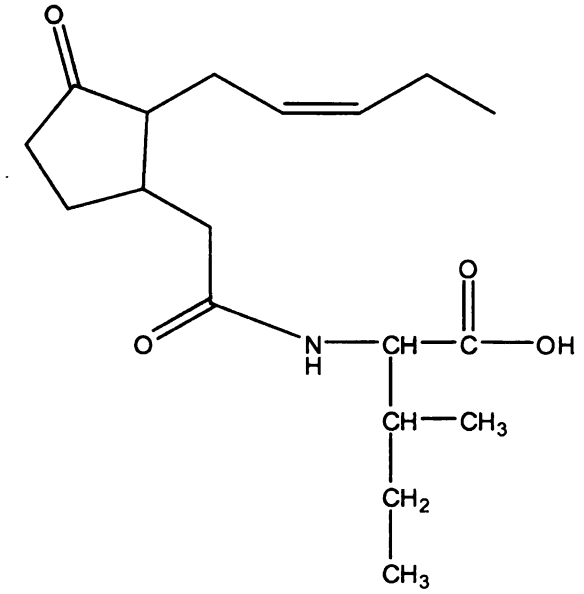

OPDA (m/z 291.20)

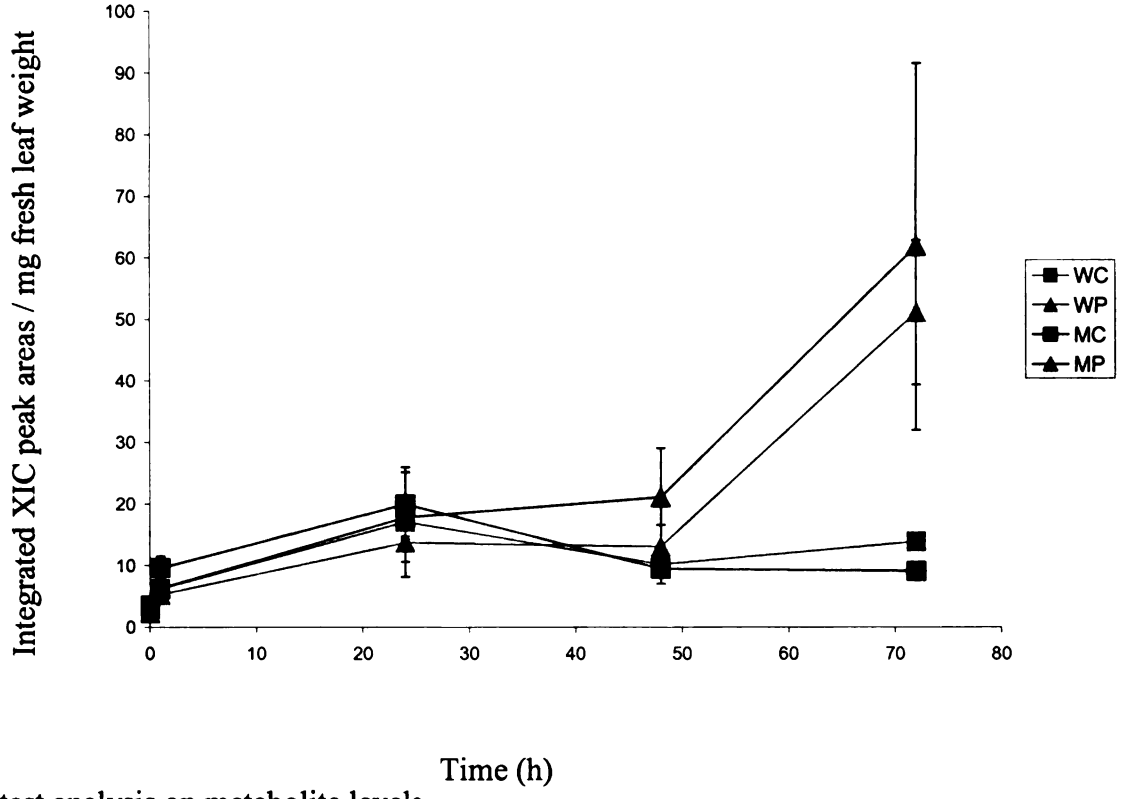

T-test analysis on metabolite levels

	1h	1d	2d	3d
WC vs MC	N.S.	N.S.	N.S.	N.S.
WP vs MP	N.S.	N.S.	N.S.	N.S.
WC vs WP	N.S.	N.S.	N.S.	*
MC vs MP	N.S.	N.S.	N.S.	*

"*" significant, $p < 0.05$
"N.S." not significant

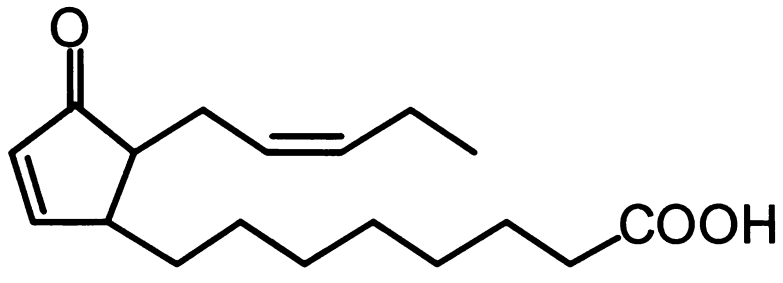

OPC:8 (m/z 293.2)

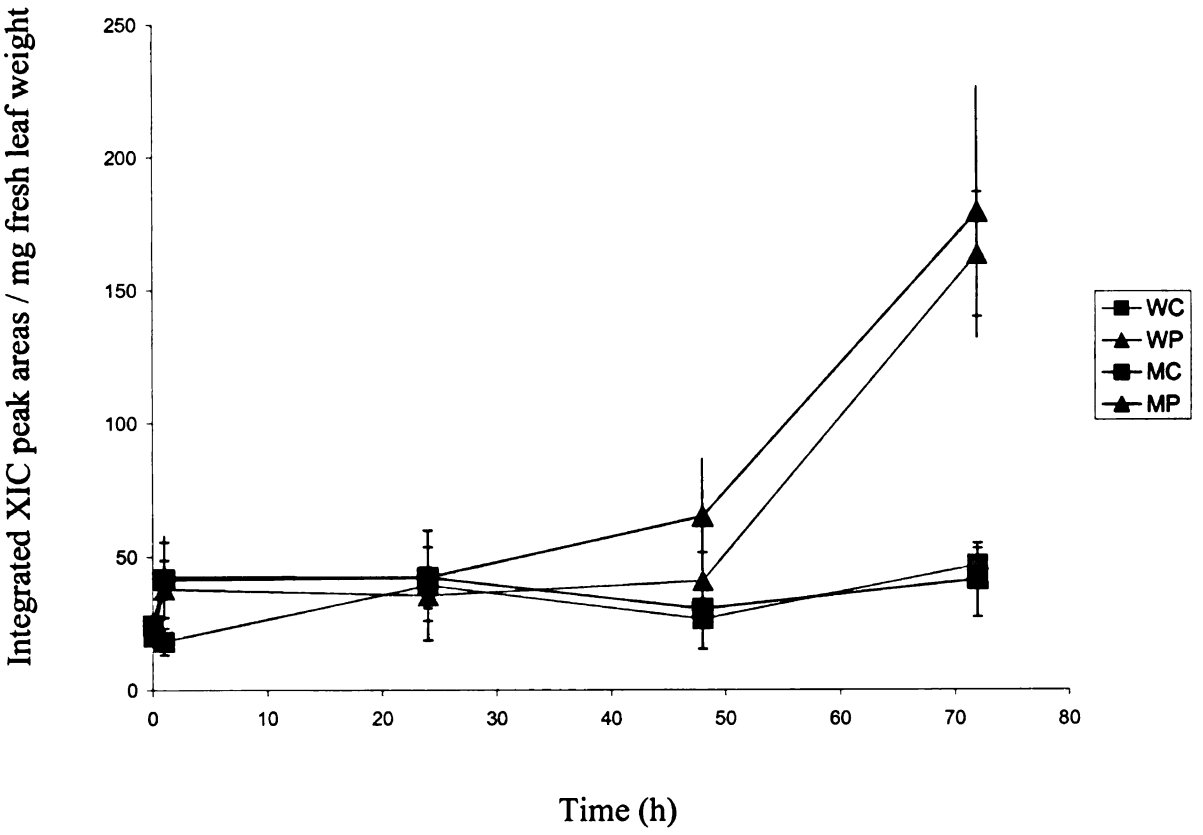

T-test analysis on metabolite levels

	1h	1d	2d	3d
WC vs MC	N.S.	N.S.	N.S.	N.S.
WP vs MP	N.S.	N.S.	N.S.	N.S.
WC vs WP	N.S.	N.S.	N.S.	*
MC vs MP	N.S.	N.S.	N.S.	*

"*" significant, $p < 0.05$
"N.S." not significant

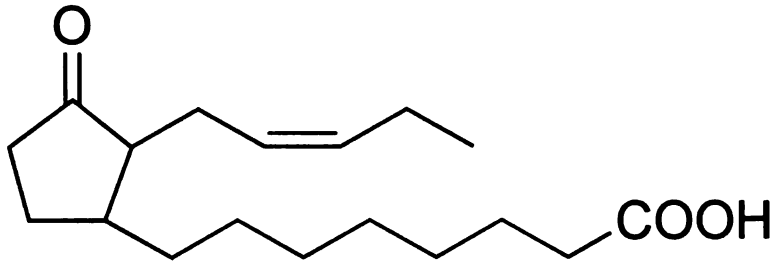

LA (m/z 277.22)

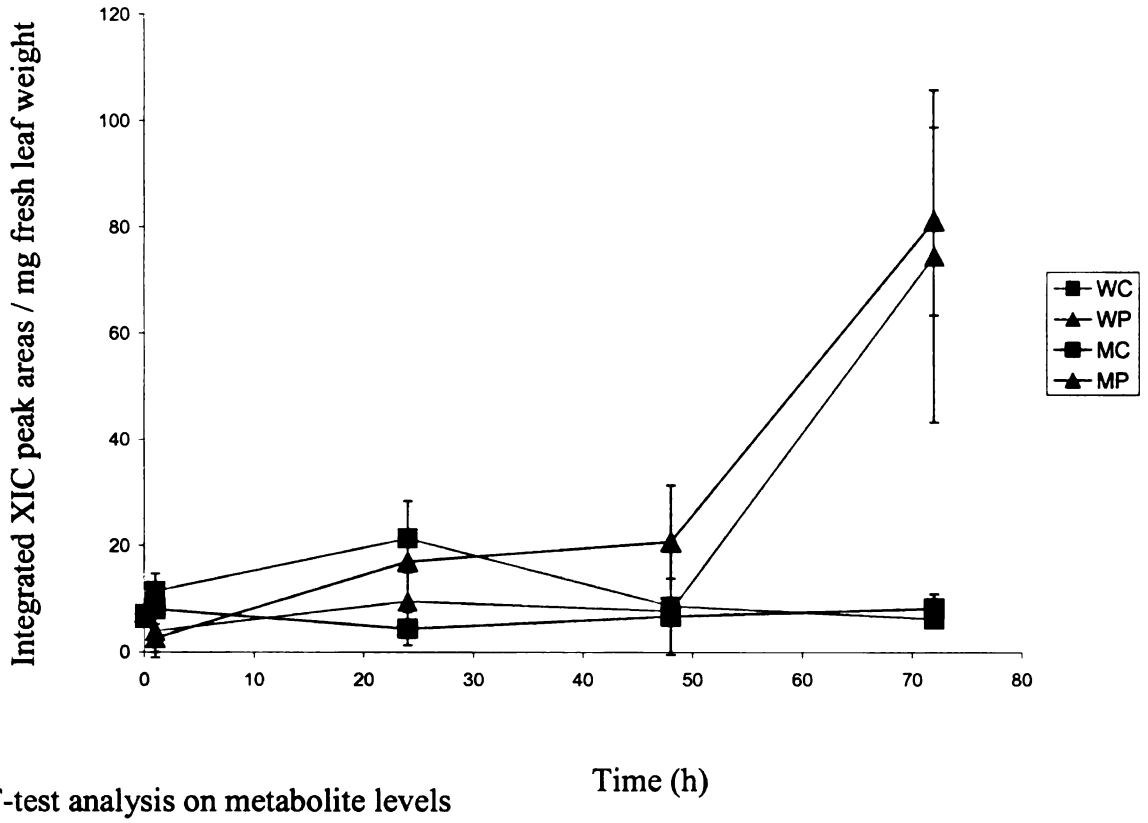

T-test analysis on metabolite levels

	1h	1d	2d	3d
WC vs MC	N.S.	N.S.	N.S.	N.S.
WP vs MP	N.S.	N.S.	N.S.	N.S.
WC vs WP	N.S.	N.S.	N.S.	*
MC vs MP	N.S.	N.S.	N.S.	*

"*" significant, $p < 0.05$
"N.S." not significant

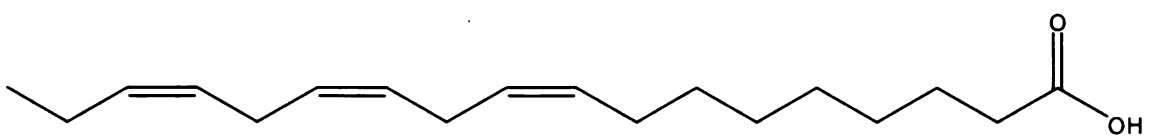

3-O-, 7-O-dirhamnosyl kaempferol (m/z 577.16)

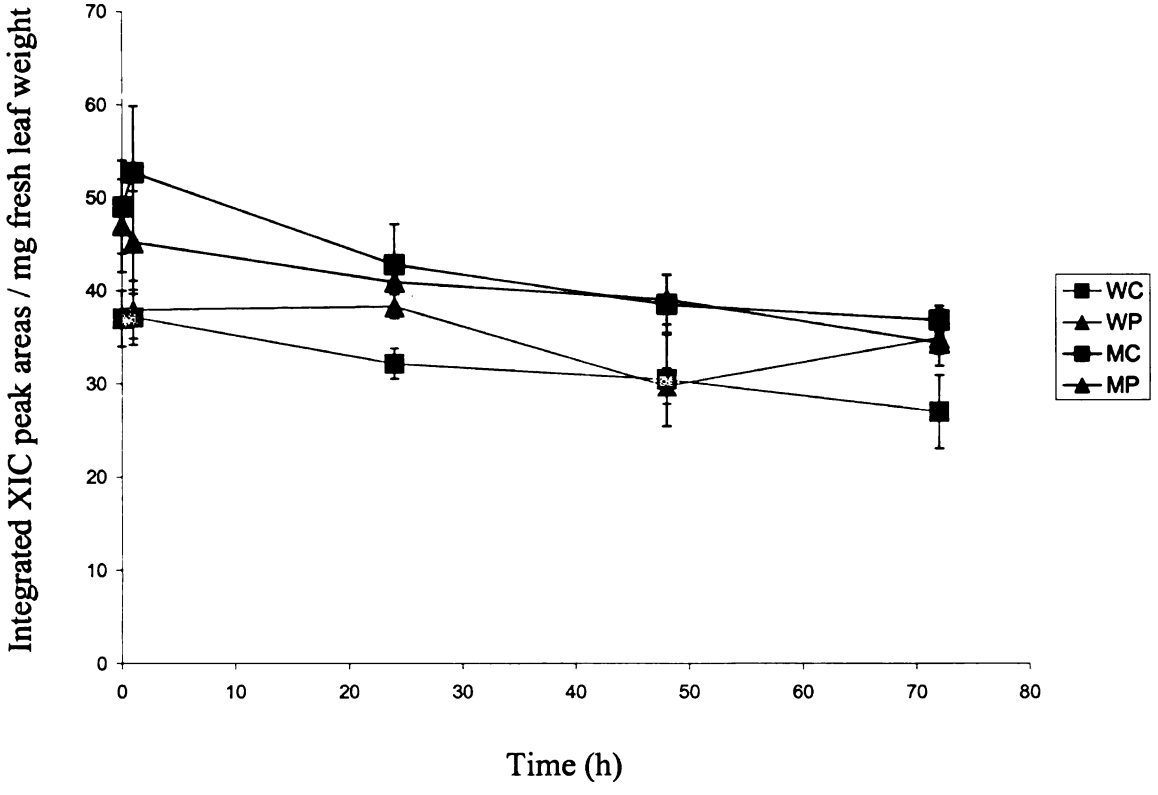

T-test analysis on metabolite levels

	1h	1d	2d	3d
WC vs MC	*	*	*	*
WP vs MP	N.S.	N.S.	*	N.S.
WC vs WP	N.S.	N.S.	N.S.	N.S.
MC vs MP	N.S.	N.S.	N.S.	N.S.

"*" significant, $p < 0.05$
"N.S." not significant

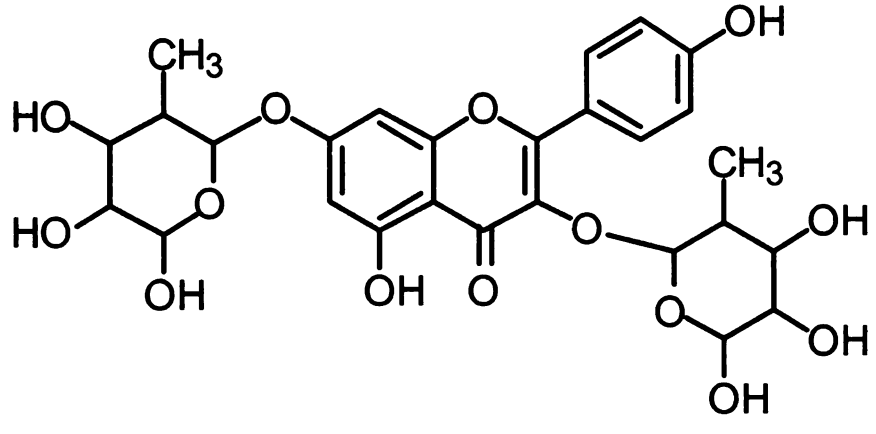

3-O-glucosyl, 7-O-rhamnosyl kaempferol (m/z 593.15)

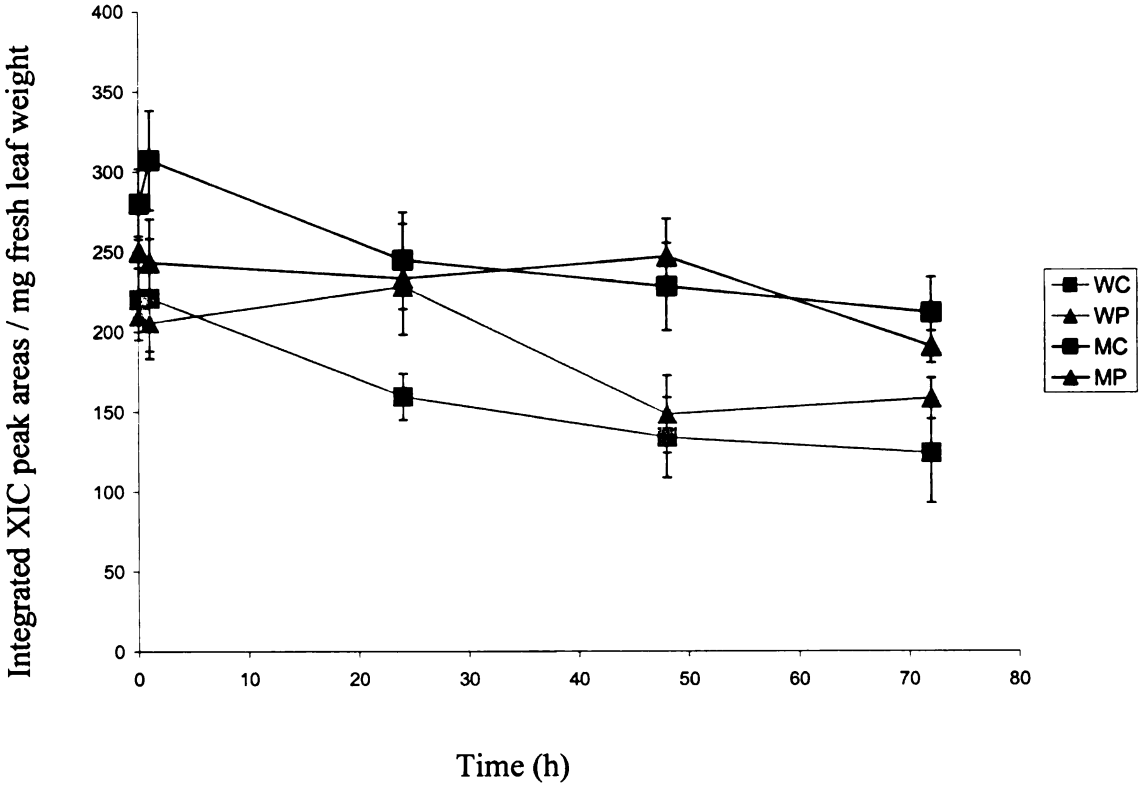

T-test analysis on metabolite levels

	1h	1d	2d	3d
WC vs MC	*	*	*	*
WP vs MP	N.S.	N.S.	*	*
WC vs WP	N.S.	*	N.S.	N.S.
MC vs MP	N.S.	N.S.	N.S.	N.S.

"*" significant, $p < 0.05$
"N.S." not significant

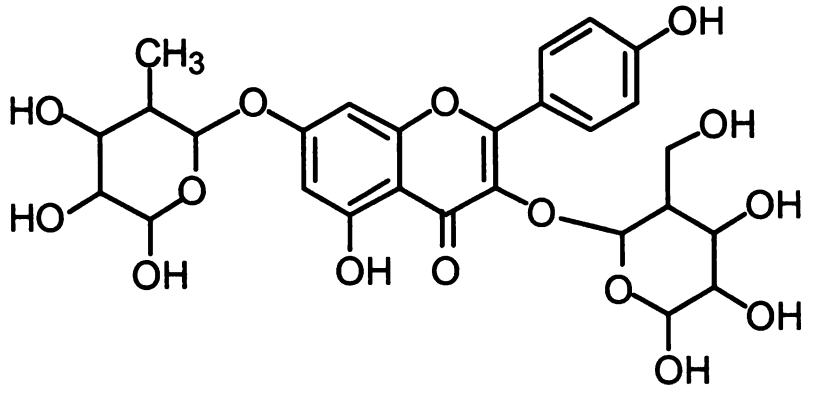

3-O-glucosylkaempferol (m/z 431.10)

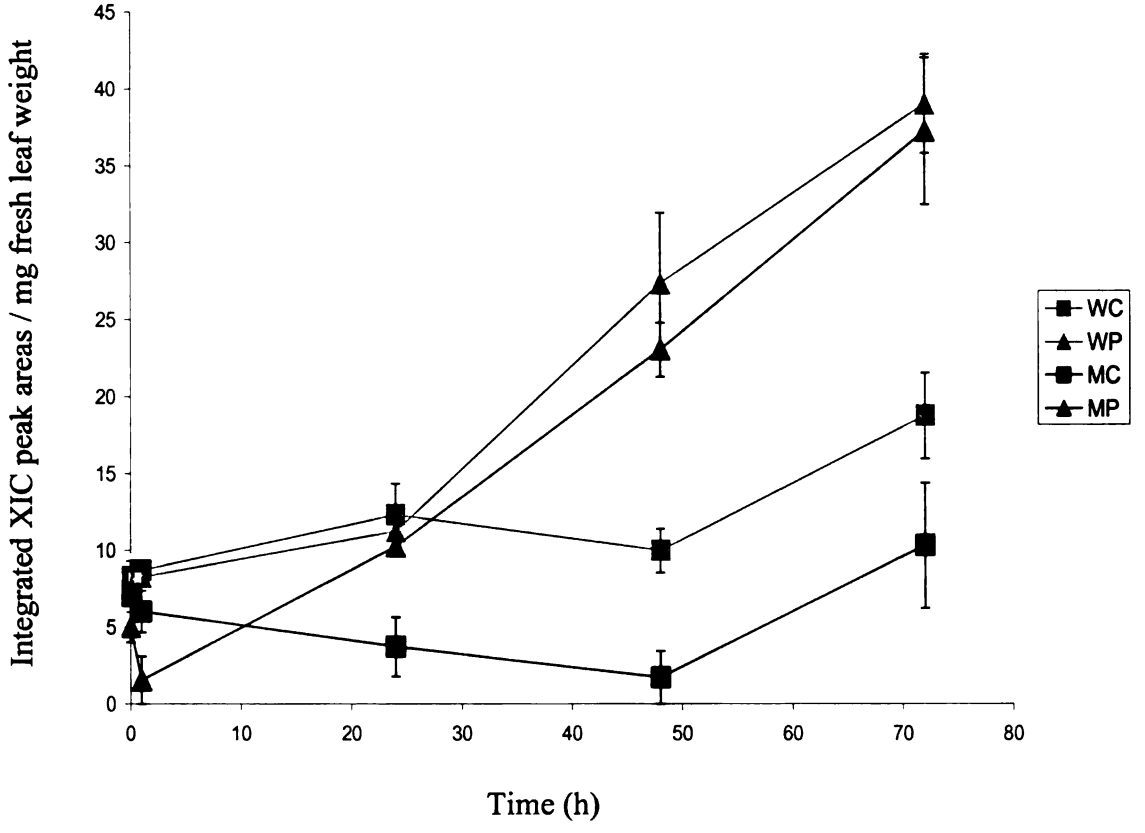

T-test analysis on metabolite levels

	1h	1d	2d	3d
WC vs MC	N.S.	*	*	*
WP vs MP	N.S.	N.S.	N.S.	N.S.
WC vs WP	N.S.	N.S.	*	*
MC vs MP	N.S.	*	*	*

"*" significant, $p < 0.05$

"N.S." not significant

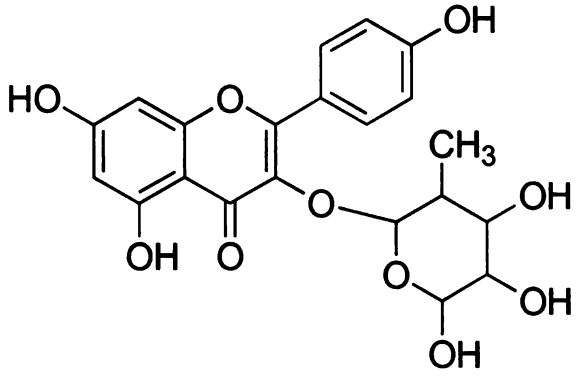

3-O-glucosyl, 7-O-rhamnosyl kaempferol with addition of OH (m/z 609.15) (the postion of -OH group is not identified)

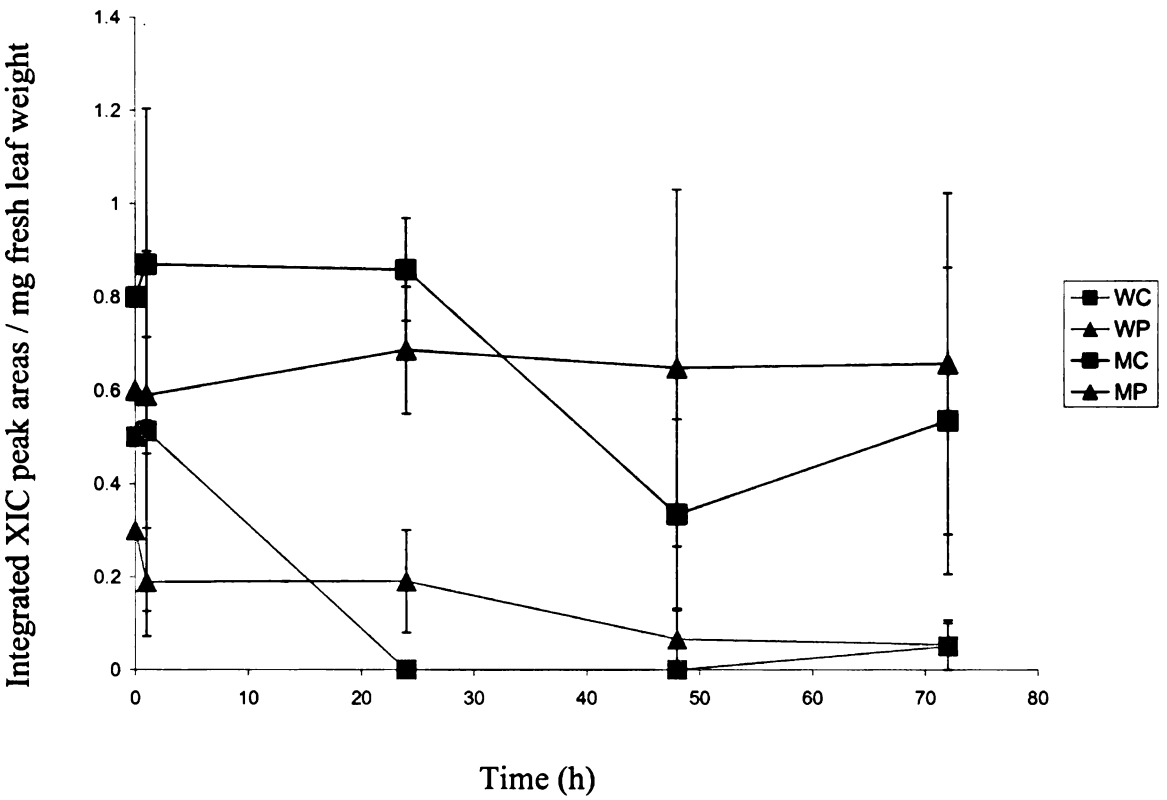

T-test analysis on metabolite levels

	1h	1d	2d	3d
WC vs MC	N.S.	*	*	*
WP vs MP	N.S.	*	*	*
WC vs WP	N.S.	*	N.S.	N.S.
MC vs MP	N.S.	N.S.	N.S.	N.S.

"*" significant, $p < 0.05$

"N.S." not significant

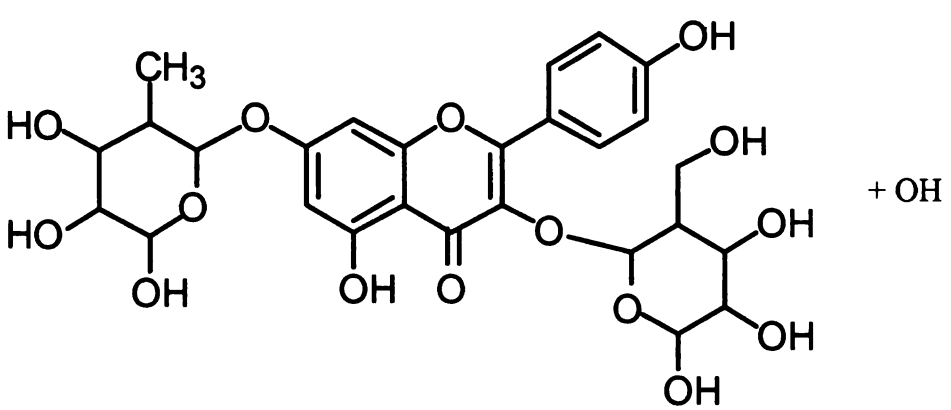

OPDA-GS (m/z 598.29)

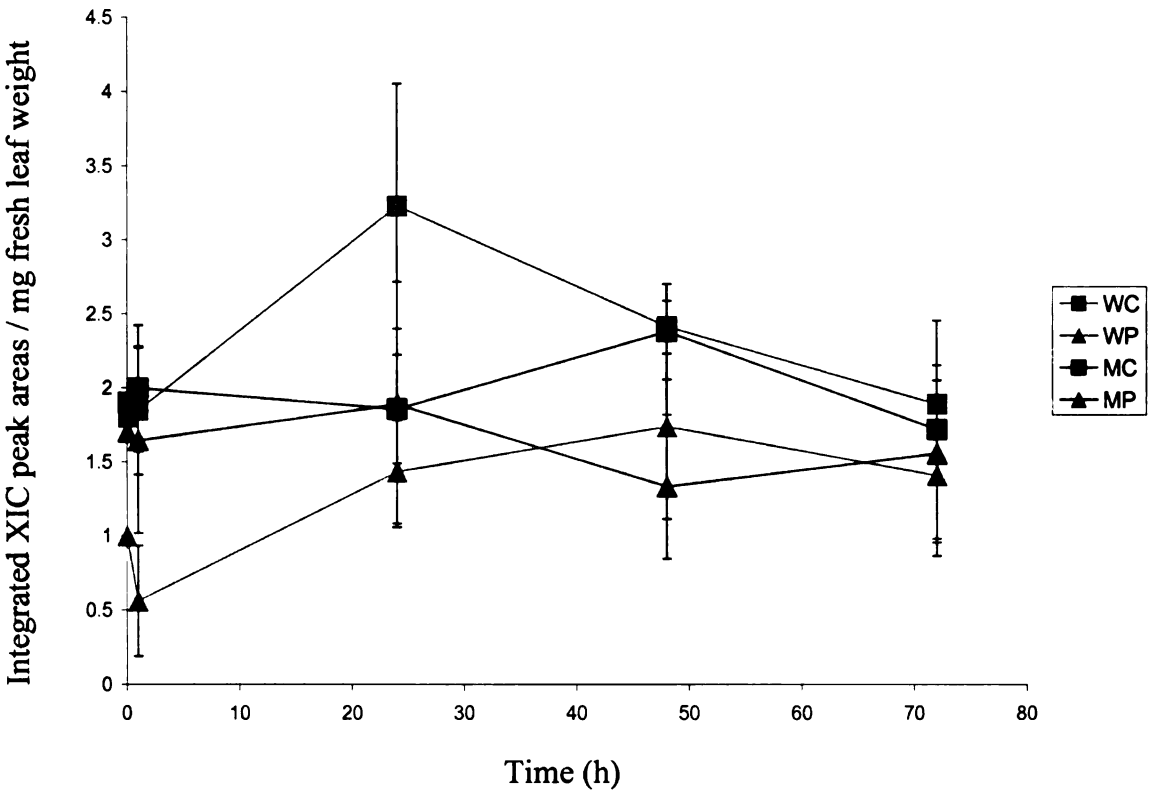

T-test analysis on metabolite levels

	1h	1d	2d	3d
WC vs MC	N.S.	N.S.	N.S.	N.S.
WP vs MP	N.S.	N.S.	N.S.	N.S.
WC vs WP	*	*	N.S.	N.S.
MC vs MP	N.S.	N.S.	N.S.	N.S.

"*" significant, $p < 0.05$
"N.S." not significant

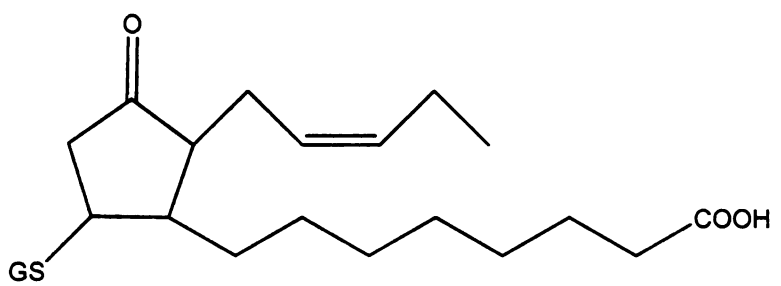

dinor OPDA-GS (m/z 570. 26)

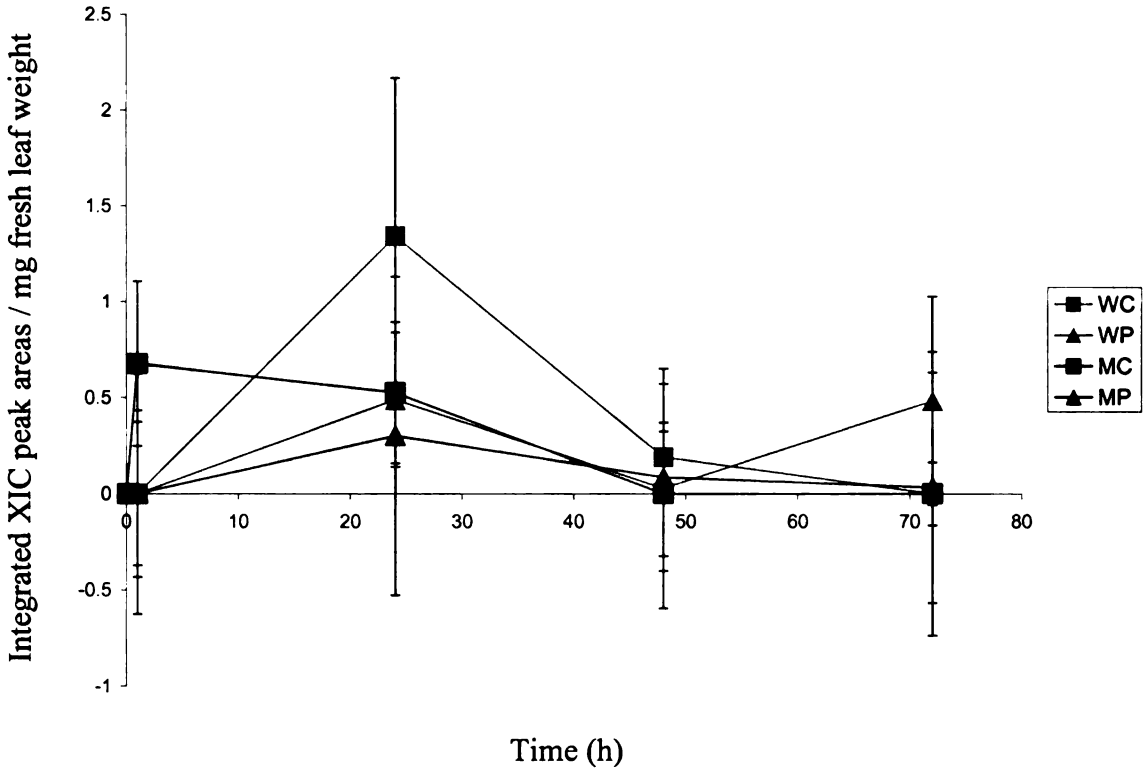

T-test analysis on metabolite levels

	1h	1d	2d	3d
WC vs MC	N.S.	N.S.	N.S.	N.S.
WP vs MP	N.S.	N.S.	N.S.	N.S.
WC vs WP	N.S.	N.S.	N.S.	N.S.
MC vs MP	N.S.	N.S.	N.S.	N.S.

"*" significant, $p < 0.05$
"N.S." not significant

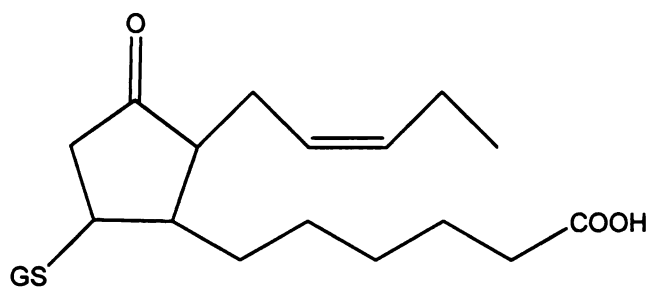

References

Agrios, G. N. (2005). Plant pathology., Elsevier academic press.

Alfenito, M. R., E. Souer, C. D. Goodman, R. Buell, J. Mol, R. Koes and V. Walbot (1998). "Functional complementation of anthocyanin sequestration in the vacuole by widely divergent glutathione S-transferases." Plant Cell **10**(7): 1135-49.

Alonso, J. M. and J. R. Ecker (2006). "Moving forward in reverse: genetic technologies to enable genome-wide phenomic screens in Arabidopsis." Nat Rev Genet **7**(7): 524-36.

Alvarez, S., E. L. Marsh, S. G. Schroeder and D. P. Schachtman (2008). "Metabolomic and proteomic changes in the xylem sap of maize under drought." Plant Cell and Environment **31**(3): 325-340.

Ames, B. N. (1983). "Dietary carcinogens and anticarcinogens. Oxygen radicals and degenerative diseases." Science **221**(4617): 1256-64.

Antolovich, M., D. R. Bedgood, Jr., A. G. Bishop, D. Jardine, P. D. Prenzler and K. Robards (2004). "LC-MS investigation of oxidation products of phenolic antioxidants." J Agric Food Chem **52**(4): 962-71.

Arabidopsis Genome Initiative. (2000). "Analysis of the genome sequence of the flowering plant Arabidopsis thaliana." Nature **408**(6814): 796-815.

Asai, T., G. Tena, J. Plotnikova, M. R. Willmann, W. L. Chiu, L. Gomez-Gomez, T. Boller, F. M. Ausubel and J. Sheen (2002). "MAP kinase signalling cascade in Arabidopsis innate immunity." Nature **415**(6875): 977-83.

Attaran, E., M. Rostas and J. Zeier (2008). "Pseudomonas syringae elicits emission of the terpenoid (E,E)-4,8,12-trimethyl-1,3,7,11-tridecatetraene in Arabidopsis leaves via jasmonate signaling and expression of the terpene synthase TPS4." Mol Plant Microbe Interact **21**(11): 1482-97.

Bargmann, B. O., A. M. Laxalt, B. ter Riet, C. Testerink, E. Merquiol, A. Mosblech, A. Leon-Reyes, C. M. Pieterse, M. A. Haring, I. Heilmann, D. Bartels and T. Munnik (2009). "Reassessing the role of phospholipase D in the Arabidopsis wounding response." Plant Cell Environ **32**(7): 837-50.

Barry, K. M. (2002). "Effect of season and different fungi on phenolics in response to xylem wounding and inoculation in Eucalyptus nitens. (vol 32, pg 163, 2002)." Forest Pathology **32**(6): 403-403.

Bednarek, P. and A. Osbourn (2009). "Plant-microbe interactions: chemical diversity in plant defense." Science **324**(5928): 746-8.

Birkenmeier, G. F. and C. A. Ryan (1998). "Wound signaling in tomato plants. Evidence that aba is not a primary signal for defense gene activation." Plant Physiol **117**(2): 687-93.

Blain, P. G. (1990). "Aspects of pesticide toxicology." Adverse Drug React Acute Poisoning Rev **9**(1): 37-68.

Blumenthal, C. Z. (2004). "Production of toxic metabolites in Aspergillus niger, Aspergillus oryzae, and Trichoderma reesei: justification of mycotoxin testing in food grade enzyme preparations derived from the three fungi." Regul Toxicol Pharmacol **39**(2): 214-28.

Boccard, J., E. Grata, A. Thiocone, J. Y. Gauvrit, P. Lanteri, P. A. Carrupt, J. L. Wolfender and S. Rudaz (2007). "Multivariate data analysis of rapid LC-TOF/MS experiments from Arabidopsis thaliana stressed by wounding." Chemometrics and Intelligent Laboratory Systems **86**(2): 189-197.

Bolwell, P. P., A. Page, M. Pislewska and P. Wojtaszek (2001). "Pathogenic infection and the oxidative defences in plant apoplast." Protoplasma **217**(1-3): 20-32.

Bostock, R. M. (1999). "Signal conflicts and synergies in induced resistance to multiple attackers." Physiological and Molecular Plant Pathology **55**(2): 99-109.

Bratton, S. B., S. S. Lau and T. J. Monks (1997). "Identification of quinol thioethers in bone marrow of hydroquinone/phenol-treated rats and mice and their potential role in benzene-mediated hematotoxicity." Chem Res Toxicol **10**(8): 859-65.

Bratton, S. B., S. S. Lau and T. J. Monks (2000). "The putative benzene metabolite 2,3, 5-tris(glutathion-S-yl)hydroquinone depletes glutathione, stimulates sphingomyelin turnover, and induces apoptosis in HL-60 cells." Chem Res Toxicol **13**(7): 550-6.

Browse, J. (2005). "Jasmonate: an oxylipin signal with many roles in plants." Vitam Horm **72**: 431-56.

Buchanan, B. B., W. Gruissem and R. L. Jones (2001). Biochemistry & Molecular Biology of Plants, Wiley.

Buell, C. R., V. Joardar, M. Lindeberg, J. Selengut, I. T. Paulsen, M. L. Gwinn, R. J. Dodson, R. T. Deboy, A. S. Durkin, J. F. Kolonay, R. Madupu, S. Daugherty, L. Brinkac, M. J. Beanan, D. H. Haft, W. C. Nelson, T. Davidsen, N. Zafar, L. Zhou, J. Liu, Q. Yuan, H. Khouri, N. Fedorova, B. Tran, D. Russell, K. Berry, T. Utterback, S. E. Van Aken, T. V. Feldblyum, M. D'Ascenzo, W. L. Deng, A. R. Ramos, J. R. Alfano, S. Cartinhour, A. K. Chatterjee, T. P. Delaney, S. G. Lazarowitz, G. B. Martin, D. J. Schneider, X. Tang, C. L. Bender, O. White, C. M. Fraser and A. Collmer (2003). "The complete genome sequence of the

Arabidopsis and tomato pathogen Pseudomonas syringae pv. tomato DC3000." Proc Natl Acad Sci U S A **100**(18): 10181-6.

Burga, L., F. Wellmann, R. Lukacin, S. Witte, W. Schwab, J. Schroder and U. Matern (2005). "Unusual pseudosubstrate specificity of a novel 3,5-dimethoxyphenol O-methyltransferase cloned from Ruta graveolens L." Arch Biochem Biophys **440**(1): 54-64.

Buseman, C. M., P. Tamura, A. A. Sparks, E. J. Baughman, S. Maatta, J. Zhao, M. R. Roth, S. W. Esch, J. Shah, T. D. Williams and R. Welti (2006). "Wounding stimulates the accumulation of glycerolipids containing oxophytodienoic acid and dinor-oxophytodienoic acid in Arabidopsis leaves." Plant Physiology **142**(1): 28-39.

Buseman, C. M., P. Tamura, A. A. Sparks, E. J. Baughman, S. Maatta, J. Zhao, M. R. Roth, S. W. Esch, J. Shah, T. D. Williams and R. Welti (2006). "Wounding stimulates the accumulation of glycerolipids containing oxophytodienoic acid and dinor-oxophytodienoic acid in Arabidopsis leaves." Plant Physiol **142**(1): 28-39.

Chapple, C., B. W. Shirley, M. Zook, R. Hammerschmidt and S. S. C., Eds. (1994). Secondary metabolism in *Arabidopsis.*, Cold Spring Harbor Laboratory Press.

Chapple, C. C., T. Vogt, B. E. Ellis and C. R. Somerville (1992). "An Arabidopsis mutant defective in the general phenylpropanoid pathway." Plant Cell **4**(11): 1413-24.

Chen, F., D. K. Ro, J. Petri, J. Gershenzon, J. Bohlmann, E. Pichersky and D. Tholl (2004). "Characterization of a root-specific Arabidopsis terpene synthase responsible for the formation of the volatile monoterpene 1,8-cineole." Plant Physiol **135**(4): 1956-66.

Cheong, Y. H., H. S. Chang, R. Gupta, X. Wang, T. Zhu and S. Luan (2002). "Transcriptional profiling reveals novel interactions between wounding, pathogen, abiotic stress, and hormonal responses in Arabidopsis." Plant Physiol **129**(2): 661-77.

Chesis, P. L., D. E. Levin, M. T. Smith, L. Ernster and B. N. Ames (1984). "Mutagenicity of quinones: pathways of metabolic activation and detoxification." Proc Natl Acad Sci U S A **81**(6): 1696-700.

Chisholm, S. T., G. Coaker, B. Day and B. J. Staskawicz (2006). "Host-microbe interactions: shaping the evolution of the plant immune response." Cell **124**(4): 803-14.

Chisholm, S. T., D. Dahlbeck, N. Krishnamurthy, B. Day, K. Sjolander and B. J. Staskawicz (2005). "Molecular characterization of proteolytic cleavage sites of

the Pseudomonas syringae effector AvrRpt2." Proc Natl Acad Sci U S A **102**(6): 2087-92.

Chiwocha, S. D. S., S. R. Abrams, S. J. Ambrose, A. J. Cutler, M. Loewen, A. R. S. Ross and A. R. Kermode (2003). "A method for profiling classes of plant hormones and their metabolites using liquid chromatography-electrospray ionization tandem mass spectrometry: an analysis of hormone regulation of thermodormancy of lettuce (Lactuca sativa L.) seeds." Plant Journal **35**(3): 405-417.

Chroust, K., T. Jowett, M. F. Farid-Wajidi, J. Y. Huang, M. Ryskova, R. Wolf and I. Holoubek (2001). "Activation or detoxification of mutagenic and carcinogenic compounds in transgenic Drosophila expressing human glutathione S-transferase." Mutat Res **498**(1-2): 169-79.

Chung, H. S., A. J. Koo, X. Gao, S. Jayanty, B. Thines, A. D. Jones and G. A. Howe (2008). "Regulation and function of Arabidopsis JASMONATE ZIM-domain genes in response to wounding and herbivory." Plant Physiol **146**(3): 952-64.

Coles, B. F. and F. F. Kadlubar (2003). "Detoxification of electrophilic compounds by glutathione S-transferase catalysis: determinants of individual response to chemical carcinogens and chemotherapeutic drugs?" Biofactors **17**(1-4): 115-30.

Constabel, C. P., D. R. Bergey and C. A. Ryan (1995). "Systemin activates synthesis of wound-inducible tomato leaf polyphenol oxidase via the octadecanoid defense signaling pathway." Proc Natl Acad Sci U S A **92**(2): 407-11.

Cook, D., S. Fowler, O. Fiehn and M. F. Thomashow (2004). "A prominent role for the CBF cold response pathway in configuring the low-temperature metabolome of Arabidopsis." Proc Natl Acad Sci U S A **101**(42): 15243-8.

Cornwell, D. G., M. V. Williams, A. A. Wani, G. Wani, E. Shen and K. H. Jones (2002). "Mutagenicity of tocopheryl quinones: evolutionary advantage of selective accumulation of dietary alpha-tocopherol." Nutr Cancer **43**(1): 111-8.

Cowan, M. (1999). "Plant Products as Antimicrobial Agents." Clinical microbiology reviews **12**: 564-582.

Cui, J., A. K. Bahrami, E. G. Pringle, G. Hernandez-Guzman, C. L. Bender, N. E. Pierce and F. M. Ausubel (2005). "Pseudomonas syringae manipulates systemic plant defenses against pathogens and herbivores." Proc Natl Acad Sci U S A **102**(5): 1791-6.

D'Auria, J. C. and J. Gershenzon (2005). "The secondary metabolism of Arabidopsis thaliana: growing like a weed." Curr Opin Plant Biol **8**(3): 308-16.

Davoine, C., T. Douki, G. Iacazio, J. L. Montillet and C. Triantaphylides (2005). "Conjugation of keto fatty acids to glutathione in plant tissues. Characterization and quantification by HPLC-tandem mass spectrometry." Anal Chem **77**(22): 7366-72.

Deem, A. K., R. L. Bultema and D. N. Crowell (2006). "Prenylcysteine methylesterase in Arabidopsis thaliana." Gene **380**(2): 159-66.

Delker, C., B. K. Zolman, O. Miersch and C. Wasternack (2007). "Jasmonate biosynthesis in Arabidopsis thaliana requires peroxisomal beta-oxidation enzymes - Additional proof by properties of pex6 and aim1." Phytochemistry **68**(12): 1642-1650.

Delong, J. M., R. K. Prange, D. M. Hodges, C. F. Forney, M. C. Bishop and M. Quilliam (2002). "Using a modified ferrous oxidation-xylenol orange (FOX) assay for detection of lipid hydroperoxides in plant tissue." J. Agric. Food Chem. **50**: 248-254.

Denekamp, M. and S. C. Smeekens (2003). "Integration of wounding and osmotic stress signals determines the expression of the AtMYB102 transcription factor gene." Plant Physiol **132**(3): 1415-23.

Dennis, C. and C. Surridge (2000). "Arabidopsis thaliana genome. Introduction." Nature **408**(6814): 791.

Dewick, P. M. (1995). "The Biosynthesis of Shikimate Metabolites." Natural Product Reports **12**(6): 579-607.

Dixon, D. P., T. Hawkins, P. J. Hussey and R. Edwards (2009). "Enzyme activities and subcellular localization of members of the Arabidopsis glutathione transferase superfamily." J Exp Bot **60**(4): 1207-18.

Dixon, R. A. (2001). "Natural products and plant disease resistance." Nature **411**(6839): 843-847.

Dixon, R. A. and N. L. Paiva (1995). "Stress-Induced Phenylpropanoid Metabolism." Plant Cell **7**(7): 1085-1097.

Do, C. T., B. Pollet, J. Thevenin, R. Sibout, D. Denoue, Y. Barriere, C. Lapierre and L. Jouanin (2007). "Both caffeoyl Coenzyme A 3-O-methyltransferase 1 and caffeic acid O-methyltransferase 1 are involved in redundant functions for lignin, flavonoids and sinapoyl malate biosynthesis in Arabidopsis." Planta **226**(5): 1117-29.

Doares, S. H., T. Syrovets, E. W. Weiler and C. A. Ryan (1995). "Oligogalacturonides and chitosan activate plant defensive genes through the octadecanoid pathway." Proc Natl Acad Sci U S A **92**(10): 4095-8.

Durrant, W. E. and X. Dong (2004). "Systemic acquired resistance." Annu Rev Phytopathol **42**: 185-209.

Engelberth, J., E. A. Schmelz, H. T. Alborn, Y. J. Cardoza, J. Huang and J. H. Tumlinson (2003). "Simultaneous quantification of jasmonic acid and salicylic acid in plants by vapor-phase extraction and gas chromatography-chemical ionization-mass spectrometry." Analytical Biochemistry **312**(2): 242-250.

Eriksson, L., H. Antti, J. Gottfries, E. Holmes, E. Johansson, F. Lindgren, I. Long, T. Lundstedt, J. Trygg and S. Wold (2004). "Using chemometrics for navigating in the large data sets of genomics, proteomics, and metabonomics (gpm)." Anal Bioanal Chem **380**(3): 419-29.

Fahey, J. W., A. T. Zalcmann and P. Talalay (2001). "The chemical diversity and distribution of glucosinolates and isothiocyanates among plants." Phytochemistry **56**(1): 5-51.

Fiehn, O. (2001). "Combining genomics, metabolome analysis, and biochemical modelling to understand metabolic networks." Comp Funct Genomics **2**(3): 155-68.

Fiehn, O. (2002). "Metabolomics--the link between genotypes and phenotypes." Plant Mol Biol **48**(1-2): 155-71.

Fiehn, O. (2003). "Metabolic networks of Cucurbita maxima phloem." Phytochemistry **62**(6): 875-86.

Fiehn, O. (2006). "Metabolite profiling in Arabidopsis." Methods Mol Biol **323**: 439-47.

Fiehn, O. (2008). "Extending the breadth of metabolite profiling by gas chromatography coupled to mass spectrometry." Trends Analyt Chem **27**(3): 261-269.

Fiehn, O., J. Kopka, P. Dormann, T. Altmann, R. N. Trethewey and L. Willmitzer (2000). "Metabolite profiling for plant functional genomics." Nat Biotechnol **18**(11): 1157-61.

Fiehn, O., G. Wohlgemuth, M. Scholz, T. Kind, Y. Lee do, Y. Lu, S. Moon and B. Nikolau (2008). "Quality control for plant metabolomics: reporting MSI-compliant studies." Plant J **53**(4): 691-704.

Flor, A. H. (1955). "Host-parasite interactions in flax rust-its genetics and other implications. ." Phytopathology **45**: 680-85.

Fobert, P. R. and C. Despres (2005). "Redox control of systemic acquired resistance." Curr Opin Plant Biol **8**(4): 378-82.

Franklin, G., L. F. Conceicao, E. Kombrink and A. C. Dias (2009). "Xanthone biosynthesis in Hypericum perforatum cells provides antioxidant and antimicrobial protection upon biotic stress." Phytochemistry **70**(1): 60-8.

Fulcrand, H., A. Cheminat, R. Brouillard and V. Cheynier (1994). "Charaterization of compounds obtained by chemical oxidation of caffeic acid in acidic conditions." Phytochemistry **35**(2): 499-505.

Galati, G., T. Chan, B. Wu and P. J. O'Brien (1999). "Glutathione-dependent generation of reactive oxygen species by the peroxidase-catalyzed redox cycling of flavonoids." Chem Res Toxicol **12**(6): 521-5.

Gallet, C., Despr'es, L., Tollenaere, C. (2004). "Phenolic response of *Trollius europaeus* to *Chiastocheta* invasion. ." Polyphenol Commun: 759–760.

Gauthier, A., P. J. Gulick and R. K. Ibrahim (1998). "Characterization of two cDNA clones which encode O-methyltransferases for the methylation of both flavonoid and phenylpropanoid compounds." Arch Biochem Biophys **351**(2): 243-9.

Glassbrook, N., C. Beecher and J. Ryals (2000). "Metabolic profiling on the right path." Nature Biotechnology **18**(11): 1142-1143.

Glauser, G., E. Grata, L. Dubugnon, S. Rudaz, E. E. Farmer and J. L. Wolfender (2008). "Spatial and temporal dynamics of jasmonate synthesis and accumulation in Arabidopsis in response to wounding." J Biol Chem **283**(24): 16400-7.

Glauser, G., D. Guillarme, E. Grata, J. Boccard, A. Thiocone, P. A. Carrupt, J. L. Veuthey, S. Rudaz and J. L. Wolfender (2008). "Optimized liquid chromatography-mass spectrometry approach for the isolation of minor stress biomarkers in plant extracts and their identification by capillary nuclear magnetic resonance." Journal of Chromatography A **1180**(1-2): 90-98.

Glauser, G., D. Guillarme, E. Grata, J. Boccard, A. Thiocone, P. A. Carrupt, J. L. Veuthey, S. Rudaz and J. L. Wolfender (2008). "Optimized liquid chromatography-mass spectrometry approach for the isolation of minor stress biomarkers in plant extracts and their identification by capillary nuclear magnetic resonance." J Chromatogr A **1180**(1-2): 90-8.

Glazebrook, J. and F. M. Ausubel (1994). "Isolation of phytoalexin-deficient mutants of Arabidopsis thaliana and characterization of their interactions with bacterial pathogens." Proc Natl Acad Sci U S A **91**(19): 8955-9.

Goujon, T., R. Sibout, B. Pollet, B. Maba, L. Nussaume, N. Bechtold, F. Lu, J. Ralph, I. Mila, Y. Barriere, C. Lapierre and L. Jouanin (2003). "A new Arabidopsis thaliana mutant deficient in the expression of O-methyltransferase impacts lignins and sinapoyl esters." Plant Mol Biol **51**(6): 973-89.

Grubb, C. D. and S. Abel (2006). "Glucosinolate metabolism and its control." Trends in Plant Science **11**(2): 89-100.

Gu, L., A. D. Jones and R. L. Last (2007). "LC-MS/MS assay for protein amino acids and metabolically related compounds for large-scale screening of metabolic phenotypes." Analytical Chemistry **79**(21): 8067-8075.

Guan, L. M. and J. G. Scandalios (2000). "Hydrogen-peroxide-mediated catalase gene expression in response to wounding." Free Radic Biol Med **28**(8): 1182-90.

Guo, X. and H. U. Stotz (2007). "Defense against Sclerotinia sclerotiorum in Arabidopsis is dependent on jasmonic acid, salicylic acid, and ethylene signaling." Mol Plant Microbe Interact **20**(11): 1384-95.

Gupta, V., M. G. Willits and J. Glazebrook (2000). "Arabidopsis thaliana EDS4 contributes to salicylic acid (SA)-dependent expression of defense responses: evidence for inhibition of jasmonic acid signaling by SA." Mol Plant Microbe Interact **13**(5): 503-11.

Gutjahr, C. and U. Paszkowski (2009). "Weights in the balance: jasmonic Acid and salicylic Acid signaling in root-biotroph interactions." Mol Plant Microbe Interact **22**(7): 763-72.

Guy, C., J. Kopka and T. Moritz (2008). "Plant metabolomics coming of age." Physiol Plant **132**(2): 113-6.

Hagemeier, J., B. Schneider, N. J. Oldham and K. Hahlbrock (2001). "Accumulation of soluble and wall-bound indolic metabolites in Arabidopsis thaliana leaves infected with Virulent or avirulent Pseudomonas syringae pathovar tomato strains." Proceedings of the National Academy of Sciences of the United States of America **98**(2): 753-758.

Hammerschmidt, R. (1999). "PHYTOALEXINS: What Have We Learned After 60 Years?" Annu Rev Phytopathol **37**: 285-306.

Hanley, J. C. (2005). Liquid chromatography/mass spectrometric methodologies for metabolomics, The Pennsylvania State University. **Ph.D.:** 282.

Harborne, J. B., Ed. (1988). The flavonoid:Advances in Research since 1980. New York, Chapman and Hall.

Harborne, J. B. (1994). Plant polyphenols and their role in plant defence mechanisms.

Heath, M. C. (2000). "Hypersensitive response-related death." Plant Mol Biol **44**(3): 321-34.

Hentze, H., F. Gantner, S. A. Kolb and A. Wendel (2000). "Depletion of hepatic glutathione prevents death receptor-dependent apoptotic and necrotic liver injury in mice." Am J Pathol **156**(6): 2045-56.

Hirai, M. Y., M. Klein, Y. Fujikawa, M. Yano, D. B. Goodenowe, Y. Yamazaki, S. Kanaya, Y. Nakamura, M. Kitayama, H. Suzuki, N. Sakurai, D. Shibata, J. Tokuhisa, M. Reichelt, J. Gershenzon, J. Papenbrock and K. Saito (2005). "Elucidation of gene-to-gene and metabolite-to-gene networks in arabidopsis by integration of metabolomics and transcriptomics." J Biol Chem **280**(27): 25590-5.

Howe, G. A. and C. A. Ryan (1999). "Suppressors of systemin signaling identify genes in the tomato wound response pathway." Genetics **153**(3): 1411-21.

Hunt, M. D., U. H. Neuenschwander, T. P. Delaney, K. B. Weymann, L. B. Friedrich, K. A. Lawton, H. Y. Steiner and J. A. Ryals (1996). "Recent advances in systemic acquired resistance research--a review." Gene **179**(1): 89-95.

Hyun, Y., S. Choi, H. J. Hwang, J. Yu, S. J. Nam, J. Ko, J. Y. Park, Y. S. Seo, E. Y. Kim, S. B. Ryu, W. T. Kim, Y. H. Lee, H. Kang and I. Lee (2008). "Cooperation and functional diversification of two closely related galactolipase genes for jasmonate biosynthesis." Dev Cell **14**(2): 183-92.

Ibrahim, R. K., A. Bruneau and B. Bantignies (1998). "Plant O-methyltransferases: molecular analysis, common signature and classification." Plant Mol Biol **36**(1): 1-10.

Ishiguro, S., A. Kawai-Oda, J. Ueda, I. Nishida and K. Okada (2001). "The DEFECTIVE IN ANTHER DEHISCIENCE gene encodes a novel phospholipase A1 catalyzing the initial step of jasmonic acid biosynthesis, which synchronizes pollen maturation, anther dehiscence, and flower opening in Arabidopsis." Plant Cell **13**(10): 2191-209.

Jander, G., S. R. Norris, V. Joshi, M. Fraga, A. Rugg, S. Yu, L. Li and R. L. Last (2004). "Application of a high-throughput HPLC-MS/MS assay to Arabidopsis mutant screening; evidence that threonine aldolase plays a role in seed nutritional quality." Plant J **39**(3): 465-75.

Jander, G., S. R. Norris, S. D. Rounsley, D. F. Bush, I. M. Levin and R. L. Last (2002). "Arabidopsis map-based cloning in the post-genome era." Plant Physiol **129**(2): 440-50.

Jimenez-Lopez, J. M., D. Wu and A. I. Cederbaum (2008). "Synergistic toxicity induced by prolonged glutathione depletion and inhibition of nuclear factor-kappaB signaling in liver cells." Toxicol In Vitro **22**(1): 106-15.

Jones, J. D. and J. L. Dangl (2006). "The plant immune system." Nature **444**(7117): 323-9.

Joshi, C. P. and V. L. Chiang (1998). "Conserved sequence motifs in plant S-adenosyl-L-methionine-dependent methyltransferases." Plant Mol Biol **37**(4): 663-74.

Kachroo, A. and P. Kachroo (2007). "Salicylic acid-, jasmonic acid- and ethylene-mediated regulation of plant defense signaling." Genet Eng (N Y) **28**: 55-83.

Katagiri, F., R. Thilmony and S. Y. He (2002). "The Arabidopsis Thaliana - Pseudomonas Syringae Interaction." The Arabidopsis Book.

Katsir, L., H. S. Chung, A. J. Koo and G. A. Howe (2008). "Jasmonate signaling: a conserved mechanism of hormone sensing." Curr Opin Plant Biol **11**(4): 428-35.

Keen, N. T. (1990). "Gene-for-gene complementarity in plant-pathogen interactions." Annu Rev Genet **24**: 447-63.

Kerhoas, L., D. Aouak, A. Cingoz, J. M. Routaboul, L. Lepiniec, J. Einhorn and N. Birlirakis (2006). "Structural characterization of the major flavonoid glycosides from Arabidopsis thaliana seeds." Journal of Agricultural and Food Chemistry **54**(18): 6603-6612.

Kim, J. K., T. Bamba, K. Harada, E. Fukusaki and A. Kobayashi (2007). "Time-course metabolic profiling in Arabidopsis thaliana cell cultures after salt stress treatment." Journal of Experimental Botany **58**(3): 415-424.

Kim, Y. S. and H. Sano (2008). "Pathogen resistance of transgenic tobacco plants producing caffeine." Phytochemistry **69**(4): 882-8.

Kliebenstein, D. J. (2004). "Secondary metabolites and plant/environment interactions: a view through Arabidopsis thaliana tinged glasses." Plant Cell and Environment **27**(6): 675-684.

Knight, M. R., N. D. Read, A. K. Campbell and A. J. Trewavas (1993). "Imaging calcium dynamics in living plants using semi-synthetic recombinant aequorins." J Cell Biol **121**(1): 83-90.

Koo, A. J., X. Gao, A. Daniel Jones and G. A. Howe (2009). "A rapid wound signal activates the systemic synthesis of bioactive jasmonates in Arabidopsis." Plant J.

Koo, A. J. K., H. S. Chung, Y. Kobayashi and G. A. Howe (2006). "Identification of a peroxisomal acyl-activating enzyme involved in the biosynthesis of jasmonic acid in arabidopsis." Journal of Biological Chemistry **281**(44): 33511-33520.

Kourtchenko, O., M. X. Andersson, M. Hamberg, A. Brunnstrom, C. Gobel, K. L. McPhail, W. H. Gerwick, I. Feussner and M. Ellerstrom (2007). "Oxo-phytodienoic acid-containing galactolipids in Arabidopsis: jasmonate signaling dependence." Plant Physiol **145**(4): 1658-69.

Kramell, R., O. Miersch, B. Hause, B. Ortel, B. Parthier and C. Wasternack (1997). "Amino acid conjugates of jasmonic acid induce jasmonate-responsive gene expression in barley (Hordeum vulgare L.) leaves." Febs Letters **414**(2): 197-202.

Kusnierczyk, A., P. Winge, T. S. Jorstad, J. Troczynska, J. T. Rossiter and A. M. Bones (2008). "Towards global understanding of plant defence against aphids--timing and dynamics of early Arabidopsis defence responses to cabbage aphid (Brevicoryne brassicae) attack." Plant Cell Environ **31**(8): 1097-115.

Lahner, B., J. Gong, M. Mahmoudian, E. L. Smith, K. B. Abid, E. E. Rogers, M. L. Guerinot, J. F. Harper, J. M. Ward, L. McIntyre, J. I. Schroeder and D. E. Salt (2003). "Genomic scale profiling of nutrient and trace elements in Arabidopsis thaliana." Nat Biotechnol **21**(10): 1215-21.

Landry, L. G., C. C. S. Chapple and R. L. Last (1995). "Arabidopsis Mutants Lacking Phenolic Sunscreens Exhibit Enhanced Ultraviolet-B Injury and Oxidative Damage." Plant Physiology **109**: 1159-1166.

Last, R. L., A. D. Jones and Y. Shachar-Hill (2007). "Towards the plant metabolome and beyond." Nat Rev Mol Cell Biol **8**(2): 167-74.

Laudert, D. and E. W. Weiler (1998). "Allene oxide synthase: a major control point in Arabidopsis thaliana octadecanoid signalling." Plant J **15**(5): 675-84.

Le Lay, P., M. P. Isaure, J. E. Sarry, L. Kuhn, B. Fayard, J. L. Le Bail, O. Bastien, J. Garin, C. Roby and J. Bourguignon (2006). "Metabolomic, proteomic and biophysical analyses of Arabidopsis thaliana cells exposed to a caesium stress. Influence of potassium supply." Biochimie **88**(11): 1533-47.

Lebel, E., P. Heifetz, L. Thorne, S. Uknes, J. Ryals and E. Ward (1998). "Functional analysis of regulatory sequences controlling PR-1 gene expression in Arabidopsis." Plant J **16**(2): 223-33.

Lee, S., S. Suh, S. Kim, R. C. Crain, J. M. Kwak, H.-G. Nam and Y. Lee (1997). "Systemic elevation of phosphatidic acid and lysophospholipid levels in wounded plants." Plant Journal **12**: 547-556.

Leon, J., E. Rojo, E. Titarenko and J. J. Sanchez-Serrano (1998). "Jasmonic acid-dependent and -independent wound signal transduction pathways are differentially regulated by Ca2+/calmodulin in Arabidopsis thaliana." Mol Gen Genet **258**(4): 412-9.

Lilienblum, W., B. S. Bock-Hennig and K. W. Bock (1985). "Protection against toxic redox cycles between benzo(a)pyrene-3,6-quinone and its quinol by 3-methylcholanthrene-inducible formation of the quinol mono- and diglucuronide." Mol Pharmacol **27**(4): 451-8.

Lim, E. K., Y. Li, A. Parr, R. Jackson, D. A. Ashford and D. J. Bowles (2001). "Identification of glucosyltransferase genes involved in sinapate metabolism and lignin synthesis in Arabidopsis." Journal of Biological Chemistry **276**(6): 4344-4349.

Lorenzen, M., V. Racicot, D. Strack and C. Chapple (1996). "Sinapic acid ester metabolism in wild type and a sinapoylglucose-accumulating mutant of Arabidopsis." Plant Physiology **112**(4): 1625-1630.

Lu, Y., L. J. Savage, I. Ajjawi, K. M. Imre, D. W. Yoder, C. Benning, D. Dellapenna, J. B. Ohlrogge, K. W. Osteryoung, A. P. Weber, C. G. Wilkerson and R. L. Last (2008). "New connections across pathways and cellular processes: industrialized mutant screening reveals novel associations between diverse phenotypes in Arabidopsis." Plant Physiol **146**(4): 1482-500.

Marrs, K. A. (1996). "The Functions and Regulation of Glutathione S-Transferases in Plants." Annu Rev Plant Physiol Plant Mol Biol **47**: 127-158.

Martin, C., K. Bhatt and K. Baumann (2001). "Shaping in plant cells." Curr Opin Plant Biol **4**(6): 540-9.

Mattsson, J. L. (2000). "Do pesticides reduce our total exposure to food borne toxicants?" Neurotoxicology **21**(1-2): 195-202.

McCallum, C. M., L. Comai, E. A. Greene and S. Henikoff (2000). "Targeted screening for induced mutations." Nat Biotechnol **18**(4): 455-7.

Meinke, D. W., J. M. Cherry, C. Dean, S. D. Rounsley and M. Koornneef (1998). "Arabidopsis thaliana: a model plant for genome analysis." Science **282**(5389): 662, 679-82.

Melotto, M., W. Underwood, J. Koczan, K. Nomura and S. Y. He (2006). "Plant stomata function in innate immunity against bacterial invasion." Cell **126**(5): 969-80.

Messerli, G., V. Partovi Nia, M. Trevisan, A. Kolbe, N. Schauer, P. Geigenberger, J. Chen, A. C. Davison, A. R. Fernie and S. C. Zeeman (2007). "Rapid classification

of phenotypic mutants of Arabidopsis via metabolite fingerprinting." Plant Physiol **143**(4): 1484-92.

Metzler, M. C., J. R. Cutt and D. F. Klessig (1991). "Isolation and Characterization of a Gene Encoding a PR-1-Like Protein from Arabidopsis thaliana." Plant Physiol **96**(1): 346-348.

Mewis, I., J. G. Tokuhisa, J. C. Schultz, H. M. Appel, C. Ulrichs and J. Gershenzon (2006). "Gene expression and glucosinolate accumulation in Arabidopsis thaliana in response to generalist and specialist herbivores of different feeding guilds and the role of defense signaling pathways." Phytochemistry **67**(22): 2450-2462.

Mewis, I., J. G. Tokuhisa, J. C. Schultz, H. M. Appel, C. Ulrichs and J. Gershenzon (2006). "Gene expression and glucosinolate accumulation in Arabidopsis thaliana in response to generalist and specialist herbivores of different feeding guilds and the role of defense signaling pathways." Phytochemistry **67**(22): 2450-62.

Mittler, R. (2002). "Oxidative stress, antioxidants and stress tolerance." Trends Plant Sci **7**(9): 405-10.

Mittler, R. (2006). "Abiotic stress, the field environment and stress combination." Trends Plant Sci **11**(1): 15-9.

Mittler, R., S. Vanderauwera, M. Gollery and F. Van Breusegem (2004). "Reactive oxygen gene network of plants." Trends Plant Sci **9**(10): 490-8.

Mizoguchi, T., K. Ichimura and K. Shinozaki (1997). "Environmental stress response in plants: the role of mitogen-activated protein kinases." Trends Biotechnol **15**(1): 15-9.

Mock, H. P., T. Vogt and D. Strack (1992). "Sinapoylglucose - Malate Sinapoyltransferase Activity in Arabidopsis-Thaliana and Brassica-Rapa." Zeitschrift Fur Naturforschung C-a Journal of Biosciences **47**(9-10): 680-682.

Moco, S., B. Schneider and J. Vervoort (2009). "Plant Micrometabolomics: The Analysis of Endogenous Metabolites Present in a Plant Cell or Tissue." J Proteome Res.

Monks, T. J. and S. S. Lau (1992). "Toxicology of quinone-thioethers." Crit Rev Toxicol **22**(5-6): 243-70.

Monks, T. J. and S. S. Lau (1998). "The pharmacology and toxicology of polyphenolic-glutathione conjugates." Annu Rev Pharmacol Toxicol **38**: 229-55.

Montesinos, E., A. Bonaterra, E. Badosa, J. Frances, J. Alemany, I. Llorente and C. Moragrega (2002). "Plant-microbe interactions and the new biotechnological methods of plant disease control." Int Microbiol **5**(4): 169-75.

Mueller, L. A., C. D. Goodman, R. A. Silady and V. Walbot (2000). "AN9, a petunia glutathione S-transferase required for anthocyanin sequestration, is a flavonoid-binding protein." Plant Physiol **123**(4): 1561-70.

Murata, M., M. Sugiura, Y. Sonokawa, T. Shimamura and S. Homma (2002). "Properties of chlorogenic acid quinone: relationship between browning and the formation of hydrogen peroxide from a quinone solution." Biosci Biotechnol Biochem **66**(12): 2525-30.

Muzac, I., J. Wang, D. Auzellotti, H. Zhang and R. K. Ibrahim (2000). "Functional expression of an Arabidopsis cDNA clone encoding a flavonol 3 '-O-methyltransferase and characterization of the gene product." Archives of Biochemistry and Biophysics **375**(2): 385-388.

Nair, R. B., K. L. Bastress, M. O. Ruegger, J. W. Denault and C. Chapple (2004). "The Arabidopsis thaliana REDUCED EPIDERMAL FLUORESCENCE1 gene encodes an aldehyde dehydrogenase involved in ferulic acid and sinapic acid biosynthesis." Plant Cell **16**(2): 544-554.

Nawrath, C., S. Heck, N. Parinthawong and J. P. Metraux (2002). "EDS5, an essential component of salicylic acid-dependent signaling for disease resistance in Arabidopsis, is a member of the MATE transporter family." Plant Cell **14**(1): 275-86.

Neuefeind, T., P. Reinemer and B. Bieseler (1997). "Plant glutathione S-transferases and herbicide detoxification." Biol Chem **378**(3-4): 199-205.

O'Donnell, P. J., C. Calvert, R. Atzorn, C. Wasternack, H. M. O. Leyser and D. J. Bowles (1996). "Ethylene as a Signal Mediating the Wound Response of Tomato Plants." Science **274**(5294): 1914-7.

Orozco-Cardenas, M. and C. A. Ryan (1999). "Hydrogen peroxide is generated systemically in plant leaves by wounding and systemin via the octadecanoid pathway." Proc Natl Acad Sci U S A **96**(11): 6553-7.

Orozco-Cardenas, M. L., J. Narvaez-Vasquez and C. A. Ryan (2001). "Hydrogen peroxide acts as a second messenger for the induction of defense genes in tomato plants in response to wounding, systemin, and methyl jasmonate." Plant Cell **13**(1): 179-91.

Orozco-Cardenas, M. L. and C. A. Ryan (2002). "Nitric oxide negatively modulates wound signaling in tomato plants." Plant Physiol **130**(1): 487-93.

Parisy, V., B. Poinssot, L. Owsianowski, A. Buchala, J. Glazebrook and F. Mauch (2007). "Identification of PAD2 as a gamma-glutamylcysteine synthetase

highlights the importance of glutathione in disease resistance of Arabidopsis." Plant J **49**(1): 159-72.

Pastore, A., G. Federici, E. Bertini and F. Piemonte (2003). "Analysis of glutathione: implication in redox and detoxification." Clin Chim Acta **333**(1): 19-39.

Patrineli, A., M. N. Clifford and C. Ioannides (1996). "Contribution of phenols, quinones and reactive oxygen species to the mutagenicity of white grape juice in the Ames test." Food Chem Toxicol **34**(9): 869-72.

Poethig, R. S. (2001). "Life with 25,000 genes." Genome Res **11**(3): 313-6.

Pontier, D., C. Albrieux, J. Joyard, T. Lagrange and M. A. Block (2007). "Knock-out of the magnesium protoporphyrin IX methyltransferase gene in Arabidopsis. Effects on chloroplast development and on chloroplast-to-nucleus signaling." J Biol Chem **282**(4): 2297-304.

Raes, J., A. Rohde, J. H. Christensen, Y. Van de Peer and W. Boerjan (2003). "Genome-wide characterization of the lignification toolbox in Arabidopsis." Plant Physiology **133**(3): 1051-1071.

Reymond, P., H. Weber, M. Damond and E. E. Farmer (2000). "Differential gene expression in response to mechanical wounding and insect feeding in Arabidopsis." Plant Cell **12**(5): 707-20.

Roessner, U. (2007). Uncovering the plant metabolome: current and future challenges. Concepts in plant metabolomics

Roessner, U., A. Luedemann, D. Brust, O. Fiehn, T. Linke, L. Willmitzer and A. R. Fernie (2001). "Metabolic profiling allows comprehensive phenotyping of genetically or environmentally modified plant systems." Plant Cell **13**(1): 11-29.

Roessner, U., C. Wagner, J. Kopka, R. N. Trethewey and L. Willmitzer (2000). "Technical advance: simultaneous analysis of metabolites in potato tuber by gas chromatography-mass spectrometry." Plant J **23**(1): 131-42.

Rogers, E. E. and F. M. Ausubel (1997). "Arabidopsis enhanced disease susceptibility mutants exhibit enhanced susceptibility to several bacterial pathogens and alterations in PR-1 gene expression." Plant Cell **9**(3): 305-16.

Rogers, L. A., C. Dubos, C. Surman, J. Willment, I. F. Cullis, S. D. Mansfield and M. M. Campbell (2005). "Comparison of lignin deposition in three ectopic lignification mutants." New Phytologist **168**(1): 123-140.

Ruegger, M. and C. Chapple (2001). "Mutations that reduce sinapoylmalate accumulation in Arabidopsis thaliana define loci with diverse roles in phenylpropanoid metabolism." Genetics **159**(4): 1741-9.

Ruegger, M., K. Meyer, J. C. Cusumano and C. Chapple (1999). "Regulation of ferulate-5-hydroxylase expression in Arabidopsis in the context of sinapate ester biosynthesis." Plant Physiol **119**(1): 101-10.

Rusterucci, C., V. Stallaert, M. L. Milat, A. Pugin, P. Ricci and J. P. Blein (1996). "Relationship between Active Oxygen Species, Lipid Peroxidation, Necrosis, and Phytoalexin Production Induced by Elicitins in Nicotiana." Plant Physiol **111**(3): 885-891.

Ryan, C. A. (2000). "The systemin signaling pathway: differential activation of plant defensive genes." Biochim Biophys Acta **1477**(1-2): 112-21.

Ryan, C. A. (2000). "The systemin signaling pathway: differential activation of plant defensive genes." Biochimica Et Biophysica Acta-Protein Structure and Molecular Enzymology **1477**(1-2): 112-121.

Ryu, S. B. and X. Wang (1998). "Increase in free linolenic and linoleic acids associated with phospholipase D-mediated hydrolysis of phospholipids in wounded castor bean leaves." Biochim Biophys Acta **1393**(1): 193-202.

Salyan, M. E., D. L. Pedicord, L. Bergeron, G. A. Mintier, L. Hunihan, K. Kuit, L. A. Balanda, B. J. Robertson, J. N. Feder, R. Westphal, P. A. Shipkova and Y. Blat (2006). "A general liquid chromatography/mass spectroscopy-based assay for detection and quantitation of methyltransferase activity." Anal Biochem **349**(1): 112-7.

Schauer, N. and A. R. Fernie (2006). "Plant metabolomics: towards biological function and mechanism." Trends Plant Sci **11**(10): 508-16.

Schilmiller, A. L. and G. A. Howe (2005). "Systemic signaling in the wound response." Curr Opin Plant Biol **8**(4): 369-77.

Schmelz, E. A., J. Engelberth, J. H. Tumlinson, A. Block and H. T. Alborn (2004). "The use of vapor phase extraction in metabolic profiling of phytohormones and other metabolites." Plant Journal **39**(5): 790-808.

Scholthof, H. B. (2001). "Molecular plant-microbe interactions that cut the mustard." Plant Physiology **127**(4): 1476-1483.

Serra, R., A. Braga and A. Venancio (2005). "Mycotoxin-producing and other fungi isolated from grapes for wine production, with particular emphasis on ochratoxin A." Res Microbiol **156**(4): 515-21.

Shulaev, V., D. Cortes, G. Miller and R. Mittler (2008). "Metabolomics for plant stress response." Physiol Plant **132**(2): 199-208.

Srivastava, L. M. (2002). Plant Growth and Development: Hormones and Environment Amsterdam: Academic Press.

Staswick, P. E. and I. Tiryaki (2004). "The oxylipin signal jasmonic acid is activated by an enzyme that conjugates it to isoleucine in Arabidopsis." Plant Cell **16**(8): 2117-27.

Stephensen, E., J. Sturve and L. Forlin (2002). "Effects of redox cycling compounds on glutathione content and activity of glutathione-related enzymes in rainbow trout liver." Comp Biochem Physiol C Toxicol Pharmacol **133**(3): 435-42.

Stobiecki, M., A. Skirycz, L. Kerhoas, P. Kachlicki, D. Muth, J. Einhorn and B. Mueller-Roeber (2006). "Profiling of phenolic glycosidic conjugates in leaves of Arabidopsis thaliana using LC/MS." Metabolomics **2**(4): 197-219.

Sumner, L. W., P. Mendes and R. A. Dixon (2003). "Plant metabolomics: large-scale phytochemistry in the functional genomics era." Phytochemistry **62**(6): 817-36.

Sumner, L. W., P. Mendes and R. A. Dixon (2003). "Plant metabolomics: large-scale phytochemistry in the functional genomics era." Phytochemistry **62**(6): 817-836.

TAIR. (2007). " The Arabidopsis Information Resource. http://www.arabidopsis.org/."

Tamogami, S. and O. Kodama (1998). "Quantification of amino acid conjugates of jasmonic acid in rice leaves by high-performance liquid chromatography turboionspray tandem mass spectrometry." Journal of Chromatography A **822**(2): 310-315.

Thilmony, R., W. Underwood and S. Y. He (2006). "Genome-wide transcriptional analysis of the Arabidopsis thaliana interaction with the plant pathogen Pseudomonas syringae pv. tomato DC3000 and the human pathogen Escherichia coli O157:H7." Plant J **46**(1): 34-53.

Thines, B., L. Katsir, M. Melotto, Y. Niu, A. Mandaokar, G. H. Liu, K. Nomura, S. Y. He, G. A. Howe and J. Browse (2007). "JAZ repressor proteins are targets of the SCFCO11 complex during jasmonate signalling." Nature **448**(7154): 661-U2.

Thoma, I., C. Loeffler, A. K. Sinha, M. Gupta, M. Krischke, B. Steffan, T. Roitsch and M. J. Mueller (2003). "Cyclopentenone isoprostanes induced by reactive oxygen species trigger defense gene activation and phytoalexin accumulation in plants." Plant J **34**(3): 363-75.

Tierens, K. F., B. P. Thomma, M. Brouwer, J. Schmidt, K. Kistner, A. Porzel, B. Mauch-Mani, B. P. Cammue and W. F. Broekaert (2001). "Study of the role of antimicrobial glucosinolate-derived isothiocyanates in resistance of Arabidopsis to microbial pathogens." Plant Physiol **125**(4): 1688-99.

Titarenko, E., E. Rojo, J. Leon and J. J. Sanchez-Serrano (1997). "Jasmonic acid-dependent and -independent signaling pathways control wound-induced gene activation in Arabidopsis thaliana." Plant Physiol **115**(2): 817-26.

Tohge, T., Y. Nishiyama, M. Y. Hirai, M. Yano, J. Nakajima, M. Awazuhara, E. Inoue, H. Takahashi, D. B. Goodenowe, M. Kitayama, M. Noji, M. Yamazaki and K. Saito (2005). "Functional genomics by integrated analysis of metabolome and transcriptome of Arabidopsis plants over-expressing an MYB transcription factor." Plant J **42**(2): 218-35.

Tohge, T., K. Yonekura-Sakakibara, R. Niida, A. Watanabe-Rakahashi and K. Saito (2007). "Phytochemial genomics in Arabidopsis thaliana: A case study for functional identification of flavonoid biosynthesis genes." Pure and Applied Chemestry. **79**(4): 811-823.

Traw, M. B., J. M. Kniskern and J. Bergelson (2007). "SAR increases fitness of Arabidopsis thaliana in the presence of natural bacterial pathogens." Evolution **61**(10): 2444-9.

Treutter, D. (2005). "Significance of flavonoids in plant resistance and enhancement of their biosynthesis." Plant Biol (Stuttg) **7**(6): 581-91.

Treutter, D. (2006). "Significance of flavonoids in plant resistance: a review." Environmental Chemistry Letters **4**(3): 147-157.

Truman, W., M. T. de Zabala and M. Grant (2006). "Type III effectors orchestrate a complex interplay between transcriptional networks to modify basal defence responses during pathogenesis and resistance." Plant J **46**(1): 14-33.

Trygg, J., E. Holmes and T. Lundstedt (2007). "Chemometrics in metabonomics." J Proteome Res **6**(2): 469-79.

van Verk, M. C., D. Pappaioannou, L. Neeleman, J. F. Bol and H. J. Linthorst (2008). "A Novel WRKY transcription factor is required for induction of PR-1a gene expression by salicylic acid and bacterial elicitors." Plant Physiol **146**(4): 1983-95.

von Roepenack-Lahaye, E., T. Degenkolb, M. Zerjeski, M. Franz, U. Roth, L. Wessjohann, J. Schmidt, D. Scheel and S. Clemens (2004). "Profiling of Arabidopsis secondary metabolites by capillary liquid chromatography coupled to

electrospray ionization quadrupole time-of-flight mass spectrometry." Plant Physiol **134**(2): 548-59.

Wang, C. X., C. A. Zien, M. Afitlhile, R. Welti, D. F. Hildebrand and X. M. Wang (2000). "Involvement of phospholipase D in wound-induced accumulation of jasmonic acid in Arabidopsis." Plant Cell **12**(11): 2237-2246.

Wang, J. and E. Pichersky (1999). "Identification of specific residues involved in substrate discrimination in two plant O-methyltransferases." Arch Biochem Biophys **368**(1): 172-80.

Wang, L., R. Halitschke, J. H. Kang, A. Berg, F. Harnisch and I. T. Baldwin (2007). "Independently silencing two JAR family members impairs levels of trypsin proteinase inhibitors but not nicotine." Planta **226**(1): 159-67.

Ward, J. L., J. M. Baker and M. H. Beale (2007). "Recent applications of NMR spectroscopy in plant metabolomics." Febs J **274**(5): 1126-31.

Wasternack, C. (2007). "Jasmonates: an update on biosynthesis, signal transduction and action in plant stress response, growth and development." Ann Bot (Lond) **100**(4): 681-97.

Weber, H., B. A. Vick and E. E. Farmer (1997). "Dinor-oxo-phytodienoic acid: a new hexadecanoid signal in the jasmonate family." Proc Natl Acad Sci U S A **94**(19): 10473-8.

Weckwerth, W. (2008). "Integration of metabolomics and proteomics in molecular plant physiology--coping with the complexity by data-dimensionality reduction." Physiol Plant **132**(2): 176-89.

Weigel, R. R., U. M. Pfitzner and C. Gatz (2005). "Interaction of NIMIN1 with NPR1 modulates PR gene expression in Arabidopsis." Plant Cell **17**(4): 1279-91.

Weiler, E. W., T. M. Kutchan, T. Gorba, W. Brodschelm, U. Niesel and F. Bublitz (1994). "The Pseudomonas phytotoxin coronatine mimics octadecanoid signalling molecules of higher plants." FEBS Lett **345**(1): 9-13.

Weisel, T., M. Baum, G. Eisenbrand, H. Dietrich, F. Will, J. P. Stockis, S. Kulling, C. Rufer, C. Johannes and C. Janzowski (2006). "An anthocyanin/polyphenolic-rich fruit juice reduces oxidative DNA damage and increases glutathione level in healthy probands." Biotechnol J **1**(4): 388-97.

Wilbert, S. M., L. H. Ericsson and M. P. Gordon (1998). "Quantification of jasmonic acid, methyl jasmonate, and salicylic acid in plants by capillary liquid chromatography electrospray tandem mass spectrometry." Analytical Biochemistry **257**(2): 186-194.

Wilson, I., P. Wardman, G. M. Cohen and M. D. Doherty (1986). "Reductive role of glutathione in the redox cycling of oxidizable drugs." Biochem Pharmacol **35**(1): 21-2.

Wingate, V. P., M. A. Lawton and C. J. Lamb (1988). "Glutathione Causes a Massive and Selective Induction of Plant Defense Genes." Plant Physiol **87**(1): 206-210.

Winkel, B. S. J. (2004). "Metabolic channeling in plants." Annual Review of Plant Biology **55**: 85-107.

Zhang, H., J. Wang and H. M. Goodman (1997). "An Arabidopsis gene encoding a putative 14-3-3-interacting protein, caffeic acid/5-hydroxyferulic acid O-methyltransferase." Biochimica Et Biophysica Acta-Gene Structure and Expression **1353**(3): 199-202.

Zhang, H., J. Wang and H. M. Goodman (1997). "An Arabidopsis gene encoding a putative 14-3-3-interacting protein, caffeic acid/5-hydroxyferulic acid O-methyltransferase." Biochim Biophys Acta **1353**(3): 199-202.

Zhang, Y., W. Fan, M. Kinkema, X. Li and X. Dong (1999). "Interaction of NPR1 with basic leucine zipper protein transcription factors that bind sequences required for salicylic acid induction of the PR-1 gene." Proc Natl Acad Sci U S A **96**(11): 6523-8.

Zhao, J., K. Fujita and K. Sakai (2007). "Reactive oxygen species, nitric oxide, and their interactions play different roles in Cupressus lusitanica cell death and phytoalexin biosynthesis." New Phytol **175**(2): 215-29.

Zook, M. (1998). "Biosynthesis of camalexin from tryptophan pathway intermediates in cell-suspension cultures of Arabidopsis." Plant Physiol **118**(4): 1389-93.

Zubieta, C., X. Z. He, R. A. Dixon and J. P. Noel (2001). "Structures of two natural product methyltransferases reveal the basis for substrate specificity in plant O-methyltransferases." Nature Structural Biology **8**(3): 271-279.

Zubieta, C., P. Kota, J. L. Ferrer, R. A. Dixon and J. P. Noel (2002). "Structural basis for the modulation of lignin monomer methylation by caffeic acid/5-hydroxyferulic acid 3/5-O-methyltransferase." Plant Cell **14**(6): 1265-77.